Santa Clara River Parkway
Floodplain Restoration
Feasibility Study

Assessment of Geomorphic Processes for the Santa Clara River Watershed, Ventura and Los Angeles counties, California

FINAL REPORT
August 2007

Prepared for
The California Coastal Conservancy
1330 Broadway, 11th Floor
Oakland, California 94612-2530

Prepared by
Stillwater Sciences
2855 Telegraph Avenue, Suite 400
Berkeley, California 94705

Stillwater Sciences

Contact:
Peter Downs, PhD.
Senior Geomorphologist
Stillwater Sciences
2855 Telegraph Avenue, Suite 400
Berkeley, CA 94705
Stillwater Sciences
(510) 848-8098 x121
downs@stillwatersci.com

Cover photography (from top to bottom):

1. Eroding uplands in the Santa Susana Mountains and floodplain agriculture in the lower Santa Clara River, upstream of Fillmore, California. January 2005. Photo California State Coastal Conservancy
2. Lower Sespe Creek, April 2005. Photo P. Downs/Stillwater Sciences.
3. Westward (downstream facing) view of the Santa Clara River and Sespe Creek (at right) in flood, January 2005. Photo California State Coastal Conservancy.
4. Dunes in the northwest corner of the Santa Clara River estuary, view east (upstream), May 2005. Photo W. Sears/Stillwater Sciences.

Acknowledgements
Our sincere thanks go to Peter Brand and the California State Coastal Conservancy for enthusiastically supporting our efforts to develop the background information necessary to understand and document how the Santa Clara River system functions, as a basis for conservation planning and river management efforts in the watershed. We would also like to thank individuals from a number of organizations who provided background information, data, advice, and support, including The Nature Conservancy, Ventura County Museum of History and Art, United Water Conservation District, Ventura County Planning Division, Ventura County Watershed Protection District, California Department of Fish Game, NOAA Fisheries, McGrath State Park, URS Corporation, and the United States Army Corps of Engineers. Antony Orme (University of California Los Angeles), Jonathon Warrick (United States Geological Survey), Howard Chang (California State University San Diego), Fred Booker (University of California, Berkeley), and Gretchen Coffman (URS Corporation and University of California, Los Angeles), provided essential data and guidance for the effort.
We have appreciated the opportunity to present and debate our findings at various conferences locally and nationally, and are particularly grateful for Tom Dunne's invitation to present our work on the Santa Clara River as a case study in his River Systems course at the University of California Santa Barbara: all these experiences sharpened our thinking about the watershed.

The project team included William Sears as the project manager and Peter Downs as the principal investigator. Technical analysis and written synthesis was provided by geomorphologists Scott Dusterhoff, Cliff Riebe, Jay Stallman, and Glen Leverich. Bill Sears performed GIS analyses of morphological change and was ably supported by Rafael Real de Asua, Sayaka Araki, and Sebastian Araya. Phoebe Bass helped tremendously with data compilation. The final report would not have been possible without the input, assistance, and cajoling of Tami Cosio. The technical team remains responsible for any mistakes and errors in this report, but we are extremely grateful for the valuable input of peer reviewers Antony Orme (University of California Los Angeles), Jonathon Warrick (United States Geological Survey), and Derek Booth (Stillwater Sciences and University of Washington) for reviews of earlier drafts of this document.

Preferred citation
Stillwater Sciences. 2007. Santa Clara River Parkway Floodplain Restoration Feasibility Study: Assessment of Geomorphic Processes for the Santa Clara River Watershed, Ventura and Los Angeles Counties, California. Prepared by Stillwater Sciences for the California State Coastal Conservancy.

Table of Contents

1 SUMMARY 1

2 INTRODUCTION 11

2.1 A Geomorphic Process-based Context for Restoration Planning 12

2.2 Regional Setting 12

2.2.1 Geology 14
2.2.2 Climate and Hydrology 15
2.2.3 Land Use/Land Cover 17

3 IMPACTS OF HISTORICAL WATERSHED CHANGES ON GEOMORPHIC PROCESSES 19

4 HILLSLOPE SEDIMENT PRODUCTION, TRANSPORT, AND DELIVERY 25

4.1 Overview of Uplift, Erosion, and Sediment Transport 25

4.2 Dominant Sediment Production and Transport Processes 26

4.2.1 Soil Creep 26
4.2.2 Overland Flow 27
4.2.3 Landslides 28
4.2.4 Earthquake-induced Landslides 30
4.2.5 Effects of Fire on Sediment Production and Transport 31

4.3 Human-Induced Changes in Sediment Production and Transport 34

4.3.1 Effects of European Settlement on Sediment Transport Rates 34
4.3.2 Effects of Conversion to Non-native Grasses on Landslide Frequency 34
4.3.3 Fire Management 34

4.4 Rates of Hillslope Processes 35

4.4.1 Rates of Rock Uplift and Dip-displacement 36
4.4.2 Rates of Hillslope Sediment Transport and Production: the Transverse Ranges 36
4.4.3 Rates of Hillslope Sediment Transport and Production: the Santa Clara River Watershed 37
4.4.4 Summary of Rates of Hillslope Processes 42

4.5 Delivery of Sediment from Tributaries to the Santa Clara River Valley 43

4.5.1 Episodic Sediment Delivery from Tributaries 44
4.5.2 Effects of Fire on Sediment Delivery 44
4.5.3 Effects of Rock Type and Local Uplift Rates on Sediment Delivery 44
4.5.4 Contributions from Tributaries along the Lower River Corridor 44
4.5.5 Effects of Infrastructure on Sediment Delivery 44
4.5.6 Sediment Particle Size 45

4.6 Conceptual Model of Hillslope Processes and Implications for Lower Santa Clara River Geomorphology 45

5 FLUVIAL SEDIMENT TRANSPORT AND MORPHOLOGICAL CHANGE 47

5.1 Frequency and Magnitude of Sediment Transport 47

5.1.1 "Dominant Discharge" Characteristics 47
5.1.2 Effects of the El Niño -Southern Oscillation on Flow Magnitude and Sediment Delivery 51
5.1.3 Bed Material and Bedload Particle Sizes 53

5.2 Potential Impact of Infrastructure and Anthropogenic Channel Modifications 57

5.2.1 Dams 58

5.2.2 Aggregate Mining *61*
5.2.3 Levees and Bank Protection *65*
5.2.4 Irrigation and Flow Diversion *67*
5.2.5 Urban Growth *68*
5.3 Morphology and Channel Dynamics 70
5.3.1 Reach-level Differences in Channel Form *72*
5.3.2 Potential for Change *76*
5.3.3 Changes in Active Channel Width: 1938–2005 ..... *77*
5.3.4 Changes in Channel Bed Level: 1929–2005 ..... *87*
5.3.5 Summary of Reach-Level Dynamics *94*
5.4 Sediment Budgets for the Lower Santa Clara River 108
5.4.1 Storm-event Sediment Budgets from Gauge Data *108*
5.4.2 Sediment Budget Accommodating Aggregate Mining *116*
5.4.3 Reach-level Differentiation of Sediment Budget *117*
5.5 Summary: Fluvial Geomorphic Processes in the Lower Santa Clara River 118
5.5.1 Linkages: Interpretation of Morphological Changes in the LCSR 1929-2005 ..... *118*
5.5.2 Conceptual Model of Fluvial Processes in the LSCR *121*

6 ESTUARINE AND COASTAL PROCESSES 123

6.1 Physical Characteristics 123
6.1.1 Geologic Setting *123*
6.1.2 Topography *123*
6.1.3 Tidal and Wave Dynamics *125*
6.1.4 Estuary Hydrology and Hydraulics *126*
6.1.5 Sediment Particle Size *126*
6.2 Sedimentation Dynamics 127
6.2.1 Fluvial Processes and Delta Dynamics *127*
6.2.2 Longshore Transport Processes and Shoreline Dynamics *129*
6.2.3 Barrier Deposition and Mouth Closure Dynamics *131*
6.3 Estuary Historical Change Analysis (1855–2002) 136
6.4 Conceptual Model and Projected Trajectory of the Santa Clara River Estuary 138

7 SYNTHESIS 141

7.1 Key Information Gaps Affecting River Corridor Management Decision-making 142

8 REFERENCES 145

TABLES

Table 2-1. Major tributaries of the Santa Clara River including areas regulated by dams. 17
Table 3-1. Indicative historical sources for the Santa Clara River watershed 20
Table 4-1. Sediment production rates inferred from 16 Ventura County debris basins. 39
Table 4-2. Suspended sediment yield by subwatershed. 41
Table 4-3. Summary of rates of uplift, displacement, sediment production, and sediment yield[a] 42
Table 5-1. Annual maximum peak discharges since 1928 on the lower Santa Clara River, gauged or estimated to be in excess of 1,416 m^3s^{-1} (50,000 cfs). 47
Table 5-2. Ranked distribution of largest instantaneous flood peaks on the Santa Clara River at Montalvo.[1] 53
Table 5-3. Characteristics of channel bed sediments for Santa Clara River at Montalvo 54

Table 5-4. Characteristics of channel bed sediment for the Santa Clara River at the Los Angeles County Line. 54
Table 5-5. Characteristics of channel bed sediments for Sespe Creek at Fillmore. 55
Table 5-6. Characteristics of bedload sediment samples from the Santa Clara River at Montalvo. 55
Table 5-7. Characteristics of bedload sediment samples for the Santa Clara River at the Los Angeles County Line. 56
Table 5-8. Characteristics of bedload sediment samples for Sespe Creek at Fillmore. 57
Table 5-9. Sand and gravel production from the lower Santa Clara River 1960–1977.* 63
Table 5-10. Irrigated acreage in Ventura County. 67
Table 5-11. Population in major settlements of Los Angeles and Ventura counties within Santa Clara River watershed. 70
Table 5-12. Lower Santa Clara River reach characteristics. 73
Table 5-13. Reach unit stream power estimates for the LSCR. 77
Table 5-14. Width statistics for the LSCR for the period of record 1938-2005 by reach. Figures in bold are referred to in the text. Reach 11 is excluded from analysis because of limited photo coverage. 79
Table 5-15. Lower Santa Clara River reach morphodynamics: a summary of reach estimates derived elsewhere in this chapter. 96
Table 5-16. Storm coarse sediment (>0.5 mm) yield. 111
Table 5-17. Flow discharge and recurrence intervals (RI) for the largest recorded floods on the Santa Clara River (Los Angeles/Ventura County Line and Montalvo stations), Sespe Creek, and Santa Paula Creek. 114
Table 5-18. A 57-year sediment budget for the Lower Santa Clara River (1949-2005), inclusive of aggregate mining. 116
Table 5-19. Reach level sediment budget for the Lower Santa Clara River, 1949-2005, inclusive of aggregate mining. 118
Table 6-1. Tidal elevations from Rincon Island (1962–1990). 125
Table 6-2. Summary of sediment discharge estimates for the Santa Clara River. 127
Table 6-3. Elements of a conceptual understanding of the Santa Clara River Estuary. 139

FIGURES

Figure 2-1. Santa Clara River watershed and vicinity. 11
Figure 2-2. Mountain ranges and elevations in the Santa Clara River watershed and vicinity. 13
Figure 2-3. Major coastal southern California watersheds. 13
Figure 2-4. Generalized geologic map showing major rock units and fault traces in the Santa Clara River watershed. 14
Figure 2-5. Distribution of mean annual precipitation based on data from the period 1900–1960. 15
Figure 2-6. Areas within the Santa Clara River watershed regulated by major dams. 16
Figure 2-7. Land cover (2000) within the Santa Clara River watershed. 18
Figure 3-1. Chronology of potential watershed impacts and events. 21
Figure 4-1. Slope distribution in the Santa Clara River watershed. 25
Figure 4-2. January 2005 view of the Santa Susana Mountains and Santa Clara River near the confluence of Piru Creek 29
Figure 4-3. Landslides triggered by the 1994 Northridge earthquake (M=6.7). 30
Figure 4-4. Documented fire reoccurrence since 1878 (major recorded fires), and areas burned in the 2003 fire season. 32
Figure 4-5. Ventura County debris basins in the lower Santa Clara River and adjacent watersheds, with approximate boundaries of regulated areas. 38

Figure 4-6. Suspended sediment yield, major dams, and selected sediment and water discharge gauges in the Santa Clara River watershed 40
Figure 4-7. Illustration of conceptual model of hillslope processes in the Santa Clara River watershed....46
Figure 5-1. Flow frequency and sediment load plotted against flow, showing conceptual, dominant discharge model of Wolman and Miller (1960). 49
Figure 5-2. Flow frequency and coarse sediment load as a function of daily mean flow for the Santa Clara River at Montalvo (USGS11114000). 49
Figure 5-3. Flow frequency and coarse sediment load as functions of daily mean flow for the Santa Clara River at the Los Angeles/Ventura County line (USGS11108500). 50
Figure 5-4. Flow frequency and coarse sediment load as a function of daily mean flow for Sespe Creek at Fillmore (USGS11113000). 50
Figure 5-5. Flow exceedence for El Niño/non-El Niño years (period of record: WY 1932–2005) for the Santa Clara River at Montalvo (USGS11114000). 51
Figure 5-6. Relationship between annual precipitation totals in Santa Paula (VCWPD11113500) and annual maximum instantaneous flood peaks recorded in the lower Santa Clara River at Montalvo (USGS11114000). 52
Figure 5-7. Santa Felicia Dam, looking downstream. 58
Figure 5-8. The remains of the Saint Francis Dam after collapsing just before midnight on March 12, 1928, in the San Francisquito subwatershed. 59
Figure 5-9. Lower Santa Clara River showing sites of instream aggregate mining and public levees. Reach numbers refer to geomorphic subreaches discussed in Section 5.3 onward. 62
Figure 5-10. Undercutting of the Highway 118 bridge over the Santa Clara River as a result of incision following the 1969 floods. 64
Figure 5-11. View across the Santa Clara River in Reach 2 (near Saticoy) on the lower Santa Clara River showing the 1961 Army Corps of Engineers levee during the recession of the 2005 flood. 66
Figure 5-12. Population in major settlements of Los Angeles and Ventura counties within Santa Clara River watershed. 69
Figure 5-13. Westward, downstream view of the Sespe Creek confluence following the January 2005 flood 71
Figure 5-14. Predicted channel pattern for the lower Santa Clara River by reach. 75
Figure 5-15. Channel width change by reach. 80
Figure 5-16. Lower Santa Clara River historical channel position: proportion of time since 1938 that the active channel bed has occupied a given location. 81
Figure 5-17. Width of channel bed in successive floods since 1938 on the lower Santa Clara River: most recent floods on top. 84
Figure 5-18. Net thalweg elevation change for the Santa Clara River from 1949 to 2005. 88
Figure 5-19. Net thalweg elevation change for the Santa Clara River 90
Figure 5-20. Reach-average bed elevation change 93
Figure 5-21. Planform, typical cross-sections and indicative photographs by reach 97
Figure 5-22. Illustration of the conceptual model of sediment transport dynamics within the lower Santa Clara River presented in Simons, Li & Associates (1983) 110
Figure 5-23. Re-calculation of coarse sediment budget for floods of January 25, 1969 and February 10, 1978. 113
Figure 5-24. Case A: Integration of storm based sediment budgets based the largest recorded flood events only 115
Figure 6-1. Topography (2000) and benthic sediment sampling locations within the Santa Clara River estuary. 124
Figure 6-2. Topographic characteristics of the Santa Clara River estuary in 2000. 124

Figure 6-3. Conceptual description of sediment deposition from jet flow. 129
Figure 6-4. Location and extent of the Santa Barbara Littoral Cell. 130
Figure 6-5. Percentage of time that the Santa Clara River mouth was open on an annual basis (1984–1997).. 132
Figure 6-6. Percentage of time that the Santa Clara River mouth was open on a monthly basis (1984–1997).. 133
Figure 6-7. Time series of Santa Clara River mouth closure (April 16–May 19, 1982). 135
Figure 6-8. Time series of Santa Clara River mouth breach and closure (May 20–June 25, 1982). 135
Figure 6-9. Approximate active channel extent in July 2002.....136
Figure 6-10. Conceptual model of the current and future maintenance of the Santa Clara River mouth/estuary complex.....139

APPENDICES

Appendix A: Geologic setting.
Appendix B: Watershed impacts chronology.
Appendix C: Determination of coarse sediment yield within the Santa Clara River watershed.
Appendix D: Reconnaissance observations following floods in January and February 2005.
Appendix E: Methods for assessing planform channel dynamics of the lower Santa Clara River: 1938-2005.
Appendix F: Bed elevation change along the Santa Clara River (1929-2005).
Appendix G: Estuary historical photos.

1 SUMMARY

This report provides a synthesis and interpretation of existing knowledge regarding geomorphic processes within the Santa Clara River watershed, located in Ventura and Los Angeles counties, California. It was conducted in support of, and as background to, the Santa Clara River Parkway Floodplain Restoration Feasibility Study, a study designed to assist the California Coastal Conservancy and its partners in developing strategies for restoring floodplain lands in a 40 km (25 mi)[1] reach of the lower Santa Clara River. The report focuses on understanding, at a watershed level, geomorphic processes in their current and historical context, with an emphasis on determining how process changes have occurred. This understanding is required as the basis for a process-based approach to restoration planning for the Santa Clara River ecosystem.

The Santa Clara River is one of the largest watersheds on the southern California coast, draining an area of approximately 4,212 km^2 (1,626 mi^2), with elevations from sea level to approximately 2,692 m (8,832 ft). The watershed is located within a geologically active area, along the San Andreas Fault, which forms the dynamic boundary between the Pacific and North America tectonic plates. Persistent tectonic uplift in the region has resulted in significant geological instability, contributing to high rates of erosion throughout the watershed.

The Santa Clara River is significant in the region because it retains many natural attributes no longer exhibited by many coastal southern California rivers that have been severely modified by urban development. In particular, it experiences high annual and inter-year flow variability as a consequence of its semi-arid, Mediterranean-type climate. During the rainy season (November and March), river flows increase, peak and subside rapidly in response to high intensity rainfall, whereas in summer months flows may be intermittent or non-existent in many tributaries and, in the mainstem, depend upon geological controls on groundwater-surface water interactions. Controlled flow releases from Piru Reservoir now supplement surface flows to the lower Santa Clara River in summer months but, in general, high flow variability still exists because only 34% of the watershed in regulated by dams. Such variability permits the survival of a complex matrix of aquatic and riparian habitats in the watershed that support a number of endangered and threatened species, including a remnant run of endangered southern steelhead (*Oncorhynchus mykiss*).

Historical land use change and the evolution of water and river management practices within the Santa Clara River watershed can be synthesized into five distinct historical periods that have influenced the response of channel morphology to natural extremes of water and sediment discharge. These periods provide the basis for a conceptual understanding of ecosystem changes in the watershed; however, clearly disentangling the impact of human activities from natural events is difficult and the subject of much of this report. The historical periods include:

1. Pre-European Colonization prior to 1820: a period in which natural events that influenced geomorphic processes (including natural wildfires) are suspected of acting relatively independent of human activities;

[1] This report utilizes the metric (SI) system as a standard for reporting units. If English standard units are used in the primary data source, a conversion to metric is provided in the text, and most tables and figures (where possible) in addition to the original unit type.

2. Ranching and Colonization from 1820–1890: characterized by significant European arrival in the watershed, the introduction of livestock, and resultant changes in watershed vegetation causing changes in rainfall-runoff relationships and hillslope erosion rates;
3. Irrigation and Diversions from 1890–1955: a period in which floodplain agriculture, especially citrus crops, required an assured water source achieved by tributary diversions and the construction of small dams, causing changes in surface water and groundwater dynamics in the lower watershed, potentially increasing the "flashy" nature of the Santa Clara River;
4. Dams and River Modifications from 1955–1990: commencing with the completion of the watershed's major dam, the Santa Felicia, impounding Lake Piru, but including subsequent construction of an extensive network of levees and bank protection in the lower watershed and an intensive period of aggregate mining from the Santa Clara River and floodplain. The period resulted in a notable decrease in runoff and sediment discharge, an increase in flood flow confinement and significant river incision;
5. Urbanization since 1990: the primary new human influence in the watershed is the continuation of rapid population increases in the watershed, causing large-scale conversion of floodplain agricultural land to residential developments, further affecting rainfall-runoff relationships in the watershed and potentially contributing to greater river erosion.

Hillslope Sediment Production, Transport, and Delivery

Highly erodible bedrock underlies much of the Santa Clara River watershed, due to a long history of shearing, fracturing and faulting at the dynamic margin of the Pacific and North America plates. Rates of uplift and displacement along faults within the watershed vary by up to two orders of magnitude, consistent with the variations in hillslope erosion rates that have been reported for the region. Uplift rates are rapid, making slopes steep and therefore prone to landslides, which are triggered episodically by earthquakes and storms, particularly during wet years associated with the El Niño Southern Oscillation (ENSO). Steep slopes promote extensive dry raveling, delivering abundant sediment to channels during the dry season, when processes that require precipitation are dormant. Hence, sediment supply and transport from hillslopes is significant throughout the year, in both wet and dry seasons.

Coastal southern California is subject to frequent, intense, and often extensive wildfires, due to the semi-arid, Mediterranean climate, the prevalence of flammable chaparral vegetation, and the hot, dry Santa Ana winds, which often blow seaward from inland deserts during the dry season. Fires increase runoff and enhance hillslope sediment supply and transport by increasing dry ravel and rain impact, and by creating hydrophobic soil horizons, which contribute to post-fire rill development. Burnt slopes rarely recover before the arrival of intense winter storms that lead to enhanced erosion and runoff, and thus complete the "fire-flood" sequence. A long-term record of large fires indicates that they are a natural part of the regional environment, occurring in spite of recent fire suppression and prevention efforts. Conversely, the frequency of smaller fires, which may affect sediment yields locally, is apparently more responsive to changes in management practices and land use. It is estimated that roughly 67% of the Santa Clara River watershed has burned since 1878. Approximately 11% of the watershed burned in the 2003 fire season alone.

Large earthquakes in the region are inevitable due to tectonic instability along the San Andreas Fault Zone. The 1994 Northridge earthquake triggered more than 7,000 landslides in the watershed and thus likely had a significant impact on sediment production and delivery from hillslopes. Future earthquakes in the area are likely to lead to new slope failures and may also reactivate old slides.

European settlement of coastal southern California led to the widespread degradation of rangelands, and subsequent increases in hillslope sediment yields. Grazing is known to increase sediment yield by reducing vegetative cover, decreasing infiltration, and increasing runoff, but the extent of these effects in the Santa Clara River watershed is poorly understood. Sediment transport and delivery in the watershed has been modified by dam building. The overall sediment delivery rate to the mainstem has been reduced by an estimated 20% by dams on Piru Creek, Castaic Creek and Bouquet Creek. On the other hand, county-maintained debris basins along the lower Santa Clara River have a much smaller effect on sediment delivery to the river corridor.

Sediment data from the debris basins was used in this study to estimate erosion rates for the small tributary watersheds that empty into the basins. Erosion rates vary by nearly 100-fold across the watersheds. This high variability is consistent with the variability of regional erosion rates from previous work, which is synthesized in this report. Localized erosion rates in the Santa Clara River watershed and surrounding mountains are among the highest on record for the world, due to contributing effects of rapid uplift, episodic earthquakes, seasonally intense rainfall, and frequent fires. Sediment delivery to the mainstem Santa Clara River is, by extension, likewise high, and is also episodic, occurring predominantly during floods associated with moderate and big storms, which are infrequent due to the semi-arid, Mediterranean-type climate. Sediment delivery to the mainstem is likely to be highest during big storms that follow fires, due to enhanced runoff and erosion that result from post-fire hillslope processes.

Fluvial Sediment Transport and Morphological Change

Sediment transport processes in the Santa Clara River mainstem are dominated by extreme events associated with the river's highest flows. These events transfer water and sediment from the hillslopes to the estuary and near-shore waters, and are integral to changes in form of the mainstem Santa Clara River and its floodplain over time. Therefore, understanding the fluvial geomorphic processes in the Santa Clara River watershed is a necessary pre-cursor for understanding the restoration planning hazards and assets possessed by the lower river corridor.

It is possible to characterize the "dominant" or channel-forming flow of the Santa Clara River (the single flow that achieves the greatest volume of sediment transport over the long-term) as the largest flow on record. This contrasts with many alluvial rivers in more humid environments with less variable flow, in which the dominant discharge is usually of an intermediate magnitude that corresponds approximately to the 1.5-year recurrence interval, or "bankfull" flow. Discharge records for the lower Santa Clara River (LSCR) indicate nine flood events in excess of 2,800 m^3s^{-1} (100,000 cfs) since 1930, with a maximum recorded flood event of 4,670 m^3s^{-1} (165,000 cfs) in January 1969, and a larger but ungauged event associated with the collapse of the St. Francis Dam in March 1928. The largest natural flood events correspond very clearly to the high intensity rainfall years associated with the El Niño Southern Oscillation, and correlate strongly with events every 3–7 years as part of the recent wet period of the ENSO cycle since 1969. Fewer floods occurred in the dry period of 1944–1968.

The episodic and extreme nature of discharge in the Santa Clara River watershed results in the majority of total sediment transport occurring in very short periods of time. For example, over a 72-year period (1928–2000), 25% of the total sediment discharge for the Santa Clara River occurred in just four days. The implication is that the morphology of the Santa Clara River does not change progressively in response to small floods, but instead will experience significant episodic changes associated with much larger floods. Bedload sampling in low to moderate flows (maximum flow of 112 m^3s^{-1} [3,970 cfs]) has collected mostly

sand and fine gravel; bedload transport calculations suggest that significant transport of coarse gravel requires flows in excess of 850 m^3s^{-1} (30,000 cfs). Limited sampling of the channel bed in the period 1971–1984 indicates that dominant bed material particle sizes range from medium sand to very fine gravel in a range that encompass fine sand to coarse gravel.

A variety of channel-related infrastructure, channel modifications, and land use changes within the watershed have affected geomorphic processes in the LSCR since the arrival of European settlers. Infrastructure changes include dams constructed during the twentieth century, the failure of the St. Francis Dam in 1928, water diversions, and the construction of roads, bridges, and levees.

Dams are estimated to have reduced flow to the Santa Clara River by 26% and have reduced suspended sediment delivery by 21%. In the Santa Clara River, morphologic effects of dams may be greatest in the reach downstream of both Castaic and Piru creeks and presumably decreases near Fillmore following significant sediment contributions from the unregulated Sespe Creek watershed.

The St. Francis Dam break is thought to have created a flood flow with a magnitude of 14,000–23,000 m^3s^{-1} (500,000–800,000 cfs), that equates to a natural recurrence interval of 200–1,000 years. While it is conceivable that many of the large-scale characteristics of the LSCR and its floodplain are relicts of this flood, evidence is not readily apparent from 1927 and 1929 aerial photography. It is possible that, as the flood was derived solely from the San Francisquito Creek tributary, its total sediment load was lower than would have occurred from a flood event of comparable magnitude generated by rainfall in the Santa Clara River watershed. The primary role of the St. Francis Dam break, therefore, might have been extensive incision.

Water diversions associated with a dramatic increase in irrigated crop land in the early twentieth century may have led to the death both of riparian vegetation and vegetation thickets on the floodplain and gravel bars of the LSCR. At the same time, vegetation was being routinely cleared from riparian areas to open them for agricultural land uses. Such reduction in vegetation may have reduced the cohesion of river banks and lowered the threshold for the transport of significant quantities of channel bed sediment. Potentially, this could have caused the river to widen and transform from a meandering to a braided stream or, at least, to have become far more susceptible to change during large flood events.

Since construction of levees first began in the 1950s, there has been a progressive increase in the extent of bank protection in Ventura County to its current total of approximately 33% of the total bank length of the Santa Clara River. The levees act to confine high discharges and to significantly reduce the width of the LSCR during large flood events. Damage and local scour has occurred to levees themselves during repeat large flood events (*e.g.*, January and February 1969; January and February 2005) and, since levees also "train" the river planform in potentially unnatural alignments during flood events, flood flows can be reflected to cause erosion on an opposite, unprotected bank. Because levees confine flood flows in-channel, they both increase the chance of bed erosion during flood events, but can also promote extensive sediment deposition as the flood recedes. In the LSCR, the net effect of levees appears to have been to promote channel bed incision, or support such incision as initiated through instream aggregate mining.

The distinct impact of levees and bank protection on geomorphic processes in the LSCR is difficult to determine, due to the competing influence of direct and indirect channel modifications associated with extensive channel and floodplain aggregate mining. Aggregate mining is cited as the single largest anthropogenic factor in changing the channel form of the LSCR. Mining operations grew in size following the Second World War and, by the 1970s, attention began to focus on impact of the extensive

incision of the Santa Clara River attributed to the mining activities. Incision was threatening to undermine bridges across the river, to damage other infrastructure including the irrigation facilities of the United Water Conservation District (and which led directly to the construction of the Vern Freeman Diversion Dam, completed in 1991), and was reducing the replenishment of beach material at the mouth of the Santa Clara River. Following "red line" restrictions on the depth of permissible gravel mining, instream mining in Ventura County ceased by 1989. Several reports indicated that the mean yearly rate of aggregate extraction was removing sand and gravel from the channel bed faster than it was being replenished by upstream sources, resulting in a net increase in the cross-sectional area of the Santa Clara River channel. The average annual extraction rate in the period 1960–1977 (*i.e.*, before the peak of mining activity) was 1.71 million tonnes yr^{-1}, as compared to an estimated post-dam sand and gravel yield of 1.08 million tonnes yr^{-1} (1956–1975), although the highly intermittent nature of sediment transport in the Santa Clara River complicates such comparisons. In addition to direct sediment extraction, aggregate mining frequently results in channel incision due to the formation of knickpoints in the channel bed when the thalweg of the stream connects with mining pits during large flood events. This causes rapid incision of the channel bed independent of the mining activity and may also prolong the morphological legacy of aggregate mining. As evidence, instream mining in Ventura County ceased in 1989 but, apart from upstream of the Freeman Diversion Dam constructed in 1991, bed level recovery has not occurred despite that a sequence of significant flood events have occurred (1992, 1995, 1998, 2005) which has the opportunity to transport in large quantities of sediment.

Land use changes that have potentially impacted the fluvial geomorphology of the LSCR include the introduction of ranching (and exotic grass species) following European colonization of the watershed in the mid-1800s and, more recently, the ten-fold growth in watershed population that has occurred since the 1940s to a current total of approximately 314,000 people. Much of the associated urban growth has occurred along the mainstem river corridor. Increase in the urban extent is frequently associated with a suite of changes to watershed hydrology and geomorphology, focused particularly in the increased frequency of moderate flood events, and ultimately causing progressive channel incision and enlargement. Potential short-term urban impacts in the Santa Clara River is less clear because geomorphic activity in the watershed is concentrated into very large magnitude flood events rather than the intermediate events that are the focus of many studies. Second, urban expansion is currently focused in the upper watershed and may have less impact in the lower watershed due to the influence of incoming tributaries (especially Sespe Creek) on the flow and sediment regimes of the lower river. In the longer-term, sediment transport research in the neighboring Santa Ana watershed (population now 6 million from 1 million in 1955) has indicated an increase in runoff and a dilution of suspended sediment concentrations which is leading to enhanced bank and bed erosion. This result is consistent with a large body of research into the geomorphic impact of urbanization, and may have implications for the future of the Santa Clara River watershed.

The LSCR flows for approximately 61 km through Ventura County with an average gradient of 0.0041. The channel morphology is of a compound type with a mixed load of sand and gravel. At low flows, the channel usually consists of a dominant low-flow channel and several secondary braids depending, in part, on whether individual reaches gain or lose baseflows according to subsurface bedrock controls. Conversely, in response to high-intensity rainfall events, the LSCR inundates the majority of its floodway and functions as a single-thread, low-sinuosity channel. The LSCR was sub-divided into 11 reaches (numbered upstream from the mouth) based on downstream changes in setting, flow regime, and human influences. Reach estimates of unit stream power—a measure of the river's ability to transport sediment—do not indicate a reduction in stream power downstream, as might be expected, but instead indicate increases, first, that follow the large step increase in discharge downstream of the Sespe Creek

confluence and, second, where channel width is confined by levees. Consequently, the downstream-most reaches (1-4) have the highest potential for change.

The active width of channel bed of the LSCR has, on average, become narrower by almost 50% from 1938-2005 (from 483 to 252 m) and, over large stretches, the expected correlation in a semi-arid river between active width and magnitude of the last flood event has diminished over time. In general, the lowermost reaches (1-4) have narrowed to the greatest extent due to the construction of bank-edge levees. The middle reaches (5-7) are the most changeable in response to flood events largely because they have not been subject to such extensive confinement by levees. Upstream reaches (8-10) have also become narrower over time, possibly due to flow reductions caused by upstream regulation. Channel profile data, including a recent (2005) LiDAR survey, indicate that the LSCR has incised on average by 0.7 m from 1949–2005. Incision is focused in the lower parts of the river, where the maximum single-station incision is 7.65 m (just downstream of the Freeman Diversion Dam), and the average incision in Reaches 1-4 is 2.4 m. There has been very little long-term incision in Reaches 5-6, and there is moderate aggradation in the upstream reaches (7-10) averaging 0.65 m (maximum single-station aggradation of 3.1 m) such that over the period of record, the gradient of the LSCR has increased slightly from 0.0040 to 0.0041. Since the construction of the Freeman Diversion Dam in 1991, significant bed level recovery has occurred in Reaches 3 and 4, upstream of the dam, whereas further incision has occurred locally in Reach 2 just downstream of the dam, and in Reach 1. Overall, due to aggregate mining and levee construction, Reaches 1-4 are confined reaches that are highly efficient at sediment transport and have incised over the period of period. Reaches 5 and 6 appear the least impacted by human activity and are the most similar in form to their 1930 channel morphology. Reaches 7-11 appear to have both narrowed and aggraded over the period of record, possibly in consequence to some combination of flow regulation and high upstream sediment supply. Episodic factors in high upstream sediment supply might include sediment pulses resulting from landslides or wildfires, or construction-related sediment released following urban development.

A sediment budget for the LSCR was constructed for ten large flood events using sediment records from gauging stations. Sediment inputs were estimated from the upper Santa Clara River (at the Ventura-Los Angeles County line), and at the major tributaries of Hopper Creek, Sespe Creek and Santa Paula Creek (scaled from Sespe Creek records). Sediment output was estimated from near the mouth of the LSCR at Montalvo. With the exception of the flood on February 10, 1978, all other floods are predicted to have results in net sediment loss. The February 1978 flood was distinctive in terms of the high magnitude and sustained duration of flood from Sespe Creek, indicating that the morphology of the LSCR will respond differently in individual flood events according to the balance of flows between Sespe Creek and the upper watershed. The result implies that there has been net incision of the LSCR over the period of record, in agreement with records of bed elevation changes. However, the volume of sediment lost through fluvial processes in large floods equates to an average decrease in bed elevation of 0.12 m, whereas records indicate average incision of 0.7 m. This difference can be resolved by adding a component into the sediment budget that accounts for the sediment directly extracted from the channel through aggregate mining.

Building on earlier analyses, and the results of the sediment budget studies and investigations into morphological changes, a six-factor conceptual model of fluvial geomorphic processes for the LSCR was developed to indicate whether individual large magnitude flood events are likely to result in net aggradation or incision in the lower river. Such information is an important pre-cursor to understanding the likely management challenges to face the Santa Clara River Parkway area. The model illustrates a potential difference in river behavior depending on the relative magnitude and duration of flood events

from the upper Santa Clara watershed and from the largest tributary, Sespe Creek. Where the flood magnitude and duration generated by Sespe Creek is relatively large (*i.e.,* rainfall is concentrated in the north of the watershed rather than the east), the apparent net result is aggradation of the LSCR. When the flood events are of relatively similar magnitude and duration, or generated primarily be rainfall in the upper Santa Clara watershed, a net export of sediment transport occurs, leading to channel incision. Morphologically, this simple conceptualization is insufficient to account for observed changes in channel bed width and elevation in the LSCR over the last 50-60 years. For this, it is necessary to accommodate the sediment mined directly from the channel. Also, it is apparent that during individual flood events, the potential for morphological change is greater if the antecedent period has been wet, and may depend also on sediment supply variations resulting from factors such as large-scale wildfire and landslide activity that are not accommodated in current sediment rating curves. Local flood impacts will also depend on the specific suite of contemporary and historical human activities as they have affected the morphology of individual reaches.

Estuarine and Coastal Processes

The Santa Clara River Estuary, lying along the axis of the Oak Ridge Fault, ranges in elevation from approximately +0.30 m (+1.0 ft) Mean Sea Level (MSL) to approximately +2.4 m (+8.0 ft) MSL, although the majority of the area of potential inundation (0.42 km^2 [105 ac]) is between +1.22 m and +1.52 m MSL (+4 ft and +5 ft MSL). Tides are mixed semidiurnal with a mean tidal range of 1.13 m (3.71 ft) and relatively small storm-induced tidal elevations compared to the tidal fluctuation. Waves averaging 1 m in height (range 0.3–7 m) generally approach from due west and are commonly of mixed plunge-spill breaker type. When river discharge is low, sediment moved onshore by wave action forms a barrier that closes the mouth of the Santa Clara River. During the summer and fall months, average daily effluent discharge form the City of San Buenaventura Water Reclamation Facility greatly exceeds river discharge and can cause the sand barrier at the river mouth to breach when it would not under natural conditions. Sediments in the estuary are characterized by highly stratified layers of coarse sand and silt deposited following flood events and due to river and ocean water mixing, although cobble and even boulder-sized sediment have been observed traveling into the estuary during large flood events. Gravel material is generally common only in the upper estuary and, seasonally, coarser material is more likely to be exposed in the spring following winter storms, than in the fall.

Sedimentation dynamics in the estuary and mouth of the Santa Clara River are driven both by fluvial and littoral sediment transport processes. Fluvial sediment discharge occurs primarily during high magnitude, low recurrence interval storm events, although it is possible that the river currently discharges 25% less sand and gravel at the mouth than prior to dam building and instream aggregate mining. The high discharge events can produce hyperpycnal flow whereby river discharge is denser than ocean water due to extremely high suspended sediment concentrations: it is possible that up to 75% of the sediment delivered by the Santa Clara River between 1950 and 1999 was delivered under hyperpycnal conditions. The importance of this condition is that the density and velocity of the hyperpycnal flows can cause suspended sediment to essentially pass through the estuary and be deposited directly on the offshore delta, which is at its greatest volume following storm events. A substantial amount of sediment discharged from the Santa Clara River is ultimately transported down-coast via longshore transport as part of the Santa Barbara Littoral Cell: the Santa Clara River may be responsible for delivering approximately 65% of the sediment to this cell. Historical surveys of the coastline indicate net accretion of the Santa Clara River mouth of approximately 274 m (900 ft) from 1855 to 1987, although shoreline accretion is predominantly the result of large flood events, and retreat can occur when there are long periods between large storm events.

Periodic closure of the river mouth occurs during summer months when low intensity wave action combines with low rates of longshore transport and low river discharge to facilitate onshore sediment transport and deposition. The mouth re-opens during winter months when higher tidal ranges, wave action and river discharge combine. The closure dynamics, in turn, influence sedimentation, salinity gradient, vegetation dynamics, and fish migration. From 1984 to 1997 the river mouth was open approximately 71% of the time, with the highest daily frequency of opening occurring in March, and the lowest in August. Long periods of opening coincided with large winter river discharges resulting from El-Niño conditions. Detailed observations of river mouth closure and re-opening confirm that mouth closure occurs when tidal activity dominates over river flows, and conclude that mechanisms shown to be important in mediating barrier closure and morphology include onshore migration of shore-parallel bars and longshore migration and eventual closure of the lagoon outlet.

Agricultural encroachment and development within the historical estuary footprint have contributed to an approximate 75% decrease in estuary extent over the past 150 years. Following from a detailed study in 1990, overlays of the 1993 and 2002 aerial photographs indicated that the shoreline and river mouth migrated to the south following the 1993 flood (compared to conditions in 1969) and that the estuary "channel" had begun to erode towards the north, while the mouth advanced to the south by 2002. Significant changes to the river mouth occurred following the 2005 floods.

Building on existing studies, a conceptual model of the geomorphic dynamics of the Santa Clara River estuary was developed. In general, it was concluded that storm-induced flows within the Santa Clara River maintain a river mouth and estuary in a fixed location on the Oxnard Plain in comparison with historical conditions (due to levees currently in place in the lower river), will migrate within the current active channel extent (*i.e.*, between levees) during high discharge events, and will supply sediment for mouth closure (near-shore deposition) and down-coast beach building (near-shore and offshore deposition). Although sediment loading to the Santa Clara River mouth is reduced compared with historical levels, hyperpycnal events occur with enough frequency to maintain the mouth/estuary and supply the offshore delta with sediment for longshore transport and down-coast deposition. Furthermore, anthropogenic encroachment does not offset the effects of hyperpycnal events enough to conclude that the mouth will not be self-maintaining.

Synthesis

A synthesis is proposed, centered on estuary, fluvial and hillslope conceptual models of geomorphic functioning. Reach-level sediment transport models for the lower Santa Clara River from the 1980s should be re-evaluated in light of subsequent flood events and accommodate differences in flood magnitudes between the tributaries. Cessation of mining means that more significant mainstem aggradation may now occur than thought possible in the mining era, but new channel surveys are required as a basis for further analyses. Investigations should also consider whether aggradation might cause levees to fail through overtopping and breaching rather than toe erosion in times of channel incision. Another consideration is whether flow confinement has increased the frequency of hyperpycnal flows at the river mouth, as floods are no longer able to spread out and deposit sediment over the Oxnard Plain. Processes in the lower Santa Clara River are also intimately conditioned by sediment supply characteristics that depend upon rates and processes of hillslope sediment production and delivery to the mainstem. Sediment supply rates to the lower Santa Clara River are high as a consequence of geological and climatic factors, but are also conditioned by significant episodic events such as landslides, earthquakes and fires. The Northridge earthquake of 1994, and the widespread fires of 2003 may still be

exerting an influence on sediment supply. Other potential influences on sediment supply and transport include flow regulation by large dams and flow diversions, the failure of the St. Francis dam, the legacy of aggregate mining, bank protection by levees, and the effects of urban growth. A series of data gaps are identified as the basis for a better understanding of the dynamics of the Santa Clara River and its estuary.

2 INTRODUCTION

Geomorphology is the study of landforms and the processes that modify them over time, encompassing spatial and temporal scales that range from the instantaneous motion of individual sand grains in rivers during floods to the uplift of entire mountain ranges over millions of years. It synthesizes information about the internal geologic processes that create topography and the external surface processes that erode and move material incrementally across the landscape.

This report investigates geomorphic processes within the Santa Clara River watershed, located in Ventura and Los Angeles Counties, California (Figure 2-1). This assessment has been guided by an unusually extensive set of previous studies of geomorphic processes in the watershed and vicinity. Hence, the report provides a synthesis and interpretation of previous work, while adding new interpretation and data wherever possible, and focuses primarily on the lower mainstem Santa Clara River.

This assessment was conducted in support of the Santa Clara River Parkway Floodplain Restoration Feasibility Study (Feasibility Study). The Feasibility Study is designed to assist the California Coastal Conservancy and its partners with the development of strategies for restoring floodplain lands within the lower Santa Clara River corridor. The primary study area (Parkway area) is a 40 km (25 mi) long reach within the lower mainstem Santa Clara River, from the river mouth to the Sespe Creek confluence and the

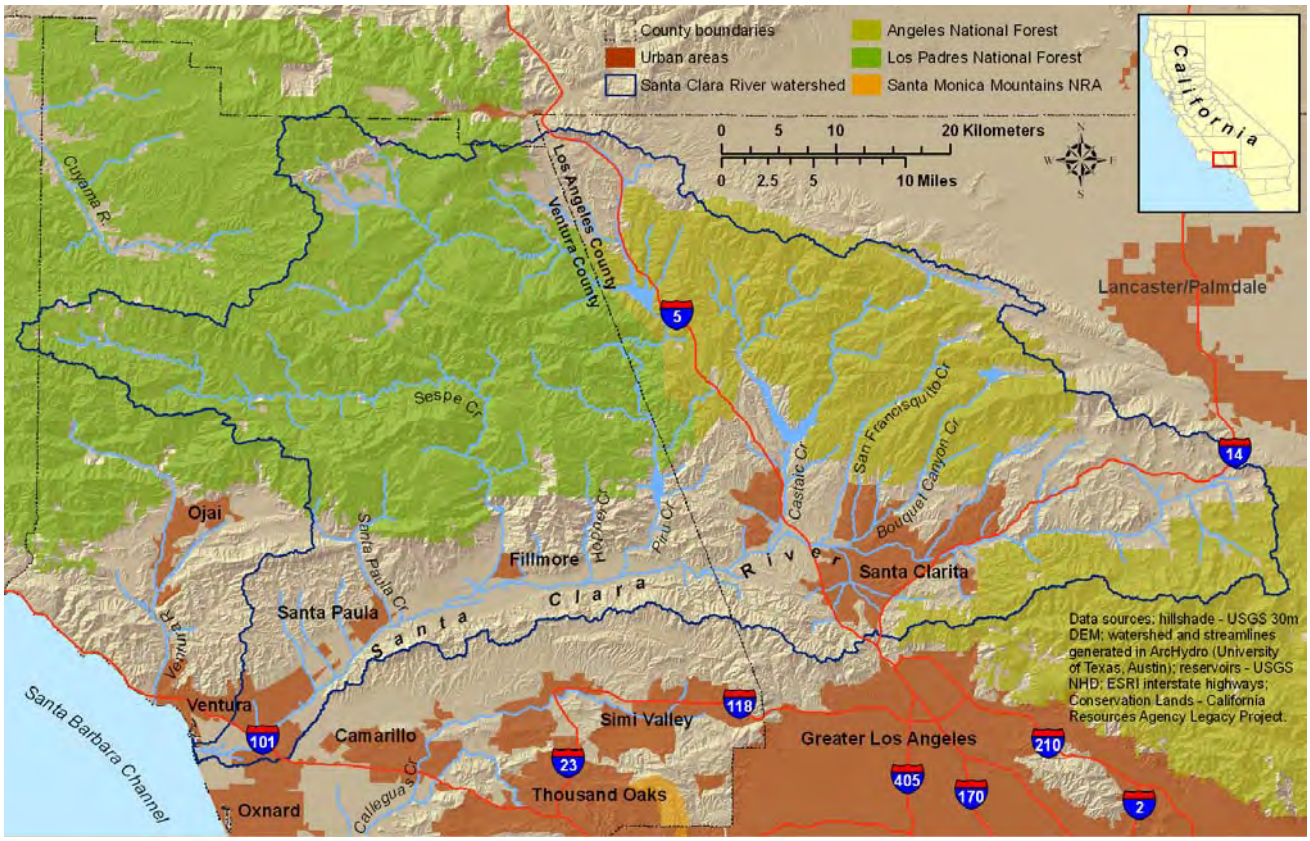

Figure 2-1. Santa Clara River watershed and vicinity.

floodplain areas adjacent to the reach. The initial phase of the Feasibility Study (which includes this report) will provide a synthesis and understanding of physical processes, habitat dynamics, and biological attributes within the corridor. In its second phase, the study will link physical processes to habitat dynamics for a discrete set of focal species, develop a desired future condition concept for the Parkway, and provide an assessment of restoration feasibility given existing constraints. Ultimately, the study will outline a recommended set of specific restoration strategies for the Parkway area.

2.1 A Geomorphic Process-based Context for Restoration Planning

Developing an understanding of physical processes and habitat dynamics of the Santa Clara River system and their effects on the Parkway area requires a detailed knowledge of the geomorphic processes operating within the watershed from the headwaters to the estuary. This information is critical in planning for management and restoration of the river corridor. Central to such planning efforts is the development of a vision for the desired future condition of the river corridor; that is, *how do you **want** the ecosystem to function?* As background for making this decision, it is necessary to understand *how the ecosystem functioned **historically**, how the ecosystem functions **now***, and, critically, *how did the changes in ecosystem function occur*? This is the essence of process-based restoration planning. Without understanding how changes occurred, restoration planning becomes an exercise in "hoping for the best" (*i.e.*, "build it and they will come").

To assess the geomorphology of the Santa Clara River watershed, Stillwater Sciences has examined geomorphic processes acting on hillslopes, within the mainstem and larger tributaries of the Santa Clara River (fluvial geomorphology), and within the Santa Clara River estuary. To address the critical questions of historical geomorphic process function and change, this study examines the watershed geomorphology under present-day and historical conditions.

The overall goal of the geomorphic assessment is to:

- provide a synthesis of existing and newly collected data to better describe the existing watershed sediment transport and deposition dynamics under existing conditions, and
- support the development of restoration strategies that consider and integrate geomorphic processes in order to sustain desired ecologic function throughout the watershed.

2.2 Regional Setting

Flowing 186 km (116 mi) from the northwestern San Gabriel Mountains to the coast, the Santa Clara River drains approximately 4,212 km^2 (1,626 mi^2)—one of the largest watersheds on the southern California coast (Figure 2-3). Elevations range from sea level to 2,692 m (8,832 ft) in the watershed (Figure 2-2). The Santa Clara River is relatively pristine in comparison with other large, coastal southern California rivers. For example, on the Los Angeles, Santa Ana, and San Gabriel rivers, flood protection and urban development modifications have been so extensive that natural physical processes have become largely ineffective at maintaining aquatic and riparian habitat.

In contrast, the Santa Clara River retains many of the natural attributes of coastal southern California rivers, including a sand-bedded, braided channel, broad floodplain terraces, and a large coastal estuarine complex—despite impacts of urbanization, agriculture, and flood control and water resources infrastructure development. The Santa Clara River and its tributaries experience high annual flow variability, multi-year droughts, and extreme seasonal flooding, which together result in a complex matrix of aquatic and riparian habitats that support a number of endangered and threatened species,

Figure 2-3. Major coastal southern California watersheds.

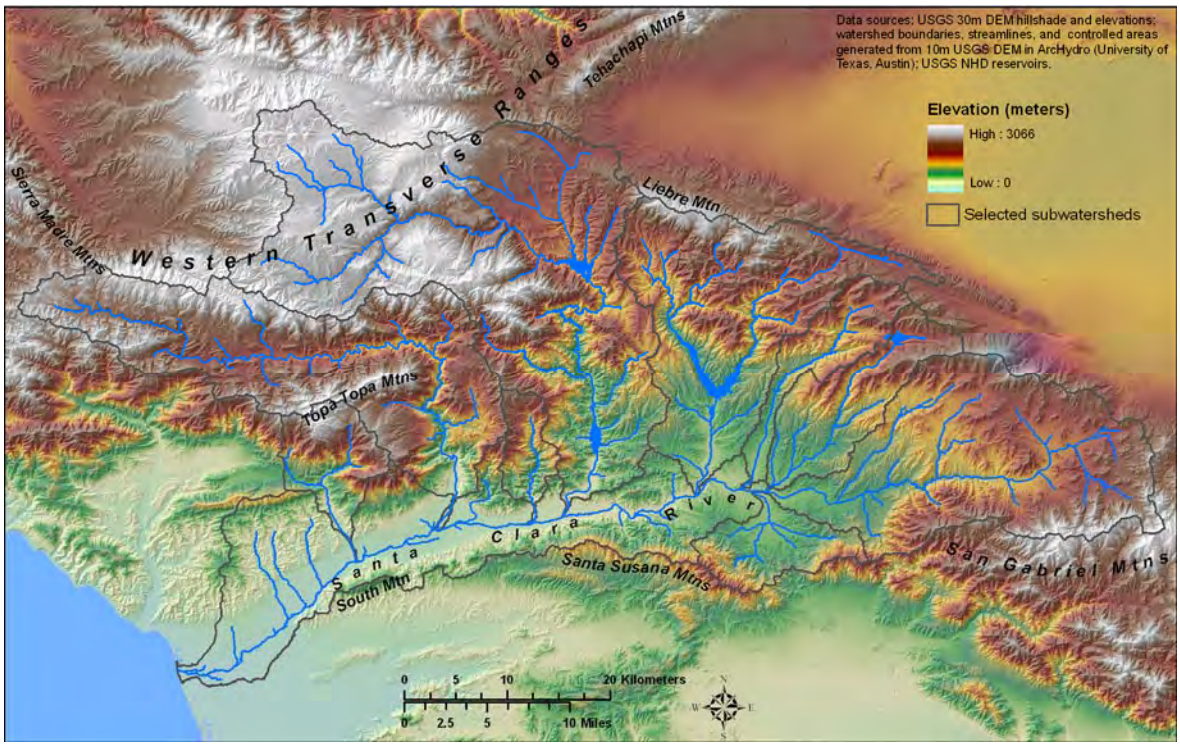

Figure 2-2. Mountain ranges and elevations in the Santa Clara River watershed and vicinity.

including tidewater goby (*Eucyclobius newberryi*), California red-legged frog (*Rana aurora draytonii*), arroyo toad (*Bufo microscaphus californicus*), southwestern willow flycatcher (*Empidonax trailii extimus*), least Bell's vireo (*Vireo bellii pusillus*), slender-horned spineflower (*Dodecahema leptoceras*), and a remnant run of federally endangered southern steelhead (*Oncorhynchus mykiss*). The run is much reduced from pre-1950s levels estimated to have been on the order of 7,000 to 9,000 adults, making the watershed a focus for regional steelhead recovery efforts (Titus *et al., in press*).

2.2.1 Geology

The Santa Clara River watershed is located within a geologically active area, within the San Andreas Fault system, which forms the dynamic boundary between the Pacific and North America tectonic plates. Relative motion of the plates includes strike-slip displacement (along the trend of the fault zone) and convergence (acting perpendicular to the fault zone). Convergence along the boundary has led to rapid uplift in coastal and interior mountain ranges throughout the region (Orme, 1998; Duvall *et al.*, 2004; Blythe *et al.*, 2000).

Persistent regional geologic instability since about 28 million years ago (Ma) has exposed a wide variety of highly deformed, fractured, and faulted rock types in the Santa Clara River watershed (Yeats, 1981; Rockwell *et al.*, 1984; Rockwell, 1988). Igneous and metamorphic rocks, including gneiss, schist, and granite, dominate in the upper watershed to the east, while younger sedimentary and volcanic rocks are more prevalent in the lower watershed, west of the San Gabriel Fault (Figure 2-4). Fractures, deformation, and faulting contribute to high bedrock erodiblity throughout the watershed. For example, the sedimentary bedrock along the mainstem valley flanks is often poorly consolidated, intensely folded, and has steeply tilted beds, making it susceptible to landsliding (*e.g.*, Harp and Jibson, 1996) and erosion by dry raveling (Scott and Williams, 1978). Even areas underlain by granite, gneiss, and schist (which are

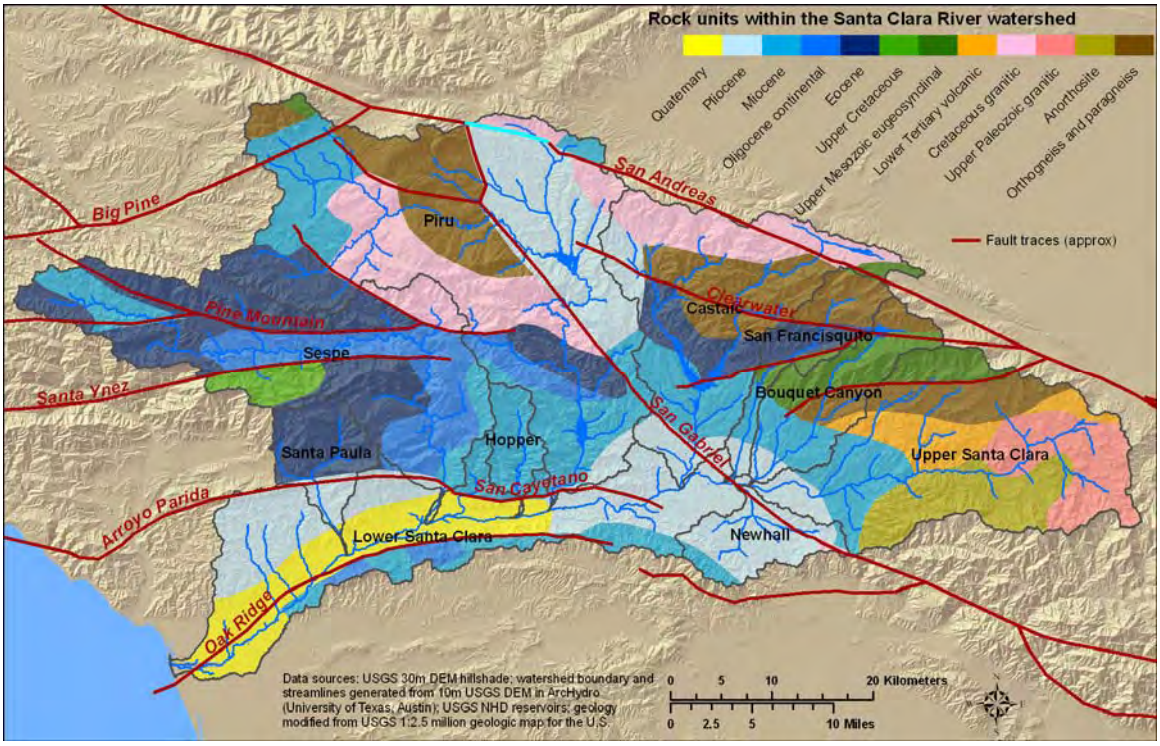

Figure 2-4. Generalized geologic map showing major rock units and fault traces in the Santa Clara River watershed.

normally thought to be relatively resistant to erosion) have been described as being highly erodible (*e.g.*, Scott and Williams, 1978; Wells *et al.*, 1987), due to extensive deformation and fracturing. The position of unchanneled valleys, creeks, and the Santa Clara River itself are strongly influenced by geologic structure and the location of active faults. Below its confluence with Sespe Creek, the river roughly follows the axis of a west-trending synclinal valley, which is bounded by active strands of the San Cayetano Fault (Rockwell, 1988) to the north and the Oak Ridge Fault (Azor *et al.*, 2002) to the south.

Intense seismic activity in the region is reflected in frequent ruptures along faults. Seven of the roughly 30 high-magnitude ($M_W \geq 6$) earthquakes that have shaken southern California over the past 80 years have occurred in the Transverse Ranges (numbers updated from Rockwell, 1988). Seismic shaking during the magnitude 6.7 Northridge event in 1994 triggered nearly 7,400 landslides in the watershed (Harp and Jibson, 1996; see further discussion in Section 4), highlighting the importance of geologic factors in the production of sediment, which ultimately affects geomorphic processes in the lower river corridor. A more detailed, technical description of geology and tectonics in the watershed and region is presented in Appendix A.

2.2.2 Climate and Hydrology

Coastal watersheds of southern California function according to a semi-arid, two-season Mediterranean-type climate, with cool wet winters and dry warm-to-hot summers. Within the Santa Clara River watershed, proximity to the Pacific Ocean moderates both seasonal and diurnal temperatures. Air moisture is greatest at the coast and decreases to near-desert conditions towards the eastern watershed boundary. Most precipitation occurs between November and March, with rainfall intensities varying significantly throughout the watershed due to complex topographic features. For example, average annual rainfall is more than 860 mm (34 in) in the mountainous headwaters of Sespe Creek, while only about 200 mm (8 in) in the drier eastern portions of the watershed near the Mojave Desert (Figure 2-5) (PWA, 2003).

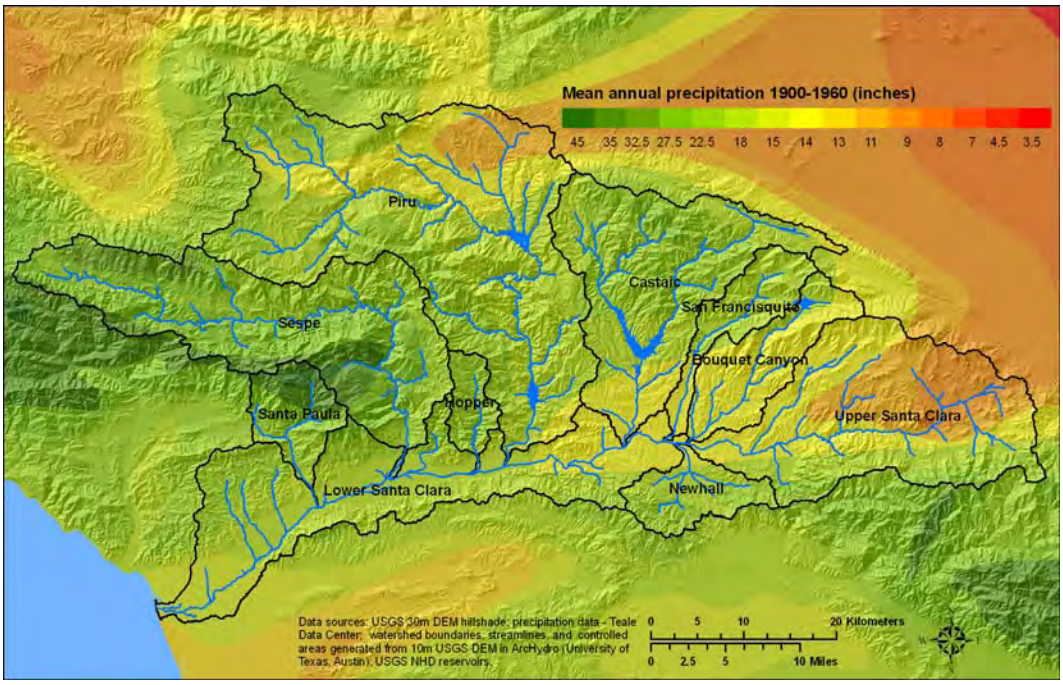

Figure 2-5. Distribution of mean annual precipitation based on data from the period 1900-1960.

The climatic and hydrologic characteristics of the watershed generally produce an intermittent flow regime in the mainstem Santa Clara River. Consistent with other rivers in the region, the Santa Clara River watershed experiences highly variable annual rainfall and peak flows. During the rainy season, flows can increase, peak, and subside rapidly in response to high intensity rainfall (the term "flashy" is commonly used to describe this characteristic), with the potential for severe flooding under saturated or near-saturated watershed conditions. Between winter rainfall events in wet years, the river may exhibit continuous baseflow to the ocean from residual watershed discharge; in dry years, flow may be intermittent.

During the dry summer season, flows in the mainstem are intermittent or non-existent, depending primarily on areas of rising groundwater or inflows from dam releases or other anthropogenic sources. Groundwater discharges to the mainstem Santa Clara River occur when groundwater levels are high and the water table is close to the surface. In the lower Santa Clara River, two geologic features are important to surface water-groundwater interactions on the mainstem – the Piru and Fillmore narrows. In these locations, constrictions in the width of unconsolidated deposits, combined with subsurface bedrock controls cause groundwater to rise and discharge to the Santa Clara River, depending on groundwater levels and surface flow conditions (URS, 2005). In areas away from the bedrock controls, surface flow is lost through the highly permeable bed materials to groundwater. Generally, flows in the river are relatively small–75% of the time flows are less than 4.2 m^3s^{-1} (150 cfs) at Montalvo and 50% of the time flows are less than 0.3 m^3s^{-1} (10 cfs) (URS, 2005). However, large peak flows associated with winter storm events cause flows to exceed 2,832 m^3s^{-1} (100,000 cfs) once every 10 years on average (URS, 2005). Major tributaries of the Santa Clara River include Santa Paula, Sespe, Hopper, Piru, Castaic, San Francisquito,

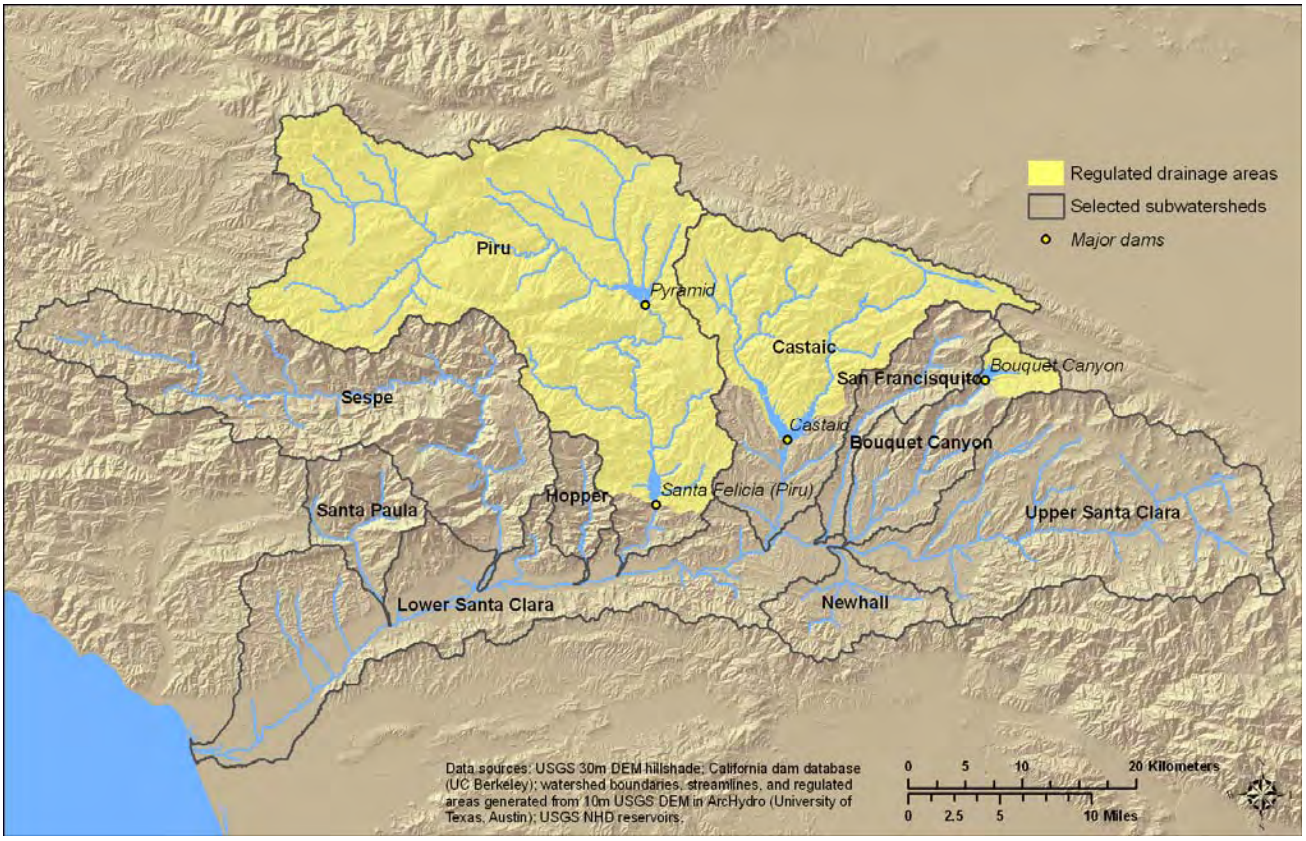

Figure 2-6. Areas within the Santa Clara River watershed regulated by major dams.

and Bouquet Canyon creeks (Figure 2-1). Other tributaries, including numerous *barrancas* (small, generally incised tributary streams) and unnamed ephemeral creeks empty into the mainstem river along its course. More than one-third of the watershed area lies upstream of dams and debris basins that regulate water and/or sediment discharge to the lower river corridor. Major dams include Santa Felicia Dam on Piru Creek and Castaic Dam on Castaic Creek (Figure 2-6 and Table 2-1). Throughout the year, controlled releases of water from Piru Reservoir supplement surface flows in the river reach in Ventura County. Additional flow is supplied from water reclamation plant discharges and imported water runoff in the middle reach from the vicinity of Santa Clarita in Los Angeles County down to the Ventura County line.

Table 2-1. Major tributaries of the Santa Clara River including areas regulated by dams.

Tributary Name	Drainage Area (km^2) [a]		Drainage Area (mi^2) [a]		Dams
	Total	Regulated[b]	Total	Regulated[b]	
Bouquet Canyon Creek	187	34	72	13	Bouquet Canyon
Castaic Creek	526	397	203	153	Castaic Dam
Hopper Creek	62	0	24	0	
Lower Santa Clara River	647	37	250	13	Debris Basins[c]
Newhall Creek	117	0	45	0	
Piru Creek	1,134	1,095	438	423	Santa Felicia
San Francisquito Creek	129	0	50	0	
Santa Paula Creek	117	0	45	0	
Sespe Creek	674	0	260	0	
Upper Santa Clara River	619	0	239	0	
Total	4,212	1,526	1,626	590	

a Areas calculated from 10 m USGS DEM using ArcHydro.
b Regulated areas are areas upstream of dams, which impound sediment and water
c Debris basins do not impound water, and only impound the coarse fraction of the sediment load to the limit of their capacity (*e.g.*, Warrick, 2002).

2.2.3 Land Use/Land Cover

The Santa Clara River watershed remains relatively undeveloped when compared with many of the coastal watersheds to the south (Figure 2-3). Large expanses of the mountainous northern portions of the watershed are part of the Angeles and Los Padres National Forest (see Figure 2-1). Land cover in upland areas of the Santa Clara River watershed is dominated by scrub/shrub (chaparral) vegetation; grasslands and mixed, deciduous, and evergreen woodlands comprise the remainder of upland land cover. Along floodplain and valley bottom areas of the Santa Clara River Valley, orchard and row crop agriculture is the dominant land use, with significant urban areas in the upper (Santa Clarita) and lower (Ventura, Santa Paula, Fillmore, Oxnard) valley areas (Figure 2-7). In the lower Santa Clara River, below the confluence with Sespe Creek, agricultural and urban use account for 22% and 9% of land cover respectively (Warrick, 2002).

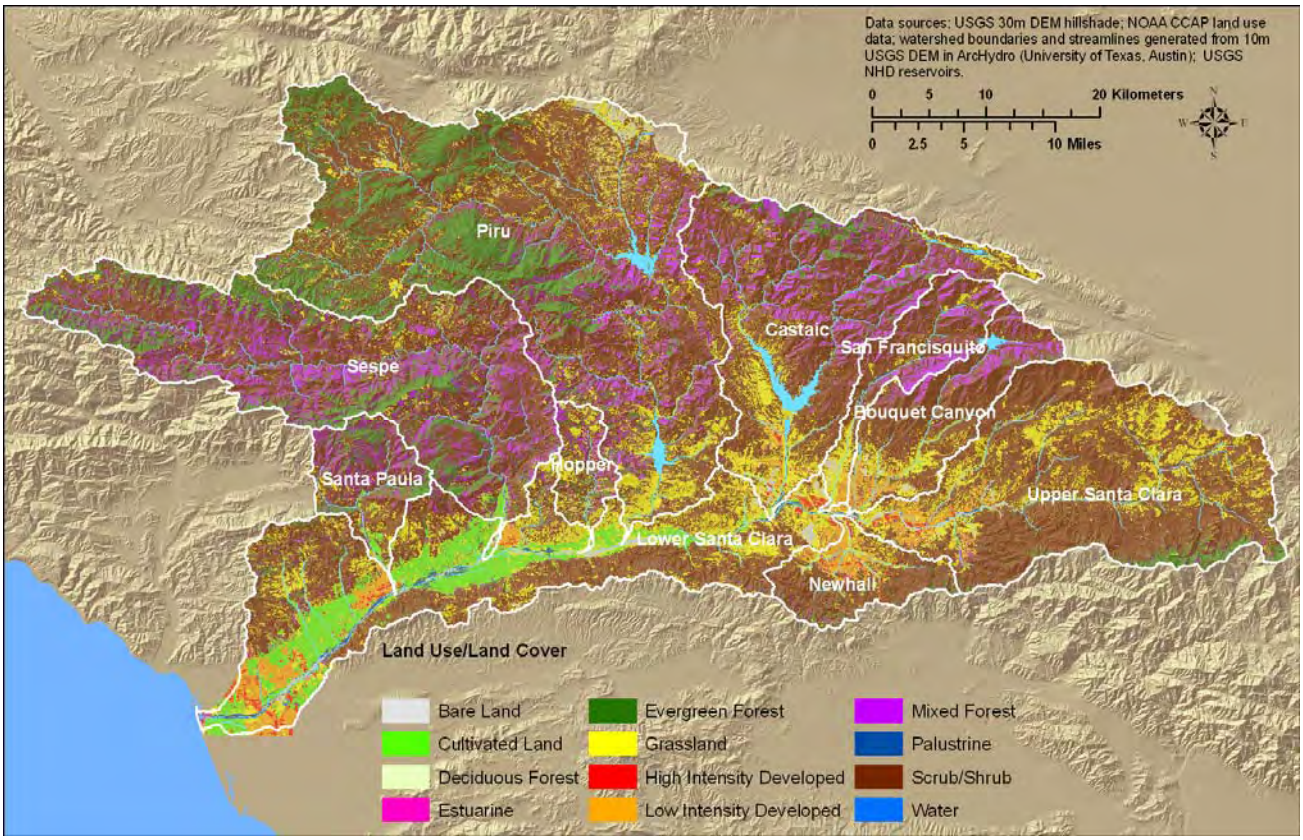

Figure 2-7. Land cover (2000) within the Santa Clara River watershed.

3 IMPACTS OF HISTORICAL WATERSHED CHANGES ON GEOMORPHIC PROCESSES

A conceptual understanding of past periods is critical in determining '*how the ecosystem **used** to function'*, while '*how the ecosystem functions **now**'* is derived from an understanding of present conditions. The integration of historical information over time helps form the foundation for determining '*how did the changes in ecosystem function occur?'* Understanding each of these three elements makes it possible to hypothesize the potential future trajectory of channel conditions and thus help to guide sustainable corridor restoration strategies. Information extracted here is combined with specific understanding gained from hillslope processes, mainstem fluvial processes, and estuarine and coastal processes (Sections 4, 5, and 6, respectively) and synthesized in Section 7.

The history of land use changes and the evolution of water and river management practices within the Santa Clara River watershed have been comprehensively documented by Schwartzberg and Moore (1995) and AMEC (2004), who summarized Schwartzberg and Moore and added extensive updates on current conditions. URS (2005) also provided a concise summary of historical land use changes, sub-dividing the history of the watershed into distinct phases related to pre-European settlements (pre–1782), the Agrarian Era (1782–1870s), the Commercial Era (1870–1920), and the Industrial Era (1920–2000). In their analysis of historical steelhead populations, Boughten et al. (2006), describe the probable baseline conditions of southern California steelhead-bearing rivers prior to the 1894–1904 period when the first USGS maps were developed for the area. More selective details have been obtained from other reports (a list of source types is presented in Table 3-1). The historical details are not repeated here but instead distilled into a time chart of historical events that may have had an effect on water and sediment discharge in the watershed, and so have influenced geomorphic processes and channel morphological responses within the mainstem river corridor (Figure 3-1). The data in Figure 3-1 and Appendix B suggest that there may be five historical periods which, in large part, have probably altered the response of channel morphology to natural extremes in water and sediment discharge.

Note that due to the "flashy", flood event-dominated nature of the Santa Clara River watershed, geomorphologic response to human influences may not be progressive, but will more likely be episodic, with channel morphology responding primarily to larger flood events. Therefore, detecting the relative effects of various human impacts (*e.g.,* the "urban signal") on natural flood events and morphological response may be difficult. As an example, in humid watersheds, urbanization can affect channel morphology by increasing the occurrence of moderate flood events because of the increased extent of impermeable ground surfaces in urban areas which produce more runoff in a shorter amount of time in comparison to native land cover. In larger (*i.e.,* less frequent), flood events when natural ground surfaces are typically saturated and thus act as impermeable surfaces anyway, the effect of the urban surfaces is diminished. However, because the Santa Clara River watershed is large, and has a flood frequency dominated by large flood events (see Section 5.1), the effect of moderate magnitude events on channel morphology is likely to be less significant, while the effect of larger events must be disentangled from other geomorphic changes that occur during high flows.

Table 3-1. Indicative historical sources for the Santa Clara River watershed.

Data	Source	Dates	Notes
Plat maps	USDI BLM http://www.blm.gov/ca/forms/mtp/index.html	1850's to 1920's	Plat maps for the Santa Clara Valley indicate general location of the Santa Clara River. They do not include any attribute information, such as riparian vegetation extent, river channel width.
Aerial photography	UCSB, VCWPD, others	1927 to present	Coverage is sparse for 1927/28, better in 1938, full for numerous years afterward.
Miscellaneous ground-based photography	UCSB, Ventura Museum of History and Art	1900's and later	None of the photography found thus far indicates the condition of historical attributes of interest, namely riparian vegetation, river channel widths.
Textual accounts	Book: Vern Freeman. 1968. People-Land-Water: Santa Clara Valley and Oxnard Plain, Ventura County, California.	1800's and later	Excellent information on historical floods (including nice table of derived historical rainfall, pre-1900's), some useful quotes from historical sources. http://www.santaclarariverparkway.org/wkb/scrbiblio/freeman1968
Textual accounts	Report: Schwartzberg, BJ, and Moore, PA (1995). Santa Clara River Enhancement and Management Plan: A History of the Santa Clara River	1700's and later	Excellent summary of the history of the Santa Clara River Valley. Includes some accounts of the river's historical condition. http://www.santaclarariverparkway.org/wkb/scrbiblio/schwarzbergmoore1995
Panoramic ground-based imagery, post St. Francis Dam disaster	Ventura County Watershed Protection District	March 1928	Excellent panoramic photos of almost the entire length of the Santa Clara River from the county line to Montalvo.
Vegetation plot and map data	UC Berkeley Wieslander Vegetation Type Mapping	approx. 1900–1930	Website contains mapping from the early part of the 1900's for the Santa Clara River Valley. Mapping is illustrated on early 1900's USGS topos. http://vtm.berkeley.edu.

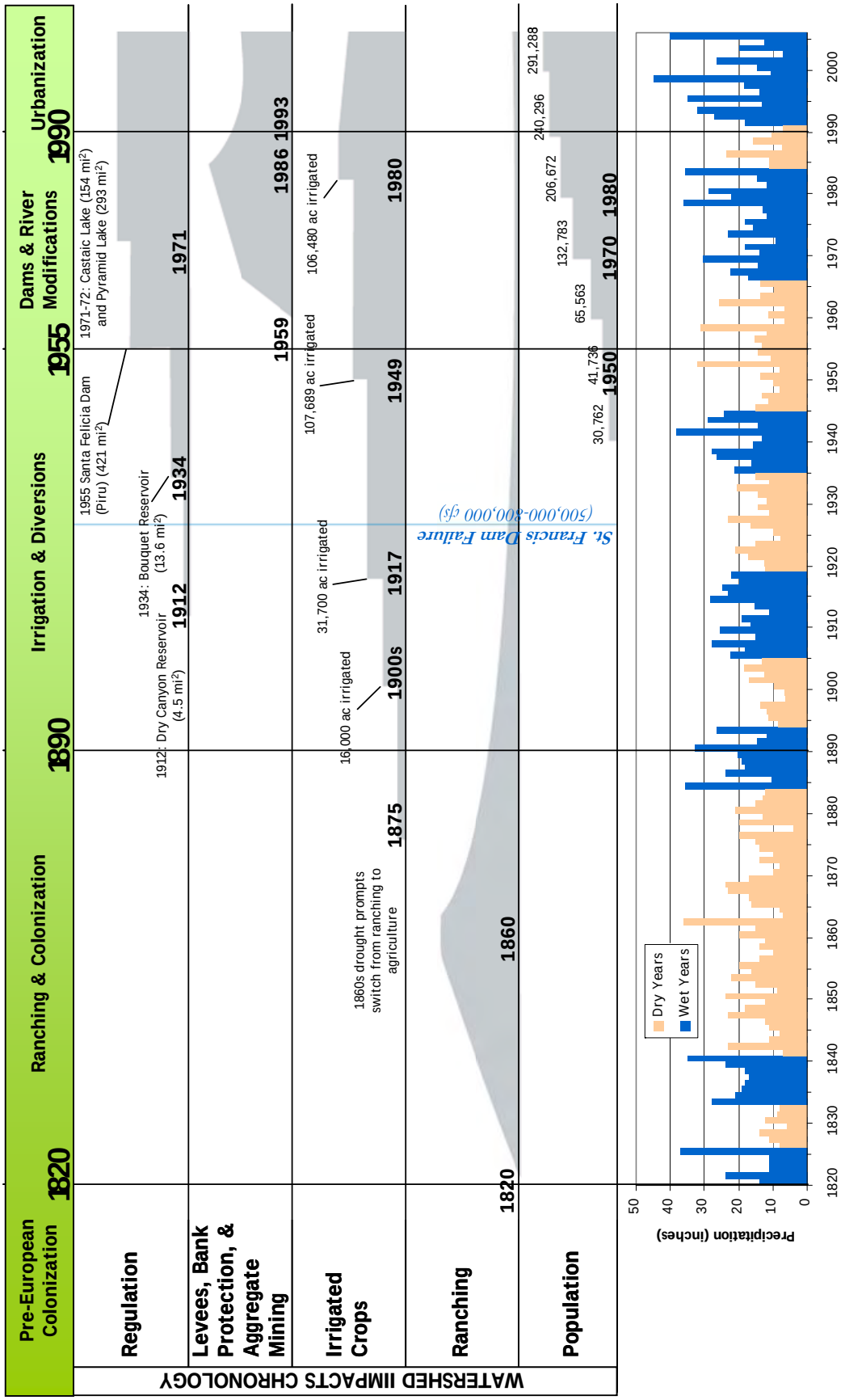

Figure 3-1. Chronology of potential watershed impacts and events. Precipitation records indicate periods of cumulatively wetter (blue) and drier periods in the watershed extended from a similar analysis by Freeman (1968). Most very wet years in the watershed are also years with large floods (see section 5.1.2).

In the period prior to widespread European ranching and colonization (approximately prior to 1820, following establishment of the first mission in 1782), the watershed is assumed to have been in a relatively undisturbed condition, responding only to fluctuating flood, drought, and fire sequences, with relatively minor impacts associated with the agricultural practices of the indigenous Chumash and Tataviam peoples. It is likely that the Santa Clara River experienced perennial stream flow in all reaches, a higher channel elevation, and supported a more-or-less continuous and broad riparian forest. There are historical reports that describe perennial stream flow for several southern California rivers, including the Santa Ana, Santa Margarita, and San Luis Rey, that are now intermittent largely as a result of water impoundment, diversion, and groundwater pumping (Boughten et al. 2006). In addition, it has been argued that the maintenance of grasslands by Native Americans increased water yield (in contrast to chaparral or sage-scrub habitats) and contributed to historical perennial stream flow dynamics (Keeley, 2002; as cited in Boughten et al. 2006). In the Los Angeles basin, perennial stream flow resulted in lower water temperatures and supported suites of aquatic species, such as redlegged frogs, threespine stickleback, freshwater lamprey, and freshwater shrimp, which are now found only in northern California (Mendenhall, 1908; McGlashan, 1930; Miller, 1961; all as cited in Boughten et al., 2006).

From the 1820s, the establishment of large-scale ranching activity is likely to have caused significant changes to rainfall-runoff relationships as deep-rooted native perennial grasses in the valleys and hillslopes were degraded and replaced by shallow-rooted, non-native annual grass species, which are less able to resist soil erosion. Drought in the 1860s caused a shift from traditional cattle grazing to sheep, potentially accelerating the removal of vegetation and subsequent erosion. The expansion of farming in the Santa Clara River valley during the 1870s probably further contributed to erosion and changes in runoff characteristics. Overall, it is likely that greater volumes of hillslope runoff were generated per unit rainfall as a result of land use change during this period, with far greater volumes of fine sediment production throughout the watershed and increased shallow landslide potential on the hillslopes. In the mainstem river corridor, Boughton et al. (2006) suggest that prior to publication of the first USGS maps in the late 1800's and early 1900's, many southern California river channels had already experienced significant incision as a result of vegetation clearing, ranching, and other land uses, as well as climatic events. Historical accounts describe the extensive effort undertaken to clear riparian forests throughout central and southern California watersheds (Gordan, 1996; as cited in Boughton et al., 2006). Floodplain forests were first cleared for fuel supply, then to prepare the land for grazing and farming, and finally to increase flood conveyance. These land uses and climatic events resulted in decreased stream bank stability and increased stream power allowing high flows to entrench the channel. Prior to incision, the Santa Clara River channel would have supported higher groundwater elevations and more frequent floodplain inundation under lower flows. These channel conditions would have facilitated the recruitment and establishment of large tracts of riparian vegetation. In addition, prior to incision and the increased supply of fine sediment that channel incision causes, rivers like the Santa Clara likely supported gravel and cobble substrates in the lower reaches (Boughton et al., 2006). These substrates would have provided suitable spawning habitat for fish species in a greater extent of the river, as well as providing habitat for benthic macroinvertebrates that fish prey upon, and would result in a quite different channel morphology from that seen today.

The period from the 1890s is characterized primarily by the expansion of water-intensive agriculture: first sugar beet and then citrus crops, which required large-scale irrigation (particularly following the First World War). In this period, irrigation using surface flow from the Santa Clara River was supplemented by pumped groundwater supplies. Following the formation of the Santa Clara River Protective Association (now United Water Conservation District) in 1925, diversions began first from Piru Creek (1930) and then Santa Paula Creek (1931). Irrigated acreage in Ventura County increased from 128.3 km^2

(31,700 ac) in 1919 to 435.9 km^2 (107,700 ac) in 1949. The likely impact was an initial reduction in baseflow within the Santa Clara River, and a subsequent lowering of the groundwater table due to pumping. Groundwater subsidence in particular may have led to further degradation of mature riparian vegetation (in areas where riparian vegetation was not replaced by orchards), which is reliant primarily on groundwater during the summer dry season. Large floodplain areas with extensive riparian vegetation may have attenuated floods within the Santa Clara River; the removal and degradation of large riparian stands would have therefore increased the "flashy" nature of the river to flood events. The removal of riparian vegetation would have also resulted in decreased complexity of floodplain habitat and increased river water temperature. Prior to disturbance, the riparian area likely supported dense, multi-stored stands of broadleaf trees, including cottonwood, sycamore, and various willows, that extended from a few to several miles wide (Boughton et al., 2006).

By 1912, the first dam in the watershed had been constructed in Dry Canyon, located in the eastern portion of the watershed (the dam was subsequently decommissioned due to leakage issues). In 1926, the St. Francis Dam was completed on San Francisquito Creek (also in the eastern watershed); however the dam failed catastrophically in March 1928, resulting in one of the largest and most tragic dam failures in United States history. The long term effects of the St. Francis Dam disaster on the morphology of the Santa Clara River are unknown, but are potentially significant and ongoing (see Section 5.2.1). From 1955, with the completion of the 61 m (200 ft) high Santa Felicia Dam on Piru Creek (regulating 1,090 km^2 [421 mi^2]) the watershed began to be subjected to an increasing amount of direct flow regulation and channel manipulation. Additional dams (see Section 5.2.1) resulted in regulation of approximately 34% of the watershed, reducing runoff to the lower watershed by approximately 26% (Warrick, 2002) and sediment discharge by approximately 21%. Further, the lower Santa Clara River floodplain and channel were increasingly modified, beginning in 1959 with the dredging of pilot channels, in 1961 with the construction of the extensive levee system from South Mountain to Highway 101 and, following the flood of 1969, construction of various additional levees, groins, and bank protection projects that continue to the present day.

Of great importance to the channel morphology, the pace of instream aggregate extraction, which began with small-scale operations in the early twentieth century, accelerated during the 1970s and 1980s and appears to coincide with increased rates of channel incision upstream of aggregate mining pits in this period. In 1986, the creation of the Ventura County 'red line', restricting the depth of instream aggregate extraction, marked the beginning of the decline in instream mining within the lower river. The construction of a permanent Vern-Freeman Diversion Dam in 1992 likely aided the stabilization of the mainstem river bed elevation and halted incision resulting from the aggregate mining operations. The geomorphic impact of such direct modifications to water and sediment discharge, and to the channel perimeter, is likely to have been significant but difficult to disentangle from the impact of previous watershed land use changes and natural flood events. For instance, it could be hypothesized that the reduction in sediment discharge caused by dam construction has acted to reverse some of the increase in sediment load that likely followed ranching and subsequent changes in upland vegetation. Clear water discharge from dams may have also led to channel incision, which could have been exacerbated by the existence of in-stream pits following aggregate extraction. Bank protection in the lower watershed may have changed instream flow patterns, deflecting erosional energy to new locations. Levees may also be increasing rates of channel incision by confining flood events to the floodway, rather than allowing overbank flooding to occur. These issues are explored further in this report.

If there is a more recent 'period' in the evolutionary history of the Santa Clara River, it is probably linked to the increasing rate of urban development in Los Angeles County and the progressive expansion of

urban areas in Ventura County into the area of the lower river corridor. The impact of the latter effect on flood response has been estimated by URS (2005) and is seen to markedly increase runoff in moderate flood events, although this is only a small proportion of the overall watershed runoff. It can be assumed that the effect in Los Angeles County is proportionately greater, although slightly attenuated by the distance of travel to the lower river and lower rainfall amounts in the eastern portion of the watershed. Increasingly, levee construction and bank protection are now linked to protecting urban communities in both counties, and so there is a potential impact of further constraining the river corridor. Such activity will clearly result if far greater flood losses as levees are breached or overtopped by flood events, but is also likely to result in increasing erosion in the mainstem river channel.

The remaining sections in this report serve to investigate further the geomorphic understanding of the lower Santa Clara River mainstem and estuary following almost two centuries of European colonization, land use changes and direct modification of water and sediment discharges and channel morphology in the watershed. It is important to note that, first, the periods outlined above are separated for convenience and that their impacts on the watershed are largely cumulative over time. Because the cumulative impact is difficult to quantify, this report requires the compilation of a large number of both quantitative and qualitative studies as the basis for a preliminary understanding of the evolutionary trajectory of the river channel. Second, sediment transport and morphological changes in the Santa Clara River occur only in brief periods during flood events, and especially when flood events follow large fires. As such, there is both a natural component to channel morphology changes and a confounding factor that human impacts in the watershed are actually expressed during natural events. This makes disentangling comprehensive human impacts from natural events one of the most challenging arenas in geomorphology.

It is has been suggested that, over a perspective of thousands of years, changes in channel morphology are "climatically driven but culturally blurred" (Macklin and Lewin, 1993) but it seems also likely that, during the last several hundred years, morphological change on the Santa Clara River may be interpreted as "climatically enacted but culturally prepared" (Downs and Gregory, 2004).

4 HILLSLOPE SEDIMENT PRODUCTION, TRANSPORT, AND DELIVERY

4.1 Overview of Uplift, Erosion, and Sediment Transport

Mountain shape and height reflect the interplay between uplift, due to tectonic processes, and the sculpting and wearing away of slopes by erosion. In general, high, steep mountains occur in areas that have been subjected to sustained, rapid uplift, whereas low, gently sloping mountains occur in areas where uplift is slow or has been followed by long periods of denudation. Steeper areas are generally thought to have higher erosion rates (*e.g.*, Ahnert, 1970), because erosion is typically more effective on steeper slopes and because steep slopes are prone to mass movement, which can enhance erosion. Hence, faster tectonic uplift rates are generally associated with steeper mountains and faster erosion rates. In general, the linkages between uplift, slope steepness, and erosion imply that slopes should tend to contribute sediment in proportion to their uplift rates over the long term.

Slopes in the Santa Clara River watershed are steep (Figure 4-1), with long-term uplift rates that are among the fastest on record for the continental United States (see discussion below). Erosion rates are likewise rapid, but are not so fast that soils are completely stripped from slopes.

Soils are produced by the physical and chemical breakdown of bedrock, which are caused by biotic processes (such as tree throw and animal burrowing) and abiotic processes (such as freeze-thaw, shear deformation, and the infiltration of water, which dissolves or alters minerals and leads to physical

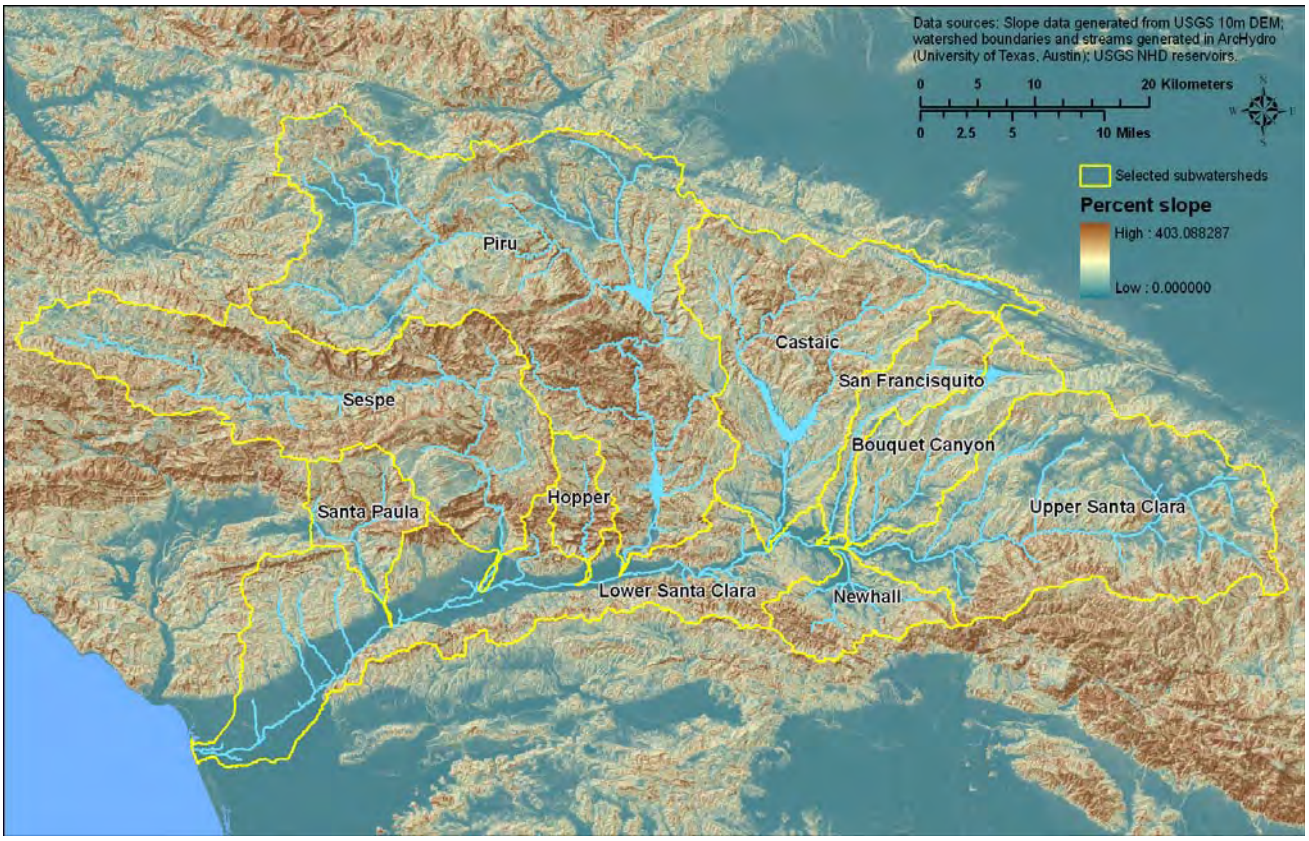

Figure 4-1. Slope distribution in the Santa Clara River watershed.

collapse of rock). Many soil production processes appear to decrease in effectiveness with increasing soil thickness (Gilbert, 1877), such that thinner soils tend to support faster soil production rates (Heimsath *et al.*, 1997).

Soil moves downslope toward channels and unchanneled valleys, transported incrementally by hillslope sediment transport processes, such as mass wasting, overland flow, and biogenic disturbances. These processes deliver sediment directly to channels from slopes, or bring it to unchanneled valleys, where it may first collect before being delivered to channels by channel-head erosion and landsliding. After entering channels, sediment is transported downstream by stream flow (*i.e.*, Newtonian viscous flow) or in concentrated (non-Newtonian) debris flows. Sediment transport by the Santa Clara River and its major tributaries is discussed in Section 5. Here the focus is on hillslope sediment production and transport.

4.2 Dominant Sediment Production and Transport Processes

4.2.1 Soil Creep

The transport of soil in the absence of running water is often referred to as soil creep—a slow, relatively continuous process that results from particle-by-particle displacement (Culling, 1963). Downslope movement by creep has been attributed to variations in soil moisture and temperature, freezing and thawing of soil water, and biological disturbances (Davis, 1892; Gilbert, 1909). Dry raveling (*i.e.,* the gravity-driven rolling, bouncing, and sliding of particles down slopes), rainsplash, and animal activity appear to be important contributors to soil creep in the Santa Clara River watershed.

Dry Ravel

In the Santa Clara River watershed, the lateral supply of sediment to channels is thought to be fairly continuous (Scott and Williams, 1978), with wet-season contributions from overland flow, landslides, and soil slumps, and dry-season contributions from dry ravel.

In general, dry raveling is thought to be important on steep, semi-arid slopes, most commonly in soils underlain by granitic rocks, coarse-grained sandstones and sheared shales, in areas that are tectonically active and undergoing rapid uplift (Scott and Williams, 1978; Wells, 1985). Hillslope soils within the Santa Clara River watershed are typically thin and coarse textured, with characteristically steep slopes that often exceed the angle of repose of the unconsolidated material. These conditions, along with the semi-arid, Mediterranean-type climate, make slopes especially prone to dry raveling. High rates of dry raveling have been documented in the San Gabriel Mountains (Anderson *et al.*, 1959; Krammes, 1960; Krammes and Rice, 1963; Krammes, 1965; Wells, 1981; Wells, 1985), which feed the Santa Clara River from the south; as much as half or more of the total sediment movement on slopes in the San Gabriel Mountains is accomplished by dry raveling (Anderson *et al.*, 1959; Krammes, 1965). Evidence from sediment traps on hillslopes in nearby Santa Barbara County indicates that dry raveling is an important process in other coastal southern California watersheds (Gabet, 2003a). Taken together, available data and field observations indicate that dry raveling is significant throughout the Santa Clara River watershed.

Local studies of sediment transport on slopes have revealed significant spatial and temporal variability in rates of dry raveling. Analysis of data from the San Gabriel Mountains reveals relatively low rates after wet winters—possibly due to residual soil moisture, which is thought to contribute to erosion-inhibiting inter-particle cohesion (Anderson *et al.*, 1959). Dry ravel appears to be especially pronounced after fires;

any sediment that has accumulated behind vegetation will be free to ravel downslope when the supporting vegetation is burned away (Gabet, 2003a).

Rain Impact

The impact of rain on slope surfaces can be an effective sediment transport mechanism (see Gabet and Dunne, 2003a, and references therein), depending on drop size, velocity, and rainfall intensity, which together regulate "rain power" (*i.e.*, the rate of transfer of energy to the surface). Larger drops and higher velocities generally lead to more efficient sediment detachment and transport. Vegetation can effectively armor surfaces against rain-induced erosion, intercepting drops and absorbing their energy before they hit the surface. Hence, erosion by rain impact can be enhanced after fires that eliminate protective vegetative cover. In general, coarser particles are harder to detach. Higher rainfall intensities should lead to more effective transport, but only up to a point; if rainfall rates are extremely high, such that overland flow is significant, the water on the surface may actually attenuate the effect of rain impact, reducing its ability to detach sediment.

Sediment transport by rain impact has been shown to be significant on steep, experimental plots in the northern Transverse Ranges, at Sedgwick Reserve, on slopes of the Santa Ynez Valley near Santa Barbara (Gabet and Dunne, 2003a), which experiences the same semi-arid, Mediterranean climate that prevails in the nearby Santa Clara River watershed. Land use history and vegetation types are similar as well. Hence, it seems reasonable to presume that sediment transport by rain impact is significant in the Santa Clara River watershed, especially after vegetation-destroying fires.

Gopher Burrowing and Other Biotic Processes

Biotic processes stir soil and transport sediment downslope (Roering *et al.*, 2002; also Gabet *et al.*, 2003 and references therein). In mountainous watersheds, biotic sediment transport processes include animal burrowing and tree throw (which causes upheaval and downslope transport of sediment from root wads). Although tree throw is unlikely to be effective in the Santa Clara River watershed, due to its paucity of forest cover, significant transport by burrowing of pocket gophers (*Thomomys bottae*) has been observed in nearby Sedgwick Reserve (Gabet, 2000; Seabloom *et al.*, 2000), with transport rates increasing as a function of increasing hillslope gradient. Given Sedgwick's proximity to the Santa Clara River, and the similarities in climate and vegetation types between the sites (as noted above), it seems reasonable to assume that burrowing by pocket gophers is an important sediment transport process in the Santa Clara River watershed as well.

4.2.2 Overland Flow

Overland flow on slopes will occur if soil becomes saturated or if the rainfall rate exceeds the infiltration capacity of the soil (Horton, 1945). Overland flow may sometimes be promoted by spare vegetation, and can occur either as a sheet of running water (called "sheet flow"), if areas of saturation and low infiltration are extensive, or in concentrated flow in shallow (1–10 cm deep) channels or "rills". Sheet flow and rilling can entrain soil particles and deliver them rapidily down slopes, leading to significant hillslope erosion.

Sheet Flow

Soil particles that are entrained in sheet flow move down the slope as "slope wash". The effectiveness of sheet flow as a sediment transport process depends on particle size and cohesion and on the extent and nature of vegetative cover. On steep slopes, such as those in the Santa Clara River watershed, sheet flow

is probably not able to dislodge particles on its own, and is most effective at moving particles that have already been detached by other processes, such as rainsplash and biotic activity.

Concentrated Flow in Rills

In contrast, concentrated overland flow in shallow rills is more likely to detach sediment on its own, and thus substantially enhance sediment transport on slopes. Concentrated flow in rills can also increase runoff to channels during periods of intense rainfall (*e.g.*, Wells, 1981) by focusing water downslope before it has a chance to infiltrate into soils. Rills characteristically appear on many coastal southern California slopes after fires, due to the development of water-repellant soil horizons (as discussed further in Section 4.2.5 below).

4.2.3 Landslides

In many soil-mantled, mountainous landscapes, shallow landsliding is an important sediment transport mechanism. Shallow landsliding links hillslopes, where sediment is produced as soil, to stream channels, where landslide material either remains in storage until it is scoured away by flood flow. These landslides also have the potential to mobilize into high-energy debris flows, which may travel far down-channel, scouring and depositing sediment along the way (*e.g.*, Dietrich and Dunne, 1978; Benda and Dunne, 1997).

Shallow Landslides

A shallow landslide or soil slip occurs when sediment is destabilized on a steep hillslope or in an unchanneled valley. Slope stability is affected by many factors including slope steepness, soil thickness and cohesion, and the presence or absence of tree roots and hydrologic flowpaths (e.g., Iverson *et al.*, 1997; Roering *et al.*, 2003). Many of these factors are directly affected by human land use. For example, the change in land cover from native sage-scrub to exotic grasses has been shown to lead to an increase in landslide frequency in coastal southern California watersheds (Corbett and Rice, 1966; Orme and Bailey, 1971; Rice and Foggin, 1971; Gabet and Dunne, 2002), as discussed in greater detail in Section 4.3 below. Shallow landslide scars are ubiquitous on steep slopes in the Santa Clara River watershed (Figure 4-2). Quantifying the relative importance of landsliding as a sediment transport mechanism is difficult without extensive field studies, but insight can be gained from recent research in the southern San Gabriel Mountains, which bound the Santa Clara River to the east. Analysis of aerial photographs and field reconnaissance suggest that landsliding has contributed only about 10% of the material that has collected over the last 70 years in debris basins at the base of a series of small watersheds draining the San Gabriels (Lave and Burbank, 2004). The other 90% of the debris-basin sedimentation is presumably due to fluvial transport of material that has sloughed into channels by dry raveling and other slope processes. Over the long term (*i.e.*, much longer than 70 years), the ratio of landslide-to-other sediment transport is likely to be higher; the 70-year sampling interval is probably too short to include large, but infrequent slides that would substantially increase the sediment contribution from slope failures. The long-term average contribution from landsliding for the watersheds that feed the debris basins (hereafter referred to as the "Los Angeles County debris basins") has been estimated to be substantially higher than the 10% inferred from short-term rates (Lave and Burbank, 2004). This is more consistent with previous studies, which have reported proportionally large sediment contributions from landslides (Rice *et al.*, 1969; Rice and Foggin, 1971).

Figure 4-2. January 2005 view of the Santa Susana Mountains (left and foreground) and Santa Clara River near the confluence of Piru Creek (downstream, westward view). Slopes in the watershed exhibit numerous landslide scars, including many that span entire hillslope lengths, from ridgetops to channel bottoms. Note snow capped peaks at upper right. (Photo courtesy of the California Coastal Conservancy)

Deep-seated Landslides

Deep-seated landslides incorporate mostly bedrock in the slide mass and do not travel long distances from their source areas. They are large (area > 0.1 km^2) and generally occur on slopes that are conditioned for failure over the long term by factors such as channel incision, slope morphology, geologic structure, shear strength loss due to weathering, and lithologic variation (*e.g.*, Miller and Sias, 1998). Human activities that contribute to initiation of deep-seated landslides include mining and dam building (*e.g.*, Voight, 1978), and possibly also timber harvesting, road building, and changes in surface hydrology. Because they are large, deep-seated landslides have a long-lived morphologic legacy (*e.g.*, Densmore and Hovius, 2000; Mather *et al.*, 2003), and may persistently contribute sediment to streams at accelerated rates. Numerous deep-seated landslides have occurred in the Santa Clara River watershed. A complete inventory of deep-seated landslides within the watershed is not currently available, but the San Martinez Grande landslide, East of Piru Creek, is perhaps the biggest, at 8,000,000 m^3 (Harp and Jibson, 1996).

Triggering Mechanisms

Slope failures, whether shallow or deep-seated, are usually associated with a triggering event, such as a rapid snowmelt (resulting from rain-on-snow, for example) or a storm of prolonged duration or high intensity. Heavy rains brought by the El Niño event of 1997–1998 triggered thousands of shallow landslides throughout California; in nearby Sedgwick Reserve alone, more than 150 slides occurred in a scant 9.5 km^2 (Gabet and Dunne, 2002). Slope failures are more likely to be triggered in areas that have

recently been destabilized by human or natural disturbances, such as fire, which destroys vegetation and roots and thus reduces soil cohesion.

4.2.4 Earthquake-induced Landslides

Ground motions during earthquakes can also trigger landslides. The Santa Clara River's location within an active seismic zone, within the San Andreas Fault system (Figure 2-4), makes its slopes especially prone to earthquake-induced landsliding—a potentially significant source of both coarse and fine sediment for the lower river corridor. The low tensile strength and high relief (nearing 1,000 m) of bedrock in the watershed generally results in steep, easily eroded canyon walls that are susceptible to failure during seismic events.

Landslides Triggered by the 1994 Northridge, California Earthquake

In 1994, a magnitude 6.7 earthquake triggered nearly 7,400 landslides in the Santa Clara River watershed and more than 11,000 landslides overall in a 10,000 km^2 area around the Northridge, California, epicenter (Figure 4-3) (Harp and Jibson, 1996). The most intense area of landslide activity occurred in the Santa Susana Mountains bordering the south-central portion of the watershed, in deformed sedimentary bedrock with little cementation and thus low tensile strength. Most of the earthquake-induced slides were shallow, with depths less than 5 m and an average volume of less than 1,000 m^3. However, many individual slides had volumes exceeding 100,000 m^3. Several tens to possibly hundreds of slides were deep (> 5 m) slumps, including the San Martinez Grande deep-seated slide (Harp and Jibson, 1996), with

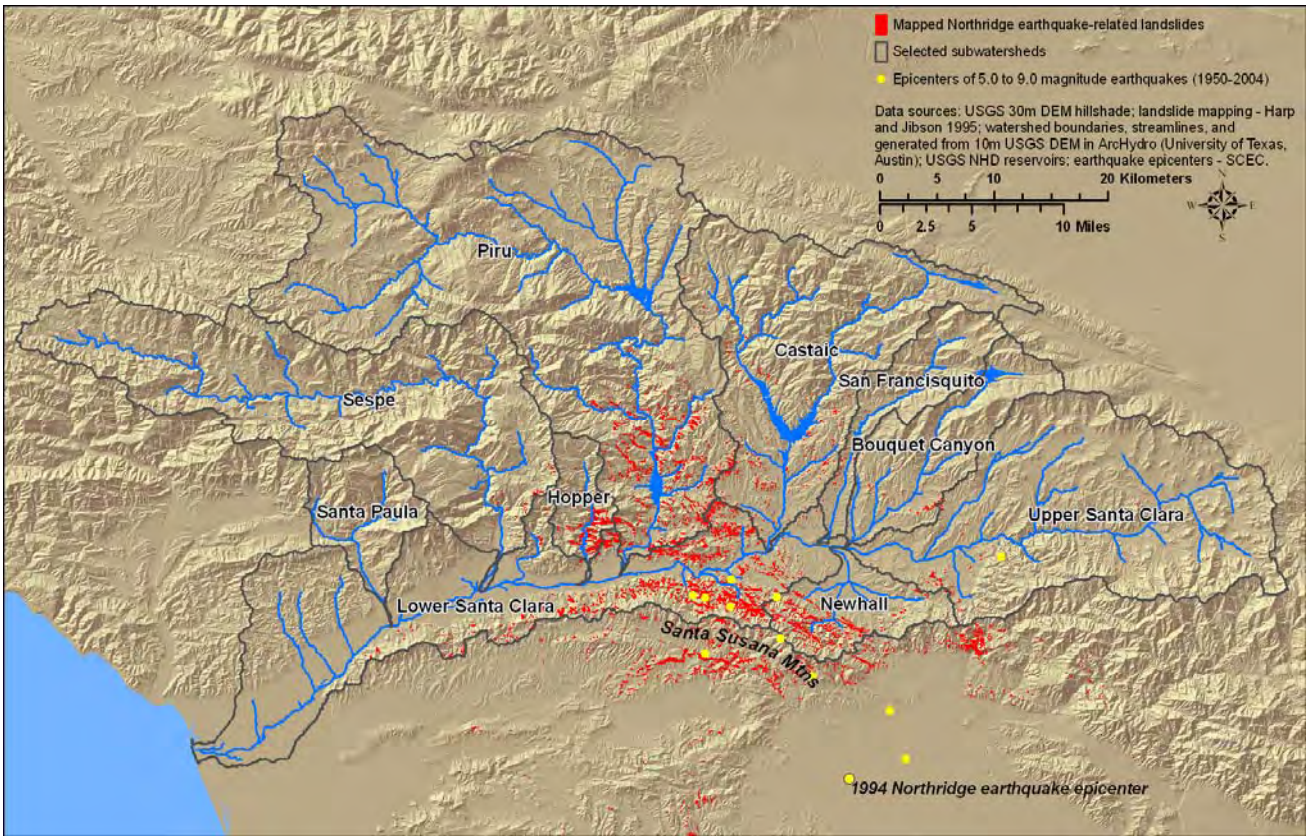

Figure 4-3. Landslides triggered by the 1994 Northridge earthquake (M=6.7). Nearly 7,400 landslides occurred in the Santa Clara River watershed alone.

an 8 million m^3 volume that corresponds to a mass that greatly exceeds the 3,357 tonnes yr^{-1} (3,700 tons yr^{-1}) average annual suspended sediment load of the Santa Clara River (see Section 4.4.2 below).

Sediment Legacy of the Northridge Earthquake

Although the shallow landslides typically traveled considerable distances (> 50 m) down-slope from their source areas (Harp and Jibson, 1996), not all of the material that was mobilized during the Northridge earthquake was transported downstream to the Santa Clara mainstem. Numerous landslide deposits remain intact in tributary channels where they came to rest immediately after being triggered by the earthquake (Orme, *pers. comm.*, 2005b). Even so, subsequent storms may have delivered significant volumes of the earthquake-related landslide sediment to the mainstem. Exactly how much of the sediment remains in the watershed is unknown. Because deep-seated landslides generally do not travel as far from their source areas as shallow landslides typically do, much of the material that was mobilized by the deep-seated landslides has probably been stabilized in place since the earthquake. However, transport of that material could be reactivated by future earthquakes or intense storms and thus add significantly to the sediment load of the Santa Clara River.

Prognosis

Earthquakes are inevitable in the region, due to active tectonics within the San Andreas fault system. In addition to the 1994 Northridge event (Wald and Heaton, 1994), the region has been the locus of several notable, recent earthquakes, including the magnitude 6.4 San Fernando earthquake of 1971 (*e.g.*, Cloud and Hudson, 1975) and the Sierra Madre earthquake of 1991 (Hauksson, 1994), which led to significant losses in lives and property. The pervasiveness of incompetent bedrock in the Santa Clara River watershed appears to have played a major role in the widespread failure of slopes during the Northridge quake (Harp and Jibson, 1996). This implies that future earthquakes in the area are likely to lead to new slope failures in the watershed, as well as the reactivation of old slides. An earthquake occurring within the watershed would be particularly devastating, as would anything close with a magnitude on par with or exceeding that of the Northridge earthquake. Local paleoseismic evidence suggests that a magnitude $M_w > 7.5$ earthquake may have occurred in the early 1800s, due to a rupture along the San Cayetano fault (Dolan and Rockwell, 2001), which cuts through the Santa Clara River watershed (see Figure 2-4). Based on the observed relationship between earthquake magnitude and area affected by landslides (Keefer, 1984), the historic San Cayetano earthquake may have affected an area of 50,000 km^2 or more—roughly 5 times bigger than the area affected by the 1994 Northridge earthquake.

4.2.5 Effects of Fire on Sediment Production and Transport

Wildfires are a major contributor to hillslope erosion throughout the arid American West and are particularly devastating in California, where expanding urbanization and fire suppression (which often increases the availability of highly flammable, natural fuels) have been the norm for nearly a century (see Booker, 1998 and references therein). Between 1919 and 1996, roughly 8.6 million ac of California burned, taking 224 lives and destroying nearly 12,000 buildings, with an ever rising annual toll of structures burned, even as the average acreage burned has remained relatively constant. Historical records indicate that much of the Santa Clara River watershed has burned at least once since the late 19th century, with many areas of the lower watershed, including South Mountain and the lower Sespe, Hopper, and Piru creek watersheds, burning up to 7 times since 1878 (CDF, 2004). Fires in 2003 alone burned 482 km^2, or 11.4% of watershed slopes (Figure 4-4).

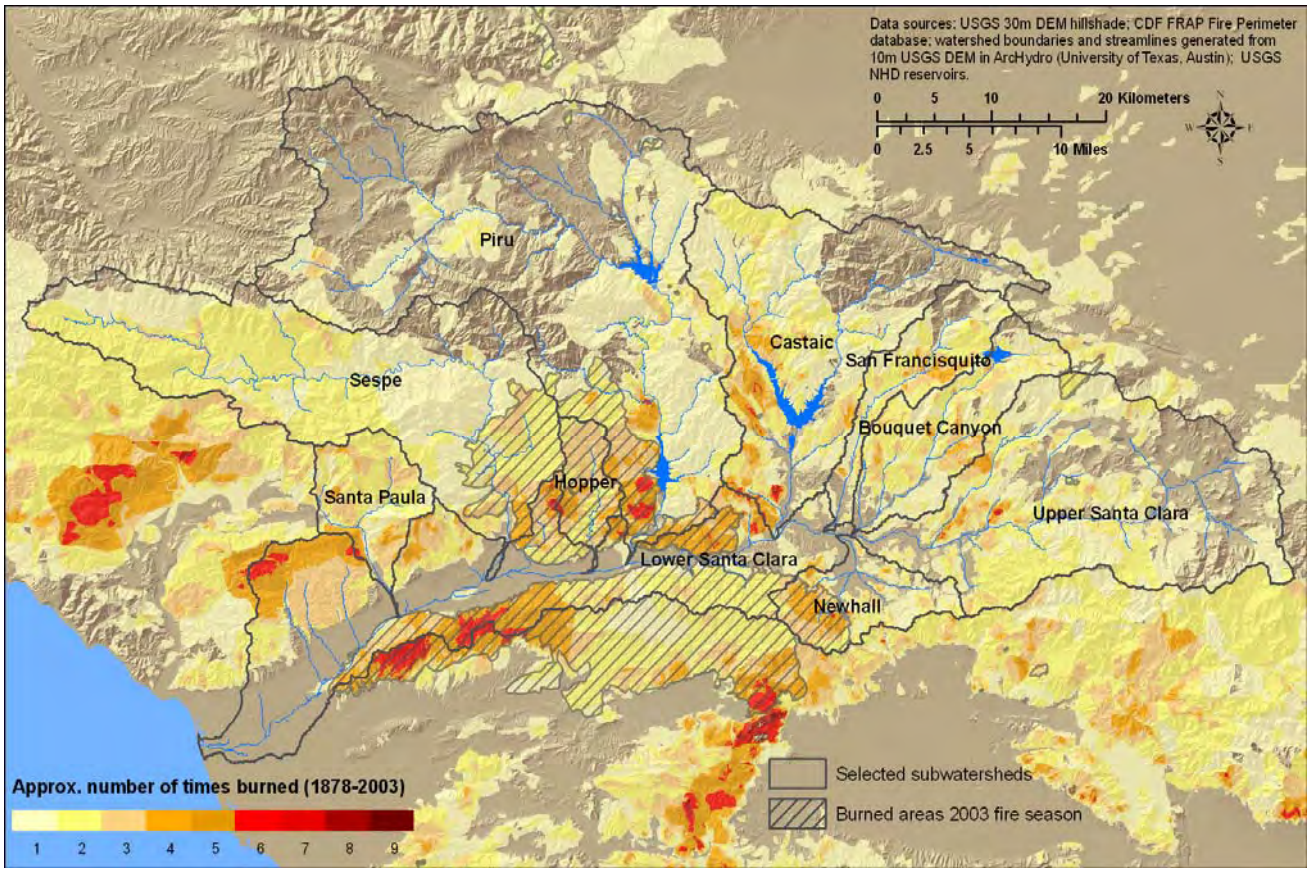

Figure 4-4. Documented fire reoccurrence since 1878 (major recorded fires), and areas burned in the 2003 fire season.

The immediate toll of a fire is often just a precursor for disasters to follow; hillslopes in steep, arid lands can respond during post-fire, winter rains with increased runoff and accelerated erosion, which results in debris flows, landslides, and floods—thus completing what has been dubbed the "fire-flood" sequence (USDA Forest Service, 1954).

As is true elsewhere in coastal southern California, fire risk in the Santa Clara River watershed is enhanced by the hot, dry Santa Ana winds, which typically blow south-southwesterly from inland deserts between August and November, when the highly flammable chaparral vegetation, which pervades over much of the landscape, is at its driest. The fire season in southern California is followed closely by the winter wet season, when multi-day storms and intense rainfall are likely. Gentle rains in early winter have been shown to promote rapid growth of an erosion-inhibiting weed cover (Orme, *pers. comm.*, 2005b), but slopes that burn in the fall are nevertheless often prone to enhanced erosion because they are devoid of protective vegetation when the first intense rains arrive. Chaparral seeds are fire-resistant and germinate into bushes that restore pre-fire fuel conditions on landscapes quickly (Ferrel *et al.*, 1959)— within 30 years (Orme, *pers. comm.*, 2005b)—making frequent fire-recurrence likely. All of these factors contribute to making the erosive destructiveness of southern California's "fire-flood" sequence intense in comparison with the post-fire responses that have been observed in other wildfire-prone landscapes (see Booker, 1998 and references therein).

Mechanisms for Fire-Enhanced Erosion

Fires can accelerate erosion in several ways. On steep slopes, vegetation can form organic dams, effectively retaining sediment that originates upslope; when fire incinerates this vegetation, sediment that was impounded behind it is released and can be quickly mobilized downslope by dry ravel and overland flow (*e.g.*, Anderson *et al.*, 1959; Wells, 1981; Booker, 1998). Incineration of vegetation by fires can also accelerate erosion by exposing surfaces to more efficient erosion by rain impact.

Fires can also accelerate erosion by causing inter-particle fusion, which makes soils coarser, and thus increases their vulnerability to raveling. Particle sizes in soils from southern California chaparral woodlands (like those that pervade throughout the Santa Clara River watershed) have been shown to shift from fine, clay-rich distributions to coarser, sand-sized distributions, when soils are subjected to temperatures that they would likely experience during wildfires. This coarsening is thought to be partly responsible for increases in raveling rates after fires (see Wells, 1981 and references therein), but is not generally widespread, except in intense, high-temperature fires (Orme, *pers. comm.*., 2005b)

Fires can also accelerate erosion by changing soil permeability. In hot fires, organic compounds in burning vegetation within soils can literally vaporize and then migrate to cooler depths where the vapor condenses to form a water-repellent, or "hydrophobic," layer (*e.g.*, DeBano, 1981). Hydrophobicity is thought to be largely responsible for the characteristic post-fire development of dense networks of narrow channels, or rills, on southern California hillslopes. These rills can be formed when soils overlying the impermeable hydrophobic layer become unstable, due to saturation, and become mobilized by downslope flow (Wells, 1981; Gabet, 2003b). Increased runoff from the rills can help to mobilize any sediment stored in channels by raveling.

Examples of the "Fire-Flood" Response from Southern California

Exceptionally dramatic post-fire responses of hillslopes have been documented during winter storms in watersheds that neighbor the Santa Clara River (Florsheim *et al.*, 1991) and also in the San Gabriel Mountains (*e.g.*, Rice *et al.*, 1969; Orme and Bailey, 1971; Wells, 1981; Wells *et al.*, 1987; Wells, 1987), which bound the Santa Clara River watershed to the southeast.

After the 1985 Wheeler fire, just north of the Santa Clara River watershed, in the Ventura River basin, dry ravel contributed large volumes of sediment to the channel (Florsheim *et al.*, 1991). The area then experienced two moderate-magnitude rainstorms. After the first post-fire rainstorm, channels aggraded by 20 to 50 cm, with an estimated 90% of the channel deposits formed by post-fire sediment delivery from slopes. Roughly 90% of the deposits were then scoured away during the second post-fire rainstorm. Hence fluvial transport of the post-fire deposits was extremely effective, even though the storm flows were of only moderate magnitude.

Field studies in the San Dimas Experimental Forest of the San Gabriel Mountains indicate that fires can lead to ten- to hundred-fold increases in sediment transport rates in California chaparral woodlands (Wells, 1981). Most of these increases can be attributed to increases in dry raveling rates, both during and immediately after fires, and increases in sediment delivery along post-fire rills (Wells *et al.*, 1987; Wells, 1987). The largest sediment transport events occurred in the first post-fire storms (Wells *et al.*, 1987). Debris torrents in channels were surprisingly abundant, given the modest intensities of the storms that followed many of the fires. These debris torrents effectively conveyed sediment in post-fire channel deposits long distances down channel, much as stream flow did during the modest storms that followed

the Wheeler fire. One avenue of further study of post-fire sedimentation might be to examine sediment accumulations in reservoirs.

4.3 Human-Induced Changes in Sediment Production and Transport

Rates of sediment production and transport on slopes can be significantly altered by human disturbance and changes in land management practices. This most certainly has been the case in the Santa Clara River watershed.

Today, significant changes in the watershed are due to expanding urbanization and changes in the way lands are managed for fire suppression. Historically, major changes followed the arrival of Europeans, the onset of extensive grazing, the California Gold Rush (which accelerated range degradation), agricultural development in the early 1900s, and the population boom that followed World War II (Warrick, 2004). Of these changes, the first three are likely to have had significant impacts on hillslope sediment transport and are considered below.

4.3.1 Effects of European Settlement on Sediment Transport Rates

Records indicate that European settlement of coastal southern California led to the degradation of native grasses on slopes starting in the early 1800s, the appearance of widespread barren lands by the mid to late 1800s, and domination by non-native animals of rangelands by the late 1800s (Pulling, 1944). This has led to significant increases in sediment yields in modern times; rates of offshore sedimentation along coastal southern California during the 20th century are many times more than they were in pre-colonial times (Sommerfield and Lee, 2003). Moreover, peak rates of sedimentation in estuaries along the California coast appear to have occurred in mid- to late-19th century, coinciding with the peak degradation of rangelands (Warrick, 2004).

4.3.2 Effects of Conversion to Non-native Grasses on Landslide Frequency

The non-native, annual grasslands of the Transverse Ranges have been shown to be three times more susceptible to mass wasting than native brush and chaparral (Rice and Foggin, 1971). Analysis of 150 landslides at Sedgwick Ranch, north of Santa Barbara, confirms that conversion of native sage-scrub to exotic-dominated grassland can lead to an increase in landsliding frequency (Gabet and Dunne, 2002) and, presumably, sediment yield. When sage-scrub cover was converted to grassland, soils became unstable (Rice *et al.*, 1969; Orme and Bailey, 1971) because the effective cohesion imparted by the shallow-rooted grass was lower than it had been for the deeper-rooted scrub. This instability led to progressive thinning of soils over time by landsliding, which will presumably continue until soils become thin enough that the shallow-rooted grass can stabilize them against failure. There is some indication that slopes may never stabilize under the new land cover, due to the high moisture-holding capacity of root masses (Orme, *pers. comm.*, 2005b). In any case, sediment yields under non-native grasses are likely to stay higher than they were under natural conditions (unless soil depth eventually adjusts to the new root cohesion). This is an example of a land use "legacy" on geomorphic processes; the conversion to grassland from native sage-scrub continues to affect sediment yields long after the land use change was initiated. This legacy effect is important in the Santa Clara River watershed.

4.3.3 Fire Management

Given the dramatic, accelerating effects of fire on hillslope sediment transport (discussed at length above), it is worth considering whether land management practices have affected fire frequency, and thus

contributed indirectly to increased sediment production in the Santa Clara River watershed and elsewhere along the southern California coast.

These considerations were the focus of a recent study of the frequency of big fires in the Santa Barbara area (Mensing *et al.*, 1999). Charcoal layers in sediment from the Santa Barbara Channel were used to derive a 560-year record of fires with area greater than 200 km^2, revealing that the recurrence interval has remained constant, at 20–30 years, despite substantial changes in management practice over the period of record. Historical records indicate that the Chumash Indians managed vegetation for thousands of years by burning slopes, until the late 1700s, when European settlers began practicing fire prevention by, for example, outlawing fires in wildfire-prone areas. A more active approach, emphasizing quick-response fire suppression, was adopted in about 1900 and continues to be used today. The unchanging frequency of big fires over a 560 year period that was marked by changing fire management suggests that big fires are a natural part of the environment, occurring irrespective of what coastal residents have been doing to suppress or prevent them (Mensing *et al.*, 1999). This challenges previous indications, from analysis of a recent time series of LANDSAT imagery (Minnich, 1983), that big fires are an artifact of changes in vegetation distributions due to increased fire suppression.

On the other hand, smaller fires, which may affect sediment yields locally, may be much more closely related to changes in land management practices. Analysis of data from the Los Angeles County debris basins suggests that encroaching urbanization in southern California wilderness has increased fire frequency locally (Lave and Burbank, 2004). Sediment yields and fire history from the small watersheds that feed the debris basins, considered together, suggest that anthropogenic fires (*i.e.,* fires caused by human inhabitants rather than natural causes) have augmented sediment yields by as much as 400% (average = 60%) (Lave and Burbank, 2004). An earlier, independent analysis of the same debris basin data yielded inclusive results about the effects of fire-frequency on sediment yield (Brozovic *et al.*, 1997; Booker, 1998). Taken together, these disparate results suggest that effects of anthropogenic fire on erosion may be difficult to quantify precisely.

4.4 Rates of Hillslope Processes

Soil production and sediment transport processes are inherently probabilistic, because they are driven by rainstorms, windstorms, fires, earthquakes, human and other biological disturbances, and other perturbations that are discrete in time and space (Benda and Dunne, 1997; Gabet and Dunne, 2003b). The inherent episodicity of erosional processes makes sediment transport rates sensitive to the timescales over which they are averaged (Kirchner *et al.*, 2001). For example, if a basin's erosion rate is averaged over a relatively dry 10-year period, it might be considerably lower than it would be if it were averaged over a 10-year period that included several wet years. In general, longer averaging timescales are more likely to include contributions from larger, more infrequent erosional events.

Erosion rates in the Santa Clara River watershed have been estimated for a variety of timescales, using historical records that span decades, and geologic records that span thousands to millions of years. A variety of spatial scales have been considered as well, including individual slopes, larger subwatersheds, and the Santa Clara River watershed as a whole. Rates from each of these spatial and temporal scales contribute to quantifying and understanding sediment delivery to the Santa Clara River corridor. We consider and discuss them below.

4.4.1 Rates of Rock Uplift and Dip-displacement

The mountains of the Santa Clara River watershed have been uplifted over millions of years, by a complex series of processes at the boundary between two tectonic plates (Blythe *et al.*, 2000; Meigs *et al.*, 2003). Long-term average uplift rates from the region's mountain ranges are among the fastest on record for the continental United States. For example, rock uplift in the San Gabriel Mountains, which rise along the southeastern edge of the watershed, are reported to range from < 0.1 to 1.0 mm yr^{-1} (Blythe *et al.*, 2000) based on geologic methods that average uplift over million-year timescales. These are somewhat lower than the 0.75 to >5 mm yr^{-1} range of uplift rates that has been reported for the Santa Ynez Mountains, which rise along the coast, to the northwest of the Santa Clara River watershed (Metcalf, 1994; Trecker *et al.*, 1998; Duvall *et al.*, 2004). A recent summary of coastal uplift rates for the Transverse Ranges region reports an even broader range of 0.05 to 9 mm yr^{-1} (Orme, 1998).

High uplift rates are corroborated locally by estimates of dip-displacement rates on the San Cayetano Fault (Rockwell, 1988), which runs roughly parallel to the lower Santa Clara River corridor, through the mountains to the north of Fillmore (Figure 2-1). Assuming that the dip-displacement rate for a section of a thrust fault such as the San Cayetano is approximately equal to the rate of vertical offset, it should also be a good first estimate of the local rate of rock uplift (and by extension, the local rate of erosion). Along eastern sections of the San Cayetano Fault, dip-displacement rates, averaged over the last < 1 million years, are as high as 8.8 mm yr^{-1}, nearly an order of magnitude faster than the long-term uplift rates of the San Gabriel Mountains. Rates of displacement along the San Cayateno Fault vary substantially along its length, dropping to about 1.1 mm yr^{-1} from east to west (Rockwell, 1988) before increasing again further to the west (Orme, *pers. comm.*, 2005b).

4.4.2 Rates of Hillslope Sediment Transport and Production: the Transverse Ranges

Extensive erosion rate data have been collected from neighboring and nearby watersheds of the Transverse Ranges. While these regional rates may not directly reflect rates of processes that affect the Santa Clara River corridor, they can be used to supplement the local data that are available, and provide additional context and insight into erosional processes that are likely to be important in the Santa Clara River watershed.

Soil production rates in the san gabriel mountains

Rates of bedrock lowering from granitic slopes in the San Dimas Experimental Forest, in the southern San Gabriel Mountains, have been reported to range from 0.05 to 0.46 mm yr^{-1} (average = 0.29 mm yr^{-1}), based on methods that average lowering rates over thousand-year timescales (Heimsath, 1998). These thousand-year averages are in the low end of the range of rates implied by the long-term, million-year average uplift rates of the San Gabriel Mountains. Assuming a bedrock density of 2.6 tonnes m^{-3} (typical for granite, which underlies the study area), the average bedrock lowering rate corresponds to equivalent soil production rate of 750 tonnes km^{-2} yr^{-1}. This rate is roughly an order of magnitude lower than sediment yields that were determined from earlier studies of fire-related effects on erosion (Scott and Williams, 1978; Wells, 1981, 1985; Wells and Wohlgemuth, 1987). This discrepancy has not been fully explained (Heimsath, 1998), but it could be due to the differences in the timescales over which the rates are averaged. The earlier studies reported sediment yields, averaged over years to decades, whereas the soil production rates are averaged over thousands of years. Hence, the fact that the short-term rates are higher could simply reflect a recent acceleration in erosion rates due to any number of factors. For example, the fact that the short-term rates are derived from areas that have been subjected to fires may explain much of the difference in rates, given that fire is a known accelerator of erosion on slopes in the San Dimas Experimental Forest.

Los Angeles County debris basins

Additional regional erosion rate data are available from the Los Angeles County debris detention basins (see Section 4.2.3), located on the southern side of San Gabriel Mountains (Lave and Burbank, 2004). Sediment yields from the debris basins imply 200 to 14,690 tonnes km^{-2} yr^{-1} of sediment production in the watersheds that feed them (Lave and Burbank, 2004). Equivalent bedrock lowering rates are 0.1 to 5.7 mm yr^{-1} (Lave and Burbank, 2004). Sediment production on slopes and in first-order channels appears to be controlled by vegetative cover and precipitation intensity, with decreasing cover and increasing precipitation intensity corresponding to increasing sediment production rates. As discussed earlier in greater detail, sediment production by anthropogenic fires has led to 60–400% increase in sediment yields compared with the background, "natural" yields (Lave and Burbank, 2004).

4.4.3 Rates of Hillslope Sediment Transport and Production: the Santa Clara River Watershed

In addition to data from regional studies of erosion, there are also data available for rates of hillslope processes from studies that were conducted within the Santa Clara River watershed proper.

Ventura County debris basins

For the past 30 years, the Ventura County Flood Control District (VCFCD) has published regular updates on its monitoring and maintenance of dozens of debris basins and debris detention dams, which are located in canyons and washes along steep mountain fronts that border heavily utilized areas (VCFCD, 1999). The dams were constructed to discourage high-energy debris flows, which would otherwise be generated in the canyons, and endanger lives and property in downstream areas. The sediment data from the debris basins has recently been used to quantify how sand retention by the dams affects the supply of sand for beach formation and maintenance (Sherman *et al.*, 2002). A useful, if unintended, additional benefit of the dam monitoring is that it permits the opportunistic determination of minimum rates of sediment production for the watersheds that feed the basins.

The array of debris basins considered here includes 8 within or immediately adjacent to the Santa Clara River watershed, 3 that line the Ventura River to the north, and 5 in watersheds of southern Ventura County (Figure 4-5). In general, rates from the basins should be applicable to the Santa Clara River watershed, even though some are located outside of it. The sediment production rates inferred from the 8 debris basins on the lower Santa Clara River are listed in Table 4-1 range from 1,000 to 22,100 tonnes km^{-2} yr^{-1} (average = 5,600 tonnes km^{-2} yr^{-1}), with estimated equivalent bedrock lowering rates of 0.4 to 8.5 mm yr^{-1} (average of 2.2 mm yr^{-1}). Sediment production rates in the 8 other Ventura County basins appear to be lower, ranging from 260 to 7,230 tonnes km^{-2} yr^{-1} (average = 1,570 tonnes km^{-2} yr^{-1}). The highest rate in each of the two data sets is considerably higher than the rest of the rates in the set. This raises the possibility that the averages are skewed, such that they exaggerate the difference between the two groups. However, when the highest rates are excluded from the analysis, the average rates of the two data sets are still very different, at 3,200 tonnes km^{-2} yr^{-1} for the Santa Clara River debris basins and 760 tonnes km^{-2} yr^{-1} for the other Ventura County debris basins. Additional analysis would be required to understand the mechanisms behind the differences.

When all of the Ventura County basins are considered together, the range of sediment production rates is 250 to 22,100 tonnes km^{-2} yr^{-1} and the average is 3,580 tonnes km^{-2} yr^{-1}. The range and average bedrock lowering rate of the Ventura County data set is roughly on par with the range and average that was inferred from the Los Angeles County debris basin data (Lave and Burbank, 2004). All sediment production rates inferred from the debris basin data (from both Los Angeles and Ventura counties) are

considered to be minimum estimates; fine sediment, which would be carried in suspended load, is unlikely to be trapped effectively in the basins. Data from similar debris basins in nearby Santa Barbara County confirm that the particle size of 80–95% of the trapped material is > 0.075 mm (fine sand and coarser), implying that debris dams have little effect on suspended sediment load (Warrick, 2002). The extent to which sand and coarser material is trapped in the basins is unknown and may be important to quantify in future studies of sediment delivery to the Santa Clara River.

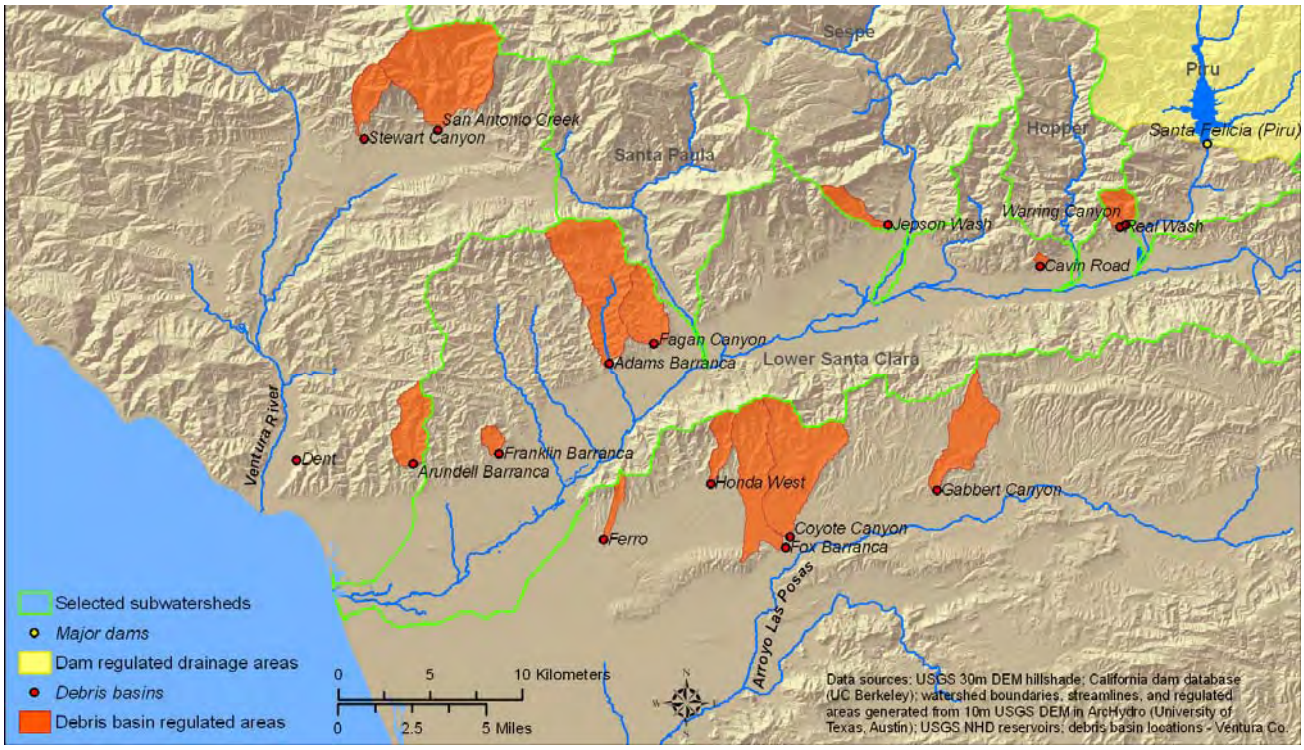

Figure 4-5. Ventura County debris basins in the lower Santa Clara River and adjacent watersheds, with approximate boundaries of regulated areas (highlighted in orange).

Evidence from sediment gauging data

Hillslope sediment delivery to streams is ultimately reflected, to some degree, in the load that actually gets transported by the streams. Rating curves, which relate suspended sediment concentration to discharge, can be used in conjunction with discharge records to calculate an estimate of what suspended sediment discharge has been over the period of the discharge record, which in this case dates back to 1928.

Table 4-1. Sediment production rates inferred from 16 Ventura County debris basins.

Name	ID	Watershed Area		Total Debris Volume[a]	Length of Record	Sediment Production Rate		Bedrock Lowering Rate[c]
		(mi^2)	(km^2)	(m^3)	(yrs)	by Volume ($m^3\ km^{-2}\ yr^{-1}$)	by Mass[b] (tonnes $km^{-2}\ yr^{-1}$)	(mm yr^{-1})
Santa Clara River Debris Basins								
Adams	DB2-07	8.22	21.24	61,836	2.8	1,025	1,948	0.7
Arundell Barranca	DB2-06	2.74	7.1	271,791	24.8	1,547	2,939	1.1
Cavin Road	DB2-03	0.14	0.36	7,737	25.7	828	1,572	0.6
Fagan Canyon	DB2-08	2.9	7.51	45,519	2.8	2,139	4,064	1.6
Franklin Barranca	DB2-01	0.52	1.34	6,333	8.3	569	1,081	0.4
Jepson Wash	DB2-02	1.34	3.47	254,852	28.1	2,614	4,966	1.9
Real Wash	DB2-04	0.25	0.65	207,673	27.6	11,628	22,093	8.5
Warring Canyon	DB2-05	1.09	2.81	237,205	26.7	3,163	6,009	2.3
Other Ventura County Debris Basins								
Dent	DB1-01	0.04	0.11	10,430	25.1	3,805	7,230	2.8
San Antonio Ck	DB1-03	9.81	25.41	43,855	11	157	298	0.1
Stewart Canyon	DB1-02	1.98	5.12	19,167	27.4	136	259	0.1
Coyote Canyon	DB3-15	7.11	18.41	136,402	25.5	291	552	0.2
Ferro Canyon	DB3-13	0.62	1.6	8,300	22.9	227	430	0.2
Fox Barranca	DB3-14	4.84	12.55	128,203	27.3	375	713	0.3
Gabbert Canyon	DB3-09	3.67	9.51	362,539	27.6	1,382	2,626	1.0
Honda West	**DB3-07**	**1.16**	**2.99**	**17,835**	**27.4**	**217**	**413**	**0.2**

[a] Calculated from debris cleanout volumes and aerial-surveyed basin volumes, which are published in the Ventura County Detention Dams and Debris Basins Manual (VCFCD, 1999). Methods for estimating volumes are detailed in the manual.

[b] Calculated using an assumed sediment density of 1.9 tonnes m^{-3}—the average density of sediment in Los Angeles County debris basins (Lave and Burbank, 2004), which presumably have deposits that are roughly similar to those in the Ventura County basins.

[c] Calculated using an assumed bedrock density of 2.6 tonnes m^{-3}.

Roughly 36% of the Santa Clara River watershed is regulated by dams, which impound sediment as well as water (Figure 2-6 and Table 2-1). This results in a net reduction of sediment load, compared with what it would be in the absence of the dams. Santa Felicia Dam and Pyramid Dam trap nearly 100% of sediment from upstream sources (Williams, 1979). Castaic Dam is also an effective sediment trap, but has a smaller drainage area than the Santa Felicia Dam on Piru Creek.

Suspended sediment yields for the subwatersheds of the Santa Clara River are summarized in Figure 4-6 and Table 4-2 (after Warrick, 2002)[2]. An estimated 540 tonnes $km^{-2}\ yr^{-1}$ and 990 tonnes $km^{-2}\ yr^{-1}$ of suspended sediment are generated in the areas upstream of the Santa Felicia and Castaic dams , with essentially all of it being impounded upstream of the lower river corridor. Roughly 410 tonnes $km^{-2}\ yr^{-1}$ of suspended sediment originates from the area upstream of the gauge at the Los Angeles/Ventura county line. Sespe Creek contributes 1,400 tonnes $km^{-2}\ yr^{-1}$ at its junction with the Santa Clara River. The highest suspended sediment yield—2,800 tonnes $km^{-2}\ yr^{-1}$—is observed in the lower Santa Clara River

[2] Subwatersheds delineated in the Warrick (2002) analysis differ from those presented elsewhere ("selected watersheds") in this report, based on the availability of suspended sediment data.

subwatershed, where weak Plio-Pleistocene siltstones predominate, and presumably contribute to enhanced erosion. This hypothesis is corroborated by the fact that suspended sediment concentrations within the nearby Santa Ynez Mountains correlate strongly with percent of contributing area underlain by Plio-Pleistocene rocks (Warrick, 2002). However, the presence of similar lithologies in the middle watershed, where sediment yields are lower, suggests that the relationship between rock-type and sediment yield (if present) is not straightforward and requires further study. Relatively intense land use has been persistent in the lower watershed over the period of record, and might have contributed to its relatively high suspended sediment yield (Warrick, 2002).

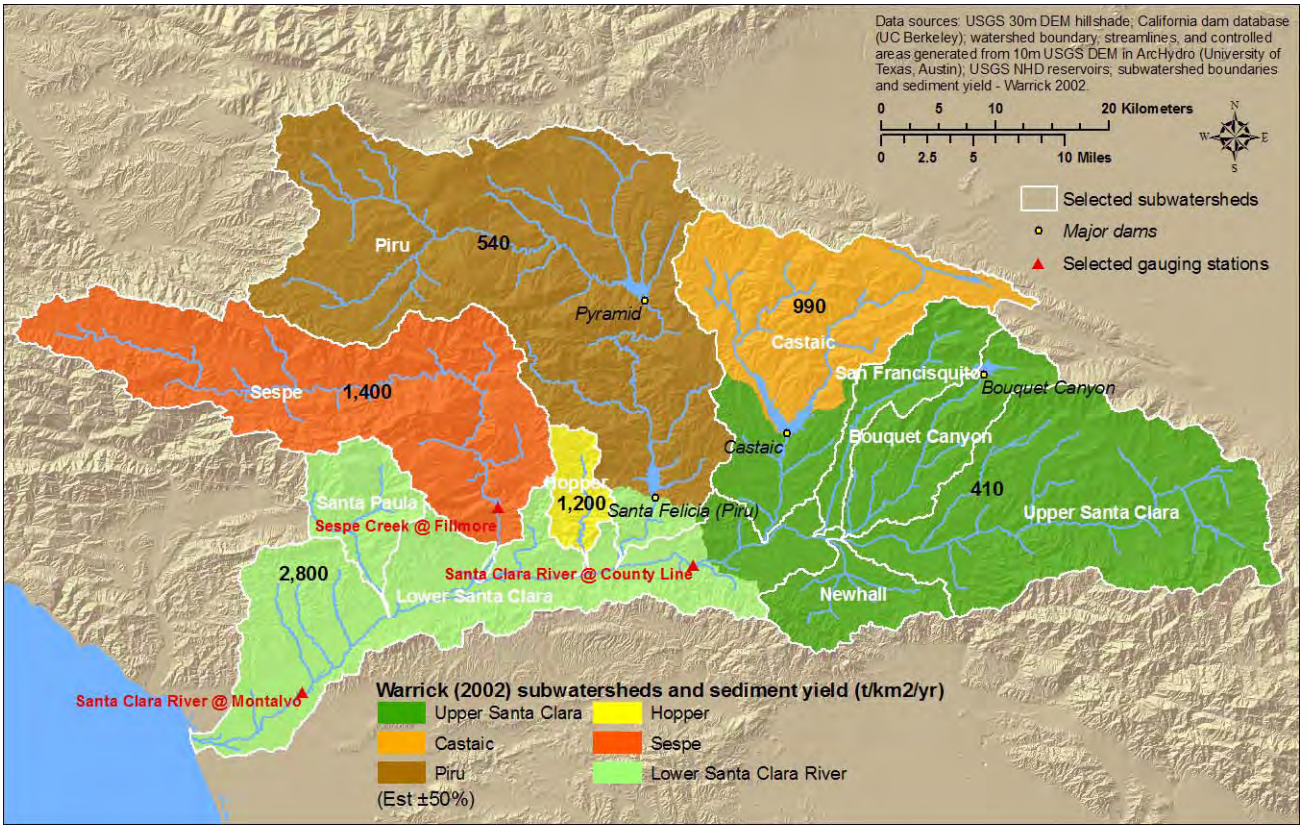

Figure 4-6. Suspended sediment yield, major dams, and selected sediment and water discharge gauges in the Santa Clara River watershed (modified from Warrick, 2002). Subwatersheds delineated in the Warrick (2002) analysis differ from those presented elsewhere in this report ("selected subwatersheds"), based on the availability of suspended sediment data.

The Santa Clara River watershed is host to most of the previously discussed, earthquake-induced landslides (Harp and Jibson, 1996), which have probably enhanced sediment delivery substantially, but are nevertheless too recent to be expressed in the sediment yields reported in Table 4-2 (which are calculated from measurements that mostly predate the earthquake). Similarly, the effects of recent fires are also not expressed in the sediment yield data.

The estimated suspended sediment yield of the Lower Santa Clara River subwatershed has the highest uncertainty, because it is calculated indirectly, by subtracting the other subwatershed sediment contributions (inferred from sediment concentrations and flow measurements) from the total load at the mouth. Hence, the suspended sediment yield of the lower watershed is the so-called "residual" term in the suspended sediment budget, and therefore includes all of the errors in the terms that were used to

calculate it (Kondolf and Matthews, 1991). In this case, the uncertainty of the lower watershed's sediment yield could be as high as 90% (or ± 2,500 tonnes km^{-2} yr^{-1}), based on Gaussian error propagation, under the assumption that the uncertainty in sediment yield for each of the subwatersheds is ± 50%. In that case, the sediment yield of the lower watershed would be indistinguishable from zero (and the other subwatershed sediment yields), from the statistical standpoint. Moreover, differences in suspended sediment yield among subwatersheds do not necessarily reflect any spatial differences in rates of hillslope sediment production, because (1) sediment produced on slopes can stay in storage if flows are insufficient to move them, and (2) river sediment loads typically include reworked contributions from floodplain deposits and other sediment storage elements, as well as sediment delivered directly from hillslopes (Trimble, 1977).

Table 4-2. Suspended sediment yield by subwatershed.

Subwatershed	Total Area[a] (km^2)	Suspended Sediment Yield[b] (tonnes km^{-2} yr^{-1})	Regulated Area[c] (km^2)	Unregulated Area[d] (km^2)	Exported Suspended Sediment (kilotons yr^{-1})
Lower Santa Clara River[e]	764	2,800	0	764	2,100
Sespe Creek	674	1,400	0	674	940
Hopper Creek	62	1200	0	62	74
Piru Creek	1,134	540	1,095	39	21
Castaic Creek	526	990	397	129	130
Eastern[f]	1,052	410	34	1,007	410
TOTAL	**4,212**	**1,390[g]**	**1,526**	**2,686**	**3,700**

[a] Adapted from Warrick (2002) using slightly different subwatershed boundaries, based on GIS analysis.
[b] From Warrick (2002).
[c] "Regulated Areas" are areas that are impounded by dams and that therefore do not contribute to sediment exports from the Santa Clara River.
[d] "Unregulated Areas" are areas that contribute to suspended sediment export from the Santa Clara River, at the rate listed under the heading "Suspended Sediment Load".
[e] Includes Santa Paula Creek.
[f] Includes Upper Santa Clara River and San Francisquito, Newhall, and Bouquet creeks.
[g] Calculated from the Total Exported Suspended Sediment (3,700 kilotons yr^{-1}) using the effective, sediment-contributing drainage area of 2,686 km^2 (*i.e.*, with the area that is regulated by dams excluded from the total); if the total Santa Clara River drainage area (4,212 km^2) were used it would produce an estimate of the "apparent" suspended sediment yield: 880 tonnes km^{-2} yr^{-1}.

The suspended sediment load of a river provides a measure of the total mass of material that is suspended in the flow, and does not account for sediment that is transported as bedload by bed traction and saltation (*i.e.*, the step-by-step bounding of relatively coarse particles due to shear stresses along the river bed). Hence, estimates of suspended sediment load under-represent the total load, and will therefore only weakly reflect hillslope sediment supply, which includes both coarse and fine sediment.

In the Santa Clara River, the bedload accounts for an average of 14% of the total, based on the few concurrent USGS measurements of bedload and suspended load that have been taken over the years (see Appendix C for references and further discussion). However, the data suggest that the ratio between suspended sediment and bedload is discharge-dependent, increasing nonlinearly with increasing discharge (see discussion below in Section 5). Hence, estimates of bedload sediment yield would be

difficult to estimate from the data that are available, with results that are likely to be highly uncertain, implying that the calculation would add little to our understanding of hillslope sediment production.

4.4.4 Summary of Rates of Hillslope Processes

The rates of hillslope sediment production and transport in the Santa Clara River region are summarized in Table 4-3. The debris basin data from Los Angeles and Ventura counties, taken together, imply bedrock lowering rates of 0.08 to 8.5 mm yr^{-1}, which are broadly consistent with the range of long-term rates of uplift that have been inferred for the region's mountain ranges. In the Santa Clara River alone, the debris basin data imply a range of 0.42 to 8.50 mm yr^{-1}, which is remarkably consistent with the 1.1 to 8.8 mm yr^{-1} range implied by rates of dip-displacement along the San Cayetano Fault, which runs through some of the watersheds that feed the debris basins.

Table 4-3. Summary of rates of uplift, displacement, sediment production, and sediment yield[a].

Location	Rate Expressed as Length per Unit Time (mm yr^{-1})			Rate Expressed in Sediment Production Units (tonnes km^{-2} yr^{-1})			Reference
	Low	High	Average	Low	High	Average	
Rates of Uplift and Dip-displacement							
San Gabriel Mts.	< 0.1	1.0	—	< 260	2,600	—	Blythe *et al.*, 2000
Santa Ynez Mts.	0.75	>5.0	—	1,950	13,000	—	Metcalf, 1994; Trecker *et al.*, 1998; Duvall *et al.*, 2004
Transverse Ranges	0.05	9.0	—	130	23,400	—	Orme, 1998
San Cayetano Fault	1.1	8.8	—	2,900	22,900	—	Rockwell, 1988
Regional Rates of Sediment Production from the Transverse Ranges							
San Gabriel Granite	0.05	0.46	0.29	130	1,200	750	Heimsath, 1998, Appendix 2
Los Angeles Co. Debris Basins	0.08	5.65	1.50	200	14,700	3,900	Lave and Burbank, 2004
Rates of Sediment Production from Ventura County Debris Basin Data							
Santa Clara Rv. Basins	0.42	8.5	2.15	1,100	22,100	6,030	This report
Other Basins	0.1	2.78	0.60	260	7,230	1,570	This report
Grand Average			*1.38*			*3,580*	*This report*
Suspended Sediment Yields from the Santa Clara River Watershed							
L. Santa Clara Rv.[b]	—	—	1.08	—	—	2,800	Warrick, 2002
Sespe Creek	—	—	0.54	—	—	1,400	Warrick, 2002
Hopper Creek	—	—	0.46	—	—	1,200	Warrick, 2002
Piru Creek	—	—	0.21	—	—	540	Warrick, 2002
Castaic Creek	—	—	0.38	—	—	990	Warrick, 2002
Eastern[c]	—	—	0.16	—	—	410	Warrick, 2002
Total Santa Clara River[d]	—	—	*0.53*	—	—	*1,390[d]*	*adapted from Warrick, 2002*

[a] uplift rates are converted to sediment production units under the hypothetical assumption that rates of mountain uplift are roughly balanced by rates of hillslope erosion (such that topography doesn't change much over time); conversions from length-per-unit time into sediment production rate units use bedrock density = 2.6 tonnes m^{-3}; blank entries indicate rates were not measured or are not applicable

[b] includes Santa Paula Creek

[c] includes Upper Santa Clara River and San Francisquito, Newhall, and Bouquet creeks

[d] applies to unregulated drainage area of the Santa Clara River (2,686 km^2)

Soil production rates from San Gabriel Mountain granites are in the low end of the range of rates inferred from the debris basins, but this could be due to sampling biases; the soil production rate analysis requires

soils with moderate erosion rates, and wouldn't yield interpretable results under conditions implied by the upper end of the debris basin data range (Heimsath, 1998).

The suspended sediment yields imply sediment production rates that are roughly consistent with those implied by the debris basin data. However, as noted above, the suspended sediment yields probably only roughly reflect rates of sediment production and delivery from slopes, especially given that coarse sediment—which is not included in suspended sediment measurements—is being supplied to the mainstem at a rate of 260 to 22,100 tonnes km^{-2} yr^{-1}, according to the analysis of the debris basin data.

Perhaps the most significant result in Table 4-3 is the substantial variability in rates implied by each of the data sets. The long-term uplift rates vary by one to two orders of magnitude, as do the dip-displacement rates for the San Cayetano Fault. The rates of denudation implied by the Los Angeles and Ventura County debris basin data vary by two orders of magnitude. The sediment yields span a seven-fold range. The least variable rates, from the San Gabriel granites, span a five-fold range. This implies that rates of sediment production in the Santa Clara River are highly variable from place to place over all timescales—from decades to millions of years.

Given the general consistency among the data sets and the high variability in the data, it is difficult to identify one set of results from Table 4-3 as being more reliable. However, given the proximity of the debris basins to the lower river corridor (which is the primary concern in this analysis), and the consistency between the debris basin data and the dip-displacement rates, the most appropriate indicators of hillslope sediment production appear to be the debris basin data, which imply an average sediment production rate of 3,580 tonnes km^{-2} yr^{-1}. The fact that much of the suspended load is not trapped by the debris basins (see above) implies that the total rate of sediment production on hillslopes is actually somewhat higher.

The upper end of the range of debris basin data implies sediment production rates that are among the fastest ever recorded, consistent with rates that have been reported for rapidly uplifting mountains in Taiwan, New Zealand and Tibet. In comparison, rates from the nearby Sierra Nevada are ten to one-hundred times slower. Rates from the Appalachian Mountains are more than one-thousand times slower (Bierman, 2004). Hence, sediment production on slopes in the Santa Clara River watershed appears by all accounts to be enormous, at least in the context of the sediment production rates that have been inferred so far for other watersheds from around the world.

4.5 Delivery of Sediment from Tributaries to the Santa Clara River Valley

In general, rates of sediment delivery from tributaries to the Santa Clara River are poorly quantified, limited to the sediment yield data of described in Section 4.4.3. However, the high rates of hillslope sediment production in the Santa Clara River watershed imply that rates of sediment delivery to the lower river corridor are high as well. Sediment that is transported from slopes can be stored briefly in tributary channels and in the floodplain, but, in general, unless tributaries are aggrading significantly, most of the sediment that is transported off of hillslopes will eventually be delivered downstream, either by floods or in debris flows. Hence, over the long term, rates of sediment delivery to the Santa Clara River should more or less reflect rates of sediment production from slopes, which are summarized in Section 4.4 above.

4.5.1 Episodic Sediment Delivery from Tributaries

Over the short term, sediment delivery to the mainstem Santa Clara River is likely to be much more episodic than the rate of supply from slopes. Storms of all sizes help move sediment down slopes and into channels, by rain impact, overland flow, and mass wasting, leading to nearly continuous inputs to tributaries from slopes during the wet season. In the dry season, hillslope sediment production continues via dry raveling (Scott and Williams, 1978). In contrast, sediment is delivered from tributaries to the mainstem more episodically, in flows associated with big storms, and also in moderate storms that follow fires (Florsheim *et al.*, 1991; Wells, 1981).

Sediment transport along mainstem of the Santa Clara River is even more episodic than delivery of sediment from tributaries. Extreme events associated with major storms are the primary movers of sediment in the watershed, as discussed in greater detail in Section 5 below.

4.5.2 Effects of Fire on Sediment Delivery

Post-fire delivery of sediment from tributaries to the mainstem may be disproportionately high, due in part to the development of rills, which not only increase sediment production rates from slopes but also help increase runoff, leading to more thorough scour of tributary channels for a given storm intensity. Big floods after fires probably lead to the highest rates of sediment delivery to the lower river corridor, because (1) fire-enhanced erosion on slopes produce thick sediment deposits in tributary channels and (2) high flows are sufficient to transport all or most of the sediment down to the mainstem.

4.5.3 Effects of Rock Type and Local Uplift Rates on Sediment Delivery

Sediment delivery rates from slopes (and ultimately to the mainstem Santa Clara River) are generally expected to be higher where the underlying bedrock is more erodible, but weak, shattered bedrock has been noted throughout the watershed, including the headwater areas that are underlain by granite and gneiss—two rock types that are often thought to have relatively high resistance to erosion. Rates of sediment delivery to the mainstem from tributaries are likely to be highly variable, depending on the proximity of tributaries to areas of rapid localized uplift and displacement along faults.

4.5.4 Contributions from Tributaries along the Lower River Corridor

The small tributaries (barrancas) along the lower Santa Clara River are connected almost directly to the mainstem, whereas upstream tributaries along Sespe Creek and the upper Santa Clara River are more remote, and therefore somewhat insulated by distance. The barrancas probably deliver a relatively higher fraction of their sediment loads to the lower river corridor, because there is less chance for material to be held up in storage before entering the mainstem.

4.5.5 Effects of Infrastructure on Sediment Delivery

The debris dams along the lower Santa Clara River margins retain significant volumes of coarse sediment, which, under natural conditions, would be delivered to the mainstem and potentially affect the lower river corridor. However, the area upstream of the debris dams is only about 37 km^2—a small fraction of the area directly adjacent to the Santa Clara River corridor. Moreover, the dams do not block delivery of suspended sediment. Hence, the reduction in sediment delivery due to the debris dams is probably a small fraction of the total load delivered to the Santa Clara River.

4.5.6 Sediment Particle Size

The grain size of sediment delivered to the Santa Clara River is reflected in the grain size distributions of suspended sediment and bedload in tributary streams. Limited grain-size distribution data are available for the tributaries, making sediment particle size difficult to quantify precisely. Key controls on the sediment particle size are expected to be geology and travel distance. In general, highly fractured, deformed rock is prevalent throughout the watershed and probably contributes to reduced sediment particle size compared with what it might be from less disrupted lithologies. However, a seemingly high abundance of boulders and cobbles has been noted in bed deposits of the lower river corridor, implying that the particle size of sediment delivered from slopes can be quite large, despite being derived from weak substrates (which would generally be expected to disaggregate into smaller sizes). It has been noted that much of the coarse load may be derived from the Sespe fan, which is a reworked mass of older rocks (Orme, pers. *comm.*, 2005b). Quantifying the effects of the Sespe fan on coarse sediment supply is important and should be the subject of further study.

4.6 Conceptual Model of Hillslope Processes and Implications for Lower Santa Clara River Geomorphology

Observations highlighted above are synthesized in Figure 4-7 and have important implications for the morphologic evolution of the lower Santa Clara River. Foremost is the fact that sediment delivery rates to the mainstem are inferred to be extremely rapid, based on available data on hillslope erosion rates, which are locally among the fastest on record for the world, due to rapid uplift, episodic earthquakes, seasonally intense rainfall, and frequent fires. By extension, the sediment load delivered to the mainstem is likewise enormous, with significant repercussions for fluvial processes in the lower river corridor (see Section 5 for further details).

Another implication is that sediment loading from tributaries, while apparently quite rapid, is inherently difficult to precisely predict. This is because it depends on numerous factors besides the rate of supply of sediment from hillslope erosion. Prediction of sediment loading is further complicated by the fact that sediment delivery is episodic, depending on the frequency, magnitude, and timing of stochastic events such as storms, fires, landslides, and earthquakes. Of critical importance, in particular, is how (and whether) these events coincide with one another. Big fires followed by droughts, for example, probably contribute less sediment to the mainstem than they would if they were followed by big storms. Similarly, earthquake-induced landslides in a dry year might become stabilized where they initially come to rest, contributing minimally to sediment delivery; there is some indication that this occurred after the 1994 Northridge earthquake (Orme, *pers. comm.*, 2005b). Hence, rates of sediment supply to the lower river, as well as the relative contributions from the various subwatersheds, are reflections of the complex interactions of probabilistic processes.

At present, the relative importance of these processes in the Santa Clara River watershed is poorly understood, and should be the focus of further study. One potential avenue of further research might involve examination of sediment accumulations in reservoirs, coupled with analysis of historical records of hydrology and fire-frequency. Such a study might help shed light on how sediment delivery rates are affected by the frequency and magnitude of storms and fires.

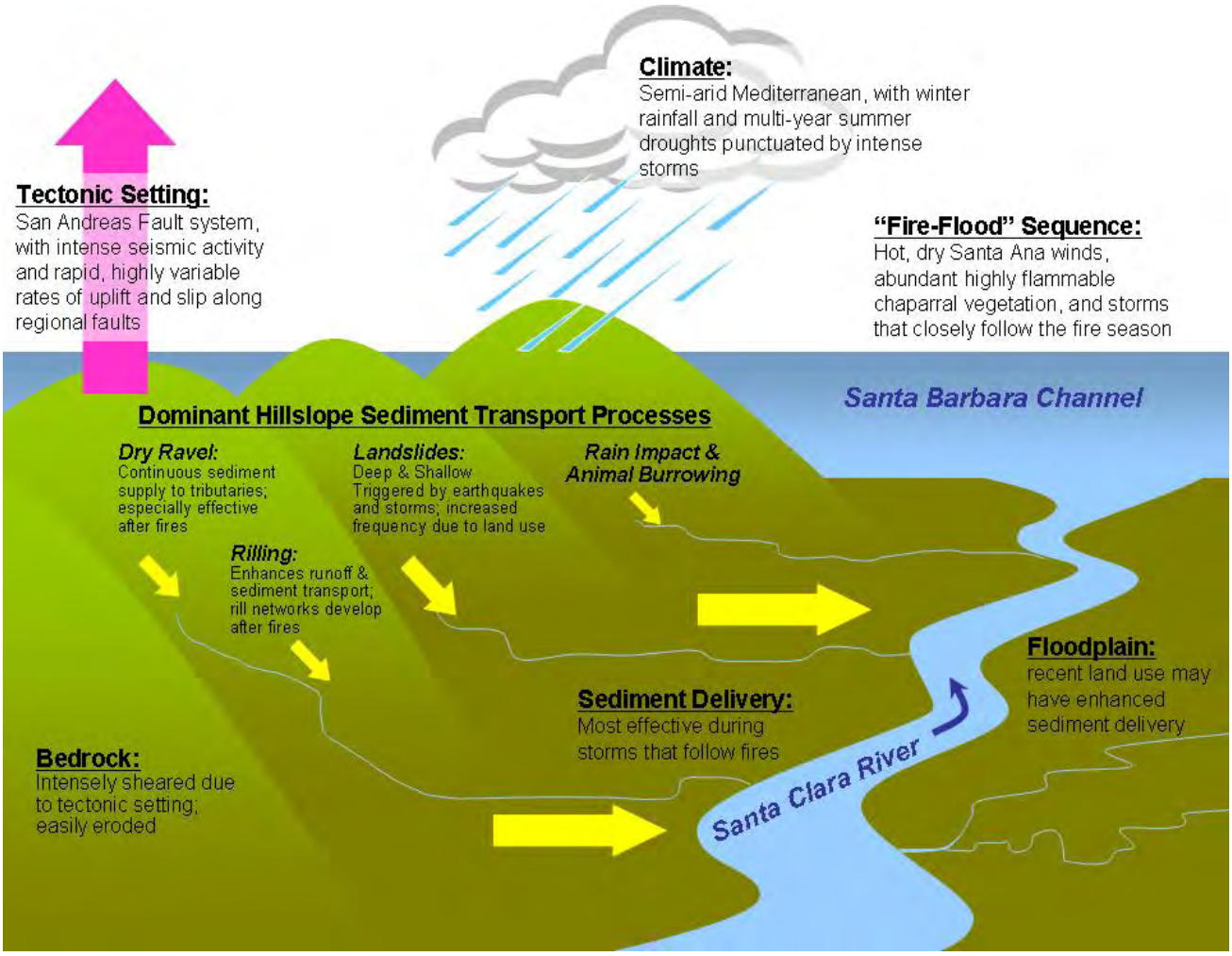

Figure 4-7. Illustration of conceptual model of hillslope processes in the Santa Clara River watershed.

5 FLUVIAL SEDIMENT TRANSPORT AND MORPHOLOGICAL CHANGE

5.1 Frequency and Magnitude of Sediment Transport

Sediment transport processes in the Santa Clara River are dominated by extreme events associated with the river's highest flows (Table 5-1). These events transfer water and sediment from the hillslopes to the estuary and near-shore waters, and are integral to changes in form of the mainstem Santa Clara River and its floodplain over time. The exchange of sediment between the river channel and floodplain during flood events (i.e., episodes of erosion and deposition) determines the hazards and assets possessed by the river corridor. In an apparent contradiction, the hydrologic and geomorphic processes that create hazards (such as flooding, unwanted bed and bank erosion, and deposition) are the same processes that help sustain river ecosystems by creating assets (such as aquatic and riparian habitat diversity). Hence, understanding the fluvial geomorphic processes in the Santa Clara River watershed is a necessary pre-cursor for understanding the hazards and assets of the lower river corridor.

Table 5-1. Annual maximum peak discharges since 1928 on the lower Santa Clara River, gauged or estimated to be in excess of 1,416 m^3s^{-1} (50,000 cfs).

Date	Discharge[a]	
	m^3s^{-1}	cfs
3/12–13/1928	14,460–22,655[b]	500,000–800,000[b]
1/25/1969	4,670	165,000
1/10/2005	3,850[c]	136,000[c]
3/2/1938	3,400	120,000
1/10/1995	3,115[d]	110,000[d]
2/12/1992	2,945	104,000
3/4/1978	2,890	102,200
3/1/1983	2,830	100,000
2/23/1998	2,380	84,000
2/16/1980	2,305	81,400
1/23/1943	2,265[e]	80,000[e]
2/11/1973	1,650	58,200
4/3/1958	1,480	52,200
12/29/1965	1,470	51,900

[a] Instantaneous peak discharges except as indicated. Source: USGS National Water Information System Annual Peak Streamflow Data for the Santa Clara River at Montalvo (USGS 11114000 Santa Clara River at Montalvo, CA).
[b] Estimated peak flood flow following the St. Francis Dam break (Simons, Li & Associates, 1983)
[c] Estimated instantaneous peak discharge at Freeman Diversion [source: VCWPD].
[d] Discharge from AMEC (2004, p. 24). Source unknown.
[e] Discharge from USACE 1968 (cited in Simons, Li & Associates, 1983)

5.1.1 "Dominant Discharge" Characteristics

The majority of sediment transport in the Santa Clara River occurs in very short periods of time. For instance, an estimated 55% of the roughly 57.6 million tonnes (63.5 million tons) of sediment that passed the USGS gauge at Montalvo near Highway 101 (Figure 4-6) between 1968 and 1975 was transported

during high flows in just 2 days (Williams, 1979). Analysis of the Montalvo gauge data for the period 1968–1985 further indicates that about 94% of the suspended load was transported by storm runoff in just 57 days, or 1% of the nearly 5,700 days covered by the flow record. A more recent study concludes that for the period 1928–2000, 25% of the total sediment discharge occurred in just four days (Warrick, 2002).

These observations contrast sharply with what has been observed in alluvial rivers in humid environments, which have provided the basis for many of the classic generalizations of fluvial geomorphology, including the concept of "dominant discharge", the flow that, over the long-term average, performs the most work in terms of sediment transport (Wolman and Miller, 1960; Emmet and Wolman, 2001). Figure 5-1 illustrates the dominant discharge concept in a hypothetical example for an idealized alluvial river. The most common flow occurs at an intermediate discharge (blue line), sediment transport rate increases steadily with increasing flow (red line), and total sediment load (black line; calculated as the product of the flow frequency and sediment transport rate) exhibits a maximum (and is therefore "dominant") at an intermediate discharge.

For the Santa Clara River, a very different picture emerges from the data, as shown in Figure 5-2, where flow frequency, sediment transport rate, and total coarse sediment load are plotted for data collected at the Montalvo gauge over the period 1928–2004. The flow frequency (blue line) shows the expected distribution of discharges over several orders of magnitude up to and exceeding 2,830 m^3s^{-1} (100,000 cfs.) Total coarse sediment load, calculated as the product of flow frequency and coarse sediment transport rate, does not follow the trend suggested by the "classic" dominant-discharge model (Figure 5-1) but instead increases with discharge across the entire range of data, with a maximum at the highest flow. Hence the dominant discharge for the Santa Clara River is also the largest discharge on record. This pattern is consistent throughout the mainstem Santa Clara River, including the Los Angeles-Ventura County line, the mouth of Sespe Creek (Figure 5-3 and Figure 5-4) and near the mouth of the Santa Clara River near Montalvo[3].

The dominant discharge corresponding to the largest flow on record has important implications for channel-forming processes. Dominant discharge is often described as the "channel-forming" flow, at the center of a range of flows that are most directly responsible for shaping and maintaining the channel in its characteristic "equilibrium" morphology (*e.g.*, Wolman and Leopold, 1957). The fact that the dominant, channel-forming flow is the largest flow on record implies that the Santa Clara River will not necessarily behave like a classic alluvial river. For example, the channel will probably not typically overflow its banks every 1 to 3 years, or maintain a well-defined, regularly-spaced riffle-pool sequence. In general, morphology will not exhibit equilibrium tendencies, with small, year-to-year fluctuations around a long-term average condition. Instead, the channel and its floodplain will experience dramatic changes due to episodically high flows that change the dynamics of the entire system, completely altering roughness and channel shape, and potentially leading to significant fluctuations in local channel bed elevation that persist for many years or decades.

[3] Appendix C describes the methods used for determining the frequency and magnitude of sediment transport at the selected gauges within the Santa Clara River watershed.

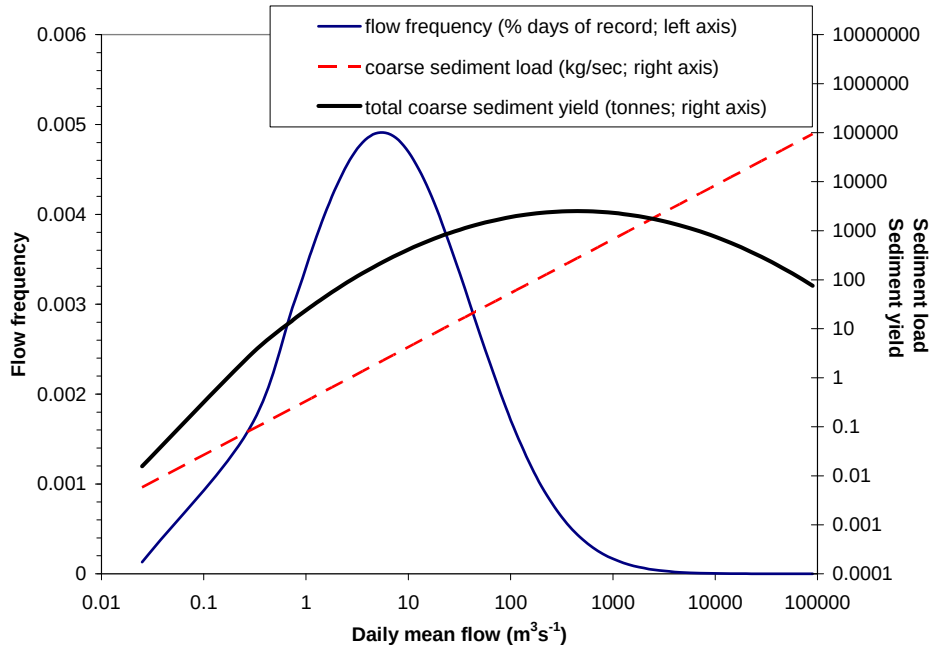

Figure 5-1. Flow frequency (left axis, scaled to 1) and sediment load (right axis) plotted against flow, showing conceptual, dominant discharge model of Wolman and Miller (1960). Blue line tracks flow frequency (for mean daily flow), red line tracks sediment transport rate (in tons/day) and black line tracks total sediment load (in tons). Sediment load increases to a maximum at an intermediate flow.

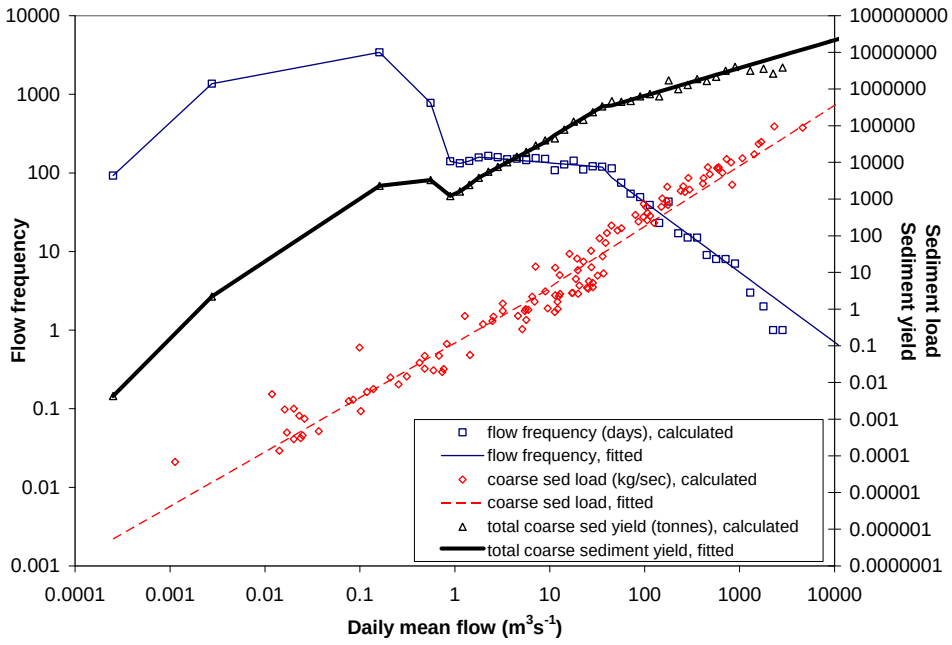

Figure 5-2. Flow frequency (left axis) and coarse sediment load (right axis) as a function of daily mean flow for the Santa Clara River at Montalvo (USGS11114000). Blue line tracks flow frequency, red line tracks sediment transport rate (in tons/day) and black line tracks total sediment load (in tons). The dominant discharge (*i.e.*, the one that carries most of the total sediment load) is the largest discharge of record. Details of this analysis are presented in Appendix C.

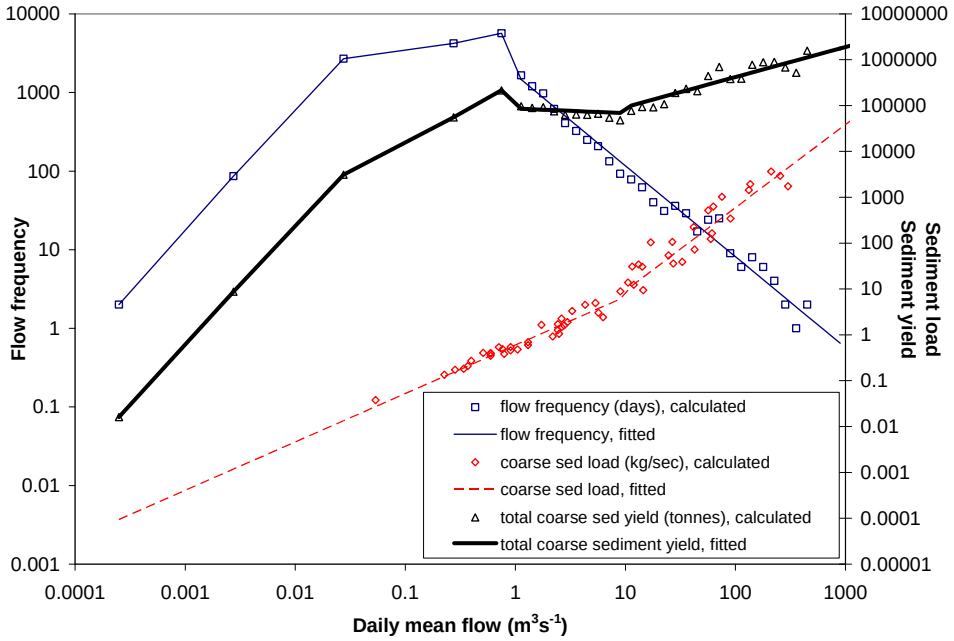

Figure 5-3. Flow frequency and coarse sediment load (right axis) as functions of daily mean flow for the Santa Clara River at the Los Angeles/Ventura County line (USGS11108500).

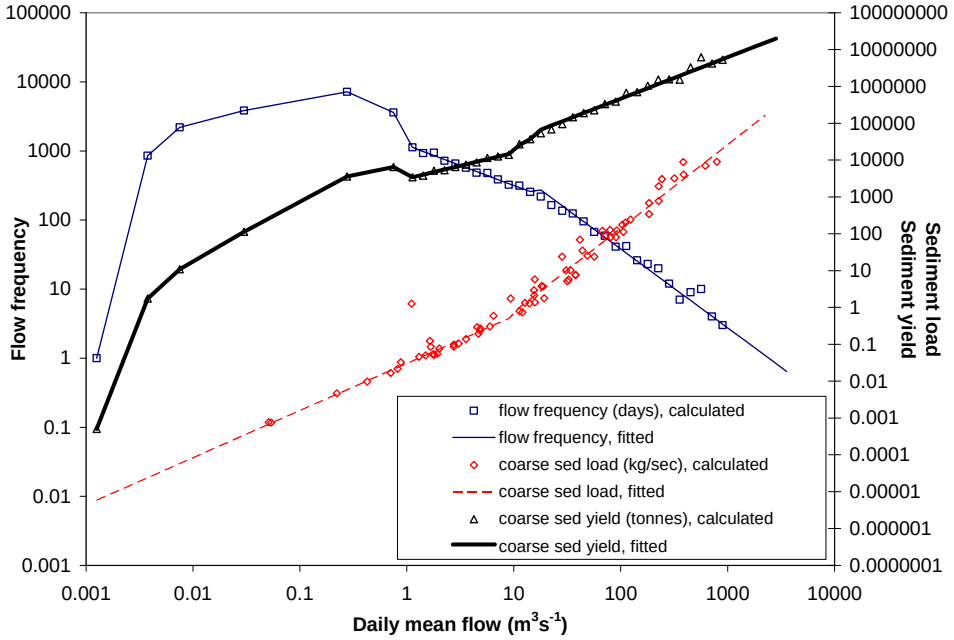

Figure 5-4. Flow frequency and coarse sediment load (right axis) as a function of daily mean flow for Sespe Creek at Fillmore (USGS11113000).

5.1.2 Effects of the El Niño -Southern Oscillation on Flow Magnitude and Sediment Delivery

The El Niño-Southern Oscillation (ENSO) is a climatic phenomenon that is characterized by warming and cooling cycles (oscillations) in the waters of the eastern equatorial Pacific Ocean. ENSO cycles have a 1–1.5 year duration and a 3–8 year recurrence interval, and they are related to changes in atmospheric circulation, rainfall, and upper ocean heat content (see Deser *et al.*, 2004, and references contained therein). In Southern California, El Niño years are characterized by relatively high rainfall intensities, with rivers and streams exhibiting higher annual peak flows than they do in non-El Niño years (Cayan *et al.*, 1999; Andrews *et al.*, 2004). This difference in flow magnitude is shown quantitatively in an analysis of the instantaneous peak flow record for the Santa Clara River (at the Montalvo gauge) for El Niño and non-El Niño years between 1932 and 2005. For El Niño years there is a greater than 70% probability of peak flow exceeding 1133 m^3s^{-1} (40,000 cfs) (Figure 5-5 open symbols) whereas a non-El Niño year has less than 10% probability of peak flows exceeding 1,133 m^3s^{-1} (40,000 cfs) (Figure 5-5 closed symbols)[4].

ENSO-induced climate fluctuations occur on a multi-decadal time scale that is consistent with the observed shift from a relatively dry climate (averaged over the period 1944–1968) to a relatively wet climate (averaged over the period 1969–1995) in North America's Pacific region (Inman and Jenkins, 1999). The wet-period ENSO cycle, which existed to the end of the Inman and Jenkins study (1995) and has likely continued, has been marked by strong El Niño years every 3–7 years, and mean sediment fluxes for Southern California rivers (from the Pajaro River south to the Tijuana River) that have been approximately 5 times greater than during the preceding dry period (1944–1968) (Inman and Jenkins, 1999). For the Santa Clara River, the annual net yield during the recent wet period was approximately 8 times greater than it was during the preceding dry period (Inman and Jenkins, 1999).

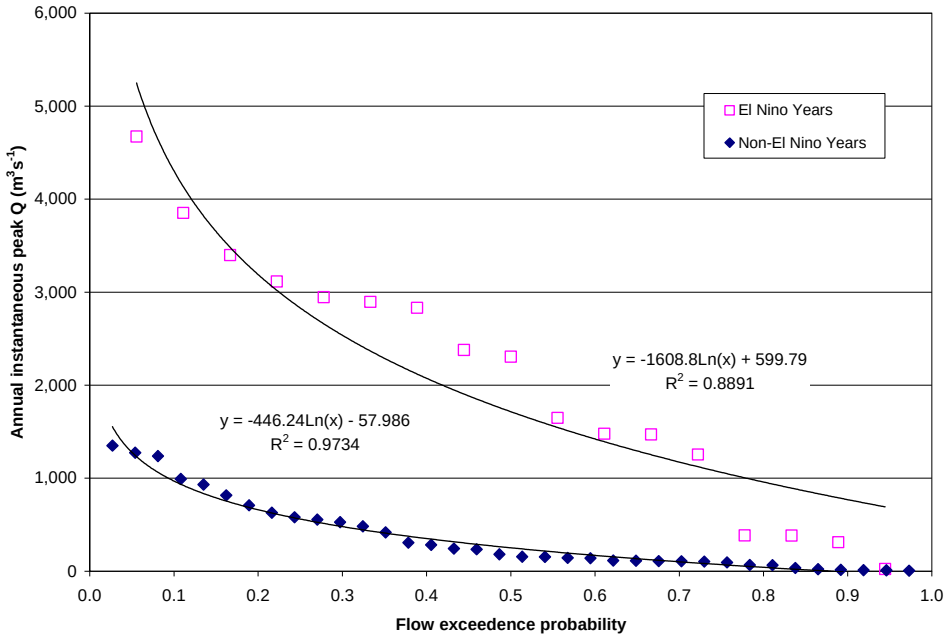

Figure 5-5. Flow exceedence for El Niño/non-El Niño years (period of record: WY 1932-2005) for the Santa Clara River at Montalvo (USGS11114000).

[4] For this analysis, El Niño years were defined as years with a multivariate ENSO index (MEI) greater than 0.5 (Wolter and Timlin, 1993).

Episodic delivery of sediment from Southern California watersheds in general, and the Santa Clara River watershed in particular, is strongly linked to ENSO-induced precipitation events with high day or multi-day rainfall totals. Because of the general aridity of the watershed, intense rainfall events are sufficient to result in high annual precipitation totals for ENSO-related Water Years. Thus years with high precipitation correlate to years with high instantaneous flood peaks. Such a relation is developed in Figure 5-6 between annual rainfall totals at the Santa Paula rainfall gauge (Venture County Water Protection District [VCWPD] gauge 11113500 by the confluence of Santa Paula Creek with the mainstem Santa Clara River) and yearly flood peaks from the Montalvo gauge on the Santa Clara River mainstem ($r^2 = 0.747$). While the Montalvo gauge has only been in continuous operation since approximately 1950, rainfall records in Santa Paula extend back to Water Year 1873, and less-reliable but nevertheless instructive rainfall data has been derived from narrative accounts back to Water Year 1770 (Lynch 1931; Freeman 1968). Using these records, it is possible to extrapolate the likelihood of large floods (*i.e.*, over 1,416 m^3s^{-1}, or 50,000 cfs) back through the historical records. In total, 22 such events are predicted (Table 5-2). Of the 22 predicted flood events, nine are gauged events known to have exceeded 1,416 m^3s^{-1}, two gauged events exceeded 1,250 m^3s^{-1}, and seven other pre-gauging events are noted as large floods by Freeman (1968). Of the 4 other predicted large events prior to gauging records, 1943 is known to have been a large flood in Sespe Creek (see Table 5-16), and 1941 is noted by Freeman as having been the wettest year of record to 1968 but consisting, unusually, of a series of relatively low intensity and well-distributed events distributed from October to April (Freeman 1968, p.181). Therefore, only two predicted events are without corroboration for producing a significant flood, and these are the smallest events in the ranked data on Table 5-2. Only three floods gauged at above 1,416 m^3s^{-1} are not predicted to have reached this threshold, and one of these, in 1992, ranks as the next flood in the sequence and so is included in Table 5-2 for completeness. The two true outliers are for Water Years 1973 (1,648 m^3s^{-1}) and 1966 (1,470 m^3s^{-1}) and presumably consist of one large flow event in an otherwise rather dry year.

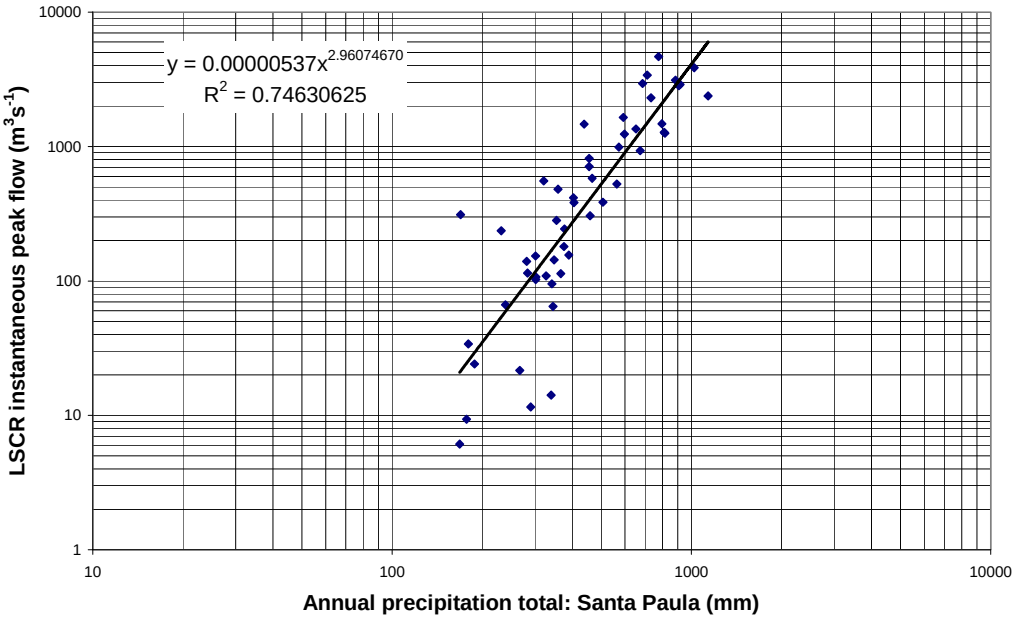

Figure 5-6. Relationship between annual precipitation totals in Santa Paula (VCWPD11113500) and annual maximum instantaneous flood peaks recorded in the lower Santa Clara River at Montalvo (USGS11114000).

Table 5-2. Ranked distribution of largest instantaneous flood peaks on the Santa Clara River at Montalvo.[1]

Water Year	Annual precipitation total (mm)	Predicted instantaneous flood peak (m^3s^{-1})	Actual instantaneous flood peak from gauged records (m^3s^{-1})	El Niño year	"Flood" event recorded by Freeman (1968), for events prior to 1965
1998	1137	6006	2379	yes	n/a
2005	1021	4363	3851	yes	n/a
1941	968	3725			no
1825	940	3413			yes
1978	916	3168	2894	yes	n/a
1862	914	3147			yes
1983	907	3075	2832	yes	n/a
1884	907	3070			yes
1840	889	2895			yes
1995	884	2846	3115	yes	n/a
1890	828	2342			yes
1993	816	2243	1254	yes	n/a
1815	813	2220			yes
1952	811	2202	1274		
1958	797	2093	1478	yes	
1969	777	1941	4672	yes	n/a
1943	736	1655			
1980	733	1633	2305	yes	n/a
1914	723	1572			yes
1938	712	1498	3398	yes	
1833	711	1495			
1907	707	1468			
1992	687	1348	2945	yes	n/a

[1] As predicted from the power relationship developed from Figure 5-6.

5.1.3 Bed Material and Bedload Particle Sizes

Bed particle sizes along the Santa Clara River channel network range from fine sand (0.12-0.25 mm) to coarse gravel (4-64 mm), with dominant sizes ranging from medium sand to very fine gravel (Simons, Li & Associates, 1983). Within the mainstem Santa Clara River at Montalvo and LA County Line, the D_{16} is sand-sized, D_{50} ranges in size from sand to very fine gravel, and D_{84} ranges from sand to medium gravel (Table 5-3 and Table 5-4)[3]. Within Sespe Creek, the finer fraction (D_{16}) is typically sand-sized, median particle sizes (D_{50}) range from very fine to medium gravel, and the coarse fraction (D_{84}) ranges from medium to coarse gravel (Table 5-5). Temporally, bed sediments (*e.g.*, D_{50}) seem to have become finer through the period of record, 1971-1984, but this may be an artifact of bed sediments coarsening following large floods, and becoming finer following smaller floods in the intervening period. Bedload particle size at the Montalvo and LA County Line gages measured during low to moderate flow has been shown to consist mainly of fine and coarse sand, with fine gravel-sized particles also being represented in the coarser bedload fraction at higher flows (Table 5-6 and Table 5-7). Bedload particle sizes in Sespe Creek at Fillmore are generally coarser than the sediment in the mainstem Santa Clara River, ranging from coarse sand to medium gravel (Table 5-8).

Table 5-3. Characteristics of channel bed sediments for Santa Clara River at Montalvo.

Sample date	Particle size (nth percentile) [mm]		
	D_{16}	D_{50}	D_{84}
8/2/1971	0.50	**2.25**	10.46
8/10/1973	0.20	0.65	2.86
3/18/1975	0.42	0.87	3.40
4/30/1975	0.44	0.91	3.82
9/30/1975	0.28	0.65	4.00
9/16/1977	0.25	0.69	8.57
9/20/1978 (7 counts)	0.22	0.55 (+1 @ **21.58 mm**)	2.5 (+1 @ 40.73 mm)
8/22/1979 (19 counts)	0.28	0.45 – finest 14 **20.43 – coarsest 5**	2.35 – finest 14 36.81 – coarsest 5
8/14/1980 (13 counts)	0.16	0.44	1.676 (+1 @ **9.14 mm**)
9/30/1981	0.21	0.58	**5.33**
8/5/1983	0.15	0.38	1.14
11/3/1983	0.16	0.40	**2.40**
12/12/1984	0.26	0.44	0.92

Source: USGS, National Water Information System, Santa Clara River at Montalvo CA (USGS 11114000).
Bold values indicate gravel-size sediment.

Table 5-4. Characteristics of channel bed sediment for the Santa Clara River at the Los Angeles County Line.

Sample date	Particle size (nth percentile) [mm]		
	D_{16}	D_{50}	D_{84}
10/21/1968	0.19	0.46	1.90
11/5/1968	0.31	0.61	1.24
2/10/1969	0.24	0.59	**7.20**
8/27/1969	0.20	0.52	1.53
11/4/1969	0.36	0.71	1.56
9/14/1970	0.37	0.76	1.63
9/30/1975	0.32	0.93	**8.00**
9/15/1977	0.38	**2.67**	**13.33**
9/20/1978 (5 counts)	0.22	1.74	**7.78**
10/7/2004 (3 counts)	0.47	1.32	**4.10**
10/16/2004 (3 counts)	0.51	1.53	**6.13**
10/21/2004 (3 counts)	0.48	1.46	**5.12**
12/17/2004 (2 counts)	0.42	0.99	**3.03**
12/30/2004 (2 counts)	0.40	1.36	**8.54**

Source: USGS, National Water Information System, Santa Clara River at the Los Angeles County Line (USGS 11108500) [1968-1978] and the Santa Clara River at Piru (USGS 11109000) [2004].
Bold values indicate gravel-size sediment.

Table 5-5. Characteristics of channel bed sediments for Sespe Creek at Fillmore.

Sample date	Particle size (nth percentile) [mm]		
	D_{16}	D_{50}	D_{84}
1/14/1969	1.26	**3.38**	**9.07**
2/19/1969	0.63	**9.60**	**31.30**
8/3/1971	0.21	**2.22**	**24.00**

Source: USGS, National Water Information System, Sespe Creek at Fillmore CA (USGS 11113000).
Bold values indicate gravel-size sediment.

Table 5-6. Characteristics of bedload sediment samples from the Santa Clara River at Montalvo.

River discharge		Bedload discharge		Particle size (nth percentile) [mm]		
m^3s^{-1}	cfs	tonnes day^{-1}	tons day^{-1}	D_{16}	D_{50}	D_{84}
0.96	34	56	63	0.27	0.42	0.82
0.99	35	29	32	0.27	0.44	0.87
2	70	132	146	0.35	0.61	0.93
8.4	297	396	437	0.39	0.82	1.95
14.5	512	661	729	0.31	0.57	1.62
15.5	549	324	358	0.34	0.70	1.93
15.6	550	299	330	0.37	0.79	**2.44**
19.5	689	224	247	0.30	0.49	1.18
19.7	695	282	311	0.33	0.63	1.57
20	714	585	645	0.34	0.66	**2.00**
21	740	1,170	1,290	0.34	0.62	1.50
22	786	478	527	0.18	0.38	0.90
24.7	872	228	251	0.34	0.62	1.09
40	1410	971	1,070	0.23	0.42	0.93
44	1560	1,243	1,370	0.54	1.41	**5.78**
47.6	1680	651	718	0.18	0.44	1.33
112.4	3970	unknown	unknown	0.29	0.85	**4.44**

Source: USGS, National Water Information System, Santa Clara River at Montalvo CA (USGS 11114000).
Bold values indicate gravel-size sediment.

Table 5-7. Characteristics of bedload sediment samples for the Santa Clara River at the Los Angeles County Line.

River Discharge		Bedload Discharge		Particle size (nth percentile) [mm]		
m^3s^{-1}	cfs	tonnes day^{-1}	tons day^{-1}	D_{16}	D_{50}	D_{84}
0.09	3.2	3.2	3.5	0.54	1.57	1.60
0.19	6.6	6.1	6.7	0.63	1.35	**3.09**
0.20	6.9	17	19	0.47	1.58	**2.31**
0.21	7.4	16	18	0.43	1.52	1.81
0.21	7.4	1.4	1.5	0.38	1.47	1.91
0.22	7.9	13	14	0.47	1.55	1.93
0.25	8.9	22	24	0.48	1.56	**2.29**
0.26	9.3	1.5	1.6	0.54	1.56	1.97
0.28	10	15	16	0.50	1.58	**2.57**
0.31	11	15	16	0.45	1.54	1.85
0.31	11	6.2	6.8	0.42	1.49	1.90
0.40	14	23	25	0.50	1.57	1.79
0.40	14	10	11	0.36	1.40	1.92
0.45	16	49	54	0.44	1.55	1.81
0.51	18	31	34	0.41	1.50	1.85
0.59	21	44	48	0.40	1.52	1.78
0.62	22	34	38	0.51	1.56	1.93
0.79	28	19	21	0.47	1.04	**3.00**
1.47	52	54	60	0.41	1.57	**2.91**
1.90	67	66	73	0.20	1.72	1.00
2.04	72	47	52	0.17	1.62	1.45
2.69	95	83	92	0.40	1.61	1.73
2.78	98	155	171	0.40	1.20	**10.13**
2.80	99	266	293	0.66	**2.75**	**8.62**
2.89	102	101	111	0.53	1.60	**5.50**
5.30	187	200	221	0.20	1.74	1.38
5.32	188	380	419	0.30	1.35	**2.80**
6.91	244	117	129	0.48	1.18	**4.00**
9.17	324	118	130	0.19	1.08	1.00

Source: USGS, National Water Information System, Santa Clara River at the Los Angeles County Line (USGS 11118500).
Bold values indicate gravel-size sediment.

Table 5-8. Characteristics of bedload sediment samples for Sespe Creek at Fillmore.

River discharge		Bedload discharge		Particle size (nth percentile) [mm]		
m^3s^{-1}	cfs	tonnes day^{-1}	tons day^{-1}	D_{16}	D_{50}	D_{84}
0.8	30	5.0	5.5	0.73	**2.23**	**6.75**
1.1	39	21	23	0.95	**2.83**	**7.24**
1.1	39	25	28	0.75	**2.48**	**6.00**
1.2	43	0.8	0.9	0.40	0.98	**6.77**
1.3	45	5.8	6.4	0.79	**2.13**	**5.43**
2.1	73	16	18	1.41	**3.45**	**7.57**
2.1	74	5.4	6.0	0.83	1.91	**4.50**
3.6	126	15	16	0.35	0.76	**2.00**
5.7	201	44	48	1.04	**2.58**	**6.18**
10.4	366	29	32	1.86	**7.57**	**14.36**
43.9	1550	836	921	1.29	**9.10**	**22.26**

Source: USGS, National Water Information System, Sespe Creek at Fillmore (USGS 11113000).
Bold values indicate gravel-size sediment.

The channel bed at Montalvo is characterized by medium to coarse gravel, whereas bedload samples (collected during moderate flood events) contain mostly sand and fine gravel. Taken together, these observations suggest that the coarser material is mobilized and deposited during relatively large floods which are not represented in the bedload sampling data. For reference, the highest flow sampled for bedload was 112 m^3s^{-1} (3,970 cfs), which has a recurrence interval of 1.3 years. Simons, Li & Associates (1983) calculated that a flow of 57 m^3s^{-1} (2,000 cfs) at the Montalvo gauge is sufficient to mobilize 907 tonnes day^{-1} (1,000 tons day^{-1}) of very fine gravel, 113 m^3s^{-1} (4,000 cfs) is sufficient to mobilize 907 tonnes day^{-1} of fine gravel, 255 m^3s^{-1} (9,000 cfs) is sufficient to mobilize 907 tonnes day^{-1} of medium gravel, and 850 m^3s^{-1} (30,000 cfs) is sufficient to mobilize 907 tonnes day^{-1} of coarse gravel. Previous studies of sediment transport dynamics within the watershed (*e.g.*, Williams, 1979; Noble Consultants, 1989; Warrick, 2002) have concentrated on characterizing the transport of fine sediment through the mainstem and out to the Santa Barbara Channel. The coarse sediment load has been less intensively studied but is a primary factor in the geomorphology of the river channel and in controlling the channel's ability to change over time (*i.e.*, the channel morphodynamics).

5.2 Potential Impact of Infrastructure and Anthropogenic Channel Modifications

Channel-related infrastructure and modifications and land use changes within the watershed since the arrival of European settlers (see Section 3) have affected fluvial geomorphology in the lower Santa Clara River (LSCR) and have contributed to several contemporary challenges for river management. Infrastructure changes include dams constructed during the twentieth century, the failure of the St. Francis Dam in 1928, water diversions, and the construction of roads, bridges, and levees. The most notable direct channel modifications have involved reductions in channel width, due to agricultural use of the floodplain, progressive increases in bank protection associated with levee construction since the 1950s, and the lowering of the channel bed that followed instream aggregate mining (especially during the peak of operations in the 1970s and 1980s). Land use changes that have potentially impacted the fluvial geomorphology of the LSCR include the introduction of ranching (and exotic grass species) following European colonization of the watershed in the mid-1800s (discussed in Section 4.3), the onset of extensive irrigation and associated water diversions (for citrus crops, starting in about 1920), and, more recently, the rapid growth in population and urban area since the 1960s. The potential geomorphic

impact of these various anthropogenic factors is outlined below. Morphological changes known to have occurred in the LSCR over the last approximately 75 years will be discussed in subsequent sections.

5.2.1 Dams

As noted in Sections 3 and 4.4.3 above, major dams (Santa Felicia, Pyramid, Bouquet and Castaic) regulate roughly 36% of the drainage area in the Santa Clara River watershed (Figure 2-6), impounding water for consumptive use and effectively reducing downstream flow compared with what it would have been in the absence of the dams.

Santa Felicia Dam and Lake Piru

Santa Felicia Dam, on Piru Creek (Figure 5-7), was completed in 1955 and operations began the following year. Lake Piru has a reservoir capacity of approximately 109 million m^3 (88,340 ac-ft). Inflow from the floods of January and February 1969 exceeded the reservoir capacity and forced the release of roughly 140 million m^3 (113,500 ac-ft) of water (Simons, Li & Associates, 1983). The intense rainfall during this period contributed to the eventual release of 816 m^3s^{-1} (28,800 cfs) on February 25, 1969, which is the largest recorded peak flow measured downstream of Santa Felicia Dam (USGS 11110000). With exception to this event, flows in Piru Creek have been regulated to below 28 m^3s^{-1} (1,000 cfs) since the completion of the dam. The second largest peak flow measured below the dam was 26 m^3s^{-1} (920 cfs) on September 6, 2000 (USGS 11109800).

Figure 5-7. Santa Felicia Dam, looking downstream. (Photo by Stillwater Sciences)

Pyramid Dam and Lake

In 1971, a second facility was completed in the Piru Creek drainage, upstream of Lake Piru, with the goal of impounding water that was to be imported from northern California under the California Water Project. Reservoir capacity is 211 million m^3 (171,200 ac-ft).

Bouquet Dam and Reservoir

Bouquet Dam impounds imported water in Bouquet Reservoir, in the relatively dry northeastern corner of the watershed. Completed in 1934, the facility has a capacity of 42 million m^3 (33,767 ac-ft), and regulates less than 1% of the watershed area. Its effects on hydrology of the LSCR are probably minimal, due to its location (in the relatively dry eastern headwaters) and its small regulated watershed area.

Castaic Dam and Lake

Castaic Dam, completed in 1972, is a California Water Project facility located on Castaic Creek, well upstream of its confluence with the Santa Clara River. The facility (capacity 401 million m^3 [325,000 ac-ft]) is designed to contain water imported from northern California. The facility is operated on a "run-of-the-river" basis, with releases that equal local natural inputs.

St. Francis Dam

In 1924, construction began on the St. Francis Dam, near Saugus in San Francisquito Canyon. Its reservoir was to serve as a backup water supply for local farmers in the event that supply from Owens Valley was interrupted. The dam was finished to a height of 56 m (185 ft) in 1926 and eventually filled with nearly 50 million m^3 (41,000 ac-ft) of water. Just before midnight on March 12, 1928, a large section of the dam suddenly collapsed, sending a wall of water down the valley towards the Pacific Ocean, 87 km (54 mi) away. The peak water level has been estimated at 24 m (78 ft), and peak flow was probably between approximately 14,000 and 23,000 m^3s^{-1} (500,000 and 800,000 cfs) (Simons, Li & Associates, 1983). Large volumes of mud and debris were entrained in the flow as it rushed first down San Francisquito canyon, and then down the Santa Clara River Valley, affecting the communities of Piru, Fillmore, Santa Paula, Saticoy and much of Ventura along the way (Figure 5-8). At Santa Paula, 68 km (42 mi) downstream from the dam, the water was reported to be nearly 8 m (25 ft) high.

Figure 5-8. The remains of the Saint Francis Dam after collapsing just before midnight on March 12, 1928, in the San Francisquito subwatershed (above). Below, a downstream view of the mainstem Santa Clara River near Santa Paula Creek, the day after the Saint Francis Dam break flood. Photos courtesy of the Ventura County Watershed Protection District.

The reservoir contents emptied into the ocean less than 5.5 hours after the dam broke, but the effects of the flood were long lasting. Nearly 500 people died in the disaster, and parts of Ventura lay under 20 m (70 ft) of mud; total property damage was approximately $5.5 million in 1928 dollars (University of Southern California, 2004). The St. Francis Dam failure changed perceptions about dam safety and water projects in California and was the impetus for the creation of the California Division of Safety of Dams, which regulates non-federal dams in the state (CDSD, 2005). The disaster may have also been the driving force behind calls for increased flood protection along the Santa Clara River in subsequent decades.

Effects of Dams on the Delivery of Water and Sediment to the Santa Clara River

Dams have reduced flow to the Santa Clara River by approximately 26% (based on water budgets reported by Warrick, 2002). Analysis of suspended sediment concentrations and flow from the Santa Clara River and its tributaries indicates that the dams reduce suspended sediment delivery to the mainstem by roughly 21% (see Section 4.4.2 above) (Warrick, 2002), assuming 100% sediment trapping efficiency (Williams, 1979). Bedload delivery to the mainstem is also estimated to have been reduced by approximately 20% due to the influence of dams (Brownlie and Taylor, 1981), but this arises because bedload is estimated partly as a function of suspended load. More research is needed to better understand changes in bedload transport within the Santa Clara River due to the influence of the dams within the watershed.

The effects of reduced sediment yield are generally most severe immediately downstream of dams, where channel incision is commonly observed due to more effective erosion of the channel bed by sediment-starved water (*e.g.*, Williams and Wolman, 1984). The effect diminishes with increasing distance downstream as sediment-laden water from tributaries is added to the flow (Petts, 1984). Therefore, in the Santa Clara River watershed, the impact of dams on channel morphology is probably greatest in the reaches downstream of both Castaic and Piru creeks. In the LSCR, dam-related morphological impacts are presumed to decrease downstream of Fillmore following flow and sediment contributions from Sespe Creek.

The St. Francis Dam break may also have resulted in long-term effects on river morphology. The peak flow of between 14,000 and 23,000 m^3s^{-1} (500,000 and 800,000 cfs), implied by anecdotal accounts, is 3 to 5 times higher than any subsequent peak flow that has occurred at Montalvo (the gauging record extends back to 1928, shortly after the flood). Based on a recent flood frequency analysis (URS, 2005), the dam-break flow had a hydrological return period of 200–1,000 years, although there is likely significant error in such an extrapolation. The relationship between magnitude and frequency implied by data presented in Section 5.1 indicates that the dominant, channel-forming discharge on the Santa Clara River is the largest flood on record. Hence, it can be argued that the St. Francis disaster is the most recent "channel-forming" flow and it is conceivable that many of the large-scale characteristics of the LSCR channel and floodway are relicts of the effects of the dam-break flood.

However, direct evidence for the morphological effects of the 1928 flood is not readily apparent from comparisons between the (somewhat poor quality) 1927 and 1929 aerial photographs. If true, this fact may be at least partly because the flood was unnatural , derived solely from San Francisquito Creek with less sediment than a comparable flood with contributing areas that included other headwater tributaries (which would have contributed additional sediment). In the situation that the St. Francis dam-break flood did indeed have a relatively low sediment load compared to a natural flood of similar magnitude, its primary morphological impact may have been extensive incision in the floodway, which would not show up clearly in aerial photographs.

5.2.2 Aggregate Mining

Aggregate mining has been the greatest single anthropogenic factor in the form of the LSCR. Large volumes of aggregate resources designated by the California Geological Survey (CGS) in both the upper Santa Clara River (USCR) (in the Saugas-Newhall Production-Consumption Region [SNPCR] of Los Angeles County) and LSCR (in the Western Ventura Production-Consumption Region [WVPCR] of Ventura County) have attracted long-standing interest in aggregate mining (Figure 5-9). Small-scale operations began in the early 1900s, often using riverbed lands leased from farmers; operations grew larger during and after the Second World War (Schwartzberg and Moore, 1995). The relatively dry period from 1944–1968 may have contributed in making the extraction of riverbed aggregate resources far less challenging than it might be under wetter conditions such as those since 1969.

Aggregate mining was largely unregulated until county permitting requirements were introduced in the early 1970s. This was followed by State regulations including the Surface Mining and Reclamation Act (1975). Years that followed were marked by growing interest in the environmental and economic impacts of mining, especially those related to channel incision. By 1979, the Ventura County Environmental Resource Agency stated "…the loss of riverbed materials and accompanying channel degradation is primarily, if not totally, the result of gravel mining from the channel" (Schwartzberg and Moore, 1995). Of particular concern was the prospect that channel incision would undermine bridges and other infrastructure. For example, the demise of Saticoy Bridge in the 1969 floods had been blamed on erosion of the bridge's pilings due to channel incision (Schwartzberg and Moore, 1995). Other effects of channel incision included the repeated need for the United Water Conservation District to move its earthen dam at Saticoy progressively upstream to retain sufficient gravity flow for water diversion until, in 1991, a permanent concrete diversion, the Vern Freeman Diversion Dam, was constructed to fix the point of water diversion. Despite these concerns, instream mining is reported to have peaked between 1981 and 1986 (Noble Consultants, 1989). Finally, in 1985, the Board of Supervisors of Ventura County and the Ventura County Flood Control District jointly issued a revised "red line" restriction on the depth of permissible gravel mining, where the red line defines a grade that is deemed to reduce the risk of upstream erosion. The new red line reduced available resources in the WVPCR to 128 million tonnes (141 million tons)—some 91 million tonnes (100 million tons) short of the CGS 1993 estimate of the 50-year aggregate demand for the WVPCR (CDMG, 1993, as cited in AMEC, 2004), and led to the cessation of instream aggregate operations in Ventura County by 1989 (SCREMP, 1996, as cited in AMEC, 2004). Two out-of-river operations continued through 1996 and all Ventura County reserves were considered depleted by 2003 (AMEC, 2004). One large-scale operation continues to extract aggregate resources within the 500-year floodplain, east of Santa Clarita in the SNPCR.

There are few recently published rates of aggregate extraction for the Santa Clara River. Simons, Li & Associates (1983) estimated annual aggregate extraction rates for the LSCR (WVPCR) for the period 1960–1977, of which an estimated 63.3% occurred directly from the Santa Clara River channel. Table 5-9 lists the extraction rates by year from instream sites. The average annual rate of extraction for the period of record is 1.71 million tonnes (1.89 million tons). More recent reports (*i.e.*, Noble Consultants, 1989; SCREMP, 1996; AMEC, 2004) discuss aggregate mining but do not contain any updates on extraction rates.

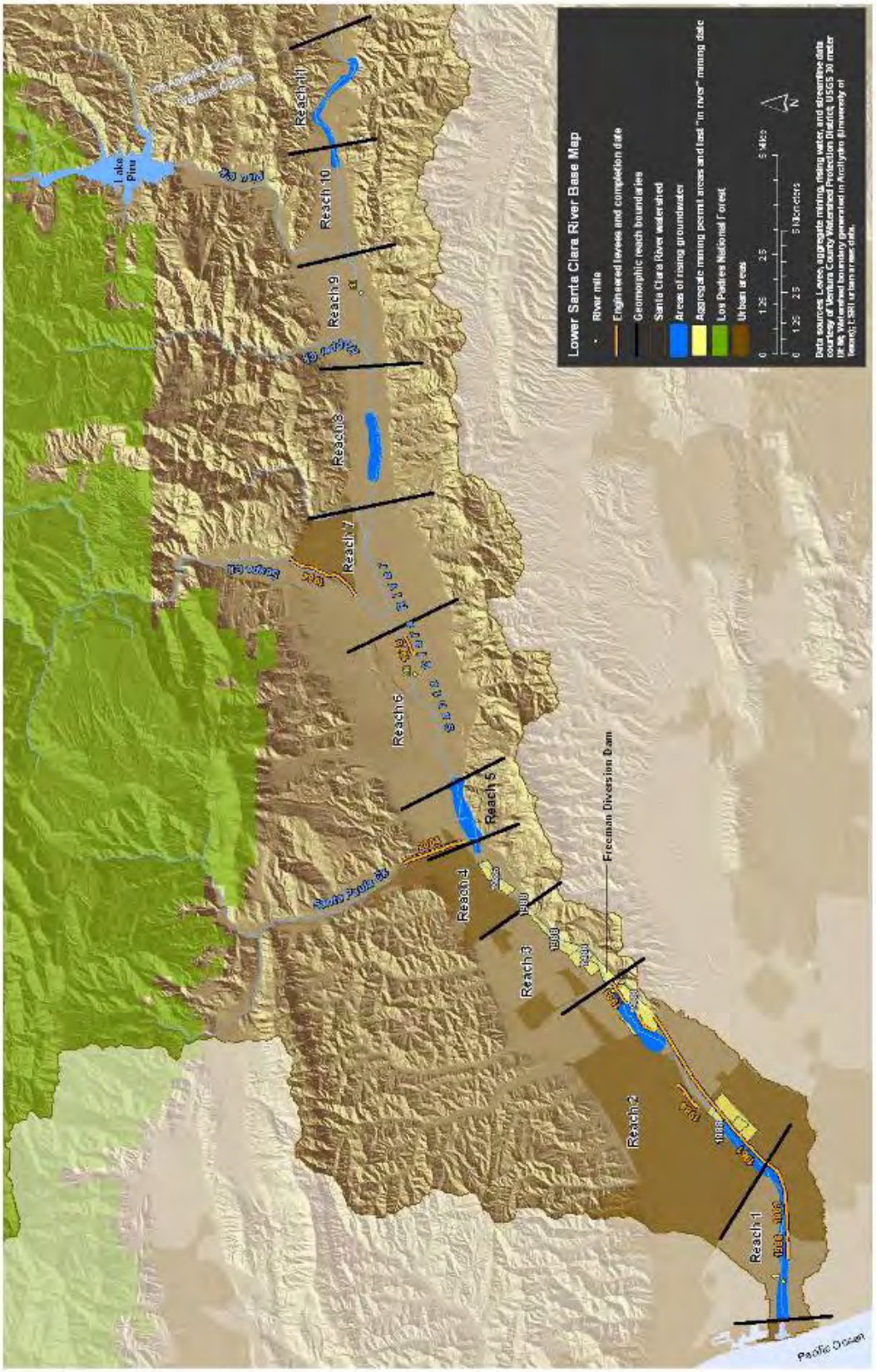

Figure 5-9. Lower Santa Clara River showing sites of instream aggregate mining (and date of last mining) and public levees. Reach numbers refer to geomorphic subreaches discussed in Section 5.3 onward.

Table 5-9. Sand and gravel production from the lower Santa Clara River 1960–1977.*

Year	Instream aggregate production	
	(thousands of tonnes)	(thousands of tons)
1960	1,260	1,389
1961	1,783	1,965
1962	2,523	2,781
1963	1,278	1,409
1964	1,242	1,370
1965	2,039	2,247
1966	1,857	2,047
1967	1,647	1,815
1968	1,606	1,770
1969	2,061	2,272
1970	1,849	2,038
1971	2,178	2,401
1972	1,908	2,104
1973	2,155	2,376
1974	1,453	1,602
1975	1,347	1,485
1976	837	922
1977	1,626	1,792
Mean	1,710	1,890

*Note: The figure given is 63.3% of the estimated total production, estimated as the direct proportion mined from the channel.
Source: CDMG (1977) in Simons, Li & Associates (1983, p 2.41).

Effects of Aggregate Mining

Aggregate mining has been identified as the primary cause of continual river bed lowering in the Santa Clara River:

> *"Preliminary studies indicated that sand/gravel mining was the dominant factor causing continuous lowering of the river bed. Mining has affected not only degradation and general river morphology, but also groundwater recharges, riparian habitat, beach sand supply and the stability of bridges, flow diversion work and pipeline crossing"* (Simons, Li & Associates, 1983, p.xiii)

The potential effect of mining activity is readily apparent when the average annual extraction rate (1.71 million tonnes yr^{-1}) is compared to Brownlie and Taylor's (1981) estimated annual sand and gravel yield (1.08 million tonnes yr^{-1} for the period 1956–1975, which post-dates dam construction) (Brownlie and Taylor, 1981), and their estimated "natural" yield (1.35 million tonnes yr^{-1}) for the entire watershed—*i.e.*, including areas regulated by dams. Extraction activities thus were removing sand and gravel faster than it was being replenished. However, comparisons between annual extraction and replenishment rates are complicated by the highly episodic nature of sediment transport in the Santa Clara River.

Instream mining has the potential indirect effect of causing knickpoint erosion, if the thalweg of the stream manages to connect with the mining pit. Mining pits beside the channel on the floodplain (*i.e.*, from out-of-stream mining) can be "captured" as well (Collins and Dunne, 1990; Kondolf, 1994a, b) when levees are breached in large flood events. For a river like the Santa Clara, which is prone to large floods, pit captures are virtually unavoidable. "Channel piloting", which involves dredging a low-flow channel

to guide flow away from the pits, was practiced on the Santa Clara River but has probably not reduced the likelihood of pit captures during high flow events, when water levels far exceed the height of low-flow channel banks. Once a river is connected to a deep pit, the headwall of the pit acts as a significant step (or knickpoint) in the channel profile. If the headwall erodes, the knickpoint may migrate upstream until such a time that the channel returns to an equilibrium long profile (*e.g.*, Parker and Andres, 1976). The distance of upstream migration will depend on (1) the ability of channel bed material to hold up as a headwall before becoming "smoothed out", and (2) on the original depth of the pit (which may also control the depth of channel bed lowering). As knickpoints migrate upstream, mass failures of river banks become likely due to an increased tendency for the channel to widen (Harvey and Watson, 1986; Simon, 1989). Erosion and undermining of bridge supports and other in-channel infrastructure may also occur.

The Simons, Li & Associates (1983) study remains the definitive work on mining-related concerns in the Santa Clara River. It includes field surveys and aerial photograph assessments of changing channel morphology and effects on levees, bridges and pipelines (Figure 5-10). It also includes hydraulic and sediment transport modeling and sediment routing studies that assess future concerns and scour potential. It resulted in recommendations for proposed mining activities, revisions to the red line standard and, in a related study, the design for the Freeman Diversion Dam. Proposed restrictions on mining were based on consideration of structural stability, sand and gravel replenishment rates and downstream channel impacts. Scour analysis identified concerns for the stability of numerous structures

Figure 5-10. Undercutting of the Highway 118 bridge over the Santa Clara River as a result of incision following the 1969 floods. (Photo courtesy of the Ventura County Watershed Protection District)

including several levees, the proposed Freeman drop structure, three bridges (Highway 101, 118 and

Willard Bridges) and the Shell Oil Pipeline. Sand and gravel replenishment rates under historical and proposed mining operations were estimated to be low. Hence it was recommended that mining should be restricted to reaches that were aggrading except for the aggrading reach upstream of Willard Bridge was was considered off-limits for mining because any downcutting would potentially threaten the bridge.

An additional sediment routing study in the LSCR was undertaken by Noble Consultants (1989). The study used an erodible-boundary model, FLUVIAL-12 (Chang, 1985), which differs from erodible-bed models in that it allows reach-scale variations in sediment yield to be reflected in changes in channel width in addition to depth. The model used design hydrographs and sediment transport rates based on the Engelund-Hansen formula, and it confirmed a complex pattern of erosion and deposition along the river. Moreover, it predicted changes in channel width and depth due to aggradation and incision associated with instream mining activities. The predicted mean annual sediment yield at the downstream end of the LSCR (at Harbor Boulevard) was 220,000 tonnes yr^{-1} (240,000 tons yr^{-1})—much lower than Brownlie and Taylor's "natural" yield estimate of 1.35 million tonnes yr^{-1} (1.49 million tons yr^{-1}). This discrepancy has been cited as an indication of the potential effect of sand and gravel mining on beach replenishment (Noble Consultants, 1989). Also, using a combination of Meyer-Peter and Müller and Einstein equations to characterize coarse (> 0.25 mm) sediment transport, and using triangular hydrographs to representing notable floods, Simons, Li & Associates (1983) estimated that the bed material replenishment rate in the LSCR averaged 145,000 tonnes yr^{-1} (160,000 tons yr^{-1}), far lower than the 1960–1977 average extraction rate, underlining the potential long-term morphologic effect of instream aggregated mining.

Significant instream mining ceased shortly after the Noble Consultants (1989) report was published. A sequence of significant flood events (in 1992, 1995, 1998 and 2005) has occurred since and, given that sediment transport during large events is far larger than the annual average sediment yield, there is little obvious sign of the former in-channel mining pits. What is less certain is whether the legacy of mining activities still affects geomorphic processes and channel form along the LSCR. Repeat bed elevation surveys from 1929–1993 supplemented by LiDAR imagery conducted after the 2005 flood is used to analyze trends in channel bed-level changes in Section 5.3.4.

5.2.3 Levees and Bank Protection

Flood flows from the LSCR historically spilled onto the Oxnard Plain and flowed towards the Pacific Ocean. However, since the 1950s, a series of 53 levees have been constructed along nearly 40 km (130,000 ft) of river bank length (URS, 2005),amounting to approximately 33% of the total LSCR bank length in Ventura county). The levees include both public and private structures, constructed independently on left and right banks, and designed variously to protect agricultural lands, urban development and floodplain mining pits. Many of the private levees are composed of riverbed materials and are designed to protect agricultural land from flooding; these typically have to be repaired or re-constructed after large floods. Several of these structures are themselves protected by earthen or stone groins projecting perpendicular from the levee and designed reduce the velocity of near-bank flood flows that might otherwise undermine the levee. Notable public levees began with the 1961 completion of a US Army Corps of Engineers structure designed to protect agricultural land along the south side (left bank) of the LSCR between South Mountain and Highway 101 (Figure 5-9). The levee was intended to prevent inundation of flows of up to the standard project flood (6,375 m^3s^{-1}, 225,000 cfs). The Ventura County Watershed Protection District now manages this stone-revetted levee, along with an adjoining structure from Highway 101 to Victoria Avenue which was reinforced with stone revetment during the

construction of the Victoria Avenue Bridge in 1976. Stone-protected or soil cement-cored levees have been constructed for flood and erosion protection of urban developments, including some that project into the historical river course.

Damage to levees occurs during flood events. In 1969, for example, a 610 m (2,000 ft) reach of the South Mountain–Highway 101 levee failed due the combined effect of the January and February flood events. Further flood damage to the downstream levee and to the Saticoy "dike" (which protects Cabrillo village) occurred during the 1978 events (Simons, Li & Associates, 1983). The damage was attributed primarily to undercutting brought about by channel incision associated with the effects of aggregate mining.

Effects of Levees and Bank Protection

Levees confine high discharges that would otherwise spill onto neighboring floodplains, reduce the effective flow width during floods, and are frequently intended to stabilize the river's planform (*e.g.*, Figure 5-11). However, because they exceed the natural elevation of the floodplain, the contained flood flows run deeper and generate increases shear stresses on the channel bed compared to the situation if the flow was able to spill over the banks. Increased shear stresses increase the chance of channel bed incision but, because flood sediments are also confined within the channel rather than being deposited onto the floodplain, large amounts of sediment may be deposited instream as the flood recedes. Hence, the net change in bed elevation along reaches that are bounded by levees depends on several factors and is difficult to predict, especially with the compounding influence of aggregate mining.

Where levees are used in conjunction with bank protection to "train" the channel to a particular planform there is the risk that, if the imposed channel planform does not align with the natural planform tendency during flood events (or if the channel is simply too narrow), the flood thalweg will flow directly towards

Figure 5-11. View across the Santa Clara River in Reach 2 (near Saticoy) on the lower Santa Clara River showing the 1961 Army Corps of Engineers levee (left bank) during the recession of the 2005 flood. Active floodplain aggregate mining in the foreground. (Photo courtesy of the California State Coastal Conservancy)

the levee in certain locations. This will lead to high near-bank flow velocities and the potential for levee

erosion. This effect is accentuated in incising channels wherein the levee toe can be prone to failure and lead to levee breaches. The 1969 flood (documented by Simons, Li & Associates, 1983) apparently produced just such an effect, with flow spilling out through a left bank breach downstream of Victoria Avenue in the direction of historical flood overflows. Many levees have been reinforced with exterior stone revetments and soil-cement cores that can help defend against such erosion and earthen and stone groins projecting into the flow are used to deflect high velocity flows before they attack the banks. However, notable erosion of some levees and other protected banks still occurred in the 2005 floods (see Appendix D). An additional impact of protected levees is that flood flows can be reflected towards an opposing, unprotected bank that would not otherwise be prone to substantial erosion.

5.2.4 Irrigation and Flow Diversion

Surface water diversions were first established during the 1860s and 1870s to irrigate the rapidly developing farmlands of the Santa Clara River valley and the Oxnard Plain. An extensive network of ground water supply wells was also established throughout the valley to supplement the increasing water demand for agricultural, domestic, and industrial purposes. In 1912, a total of 16,580 acres were being actively irrigated by surface waters diverted from the Santa Clara River and its tributaries (Freeman, 1968). As agriculture in the Santa Clara River watershed grew and shifted more towards producing citrus crops, especially after World War I, surface water irrigation became an increasingly unreliable source for large scale irrigation enterprises. By 1965, the total number of irrigated acres from diverted surface water originating from the river and its tributaries decreased to approximately 2,500 due to reductions in surface water availability (Freeman, 1968) and more than 90% of water required for all uses in the SCR valley and Oxnard Plain was supplied by ground water (~800 wells).

Following its formation in 1925, the forerunner to United Water Conservation District began surface water diversions from Piru Creek in 1930 and from Santa Paula Creek in 1931 to meet the growing water demands in the valley (see Figure 3-1). The amount of irrigated area therefore increased markedly due to the combined efforts of these surface water diversions, several water supply reservoirs, and vast network of groundwater supply wells (see Table 5-10). More recently, the main diversion from the Santa Clara River at Saticoy was stabilized by the construction of the Vern Freeman Diversion Dam following a period in which the diversion had to be moved progressively upstream to maintain sufficient gravity flow for the water diversion.

Table 5-10. Irrigated acreage in Ventura County.

Year	Irrigated Area[1]	
	km²	acres
Early 1900s	65	16,000
1912	69	16,580
1919	128	31,700
1925	142	35,000
1949	436	107,689
1969	409	101,140
1980	431	106,480
1991	**421**	**103,921**

Source: Freeman, 1968; SCREMP, 2005.

[1] Comprises (a) surface water diversions until 1912, (b) surface water diversions and ground water wells from 1919 to 1925, and (c) a combination of diversions, wells, and reservoirs since 1949.

Effects of Irrigation and Flow Diversion

The increase in irrigated crop land caused a general lowering of the groundwater table in and near the Santa Clara River mainstem. The first water wells drilled on the Oxnard Plain in the 1870s were initially free-flowing, or artesian; however, by the 1900s decreased water pressures resulting from over-drafting of the groundwater supply from the underlying aquifer required pumps to be installed (Freeman 1968). Since the 1930s, active replenishment of the over-utilized groundwater supplies has been managed within the Santa Clara River watershed using both surface water diversions and reservoir releases to infiltrate directly into the stream beds or onto spreading grounds (e.g., Piru and Saticoy Spreading Grounds). Zones of both rising groundwater and surface water loses to the subsurface continue to occur throughout the LSCR due to interactions between tributary basin inputs and geologic constraints (Figure 5-9). However, present day groundwater withdrawls and recharge management activities have strongly influenced these gaining and losing reaches, especially during dry years when water supplies are insufficient to meet demand thus resulting in significant lowering of the water table.

The lowered floodplain groundwater tables may have led to the death of riparian vegetation and to reductions in vegetation thickets on the floodplain and gravel bars since the 1930s (Faber *et al.*, 1989), but also at this time, vegetation was routinely cleared from riparian areas for fule supply, grazing and farming, and flood conveyance (see Section 3.1). Either way, the potential geomorphic impact of this reduction in riparian vegetation would likely result from the reduction in vegetative roughness on the channel bed which would allow flows to entrain bed sediments at lower discharges and thus potentially to increase sediment loads during floods—especially during moderate events which might previously not have been sufficient enough to remove established vegetation from the channel bed. Reduced riparian vegetation can also reduce the threshold for channel-bank erosion, which could lead to rapid widening of the river. Such an effect has been documented along the Carmel River in central California, where water supply wells reduced groundwater levels, causing riparian dieback and channel widening (Kondolf and Curry, 1986). For rivers whose slope and sediment load places them on the boundary between being a meandering river and a braided river (see Section 5.3.1), vegetation reductions may cause the river to transform into a braided channel more frequently. As braided rivers are generally very wide, this can have substantial effects on riparian land use.

5.2.5 Urban Growth

Population in the watershed has increased approximately ten-fold since the 1940s (Figure 5-12), with much of the growth occurring along the mainstem corridor where increases in urbanization have been substantial. Increases in population and urbanization will undoubtedly continue into the foreseeable future and are likely to have an increasingly noticeable effect on geomorphic processes in the lower river corridor.

Effects of Urbanization

There are two major geomorphic effects on the LSCR that are related to urbanization. The first arises where construction occurs close to the river and requires levees for flood protection. Where the levees constrain the width of the river, accelerated erosion can result. This local effect has been considered under levees and bank protection in Section 5.2.3. The second impact may be of greater regional consequence. It arises as a consequence of hydrological changes bought about by the increasing area of impermeable surface that accompanies population growth and urban expansion (*e.g.,* Leopold, 1968). The hydrological changes generally take the form of higher peak flows and a shorter time-to-peak discharge for the flood flow.

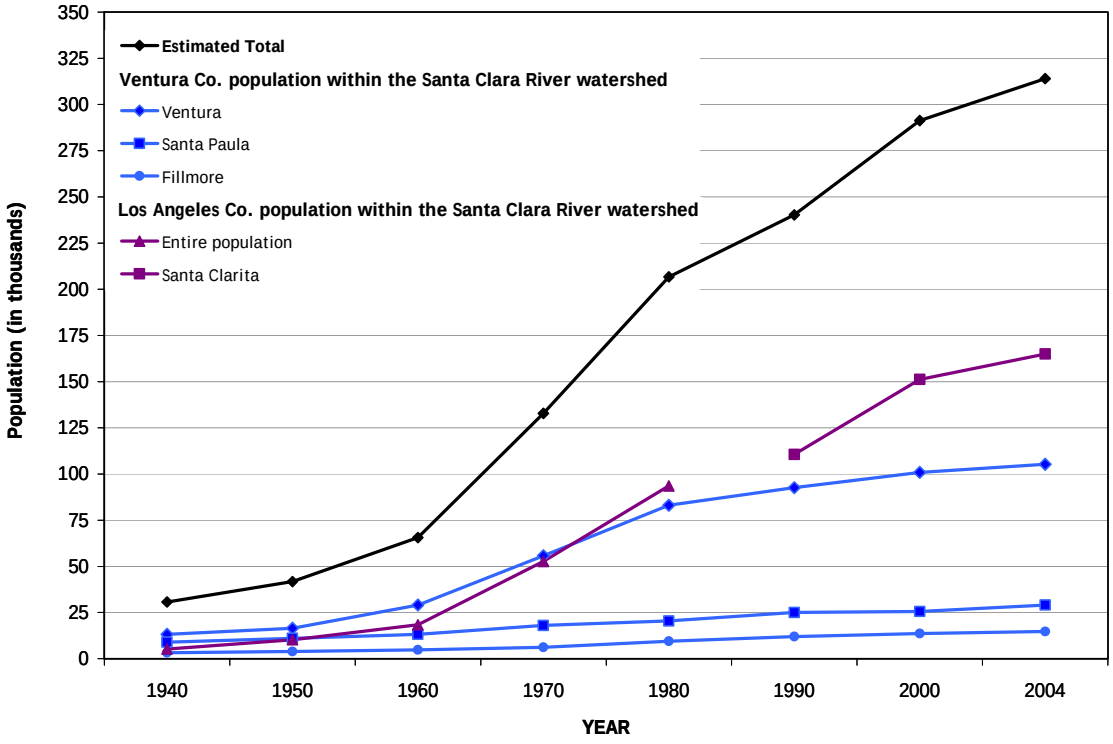

Figure 5-12. Population in major settlements of Los Angeles and Ventura counties within Santa Clara River watershed.

Geomorphic impacts are usually associated with the increasing frequency of intermediate flood flows that cause progressive channel incision and enlargement (*e.g.*, Roberts, 1989; Bledsoe and Watson, 2000, 2001) and armoring of the channel bed following erosion of the initial pulse of construction-related sediment (*e.g.*, Wolman, 1967). However, these impacts have to be taken in context when considered within the LSCR. First, geomorphic activity is concentrated into very large-magnitude flood events; therefore, it is unclear whether increasing the magnitude of intermediate flood events from the upper watershed will have a significant impact on the downstream channel morphology. Second, urban expansion is currently focused in the Santa Clarita region of the upper watershed and may have less impact in the lower watershed due to the influence of incoming creeks (*e.g.*, Santa Paula, Sespe) on the morphology of the lower river. Farther downstream, the effects of urban expansion in Ventura County, which has also been significant (Table 5-11), may have been manifested primarily by erosion in the barrancas leading to the Santa Clara River rather than in the Santa Clara itself. Whether the barrancas provide significant sediment supply to the mainstem Santa Clara River remains unclear.

Table 5-11. Population in major settlements of Los Angeles and Ventura counties within Santa Clara River watershed.

	Los Angeles Co. population within the Santa Clara River watershed		Ventura Co. population within the Santa Clara River watershed			
Year	Santa Clarita	Entire population	Ventura	Santa Paula	Fillmore	Estimated Total
1940		5,260	13,264	8,986	3,252	**30,762**
1950		10,269	16,534	11,049	3,884	**41,736**
1960		18,362	29,114	13,279	4,808	**65,563**
1970		52,700	55,797	18,001	6,285	**132,783**
1980		93,600	83,084	20,450	9,538	**206,672**
1990	110,642		92,600	25,062	11,992	**240,296**
2000	151,131		100,916	25,598	13,643	**291,288**
2004	164,900		105,299	29,056	14,736	**313,991**

Sources:
http://www.santaclaritamagazine.com/Pages/scvdemo02.html;
http://www.dof.ca.gov/HTML/DEMOGRAP/Hist_E-4.xls;
http://www.dfg.ca.gov/HTML/DEMOGRAP/90e-4.xls;
http://www.dof.ca.gov/HTML/DEMOGRAP/E4call.htm

As potential context, there has been recent analysis of the sediment gauging record from the nearby Santa Ana River (Warrick and Rubin, 2007; Warrick, 2003). The Santa Ana is also a large southern Californian watershed but one in which approximately 40% of the watershed has been developed to house a population of approximately 6 million people (from 1 million in 1955; Warrick, 2003). Because of increased runoff due to urban development since the late 1960s, flow discharge has increased while the suspended sediment concentrations have decreased. The total annual sediment discharge has not changed, even though it is now delivered in lower concentrations throughout the year. In relative terms, flow discharge has increased ahead of sediment discharge resulting in clearer flows that have proved capable of incising the channel bed. While the effects observed in the Santa Ana may not yet be relevant to geomorphic processes of the less-urbanized Santa Clara River watershed, it is nevertheless possible that continued population growth along the corridor will eventually lead to similar relative increases in runoff over sediment load, enhancing prospects for bank and bed erosion in the LSCR, leading to additional morphologic change of the river planform and long profile.

It is not yet possible to reach a conclusion on the overall impact of upstream urban development on the LSCR. In part any effects of urbanization cannot be distinguished from impacts related to rainfall variability, aggregate mining, levee construction, flow impoundment and diversions, land use changes and, potentially, the Saint Francis dam-break. However, as illustrated by the Santa Ana watershed, it is likely that continued urban development will eventually result in a discernable morphological response at some point in the future and the response will be similar in style to those seen in many urbanized watersheds around the world.

5.3 Morphology and Channel Dynamics

The lower Santa Clara River (LSCR) today flows for approximately 61 km (38 miles) through Ventura County (Figure 5-9) to the Pacific Ocean. In planform, it is characterized by a wide, relatively straight floodway with one or more low-flow channels that are re-configured after each flood event. The overall mainstem channel is filled only during high-magnitude floods. Erosion of alternate outer banks of the

active floodway in some reaches following large floods in January-February 2005 (see Appendix D and Figure 5-13) suggests that the entire floodway of the contemporary LSCR behaves in a manner similar to a broad, single-thread meandering channel at very high flows. As floods recede, the river becomes more braided in character, with multiple flow courses. There is insufficient perennial flow to retain multiple flowing channels in a majority of the LSCR and, in general, a single dominant channel defines the channel thalweg. In some reaches, however, residual flow continues to be carried by secondary channels.

The long profile is gently concave, with gradients ranging from approximately 0.0060 to 0.0025 near the river's mouth and an average gradient of 0.0041. The LSCR transports a mixed load of sediment ranging from fine sand to coarse gravel (see Section 5.2.3). Dominant sediment sizes have been recorded to range from medium sand to very fine gravel (Simons, Li & Associates, 1983), but this may partly reflect a bias towards finer sediment that covers the bed as flood flows recede. Reconnaissance following the January-February 2005 high-magnitude floods indicated that the river can transport coarse gravel to the Santa Clara estuary. The channel morphology occupied by the 1.5-year recurrence interval flood event (186 m^3s^{-1}; 6565 cfs downstream from the confluence with Sespe Creek: equivalent to a "bankfull" event for humid single thread channels) is not clearly defined in morphological terms (for reasons, see Section 5.1) but, according to hydraulic model calculations undertaken in HEC-RAS (URS, 2006), would result in average wetted channel dimensions of 247 m (810 ft) wide, and 1.0 m (3.3 ft) deep.

The morphology and dynamics of the current LSCR likely differ quite significantly from the LSCR prior to Euro-American colonization of the Santa Clara watershed. Prior to the availability of detailed

Figure 5-13. Westward, downstream view of the Sespe Creek confluence (two channels entering from right) following the January 2005 flood. South Mountain is in the upper left of photo. (Photo courtesy of the California Coastal Conservancy)

morphological data from approximately 1930, two aspects of particular influence may have involved land-cover changes that accompanied large-scale ranching activities (the Ranching and Colonization phase in Figure 3-1), and groundwater changes that occurred following groundwater abstraction for crop agriculture (the Irrigation and Diversions phase in Figure 3-1). As indicated in Section 3 and Section 4.4, ranching is likely to have resulted in changes to the rainfall-runoff regime and erosion regime on hillslopes, resulting in flashier flood flows of higher magnitude carrying larger quantities of sediment, especially fine sediment. River changes linked to ranching would quite probably have occurred in 1862 and 1884; two large floods that occurred in a period of prolonged dry conditions (1841–1884). The onset of crop agriculture, involving the draining of groundwater from the Oxnard Plain and the wholesale removal of riparian vegetation, is likely to have resulted in notable reductions in baseflow in the LSCR, and far easier erosion of river channel sediments in flood events because of reduced protection by riparian vegetation. River modifications associated with this activity would have been most acutely felt following large flood events such as the large flood of 1914. Overall, the LSCR seems likely to have undergone a fundamental shift in its hydrology and sediment supply regime towards higher-magnitude flood flows carrying greater amounts of finer-textured sediment, and with less protection of the bed and banks from erosion. Thus, the river was more vulnerable to rapid changes in channel morphology during highly concentrated flood events. Near to 1930, the impact of the 1928 St. Francis dam break is not clearly demarked. As postulated in Section 5.2.1, the event may have resulted in considerable incision but conversely, as the LSCR channel was not confined by levees at this time, the flood flows may have spread across the floodplain thereby reducing the overall impact on channel morphology.

These potential historical impacts serve as context in examining the morphology and river channel dynamics of the LSCR since 1930. Significant river channel changes resulting from Euro-American population growth in the watershed had already occurred, so that some of the post-1930 changes identified in the following sections may have been, at least in part, legacy responses to impacts caused by watershed changes prior to 1930.

5.3.1 Reach-level Differences in Channel Form

It is unlikely that the morphology and channel dynamics of the 61-km (38-mile) LSCR varies consistently along the entire length of channel: instead there are most likely reach-level differences in the channel response that may have important implications for river management, including that management solutions may vary from reach to reach. As such, the LSCR was sub-divided into 11 reaches, ranging from approximately 2.5 to 10-km in centerline length (1.5 to 6 miles) according to criteria that were expected to lead to different morphological properties between reaches (Table 5-12). These criteria include tributary junctions (where additional flow and sediment are received) and degree of channel confinement, whether by valley walls or by constructed levees. Using post-flood 2005 aerial photographs, the active channel width varied from approximately 220–570 m (720–1870 ft), with the large 2005 flood scouring the channel bed clear of vegetation over widths ranging from 180 to 510 m (590–1670 ft). These 11 reaches are the basis for all later analyses in this section.

Table 5-12. Lower Santa Clara River reach characteristics.

	Reach 1	Reach 2	Reach 3	Reach 4	Reach 5	Reach 6	Reach 7	Reach 8	Reach 9	Reach 10	Reach 11
Reach Boundaries (downstream to upstream)	*Harbor Blvd Bridge* – *101 Bridge*	*d/s Freeman Dam* – *u/s Freeman Dam*	*Shell Rd*	*Santa Paula Ck.*	*East flank South Mt.*	*Sespe Ck.*	*1 mi E Cham'berg Rd.*	*Hopper Ck.*	*Piru Ck.*	*2.5 mi E Piru Ck.*	*LA County Line*
Indicative River Mile	0.00	4.10	10.23	13.00	15.19	17.00	21.53	24.50	27.99	31.10	33.50
Start distance[1] (ft)	2,800	24,448	56,800	71,440	83,000	92,560	116,500	132,160	150,600	167,000	179,680
End distance[1] (ft)	24,448	56,800	71,440	83,000	92,560	116,500	132,160	150,600	167,000	179,680	203,000
Centerline reach length[2] (m)	6,412	9,967	4,715	3,503	2,545	6,803	5,267	5,710	4,745	4,445	6,076
Reach-average slope[2]	0.0025	0.0027	0.0025	0.0039	0.0031	0.0036	0.0048	0.0055	0.0053	0.0062	0.0055
Active channel width 2005[3] (m)	222	350	265	384	456	474	570	422	542	555	146
Fully-scoured width 2005[3] (m)	203	305	185	195	396	368	444	394	434	511	117
Bankfull width[2] (m)	223	215	159	156	186	365	312	317	287	360	104
Bankfull depth[2] (m)	1.44	1.37	1.51	1.34	1.20	1.01	0.78	0.60	0.56	0.47	0.70
Bankfull discharge[2] (m^3s^{-1})	185.9	185.9	185.9	185.9	185.9	185.9	89.5	60.6	60.6	54.2	52.9
Local characteristics	Wide floodplain, part of natural distributary area for the river. Largely straight channel, levees on left bank, urban area behind.	Wide floodplain, part of natural distributary area for the river. Levee along most of left bank, and a short stretch of the right. Urban development to channel edge along most of the right bank, and downstream along the left bank. Gravel mining until 1988 in the lower and upper reach. Upstream extent bounded by Freeman Dam.	Left bank impinges on South Mountain. Gravel mining throughout the reach until 1988. Freeman Diversion Dam provides grade control at the downstream end.	Left bank close to South Mountain, urban development to edge of right bank. Some revetment on right bank. Gravel mining until 1986. Receives unregulated inflow from Santa Paula Creek.	Left bank impinges on South Mountain. Downstream end is confluence with Santa Paula Creek	Wide floodplain, channel in center: sinuous and braided. Levee at upstream end opposite Sespe Creek confluence. Receives unregulated inflow from Sespe Creek.	Urban development to right bank edge in upper part of reach, right bank leveed in this area. Downstream end is confluence with Sespe Creek	Wide floodplain floor. Upstream left bank close to mountains. Sinuous and braided. Inflow from Hopper Canyon	Wide floodplain floor, channel veers towards towards left bank mountains. inuous and braided. Received highly regulated flow from Piru Creek.	Wide floodplain floor. Channel in valet center. Highly regulated flows.	Last narrow valley segment. Highly regulated flows (upstream from Castaic Creek). Heavy agriculture use adjacent to floodway.

Notes:
[1] Derived using SCREMP report, supplemented by data from 2005 LiDAR images, where necessary
[2] Derived from HEC-RAS output
[3] Derived from GIS analysis of post-flood aerial photography (Flood peak 3,851 m^3s^{-1})

Classification of the channel pattern into a distinct typology provides important first step in understanding the morphodynamic behavior of river systems. However, channel pattern within the LSCR is clearly stage-dependent and does not fit neatly into simple classification schemes (*e.g.*, Rust 1978's division into straight, meandering, braided or anastomosing channels). Using more complex graphical classifications, the LSCR at various flow stages could qualify as one of several of the 14 patterns identified by Schumm (1981, 1985, as developed by Knighton 1998, p.206) and does not obviously fit any of the channel patterns in Shen et al.'s (1981) graphical matrix of possibilities, reinforcing the sense that the LSCR does not operate like a "classic" alluvial channel. To explore the poorly predicted character of the LSCR, various "discriminant" analyses were performed (Figure 5-14a-d) to evaluate channel typology by reach. All reaches conform to the braided category using Wolman and Leopold's (1957) slope-discharge-based distinction (Figure 5-14a), but the number of braids should range from 1-2 to 10 (generally increasing upstream) according to ratios devised by Parker (1976; Figure 5-14b). Additionally incorporating grain size, the river plots between the gravel-bed braided and sand-bed braided distinction implied in analyses by Ferguson (1987) and Knighton and Nanson (1993) (Figure 5-14c). Conversely, average reach conditions plot into the single-thread channel conditions predicted by Van den Berg (1995) on the basis of median grain size and unit stream power (Figure 5-14d), although the channel is less sinuous than those forming Van den Berg's data set.

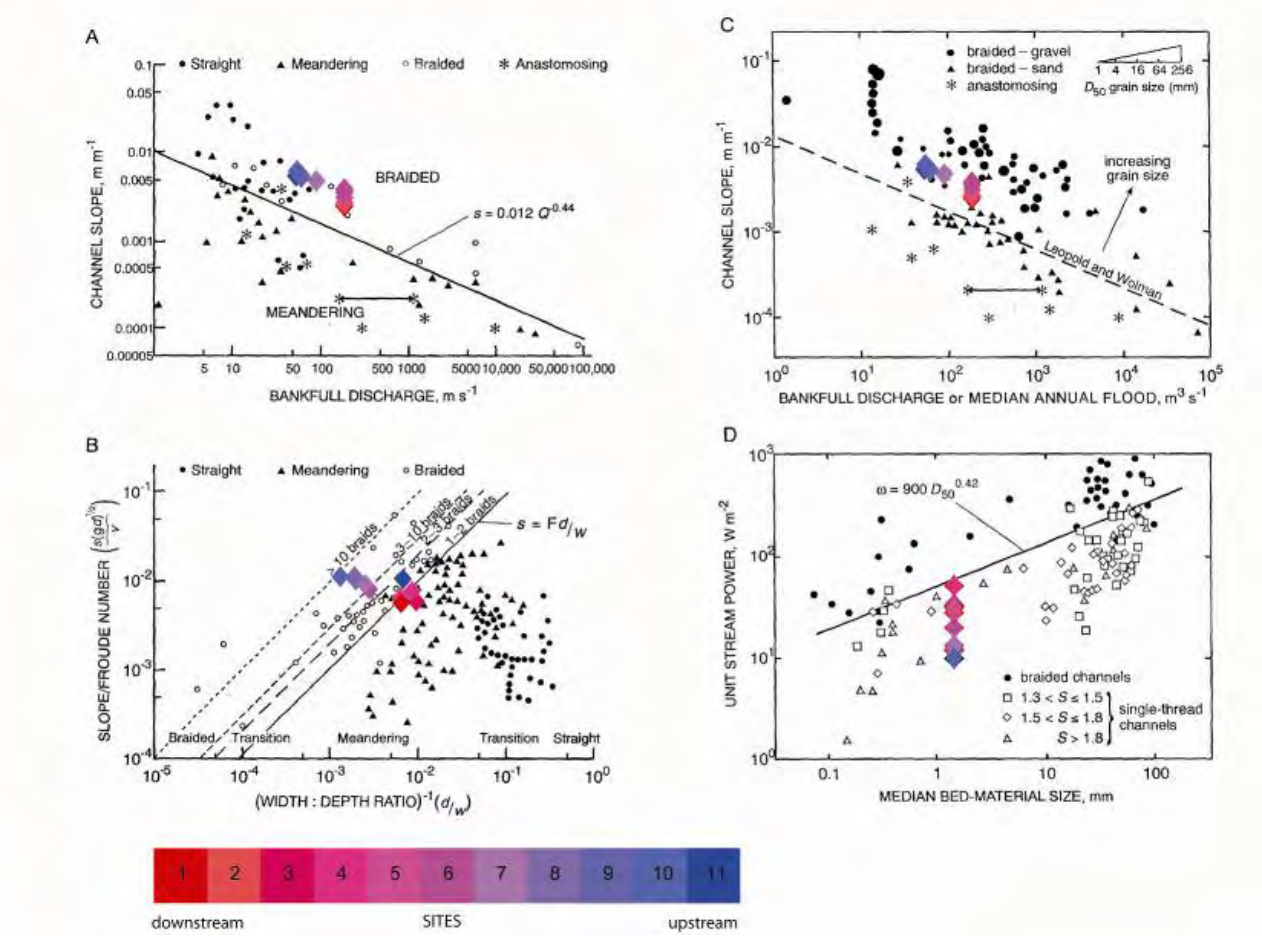

Figure 5-14. Predicted channel pattern for the lower Santa Clara River by reach. See text for details of data sources. Note that the pattern is classified variously as braided (A) and meandering (D), between braided and meandering (B), and on the transition between sand- and gravel-bed braided rivers (C).

Using a pattern classification developed for dryland rivers with highly variable flows (Graf 1983, 1988a, 1988b), or implied in regions with extended drought- and flood-dominated flow regimes (*e.g.*, Warner 1987, 1994; Erskine and Warner 1988), the LSCR can be classified as a "compound" channel. Graf's compound channel definition arises from research primarily in Arizona. He described compound channels as having two modes of operation: a single meandering channel at low flow and a braided channel at higher flows (1988b, p.202). Compound channels are differentiated from braided channels by the existence of a dominant sub-channel and because the meandering channel fits within the overall braided channel form (Graf, 1988b, p.202). While the LSCR shares several of these characteristics, especially the nested channel form and, usually, a dominant sub-channel, it is clearly differentiated from Graf's examples because the floodway is retained within reasonably component channel banks (unlike Graf's) and so exhibits more of a single thread form at higher flows, while it is braided at lower flows. Compound channel morphology has also been described in south-east Australia where flood and drought cycles lasting on the order of decades result in a distinct "channel-in-channel" morphology for single thread channels during drought periods as the channel narrows, and subsequent widening during the flood-dominated periods (Warner 1987, 1994 ; Erskine and Warner 1988). While the LSCR is affected by multi-decade wet and dry periods, analyses of channel width changes in the less incised reaches (see Section 5.3.2) suggest that the active channel width is apparently correlated most strongly with the influence of *individual* flood events, primarily those resulting from ENSO oceanic conditions (see Section 5.1.2; Figure 5-5), than any overall equilibrium 'wet' and 'dry' condition.

On balance, the planform of current LSCR is unusual and does not fit neatly into any reviewed classification. Primarily because the river has two distinct functional regimes, it is a variation on a compound mixed-load channel. The low-flow regime exists for the majority of the time and consists of a dominant low flow channel and, occasionally, several minor channels, which meander across the sand and gravel bed of the active channel bed. During these periods, little sediment transport occurs. Summer flows are maintained by dam releases and urban effluent flows. In some areas, subsurface bedrock controls cause groundwater to flow towards the surface; elsewhere, flow is lost to the channel bed (Figure 5-9).

The LSCR's high-flow regime occurs very intermittently in response to high-intensity rainfall events, usually occurring between December and March. Such flows are capable of inundating the majority of the channel floodway (average width of flow during the 1969 flood of record was 922 m; 3024 ft) and cause the channel to function as a single-thread, low-sinuosity channel. Rates of sediment transport are very high and morphological change occurs primarily by bed scour during flood events. Events can result either in the net transport of material out of the LSCR (i.e., channel incision), or into the LSCR resulting in channel bed aggradation (see Section 5.4.1). In the largest events, alternate erosion of the outer banks of the active floodway can occur (observed following the January-February 2005 floods, see Figure 5-13 and Appendix D). It is possible that the river had more in common with Graf's dryland river examples prior to human impacts that have resulted in considerable channel incision (see Section 5.3.3).

Overall, this indeterminacy of channel form relative to 'classic' channel typologies described elsewhere means that caution should be used in interpreting behavior of the LSCR, and that management solutions must be drawn distinctly from the observed characteristics of the LSCR rather than being imported from potentially dissimilar river elsewhere.

5.3.2 Potential for Change

More changeable river channels generally pose a greater risk to nearby human activities and infrastructure. For example, land uses next to a channel that erodes its banks frequently are more likely to be compromised than

those next to a stable channel. Therefore, gauging the likelihood of potential change can be one means to assess relative hazard between multiple river reaches.

An index for reach-level potential for morphological change can is the unit stream power. Unit stream power is the energy available per unit area of river bed to overcome friction and transport sediment. It can be used in predicting sediment transport (*e.g.*, Bagnold 1960, 1966, 1973, 1977; Gomez 2006; Gomez and Church 1989), and more generally it is a surrogate for the energy available to "do work" in the channel (Bull 1979). Higher stream power is indicative of channels more likely to change their form (Richards 1982, Graf 1983). Stream power has also been used in typing river channels, but as with channel planform predictions, the observations for the LSCR do not correspond well with published studies elsewhere in the world (Nanson and Croke, 1992; Ferguson, 1981). Of further note, stream power in the LSCR increases dramatically with larger flood events, due to orders-of-magnitude increases in discharge between small and large flood events. Unit stream power values in a 1.5-year flood event average 24 Wm^{-2}, while stream power values reach an average of 126 Wm^{-2} in a 10-year event, suggesting the rapid increase in the river's ability to adjust and transport sediment in larger floods.

In addition, unit stream power does not decay smoothly toward the river's mouth (*i.e.*, from Reach 11 to Reach 1 in Figure 5-13), as commonly found at the downstream end of an alluvial river (*e.g.*, Lawler, 1992; and others). This occurs, first, because of a significant step increase in discharge in the LSCR that occurs below Reach 7 at the confluence of Sespe Creek. The additional discharge imparts a quite different ability to transport sediment above and below the Sespe Creek confluence, necessary to accommodate the influx of sediment from Sespe Creek. Second, the downstream decay trend is also interrupted because of reach-scale variability in slope and channel width: slope is 'anomalously' high in Reach 4 and width is especially narrow through Reaches 3 and 4. The result is that unit stream power peaks in Reach 4, rather than in Reach 11, as might otherwise be expected. Such local deviations in stream power values indicate differential sediment transport and adjustment capacities at a scale of resolution finer than can be achieved by comparing transport capacities at a few individual gauging stations. Hence, the pattern implies that the potential for erosive change is greatest in Reach 4, alongside and downstream of the city of Santa Paula, and the likelihood of erosion-based adjustment remains high in Reaches 1 to 5. Normally, rivers approaching their mouth would be expected to trend towards deposition. In the LSCR, the relative potential for depositional adjustment is greatest in Reaches 7–10. Such patterns may partly result from natural factors, but are also undoubtedly related to human activities (see Section 5.2).

Table 5-13. Reach unit stream power estimates for the LSCR.

Recurrence interval flood event	Unit stream power (Wm^{-2})										
	1	2	3	4	5	6	7	8	9	10	11
1.5-year	27	27	32	51	31	20	13	12	12	10	33
2-year	47	54	58	94	42	28	19	17	18	15	57
5-year	95	118	136	244	62	44	38	37	42	39	159
10-year	99	185	199	286	83	56	45	58	69	66	227
50-year	168	392	214	540	98	108	85	113	148	135	425

5.3.3 Changes in Active Channel Width: 1938-2005

The compound channel of the LSCR comprises a primary low-flow channel and various short-lived secondary channels, inset within a larger mainstem channel that is filled only during large-magnitude floods. The low-flow channel boundary changes rapidly and completely during flood events according to the magnitude of the event and other factors, whereas the boundary of the mainstem channel changes relatively less frequent but carries greater importance in determining the relationship between the river's geomorphology and human

activities on the adjacent floodplain. The risk of bank erosion is focused primarily where the flow thalweg is directed towards the mainstem banks during individual flood events. An earlier attempt to identify bank erosion risk on the LSCR between Willard Bridge in Santa Paula downstream to the Highway 118 bridge (PWA *et al.*, 1997), using a numerical model of potential meander progression (Johannesson and Parker, 1989; Larsen, 1995, and see Larsen and Greco, 2002), met with only limited success. This shortcoming is another consequence of the differences between the Santa Clara River and a more "classic" perennial meandering river, both in terms of its morphology and because the concept of dominant discharge does not readily apply (see Section 5.1.1). In morphological terms, the thalweg prescribed by the Santa Clara River during the 2005 flood event, as indicated by the areas of bank erosion and preserved in the primary (low flow) channel, appeared to switch back and forth across the river far more frequently than predicted by the meander progression model. This may arise through the influence of natural constraints (*e.g.,* river bluffs) and levees in deflecting flow, but it is also a characteristic of braided rivers, wherein single braids act like an individual meandering river of far smaller width and consequently far shorter meander wavelength than would be prescribed by the overall mainstem flow width.

Unlike meandering channels that generally have a well-defined break between the mainstem channel and its floodplain, the mainstem boundary of the LSCR is less well-defined. Because of the intermittent flow, changeable morphology, and rapid colonization of the channel bed by riparian vegetation between flood events, the divide between the floodplain and the "active channel" (that defines the mainstem boundary) is only evident following relatively large flood flows and is even then subject to interpretation according to the extent of apparent flow inundation and re-working of channel bed sediments achieved by the flood event. Prior empirical investigations of channel change have focused both on the position of the primary low-flow channel, to the extent it is discernable, and on the extent of the full width of flood flow evident from aerial photographs of the LSCR (*e.g.,* the maps and supporting text in Section III of Simons, Li & Associates, 1983). However, for this geomorphological analysis, the "active channel width" is a more useful metric.

The "active channel width" is defined here as that part of the channel bed that carried a significant part of the flood and sediment discharge during the recent flood event. The active channel width was designated using an analysis of large-scale aerial photographs from 1938, 1945, 1969, 1978, 1992, 1995, and 2005, in ESRI ArcGIS, using similar methods to studies in dryland rivers by Graf (1984, 2000), Tiegs and Pohl (2005), and Tiegs et al. (2005). A technical account of the methods is found in Appendix E. Partial coverage provided by photographs from 1927 and 1929 were excluded from analysis because of their poor textural quality. Discrete polygons were digitized on the channel bed to define (1) clear-scoured channel bed without vegetation, and so clearly subjected to significant flow; (2) partially vegetated areas showing evidence of having been subject to flow and erosion and/or deposition; and (3) densely vegetated areas on the channel bed without evidence for scour or deposition in the last flood. Hydrologically, the latter areas may have been inundated during the last flood event, but the effects related to geomorphic processes were minor. The extent of active channel was designated to include all polygon types (1) and (2). The analysis was run for each set of aerial photographs over the entire LSCR, or to the extent possible according to photographic coverage (see Appendix E).

Dividing the total area of active channel by the length of each channel reach provided a measure of the average active channel width for each date (Figure 5-15) and a variety of associated statistics (Table 5-14). Figure 5-15 shows a general trend for the active channel width to have become narrower over time. In Table 5-14, the normalized standard deviation of active channel widths indicates two distinct reach groups: those reaches that have been more changeable over time (Reaches 1, 5, 6, and 7: normalized standard deviation ≥ 0.49) and those that have been less changeable (Reaches 2, 3, 4, 8, 9, 10: normalized standard deviation ≤ 0.36). In a dryland river like the SCR that is subject to episodic large floods, it would be reasonable to assume that in its natural condition the active channel width varies proportionally with the magnitude of the previous flood event: as

such, a statistically strong positive correlation between the parameters would be expected. However, Table 5-14 shows this relationship to exist only in four of the reaches (5, 6, 7, and 10: $r^2 \geq 0.48$), while far stronger relationship exists between discharge and time (except in Reaches 5 and 6). Together, these results suggest that in the LSCR only Reaches 5 and 6, from the confluence with Santa Puala Creek upstream to the confluence with Sespe Creek, are freely adjusting according the magnitude of individual floods. This result would not be expected in a naturally fluctuating semi-arid river channel and it suggests that there are additional influential factors. These factors are likely the human activities that have acted to reduce the width of the active channel bed in the last 65 years.

Table 5-14. Width statistics for the LSCR for the period of record 1938-2005 by reach. Figures in bold are referred to in the text. Reach 11 is excluded from analysis because of limited photo coverage.

Date	Follows flow (m^3s^{-1})	Active Channel Width (m)										
		1	**2**	**3**	**4**	**5**	**6**	**7**	**8**	**9**	**10**	**11**
2005	3,851	222	350	265	384	456	474	570	422	542	555	146
1995	3,115	209	331	277	224	391	402	463	305	473	470	99
1992	2,945	229	357	204	265	279	528	465	297	515	521	112
1978	2,890	347	405	393	431	508	677	584	586	519	487	
1969	4,670	1412	511	624	519	1230	1406	1542	642	687	738	
1945	2,265	497	662			330	519					
1938	3,398	1501		605	583	561	847			758	743	256
Weighted Average (m)		603	493	473	458	502	660	745	480	623	617	
Standard Deviation (m)		473	150	168	151	297	323	446	163	159	161	
Normalized StdDev		**0.78**	0.30	0.36	0.33	**0.59**	**0.49**	**0.60**	0.34	0.25	0.26	
r^2 of width vs magnitude of last flood		0.28	-0.04	0.33	0.25	**0.71**	**0.53**	**0.77**	0.32	0.29	**0.48**	
r^2 of width versus time		-0.49	-0.92	-0.74	-0.67	**-0.031**	**-0.14**	-0.56	-0.62	-0.76	-0.59	

Further detail on the factors acting to constrain flood flows was obtained by creating two sets of maps, overlaying the active channel bed width from each set of aerial photographs. First, the channel bed was plotted first in terms of the time (as a proportion since 1938) that the bed has occupied a given position (Figure 5-16a-g) to indicate the relative likelihood of channel courses and, second, the width of the bed in successive floods was overlaid with the most recent on top (Figure 5-17a-g) to indicate trends in flood width. Reach 1 is anomalous in that the active channel width is highly changeable and yet has narrowed in time. Comparison of the two map sources indicates that this occurs because, whereas the reach was previously free to inundate and move sediment across a wide extent of floodplain (*i.e.*, 1938; Figure 5-17a), levees have confined all subsequent floods except 1969, which broke through the levees and re-occupied the former flood extent. Reach 1 is the reach that has previously been described as loosing more of its floodway than any other reach (SLA, 1983): the maps confirm this conclusion and indicate that, since the 1990s, active channel width during floods has become narrower still (see Table 5-14 and Figure 5-15).

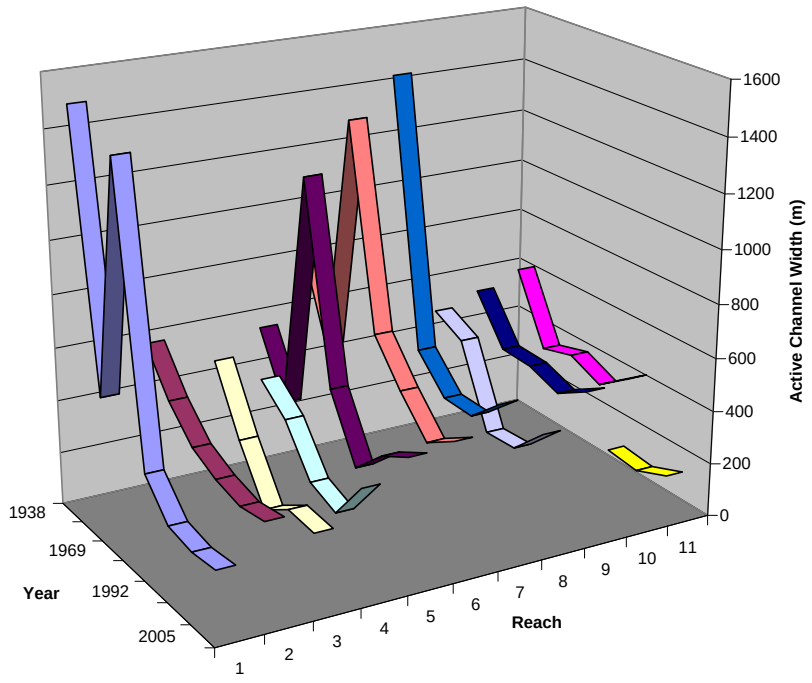

Figure 5-15. Channel width change by reach.

Reaches 2, 3, and 4 share similar attributes in that each has become narrower in time, irrespective of the flood event magnitude, and they are not highly changeable in planform. Whereas the lack of adjustment in Reach 3 may be partly an attribute of the confinement of the left bank by South Mountain, Reach 2 has been stabilized by levees and the course of Reach 4 may have been influenced by short lengths of bank protection. Although the flood in 2005 was the second largest on record, the flood outline occupied a relatively narrow trace through Reaches 2, 3, and 4. Significant extents of each of these reaches were permitted for aggregate mining, indicating that changes may have been partially related to channel incision that typically follows aggregate mining.

Reaches 5, 6, and 7 also display similar planform response attributes to the recent flood events. These three reaches are the most changeable in the LSCR and are largely free to adjust in accord with the magnitude of the flood event. Large areas along Reaches 5 and 6 have been inundated in the last flood events, and their changeability is highlighted in Figure 5-16 by the lack of a contiguous course of channel occupation (i.e., breaks in the polygon recording a probability of occupation between 0.86–1.0). These reaches are both downstream of the confluence with Sespe Creek and thus may owe their behavior to the pattern of deposition of sediments emanating from Sespe Creek. Conversely, Reach 7 is upstream of the Sespe Creek confluence and it holds a more stable planform alignment even though the flood width varies according to the flood magnitude. This attribute is presumably a response to backwater effects of the mainstem in response to the frequently greater discharge emanating from Sespe Creek.

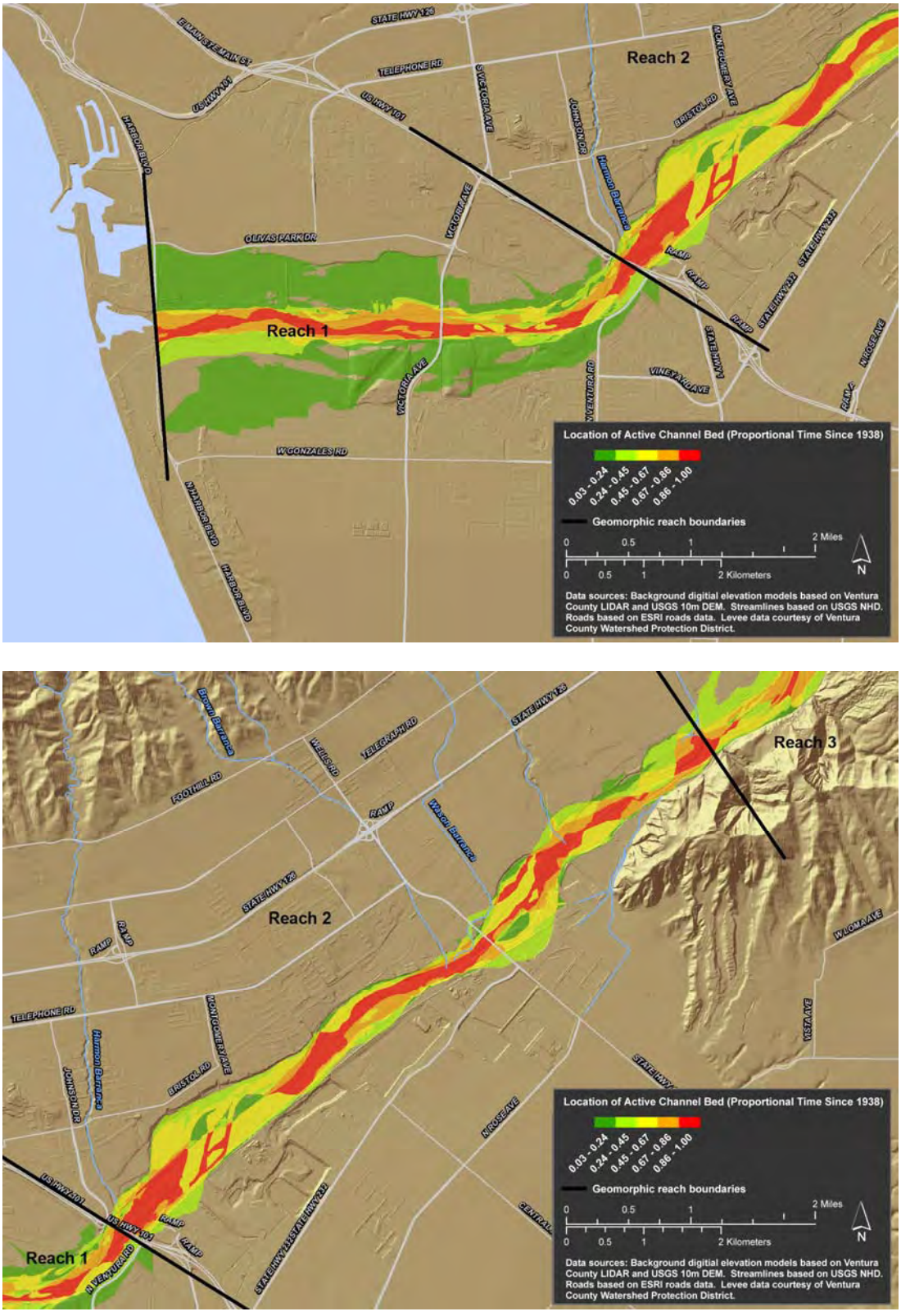

Figure 5-16. Lower Santa Clara River historical channel position: proportion of time since 1938 that the active channel bed has occupied a given location.

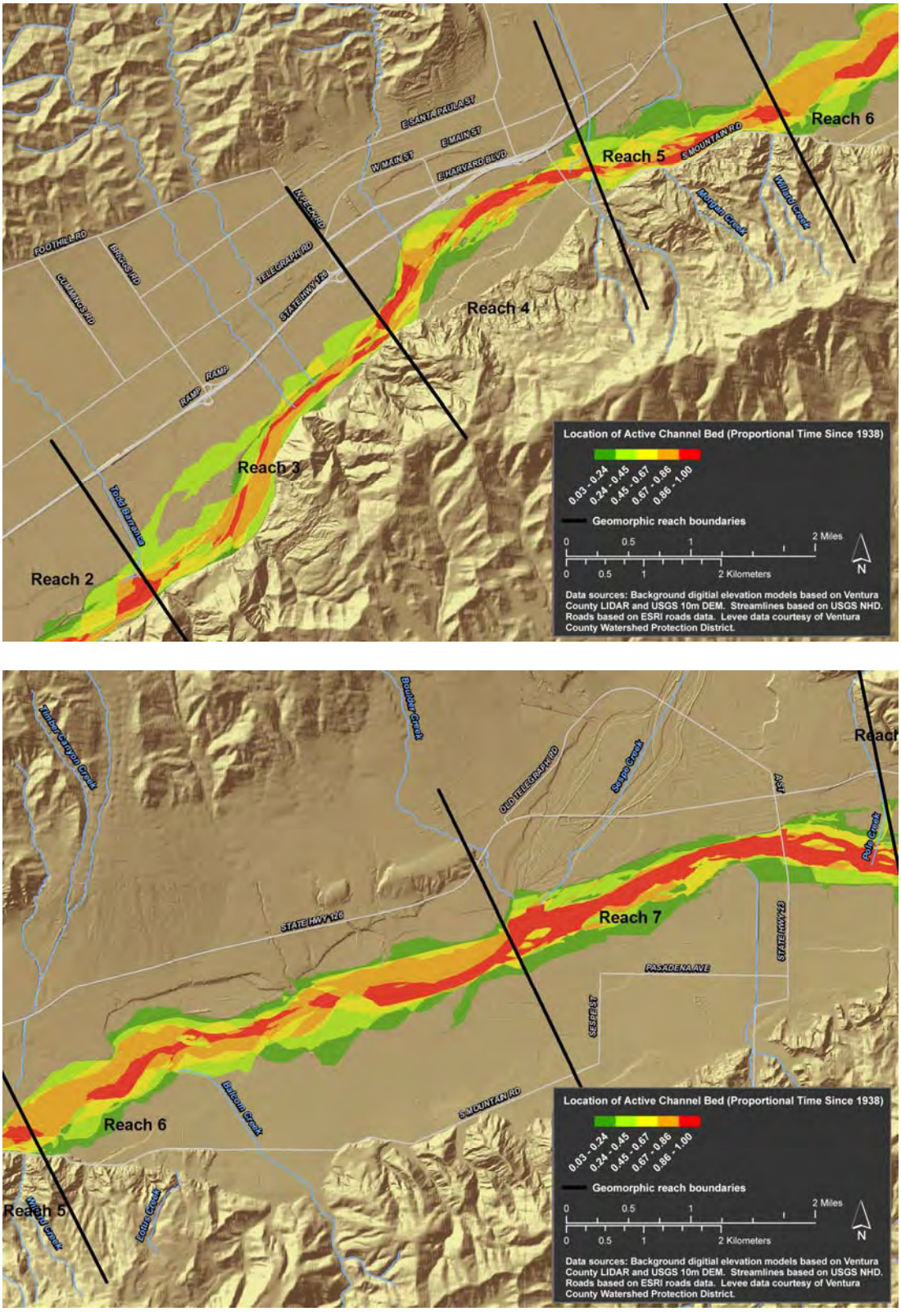

Figure 5-16. Lower Santa Clara River historical channel position: proportion of time since 1938 that the active channel bed has occupied a given location (continued).

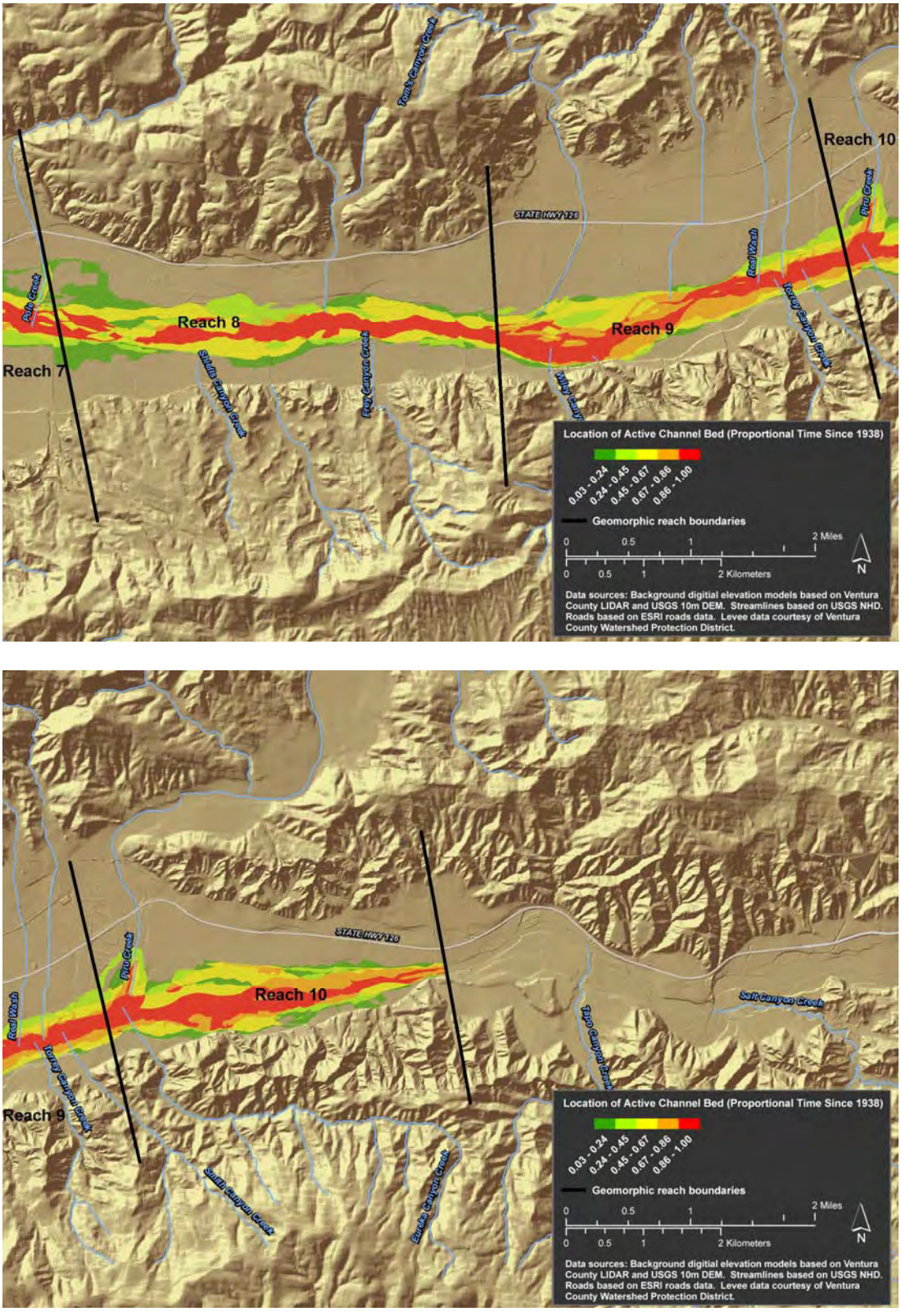

Figure 5-16. Lower Santa Clara River historical channel position: proportion of time since 1938 that the active channel bed has occupied a given location (continued).

Figure 5-17. Width of channel bed in successive floods since 1938 on the lower Santa Clara River: most recent floods on top.

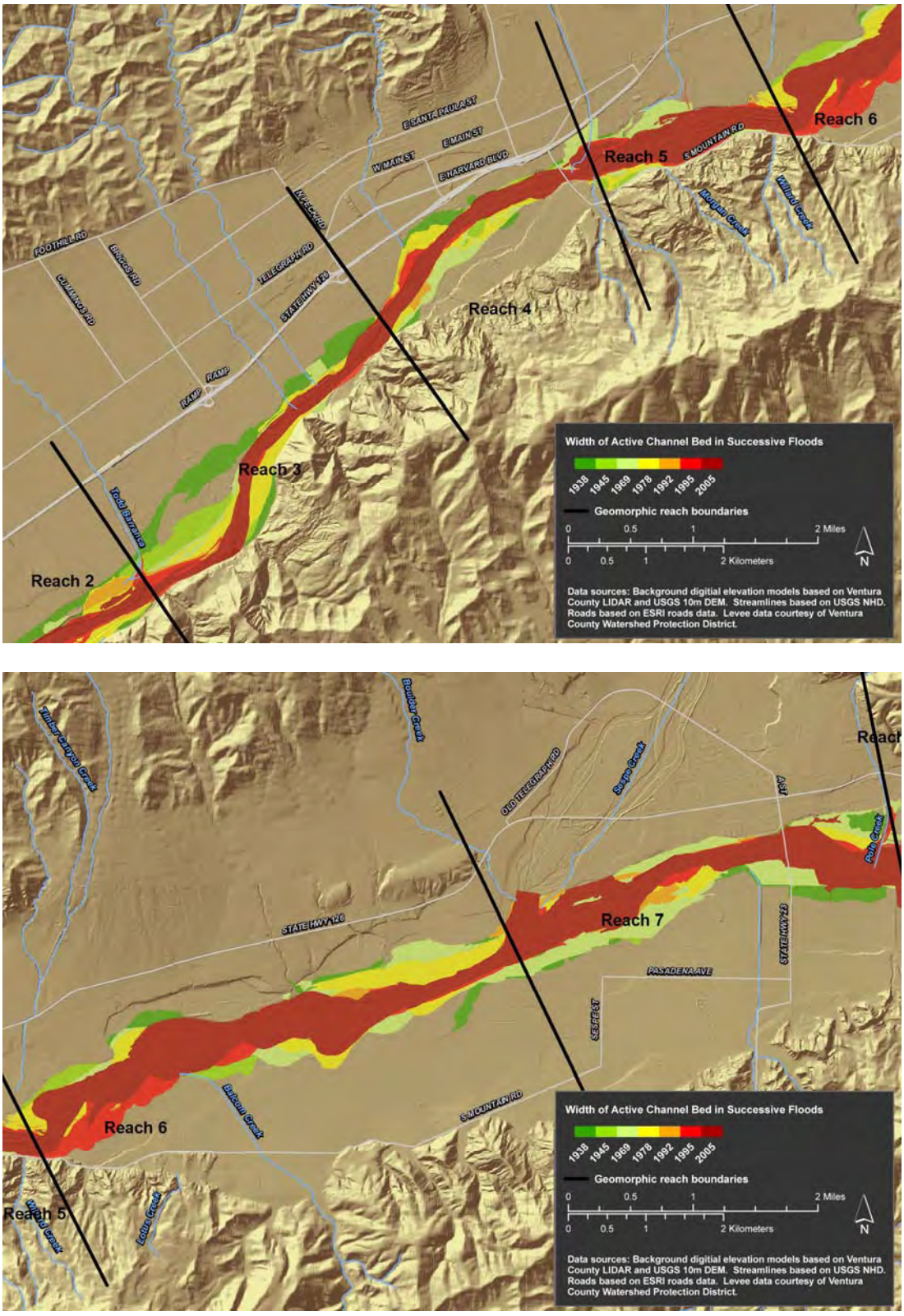

Figure 5-17. Width of channel bed in successive floods since 1938 on the lower Santa Clara River: most recent floods on top (continued).

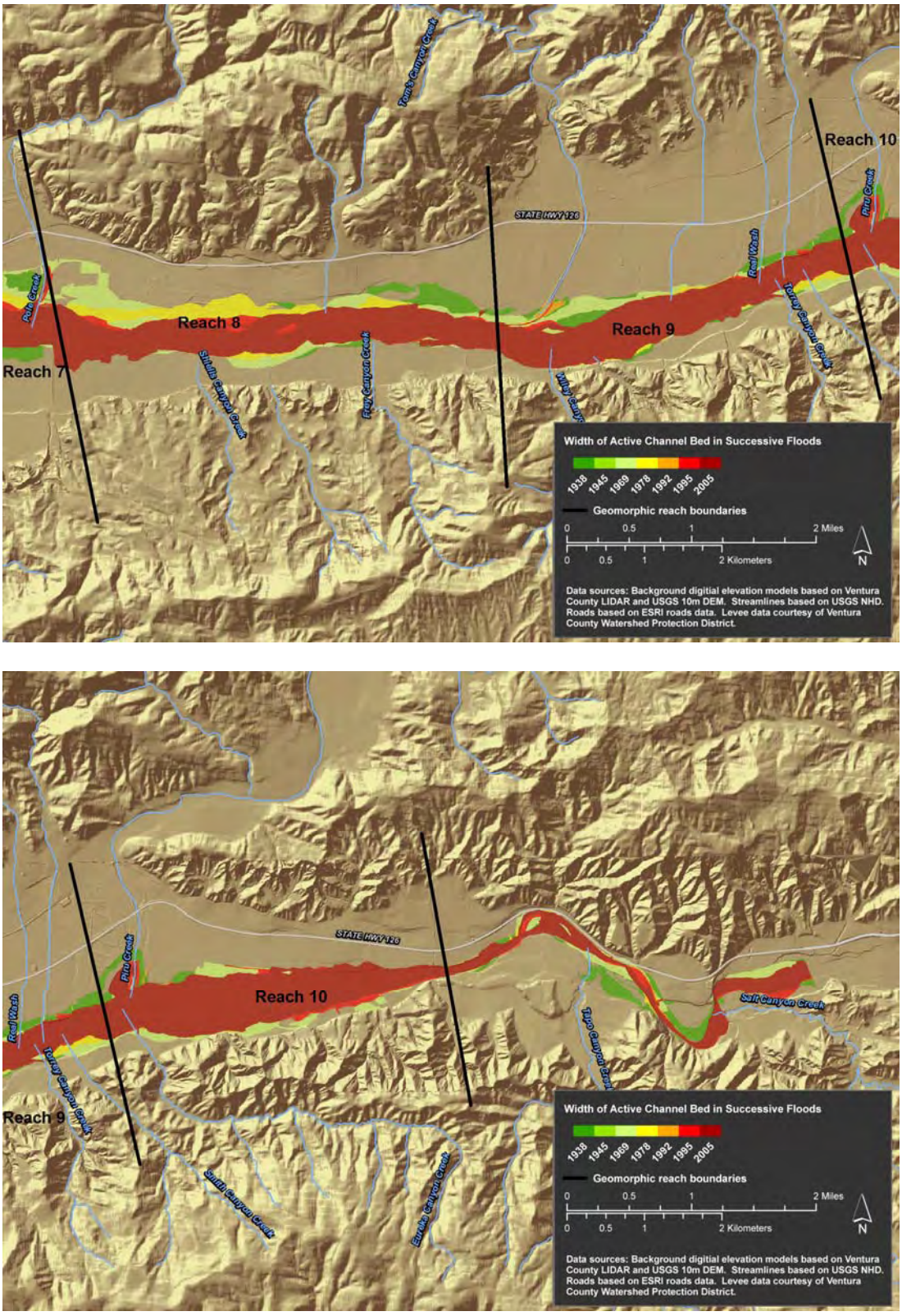

Figure 5-17. Width of channel bed in successive floods since 1938 on the lower Santa Clara River: most recent floods on top (continued).

The active channel bed through Reaches 8, 9, and 10 is less changeable than that of the reaches downstream, and it has become narrower over time. Unlike Reaches 2, 3, and 4, these reaches are not confined by engineered levees, and have not been subject to in-stream aggregate mining. The reaches may be less changeable than those downstream because the reaches do not experience the extreme flows promoted downstream of the confluence of Sespe Creek. The estimated 1.5-year recurrence interval discharge in Reaches 8-10 is approximately 60 m^3s^{-1} (2,120 cfs) (URS, 2006), whereas flow is estimated at 186 m^3s^{-1} downstream of Sespe Creek (Table 5-12). Consequently these reaches generate lower unit stream power in the 1.5-year recurrence interval event (Table 5-13) than farther downstream, exhibiting values that might be expected in a lowland river. As such, they may be naturally less changeable. However, these reaches also show a consistent reduction in width over time (Figure 5-15), suggesting that other factors are influential. Chief among these may be flow regulation, especially of Piru Creek by Santa Felicia Dam. Since its construction in 1955, all flows except those in 1969 have been regulated to below 28 m^3s^{-1} (1,000 cfs) (the 1969 peak discharge was 816 m^3s^{-1}: 28,800 cfs). Using gauge information from above Lake Piru (USGS11109600) indicates that, without regulation, large flows ($\geq$283 m^3s^{-1}: 10,000 cfs) would have occurred also in 1962, 1969, 1978, 1983, 1992, 1998, 2001, and 2005. Therefore, the active channel width in Reaches 8 and 9 may have narrowed simply because of reductions in flood magnitudes since completion of Santa Felicia Dam. Reach 10 is situated above the Piru Creek confluence; although it is subject to regulation by Castaic Dam, this facility is operated as "run-of-the-river" and, by comparing upstream and downstream gauge data (USGS11108075, USGS11108145, USGS11108134, USGS11108135), has far less impact on flood flood magnitudes.

5.3.4 Changes in Channel Bed Level: 1929–2005

The change in channel bed elevation over time reveals trends of incision and aggradation for discrete reaches within the LSCR. Changes in the active channel width are also very likely to be linked to changes in bed elevation. Combining these data with known impacts to the river channel and surrounding watershed can help reveal causes for past incision/aggradation trends, and they can contribute to the understanding of future trends in incision/aggradation.

Because river-bed elevations were needed to plan water abstraction, repeat thalweg elevation surveys (i.e., surveys linking the deepest point of the channel bed) for the Santa Clara River from the mouth to the Ventura-Los Angeles County line are available from 1949 to 1993, and additional data exist from a survey undertaken in 1929 between the confluence of Piru Creek downstream to approximately the confluence of Santa Paula Creek. Data were extracted from graphical plots of thalweg elevation to the nearest 0.5 ft (the original unit of measurement). These data have been supplemented by information extracted from aerial LiDAR taken in 2005. Bed level changes in the LSCR can thus be established for the last 76 years (i.e., 1929–2005) in Reaches 6–10, and for the last 56 years (1949–2005) in Reaches 1–5 and Reach 11.
Thalweg survey elevations were extracted at intervals of approximately every 305 m (river station increments of 1000 ft) and are detailed in Appendix F (Table F-1). Appendix F also shows changes in thalweg elevation for discrete time periods (Table F-2). Absent independent validation of the 1929–1993 survey data or methods, we have assumed their approximate accuracy through the fact that the data were used in decision-making regarding water abstraction and, later, in relation to in-channel aggregate mining and infrastructure provision. Changes in sinuosity of the low-flow channel over time will cause changes to the exact location represented by a particular stationing, and these may have somewhat greater impact at higher station numbers. The 2005 LiDAR data were taken over a period of several weeks before the onset of dry weather flow conditions in the LSCR. Because standard LiDAR does not scan through water, the 2005 "thalweg" elevations are in fact water surface elevations and may therefore *over*-estimate thalweg elevations by up to 0.15-0.6 m (i.e., approximately 0.5-2 ft based on estimated flow depths.

LSCR Channel Bed Level Trends: 1949–2005

Using a base date of 1949 for consistency, the LSCR shows:

- a trend of incision from 1949 to 2005 downstream of the Santa Paula Creek confluence (i.e., Reaches 1–4), averaging 2.4 m (7.9 ft);
- a variable trend of minor incision and aggradation from Santa Paula Creek to Sespe Creek (Reaches 5-6), and
- moderate aggradation upstream towards the LA County Line (Reaches 7–11), averaging 0.65 m (2.1 ft) (Figure 5-18).

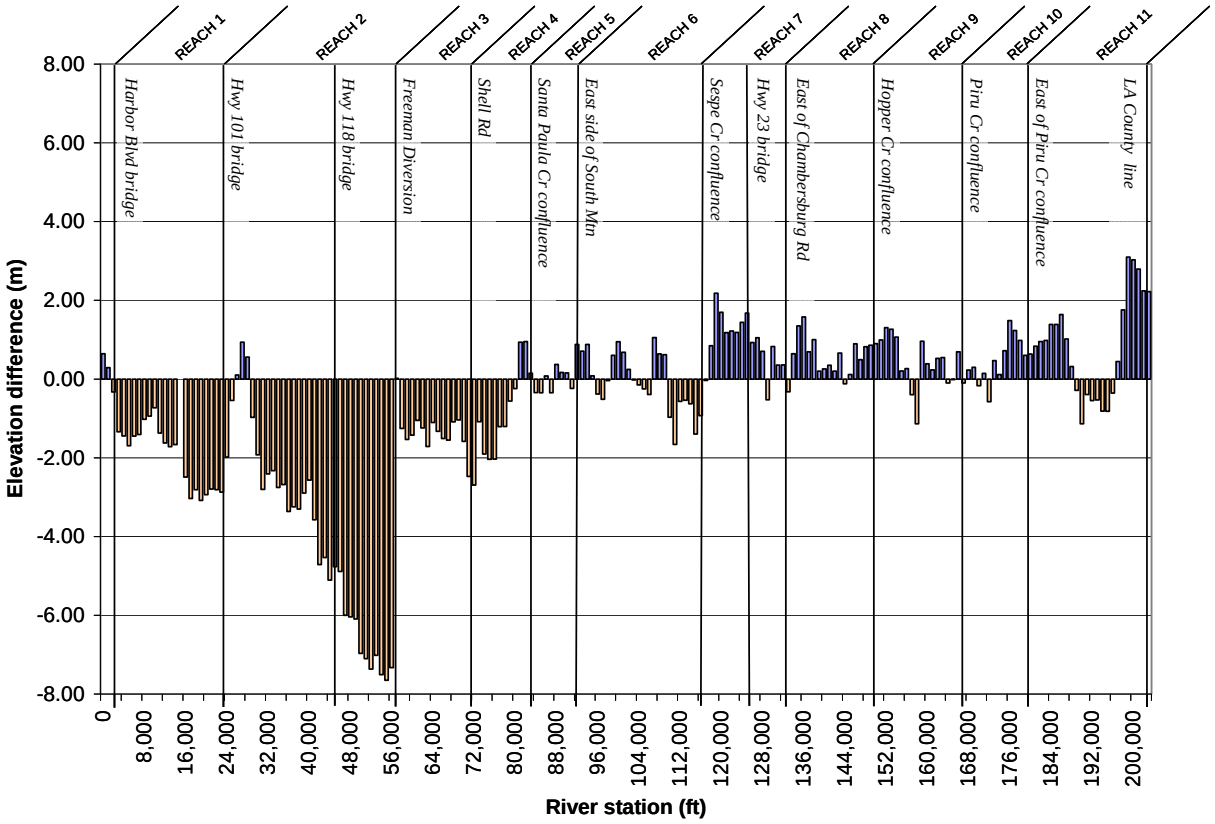

Figure 5-18. Net thalweg elevation change for the Santa Clara River from 1949 to 2005.

Consequently, the average gradient of the LSCR has increased slightly over the period of record, from 0.0040 to 0.0041. In average terms, the entire LSCR has incised approximately 0.7 m (2.3 ft) over the period 1949–2005. For individual river stations (recorded in feet upstream of the river mouth), maximum incision of 7.65 m (25.1 ft) occurred at station 55,000, at the upstream end of Reach 2 (i.e., just below Freeman Diversion dam), while maximum aggradation of 3.1 m (10.2 ft) occurred at station 199,000, at the upstream end of Reach 11.

Channel Bed Level Trends: 1929–1949

In Figure 5-19a-e, the 1929–2005 data are sub-divided into shorter time periods. Between 1929 and 1949 (Figure 5-19a), the partial survey indicates variable incision and aggradation of up to 2 m along the LSCR, with notable aggradation apparently focused downstream of Sespe Creek and (the then, unregulated) Piru Creek. It is possible that the changes reflect local adjustments caused by the 1938 and/or 1943 flood events following the large flood event caused by the 1928 St. Francis Dam break.

Channel Bed Level Trends: 1949–1967/71

In the period 1949 to 1967–71[5] a general trend for 1–2 m of incision exists (Figure 5-19b) throughout much of the LSCR. Maximum incision coincides with the area of active in-channel gravel extraction (Reach 2–3, maximum of 3.8 m [12.5 ft]), whereas aggradation of 1–2 m occurs upstream of the Sespe Creek confluence (Reach 7 into Reach 8) and below the LA/Ventura County line (Reach 11, up to 3.5 m [11.5 ft]). Aggradation upstream of Sespe Creek presumably reflects the effect of large flood flows exiting Sespe Creek, causing velocity reductions in the lower magnitude flows from the USCR upstream of the confluence zone. If data upstream of Sespe Creek do reflect a 1971 survey date, it is possible that aggradation upstream of Sespe Creek reflects the deposition of sediments during the (gauged) flood of record in 1969. Overall, especially for the surveys taken prior to 1969, the general trend for incision may represent thalweg incision as the channel bed was re-worked during relative smaller flood events (*e.g.,* 1958, 1962, 1965, 1966) that did not bring appreciable amounts of new hillslope sediment into the LSCR.

Channel Bed Level Trends: 1971–1993

Gravel mines were operated from upstream of Highway 101 Bridge (station 24,000) to Santa Paula (approximately station 80,000) during this period (see Figure 5-9). Multiple partial surveys occurred downstream of the Santa Paula Creek confluence in the period 1971–1986 (Figure 5-19c; surveys in 1975, 1978, 1980, 1983, 1986) amid growing concerns for the potential impact of in-channel aggregate mining on flow abstraction and local bridges and other infrastructure. The concern appears well-founded as incision occurs almost everywhere in Reaches 1–4, frequently in the range of 2–4 m in the extensive area of mining between the upper end of Reach 2 and the middle of Reach 4, reaching a maximum (up to 4.6 m [15.0 ft]) in Reach 3, above what is now Freeman Diversion dam.

The impact of the construction of Freeman Diversion Dam in 1991 is shown clearly in the period 1986–1993 (Figure 5-19d including partial LSCR surveys in 1986, 1989, 1992, 1993). Rapid aggradation occurs upstream of the dam throughout Reaches 3-5, from 4.5 m (15 ft) immediately upstream of the dam to 1.2 m (4 ft) at the upstream end of Reach 5. Conversely, local scour has occurred below Freeman Dam in Reach 2 (maximum of 1.7 m [5.5 ft]) over a distance of approximately 1,800 m (6,000 ft). Farther downstream, especially in Reach 1, some channel aggradation (up to 1.5 m [5ft]) occurred, and this may be related to deposition resulting from a flood that occurred in February 1978 (see Section 5.4.1).

Channel Bed Level Trends: 1993–2005

LiDAR data, taken in spring 2005 following the large floods of January and February 2005 has provided a means of understanding trends in bed levels since regular thalweg surveys ended after the construction of Freeman Diversion Dam subject to the potential errors in vertical accuracy outlined above. Aggradation in Reach 1 in the period 1986–1993 could have been a precursor to more general channel bed recovery following the cessation of in-channel aggregate mining in about 1989 but the 2005 LiDAR data does not confirm this trend (Figure 5-19e) and instead shows consistent incision of 1–2 m has occurred since 1993. Reach 2 suggests an accentuated impact of Freeman Diversion Dam with further incision near to the dam face (up to 1.5 m), with aggradation (possibly the deposition of the sediments eroded below the dam) only at the downstream end of Reach 2. Localized incision also occurs in Reaches 3 and 4 (possibly related to active meander growth in the 2005 flood) while further aggradation occurs around the confluence with Santa Paula Creek. Aggradation downstream of Santa

[5] A U.S. Army Corps of Engineers survey took place progressively over the LSCR working upstream from 1967-1971. Data downstream of Sespe Creek in Figure 5-19a pre-dates the flood of record in 1969, whereas upstream data have dates in both 1968 and 1971, making it unclear exactly which data were collected before and after the 1969 event.

Paula Creek confluence in the period 1986-2005 (*i.e.,* Figure 5-19d and e) may also be related to the delivery of sediment locally in response to observed rapid incision in Santa Paula Creek that coincided with channelization in Lower Santa Paula Creek started in the late 1970s. Mild aggradation has occurred through Reaches 6–8 while a small amount of incision occurs in Reach 11 and is presumed to be associated with meander bend development.

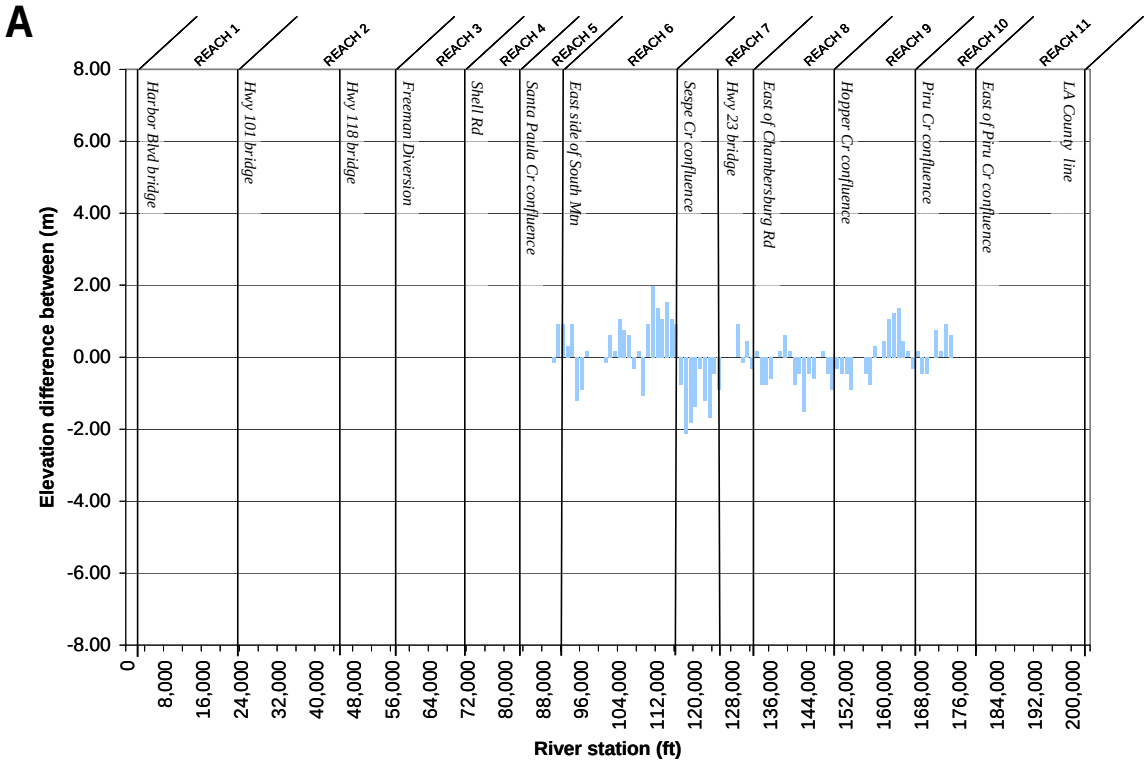

Figure 5-19. Net thalweg elevation change for the Santa Clara River from (a) 1929-1949; (b) 1949-1967 through 1971; (c) 1971-1986; (d) 1986-1993; and (e) 1993-2005.

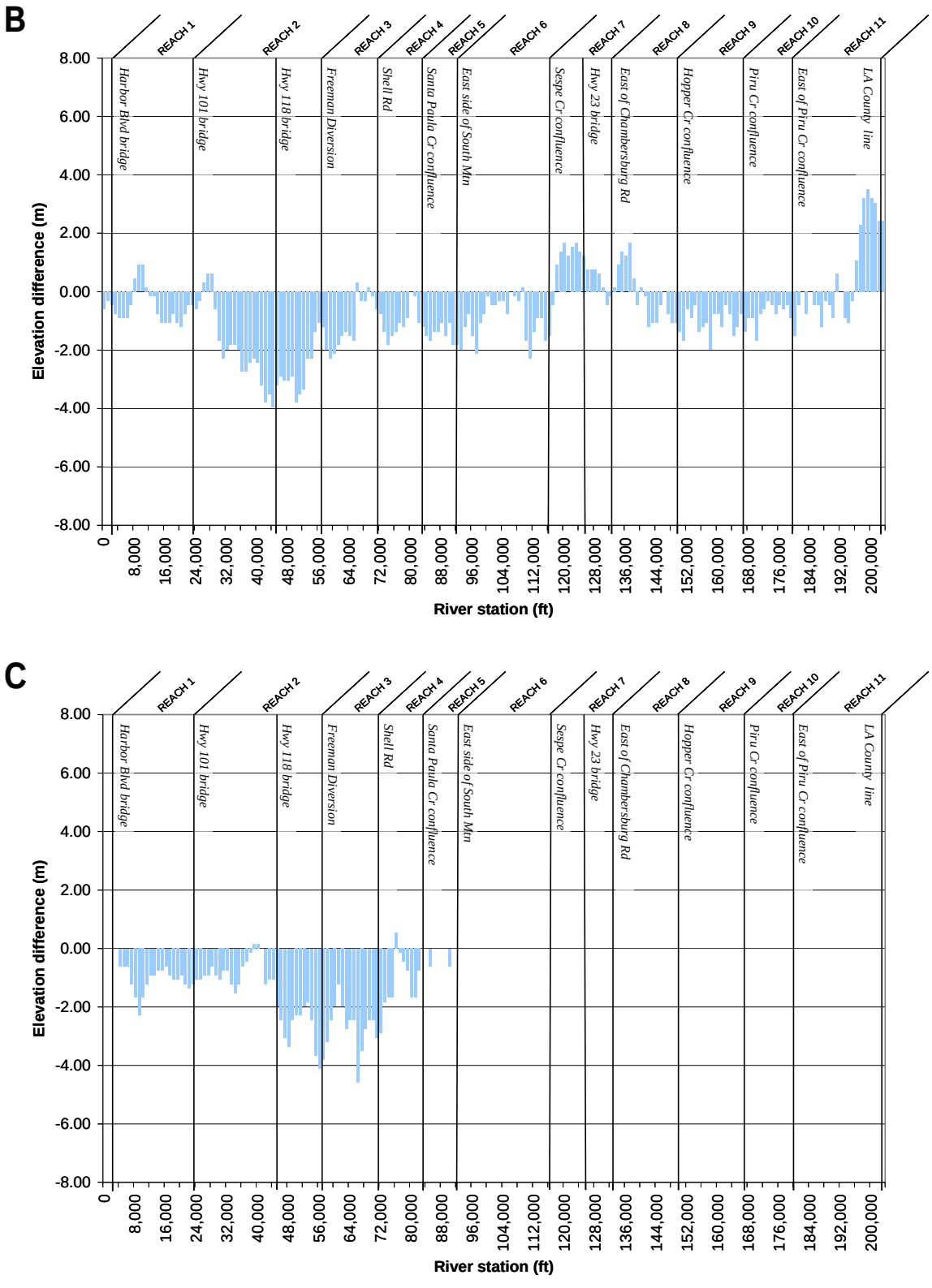

Figure 5-19. Net thalweg elevation change for the Santa Clara River from (a) 1929-1949; (b) 1949-1967 through 1971; (c) 1971-1986; (d) 1986-1993; and (e) 1993-2005.

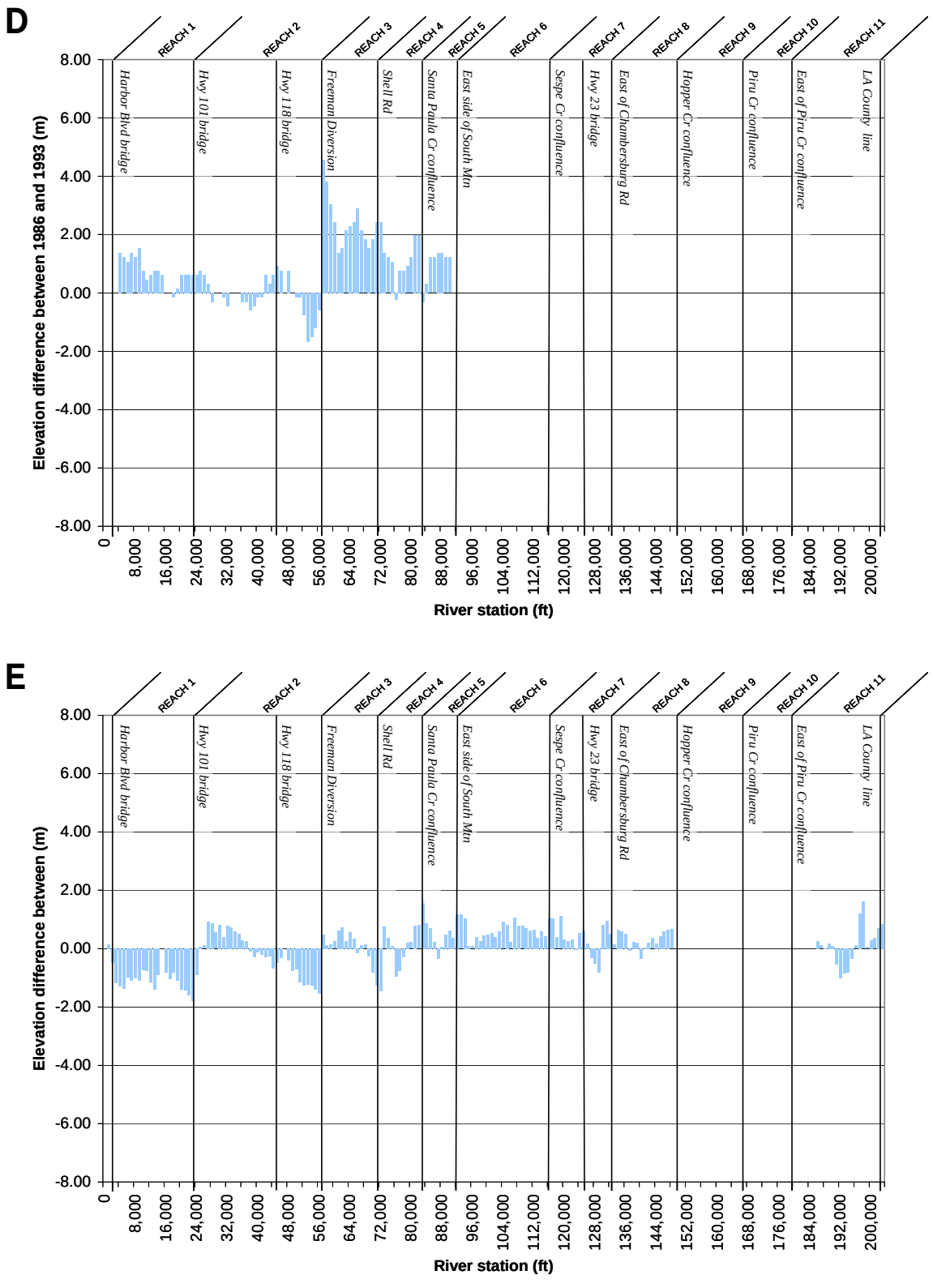

Figure 5-19. Net thalweg elevation change for the Santa Clara River from (a) 1929-1949; (b) 1949-1967 through 1971; (c) 1971-1986; (d) 1986-1993; and (e) 1993-2005.

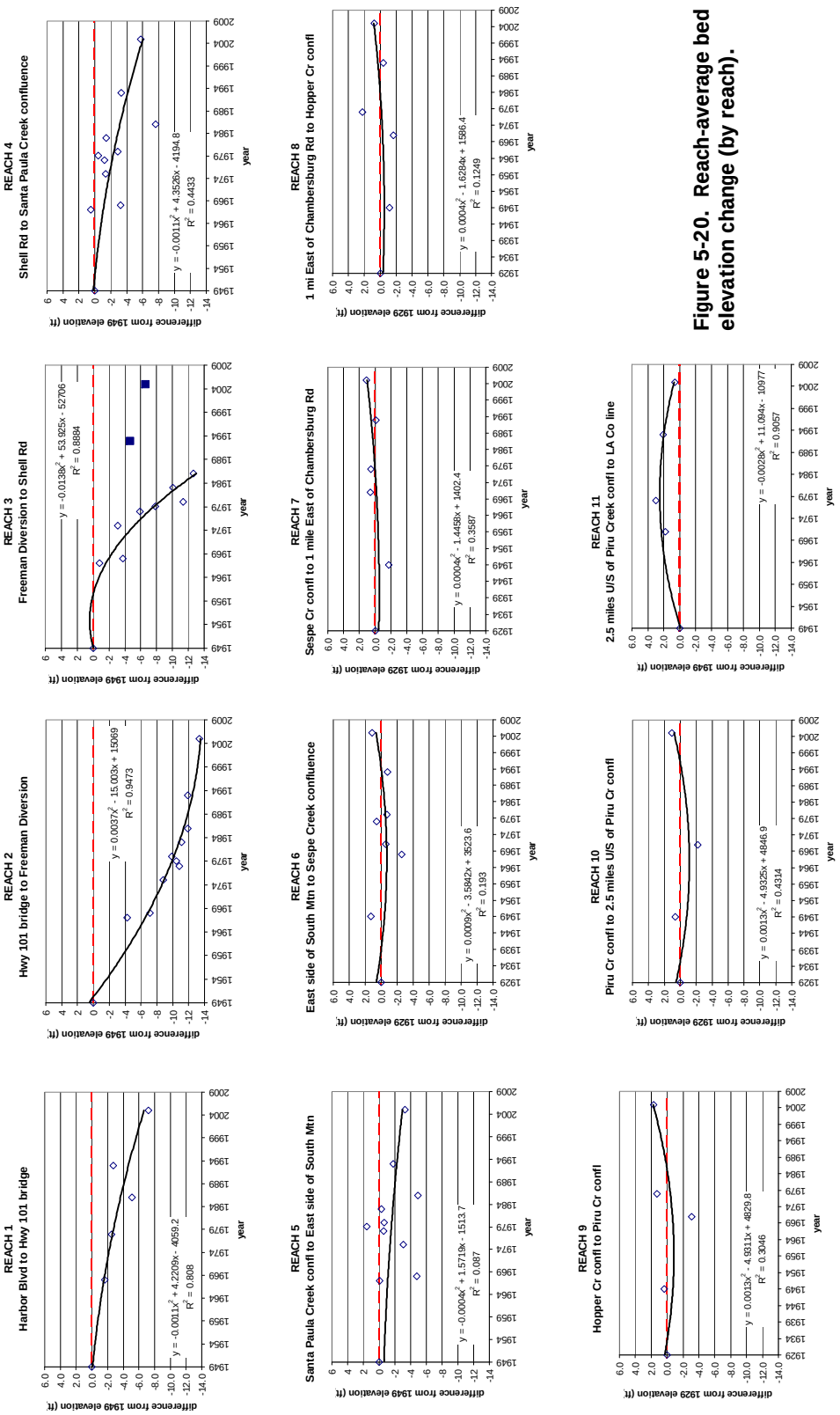

Figure 5-20. Reach-average bed elevation change (by reach).

Elsewhere, conceptual models of river response to the passage of a single knickpoint indicate that a suite of interrelated channel adjustments will occur, including channel bed recovery towards the original bed level (Schumm et al., 1984; Simon, 1989). Typically, following a period of incision caused by upstream knickpoint erosion, bed elevation recovery begins rapidly and then becomes slower as the original bed elevation is approached, forming an exponential decay curve of channel bed recovery (*e.g.*, Barnard and Melhorn, 1982). Significant channel bank erosion occurs as the bed levels recover. However, reach-averaged trends in channel thalweg elevation over time confirm that channel bed elevations have not consistently recovered (i.e., increased in elevation) since the cessation of in-channel aggregate mining. Instead, five separate trends in reach-level bed adjustment are recognized (Figure 5-20a-k):

- Reach 1 illustrates a trend towards mild but increasing incision over time (Figure 5-20a).
- Reach 2 experienced more rapid incision until the upstream construction of the Freeman Diversion Dam and on average, has stabilized thereafter (Figure 5-20b). The resulting trend therefore combines responses expected following knickpoint migration and placement of the dam (*e.g.*, Williams and Wolman 1984). Since construction of the diversion dam, trends are different in the upper (incising) and lower (aggrading) parts of the reach.
- Reach 3 was experiencing an increasing rate of incision until the construction of Freeman Diversion Dam (Figure 5-20c), at which time the infilling behind the dam caused rapid bed aggradation between 1986 and 1993.
- Reaches 4 and 5 show mild and more variable trends towards incision but, with bed aggradation between 1986 and 1993 as a result of the Freeman Diversion Dam is visible (Figure 5-20d,e).
- There are no appreciable trends over time for Reaches 6–11 (Figure 5-20f-k).

Major trends are thus mild incision following bed aggradation upstream of Freeman Diversion Dam in Reaches 3–5 (blue line in Figure 5-20c-e), and incision in Reach 1 that appears to be increasing. These trends may be related to continued prevalence of floods in the recent period (see below), to apparent active meander growth in Reaches 3 and 4 following the 2005 flood, and to the effects of levees in confining flood flows and causing additional channel thalweg scour (e.g., Reach 1). Also, in reasoning why channel bed response may not follow the common conceptual model (other than because of local adjustments caused by the Freeman Diversion Dam), one notable feature in the LSCR is that many reaches have been actively narrowed and are retained narrow by protected levees: as such, there is no opportunity for channel widening following knickpoint incision and this may prevent channel bed recovery. Because of the absence of thalweg surveys from 1993–2005, confirmation of these trends will require surveys following the next several large floods in the LSCR.

5.3.5 Summary of Reach-Level Dynamics

Based on apparent differences in criteria such as flow, planform pattern, the degree of valley confinement, and levees, the LSCR was split into 11 reaches, numbered up from the river estuary. Subsequent analysis indicated similarities between Reaches 1–4, from the river estuary to the confluence with Santa Paula Creek, 5 and 6 from the confluence with Santa Paula Creek to the confluence with Sespe Creek, and Reaches 7–11 upstream of the confluence with Sespe Creek. Over the last 57years, Reaches 1–4 have incised on average 2.4 m, have narrowed considerably and have an active width that is no longer related to the magnitude of the last flood, but instead to a legacy of in-stream aggregate mining and the existence of extensive levees. Reaches 5 and 6 are the most 'natural' reaches in the LSCR. They have not appreciably changed bed elevation over the period of record, and they have a highly changeable active channel width related to the magnitude of the last flood rather than to constraints provided by human activity. Reaches 7–11 have aggraded 0.65 m since 1949, and they have narrowed in width over time but are still somewhat responsive to flood magnitude, possibly in response to flow regulation, to the passage of construction sediments or to sediments deriving from episodically high natural supply rates (e.g., in response to wildfire or landslide activity). A summary of the morphodynamic features of

each river reach is provided in Table 5-15, and several example cross-sections from each reach are provided in Figure 5-21a-k.

Reaches 1–4, below the confluence with Santa Paula Creek, have experienced the greatest amount of incision since the mid-twentieth century and so are the source of the net export of sediment from the LSCR. The formation of an inset channel (Figure 5-21a), caused by the incising thalweg stands in contrast to the lack of a clearly defined channel in many of the upper LSCR cross-sections. The current channel thus has a compound structure, with a highly changeable low-flow channel inset within a far larger channel that is largely straight in response to both regional tectonic controls and confinement caused by human activities such as levee construction and in-channel gravel mining. The thalweg of Reaches 1–4 has incised from 1–4 m on average, and levee construction since 1960 has narrowed the active channel bed of the reaches considerably. Thalweg incision began with in-stream aggregate mining which caused the development of upstream migrating knickpoints that have extended into the lower end of Reach 5. Whereas, a subsequent process of (at least partial) bed elevation recovery might be expected following incision, it appears that the levee construction in combination with the flashy nature of large floods in the watershed have prevented recovery in the LSCR. Recovery has been achieved structurally in Reaches 3 and 4 following the construction of Freeman Diversion Dam. Scour has occurred downstream of the dam, in the upper end of Reach 2, with aggradation in the lower end of the reach. Reach 1 continues to incise mildly. Unit stream power values in Reaches 1–4 are higher than in the reaches upstream, whereas naturally it would be expected that stream power values would diminish approaching the mouth of the river. As stream power is a surrogate for sediment transporting potential, Reaches 1-4 continue to possess the energy to transport more sediment than supplied to them from upstream, indicating a possibility of further incision into the future.

Table 5-15. Lower Santa Clara River reach morphodynamics: a summary of reach estimates derived elsewhere in this chapter.

	Reach 1	Reach 2	Reach 3	Reach 4	Reach 5	Reach 6	Reach 7	Reach 8	Reach 9	Reach 10	Reach 11
Reach Boundaries (downstream to upstream)	*Harbor Blvd Bridge* / *101 Bridge*	*d/s Freeman Dam*	*u/s Freeman Dam* / *Shell Rd*	*Santa Paula Ck.*	*East flank South Mt.*	*Sespe Ck.*	*1 mi E Cham'berg Rd.*	*Hopper Ck.*	*Piru Ck.*	*2.5 mi E Piru Ck.*	*LA County Line*
Centerline reach length[1] (m)	6,412	9,967	4,715	3,503	2,545	6,803	5,267	5,710	4,745	4,445	6,076
Bankfull discharge[1] (m^3s^{-1})	185.9	185.9	185.9	185.9	185.9	185.9	89.5	60.6	60.6	54.2	52.9
Reach-average slope[1]	0.0025	0.0027	0.0025	0.0039	0.0031	0.0036	0.0048	0.0055	0.0053	0.0062	0.0055
Unit stream power at 1.5-year flow	**27**	**27**	**32**	**51**	**31**	20	13	12	12	10	**33**
Channel type[2]											
Active channel width 2005[3] (m)	222	350	265	384	456	474	570	422	542	555	146
Width variability[4]	**0.78**	0.30	0.36	0.33	**0.59**	**0.49**	**0.60**	0.34	0.25	0.26	
Correlation (r^2) of width with magnitude of last flood[5]	0.28	-0.04	0.33	0.25	**0.71**	**0.53**	**0.77**	0.32	0.29	**0.48**	
Correlation (r^2) of width with time[5]	-0.49	-0.92	-0.74	-0.67	**-0.03**	**-0.14**	-0.56	-0.62	-0.76	-0.59	
Reach average bed elevation change, 1949-2005[2] (m)	**-1.96**	**-3.90**	**-1.24**	**-1.13**	0.05	-0.05	0.86	0.58	0.42	0.42	0.83
Trend in bed level elevation	Progressive mild incision	Incised and stabilizing, local scour upstream, aggradation downstream	Rapid incision prior to Freeman Dam. Recovered but slight incision recently	Recovered after Freeman Dam built. Slight incision recently	Recovered after Freeman Dam built. Slight incision recently	No trend	Slight aggradation, no trend	Slight aggradation, no trend	Slight aggradation, no trend	Slight aggradation, no trend	Slight aggradation, no trend
Net sediment balance 1949-2005 (M t)	**-5.33**	**-15.90**	**-1.76**	**-1.17**	0.05	-0.23	2.68	1.99	1.09	1.28	0.99

[1] Derived from HEC-RAS output
[2] Derived from discriminant analysis, Figure 5-14
[3] Derived from GIS analysis of post-flood aerial photography (flood peak 3,851 m^3s^{-1})
[4] Defined as the normalized standard deviation of the ratio of weighted average width and standard deviation of the width, Table 5-14.
[5] Table 5-14.
Bold text used to distinguish similarities in channel character between reaches

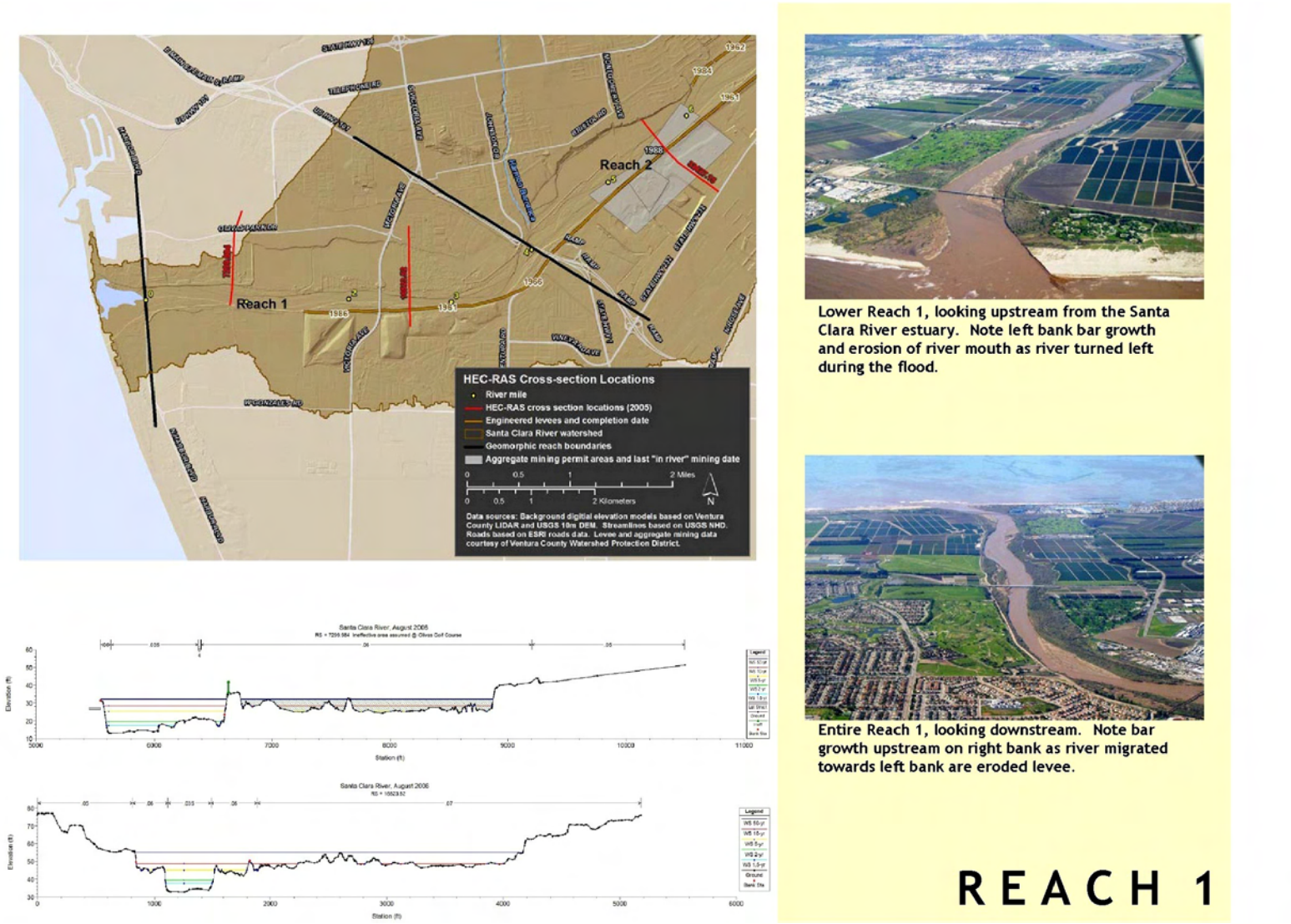

Figure 5-21. Planform, typical cross-sections and indicative photographs by reach. Cross-sections derived from HEC-RAS analysis (URS, 2006). Photographs taken January 12, 2005 during recession of January 10, 2005 flood (peak flow 3,850 m^3s^{-1}). (Photographs courtesy of California Coastal Conservancy)

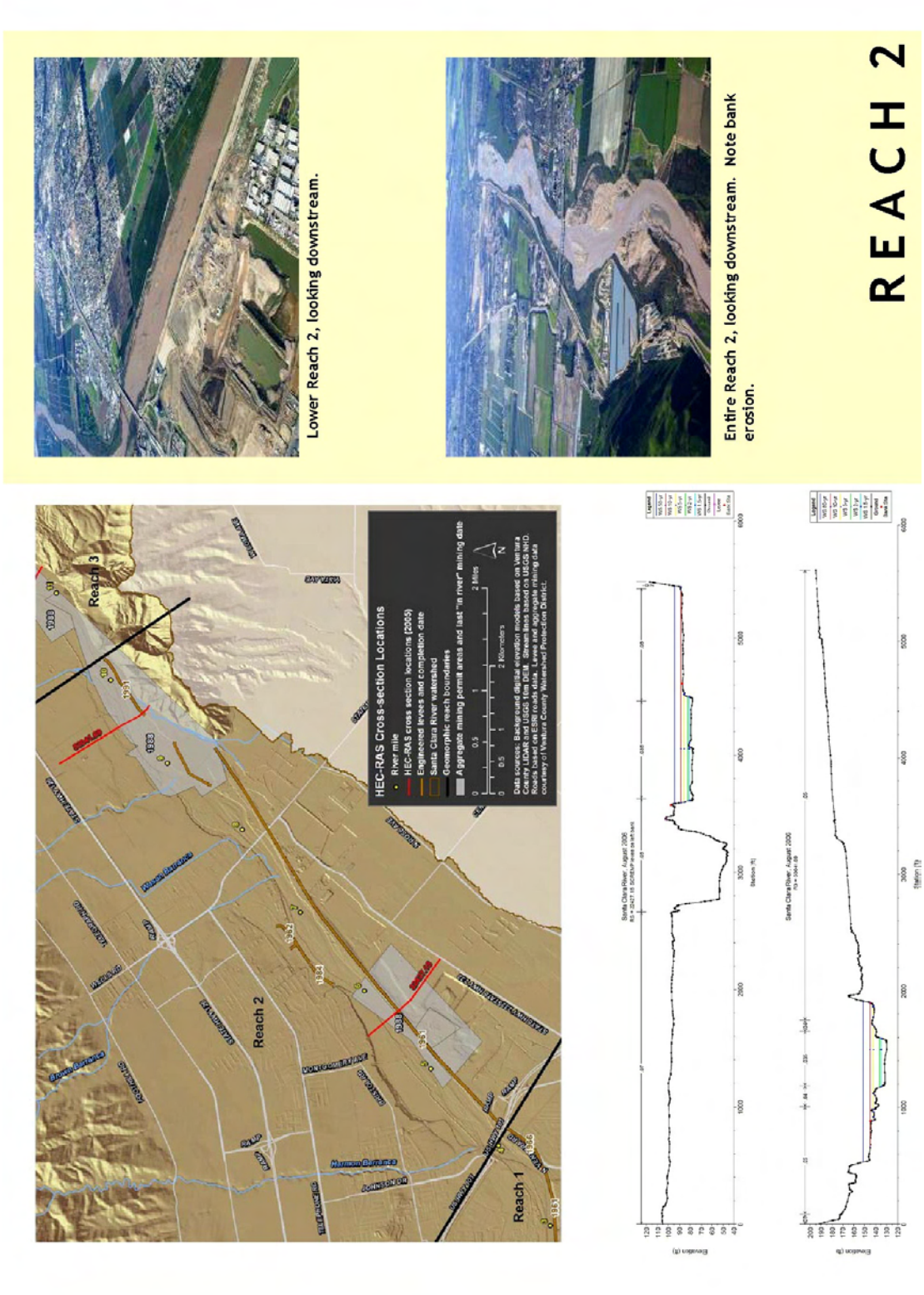

Figure 5-21. Planform, typical cross-sections and indicative photographs by reach. Cross-sections derived from HEC-RAS analysis (URS, 2006). Photographs taken January 12, 2005 during recession of January 10, 2005 flood (peak flow 3,850 m^3s^{-1}). (Photographs courtesy of California Coastal Conservancy)

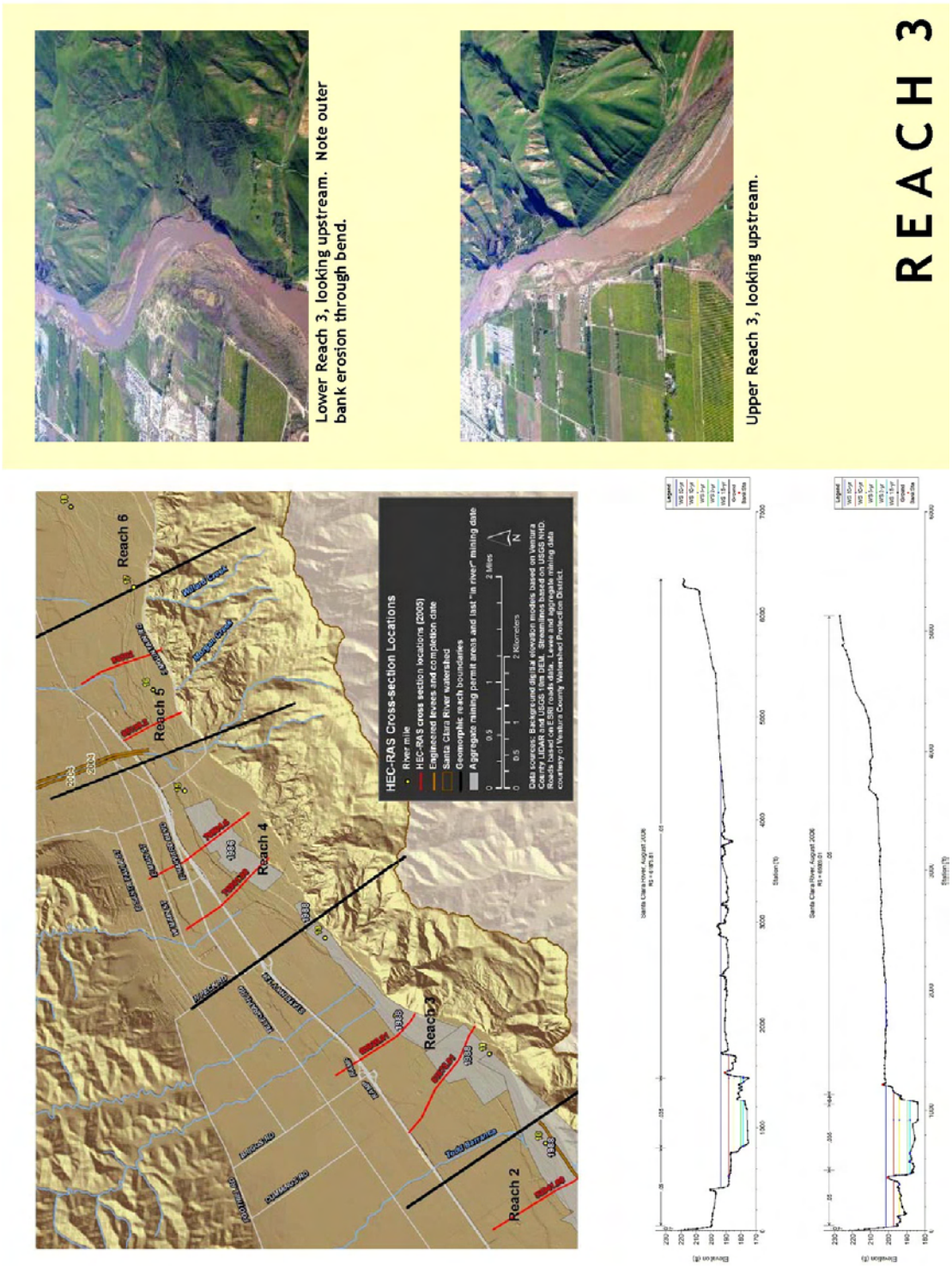

Figure 5-21. Planform, typical cross-sections and indicative photographs by reach. Cross-sections derived from HEC-RAS analysis (URS, 2006). Photographs taken January 12, 2005 during recession of January 10, 2005 flood (peak flow 3,850 m^3s^{-1}). (Photographs courtesy of California Coastal Conservancy)

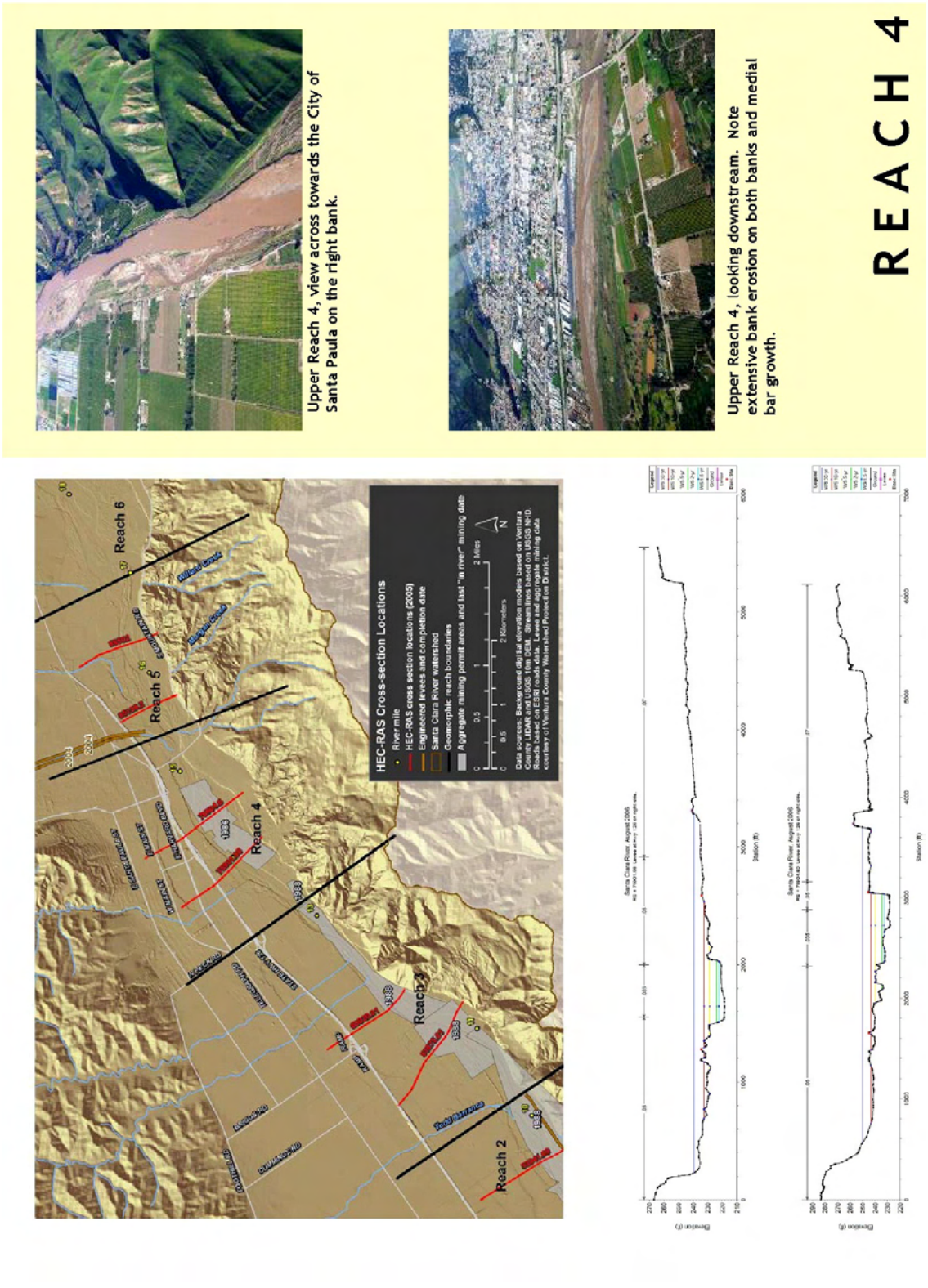

Figure 5-21. Planform, typical cross-sections and indicative photographs by reach. Cross-sections derived from HEC-RAS analysis (URS, 2006). Photographs taken January 12, 2005 during recession of January 10, 2005 flood (peak flow 3,850 m^3s^{-1}). (Photographs courtesy of California Coastal Conservancy)

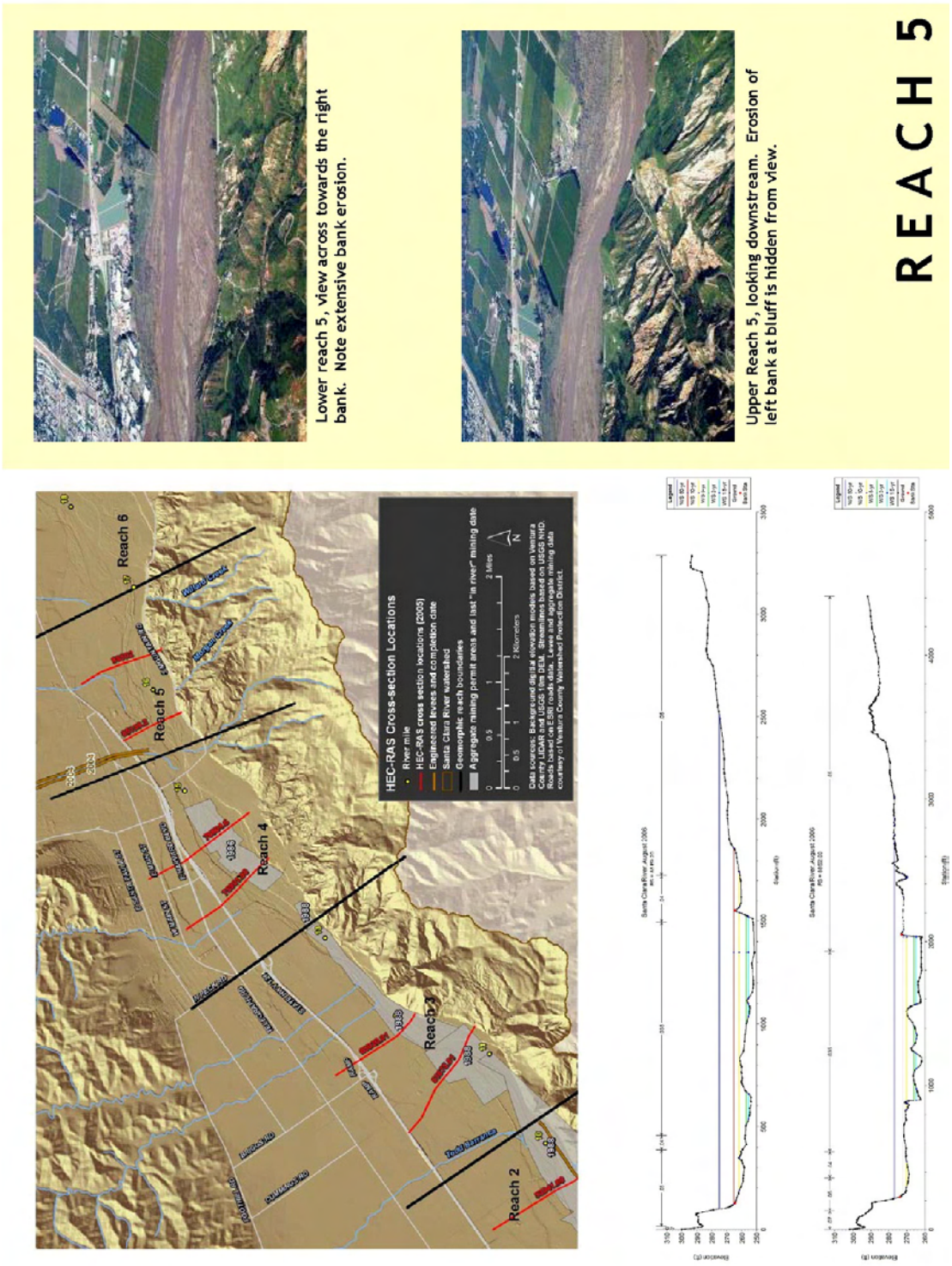

Figure 5-21. Planform, typical cross-sections and indicative photographs by reach. Cross-sections derived from HEC-RAS analysis (URS, 2006). Photographs taken January 12, 2005 during recession of January 10, 2005 flood (peak flow 3,850 m^3s^{-1}). (Photographs courtesy of California Coastal Conservancy)

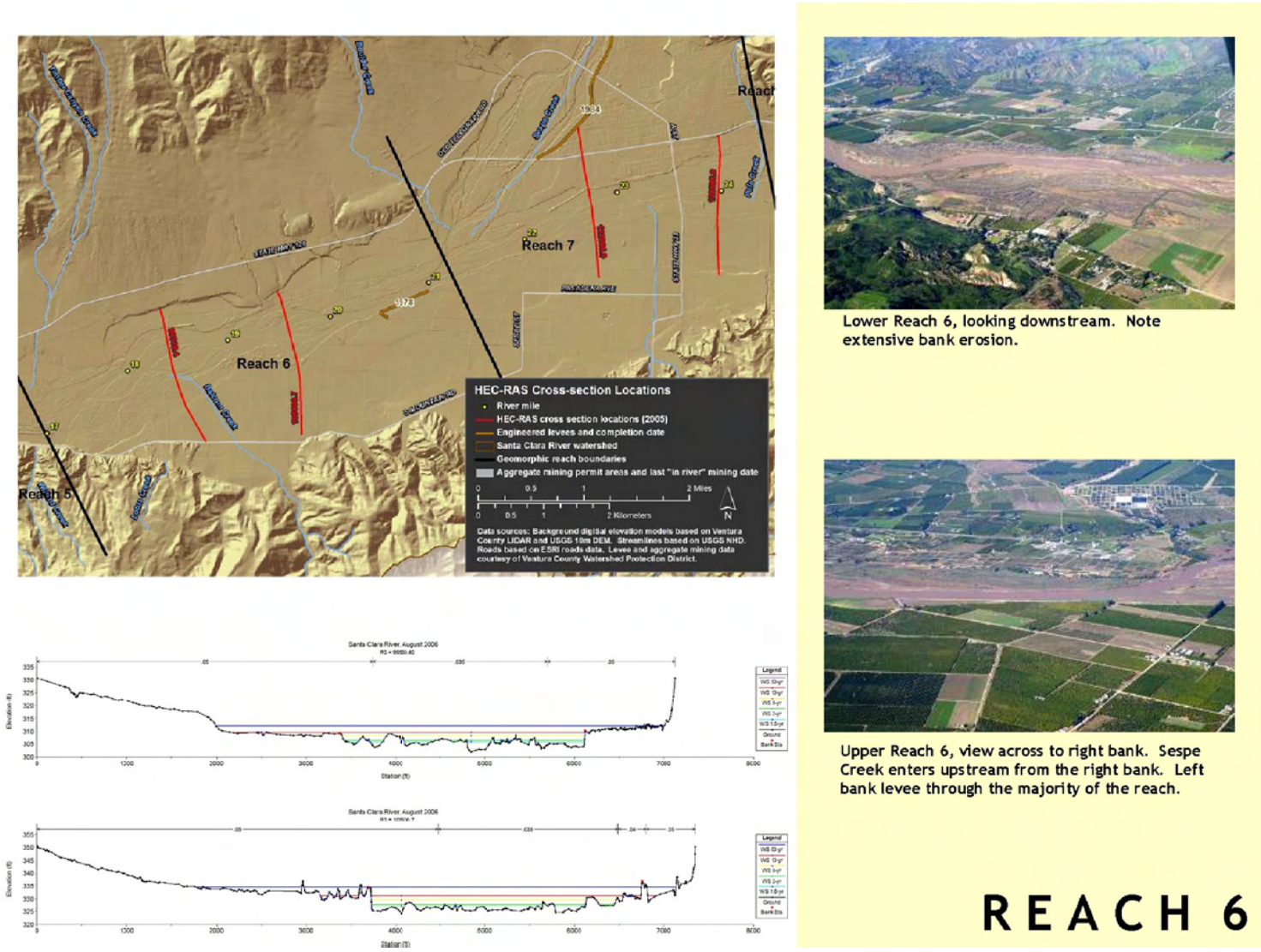

Figure 5-21. Planform, typical cross-sections and indicative photographs by reach. Cross-sections derived from HEC-RAS analysis (URS, 2006). Photographs taken January 12, 2005 during recession of January 10, 2005 flood (peak flow 3,850 m^3s^{-1}). (Photographs courtesy of California Coastal Conservancy)

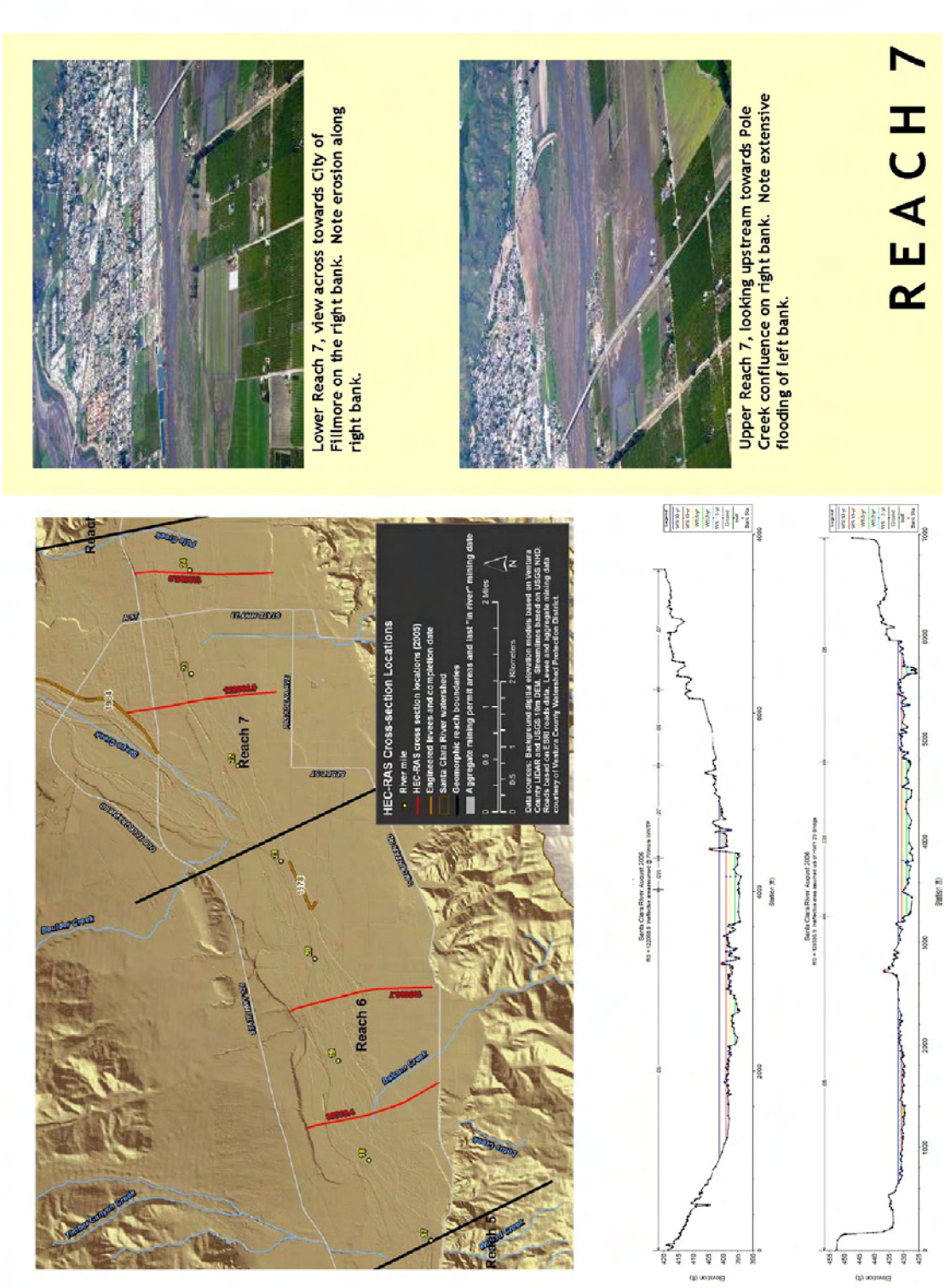

Figure 5-21. Planform, typical cross-sections and indicative photographs by reach. Cross-sections derived from HEC-RAS analysis (URS, 2006). Photographs taken January 12, 2005 during recession of January 10, 2005 flood (peak flow 3,850 m^3s^{-1}). (Photographs courtesy of California Coastal Conservancy)

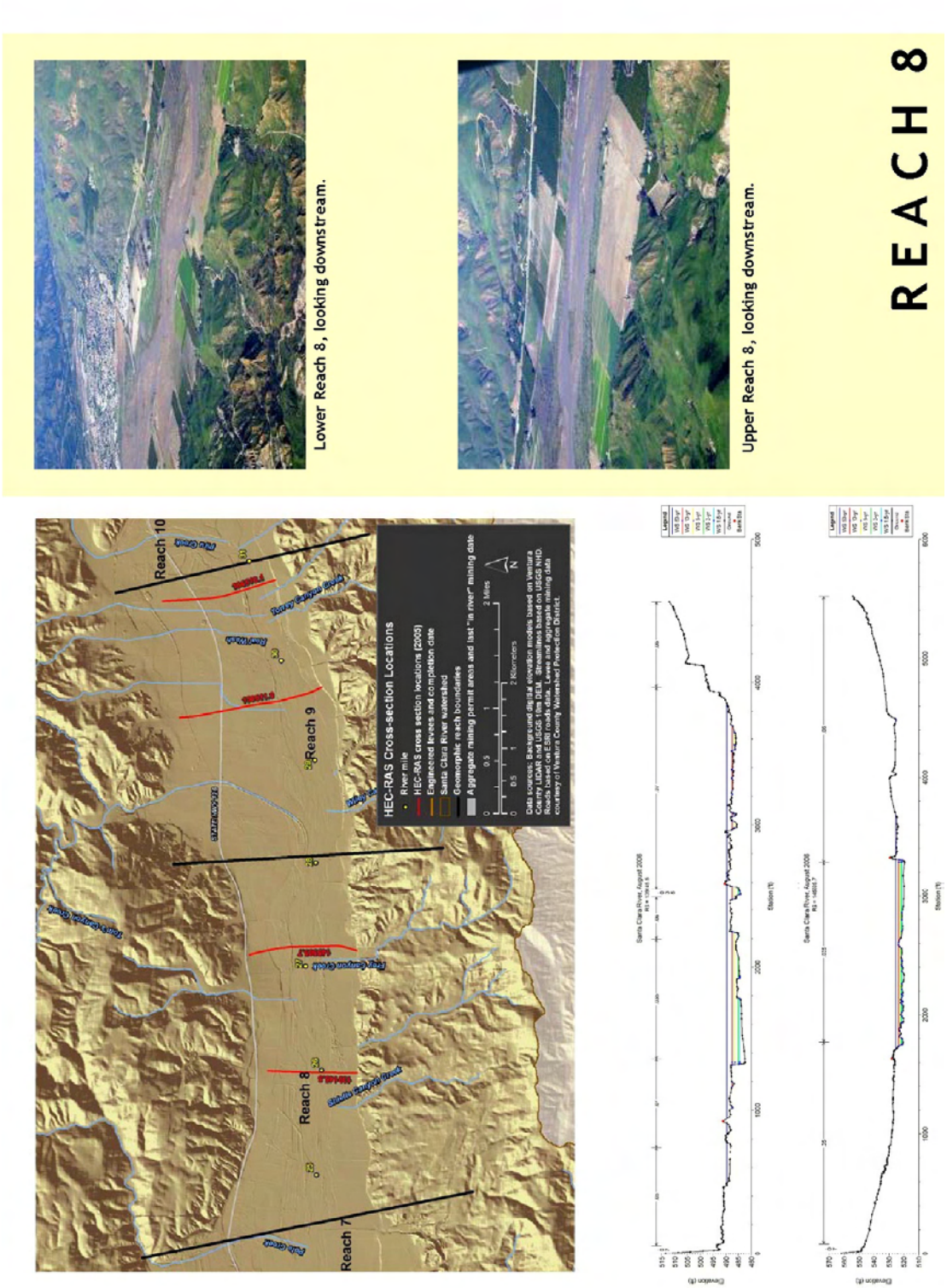

Figure 5-21. Planform, typical cross-sections and indicative photographs by reach. Cross-sections derived from HEC-RAS analysis (URS, 2006). Photographs taken January 12, 2005 during recession of January 10, 2005 flood (peak flow 3,850 m^3s^{-1}). (Photographs courtesy of California Coastal Conservancy)

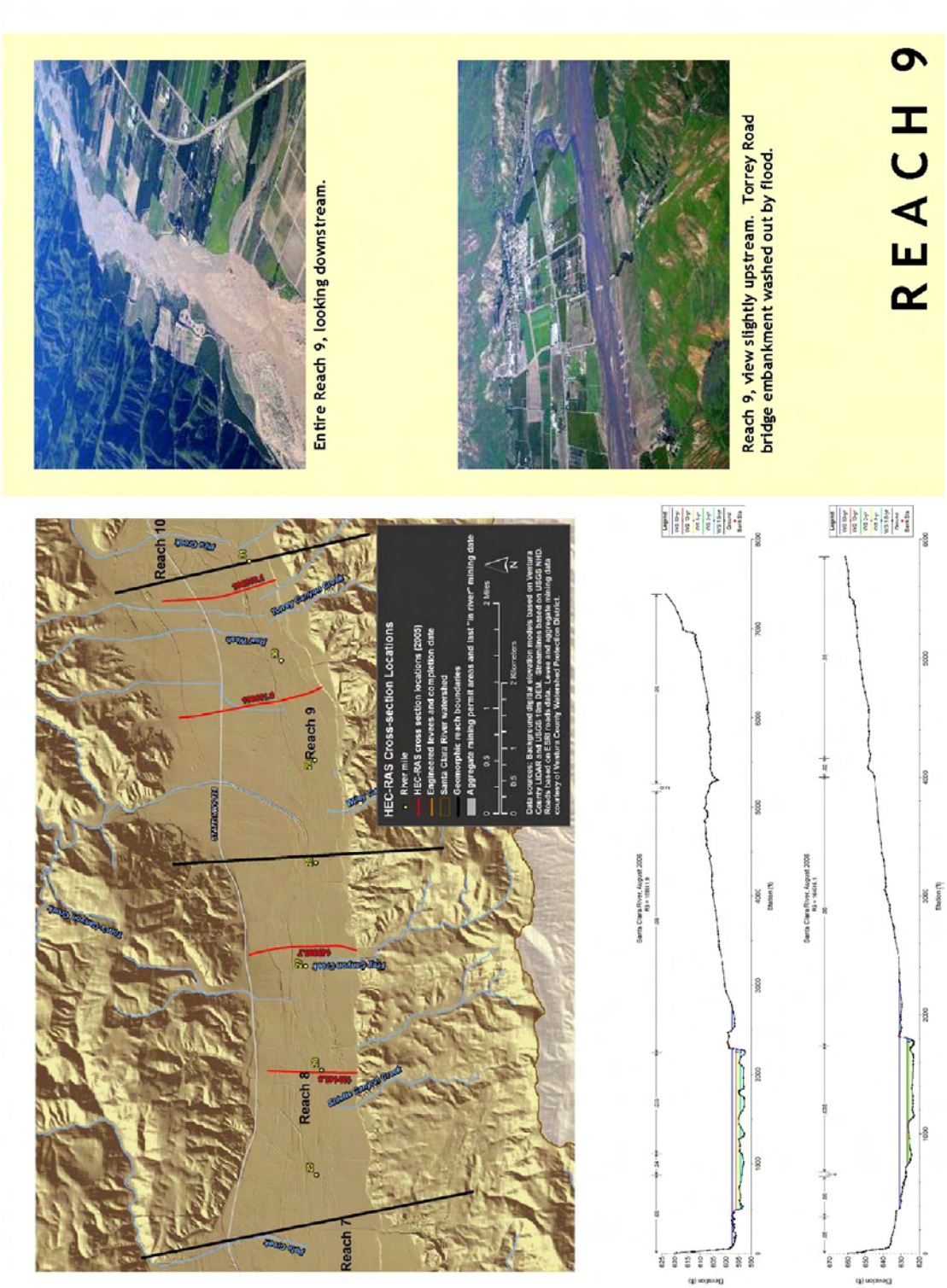

Figure 5-21. Planform, typical cross-sections and indicative photographs by reach. Cross-sections derived from HEC-RAS analysis (URS, 2006). Photographs taken January 12, 2005 during recession of January 10, 2005 flood (peak flow 3,850 m^3s^{-1}). (Photographs courtesy of California Coastal Conservancy)

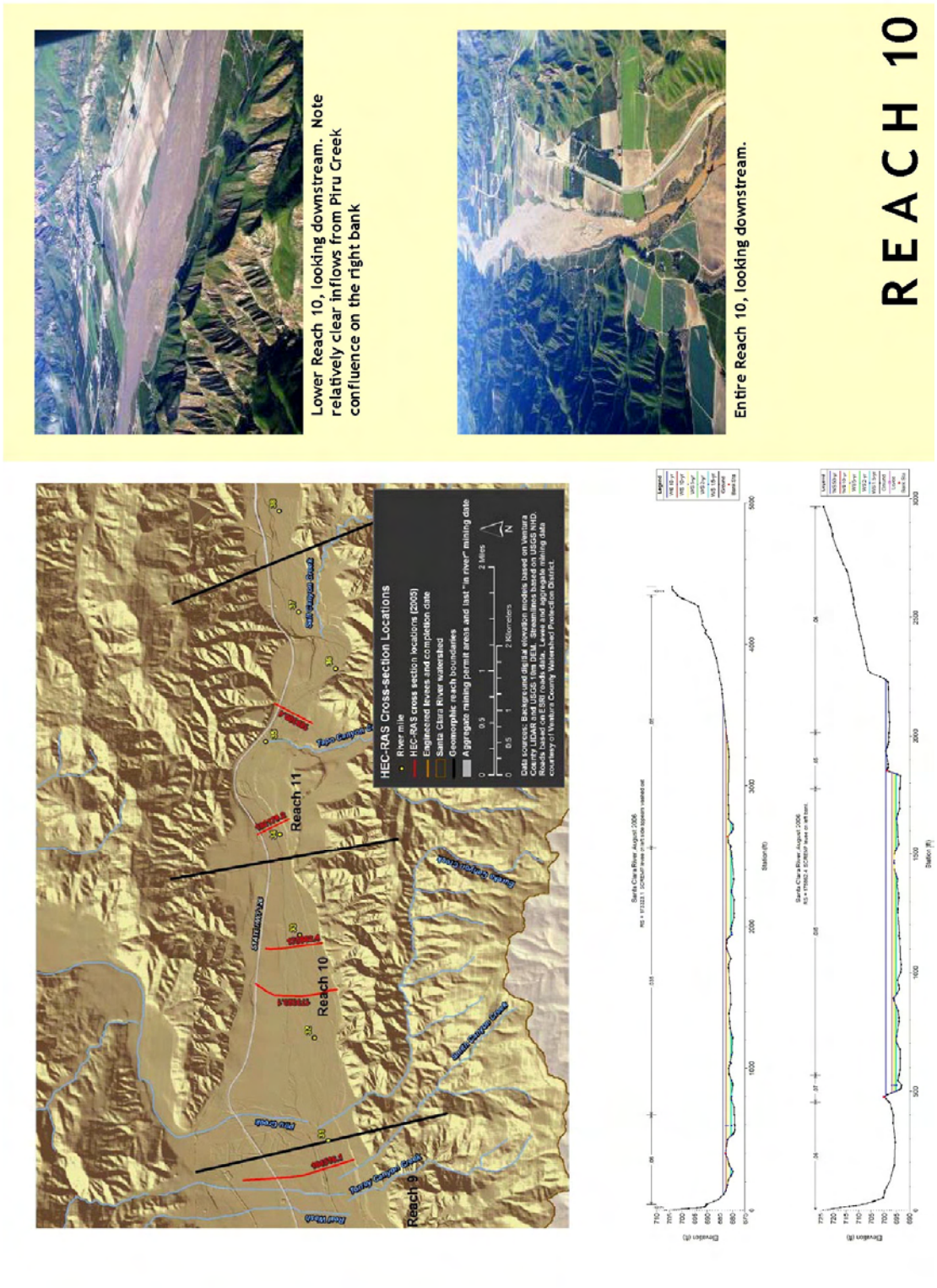

Figure 5-21. Planform, typical cross-sections and indicative photographs by reach. Cross-sections derived from HEC-RAS analysis (URS, 2006). Photographs taken January 12, 2005 during recession of January 10, 2005 flood (peak flow 3,850 m^3s^{-1}). (Photographs courtesy of California Coastal Conservancy)

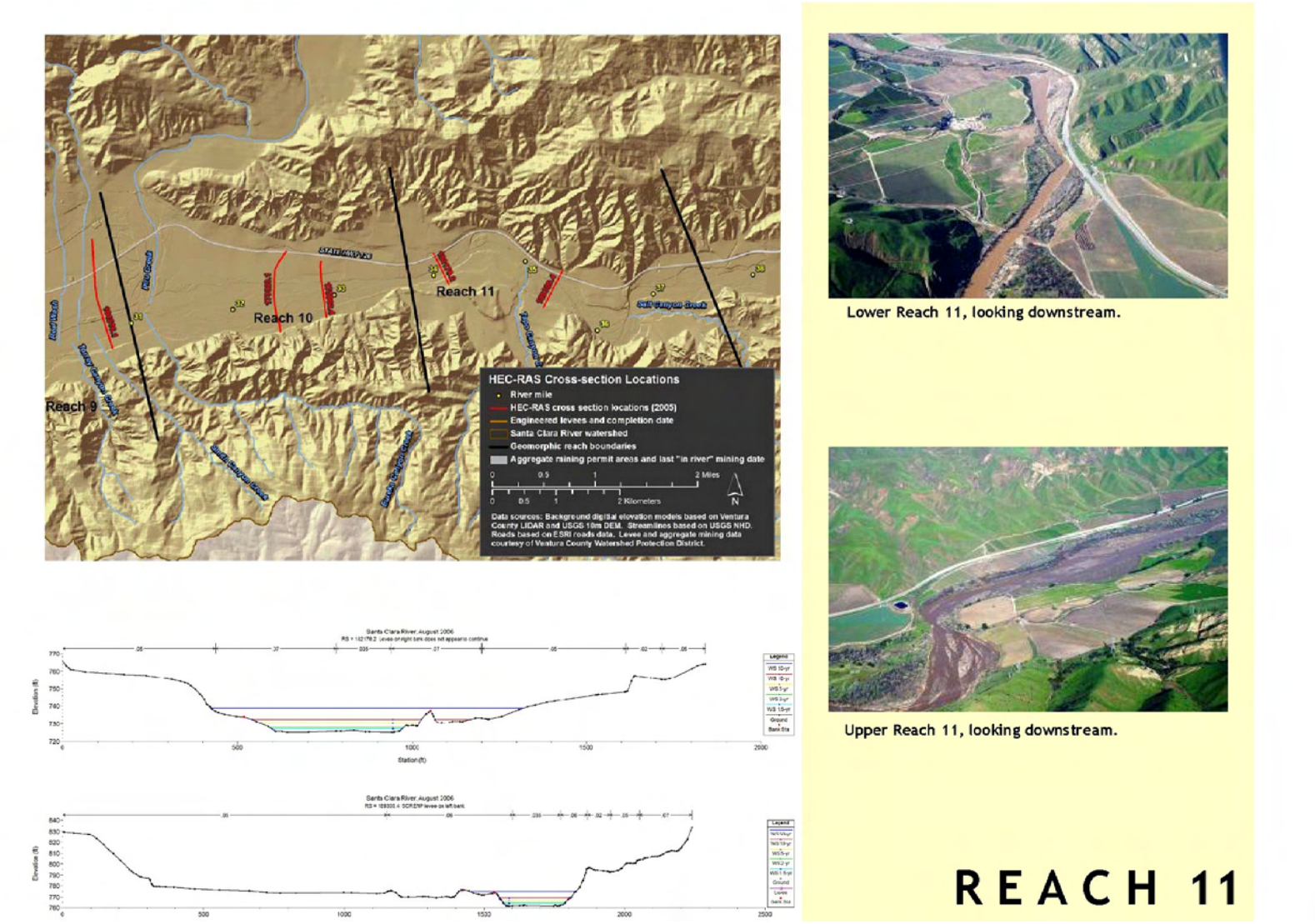

Figure 5-21. Planform, typical cross-sections and indicative photographs by reach. Cross-sections derived from HEC-RAS analysis (URS, 2006). Photographs taken January 12, 2005 during recession of January 10, 2005 flood (peak flow 3,850 m^3s^{-1}). (Photographs courtesy of California Coastal Conservancy)

Between the Santa Paula and Sespe Creek confluences, Reaches 5 and 6 appear to be the least affected by human activity in the LSCR. Neither reach has incised or aggraded appreciably overall, while the active bed width continues to vary in harmony with the magnitude of the last major flood event—a natural response in a semi-arid channel. Both reaches possess a wider and more irregular channel bed as a function of the low-flow channel migrating across the active channel bed during flood events. Reach 5 and parts of Reach 6 did incise during the period 1949–1967/71, but Reach 5 recovered in the period 1986–1993 following the construction of Freeman Dam. This may suggest that instream aggregate mining, rather than the effect of the 1969 flood of record, was responsible for the observed incision. Recent slight incision in the downstream end of Reach 5 may herald further incision in Reach 5, especially as incision also occurs in the reaches below. Local thalweg incision has occurred at the upstream end of Reach 6, and this may be due, at least in part, to the existence of a levee opposite the Sespe Creek confluence. Bed elevations at the upstream stations 112,000 and 116,000 had increased by 1.7 m (5.5 ft) and 0.9 m (3 ft), respectively, between 1929 and 1949 (Table D-2) but, from 1949-1993, incised by approximately 1.2 m (4 ft) and 2.1 m (7 ft), respectively, coinciding with levee construction in 1978. Apparent meandering during the 2005 flood event may also have been assisted by the existence of the levee opposite the Sespe creek confluence serving to turn flow back across the channel sharply, and promoting a meandering flow thalweg.

While there have been fewer thalweg surveys in Reaches 7–11, upstream of the Sespe Creek confluence to the L.A.-Ventura County Line, the reaches apparently share the common attribute of approximately 0.5–1 m of bed aggradation since 1949 in addition to narrowing of the active channel bed width since 1938. The trend for aggradation has been greatest since 1969. Reach 7, just upstream of the Sespe Creek confluence, is distinct in that its active channel bed width is still linked strongly to the magnitude of the last flood event, possibly because it functions to backwater during significant flood events emanating from Sespe Creek or because of flow constriction upstream of the Highway 123 bridge. There are several potential causes of the aggradation. First, Reaches 7–10 have low 1.5-year recurrence interval unit stream power and as such, they may be quite responsive to flood event frequency so that since 1969, mild aggradation has occurred in relation to the increased frequency of large flood events that bring appreciable hillslope sediment into the reach (possibly aided by wildfire or landslide activity). Alternatively, the apparent contradiction of the narrower but aggraded channel may be explained by flood flow reductions, especially due to regulation of Piru Creek, making the reaches somewhat less capable of transporting the sediment delivered to them, or to the passage of a sediment pulse resulting from upstream urban construction.

5.4 Sediment Budgets for the Lower Santa Clara River

5.4.1 Storm-event Sediment Budgets from Gauge Data

The morphological evolution of the LSCR is a complex interaction between periodic flood events and discrete human actions in and around the river that have altered the river's ability to transport sediment throughout the historical period. Furthermore, the morphological impact of individual flood events also varies in time as a function of runoff and sediment supply factors governed by watershed hillslope processes. As such, influences on channel morphology are both temporally and spatially variable.

As an aid in managing future reach-scale changes in morphological activity, it is necessary to understand whether individual flood events will result in net aggradation or incision in the LSCR. In this regard, a sediment budget analysis of the lower river is highly instructive in understanding system behavior. Fundamentally, it addresses the question "does sediment supply at the upper limit of the LSCR exceed

the river's ability to transport the received sediment to the ocean?" on an event-by-event basis. When the answer is yes, then net aggradation should occur; if no, then net incision may be expected. A sediment budget approach is preferred to a "design flood" basis for this conceptualization, where each source tributary is assigned an equal recurrence interval flood event (*e.g.*, the 10-year flood) because the size, topography and climate of the Santa Clara River watershed results in flood events of different relative magnitudes depending upon where rain is falling in the watershed . Rainfall is generally spread unevenly around the watershed: if the event generates high amounts of rainfall in the eastern watershed, flows from the less erodible upper river may be relatively higher than from Sespe Creek, increasing the chance for net incision to result. Conversely, when rain falls primarily over the northern portion of the watershed, in the highly erodible headwaters of the Sespe and Santa Paula Creeks, net aggradation may occur.

A template for this sediment budget approach was first provided by Simons, Li & Associates (1983), based on gauging records and a sediment transport model for coarse particles (*i.e.*, medium sand and coarser), that have the greatest influence on river channel morphology. Their model (Figure 5-22) was based on the major sediment supply inputs provided by the USCR and Sespe Creek (and a proportional estimate of 'other' sources), and sediment export as estimated from the Montalvo gauge in the LSCR. Figure 5-22a predicts that, in January 1969, there was a net transport of sediment out of the reach (net loss) because flows at Montalvo had the ability to transport more sediment than the total sediment supplied from the upstream sources. Conversely, in February 1978 (Figure 5-22b), the reverse applied and there was a net supply of sediment to the LSCR. This condition, which was demonstrated to be "unusual" in the context of the other compared floods (January 1969, February 1969, March 1978, February 1980), was largely the result of an exceptional load of sediment supplied to the LSCR by Sespe Creek. This occurred because Sespe Creek inherently supplied a greater concentration of sediment per unit area (see Table 4-2), and because the flood in Sespe Creek was of far greater magnitude than that in the upper river (see Table 5-9) and of greater duration (Simons, Li & Associates, 1983). Although the local impact of these net results depends upon the character of individual reaches, the flood of January 1969 should have generally resulted in channel bed incision and banks undercutting (see descriptions in Section 5.2.2 and 5.2.3). Conversely, in February 1978, aggradation and lateral migration caused by flow deflection around deposited sediment may have been more likely.

The analysis first performed by Simons, Li & Associates (1983) is replicated and extended in Table 5-16 to encompass four storms since 1980 and the storm of March 2, 1938. As such, the analysis covers eight of the nine annual maximum peak instantaneous discharges to have been recorded in excess of 2,265 m^3s^{-1} (80,000 cfs; see Table 5-1) and includes the secondary floods of February 1969 (estimated at 4,248 m^3s^{-1}; 150,000 cfs) and February 1978 (estimated at 2,690 m^3s^{-1}; 95,000 cfs). The 1998 event was not included due to gauge malfunctions that prevented the collection of hourly discharge data, the minimum necessary for the analysis.

Overall, sediment supply inputs from the upper watershed were estimated as a function of flows from the Santa Clara River at the Los Angeles-Ventura County line/Piru (USGS11108500/11109000), Hopper Creek near Piru (USGS11110500), Sespe Creek at Fillmore (USGS1113000), and Santa Paula Creek at Santa Paula (USGS11113500) (see Appendix C for details). This improved resolution over the original analysis by replacing the "other sources" in the Simons, Li & Associates analysis (estimated as 50% of the contribution from the USCR) with explicit values for Santa Paula Creek and Hopper Creek. Long-term flow records exist in Santa Paula Creek but no sediment measurements have been made at the gauge: as a first estimate, the sediment rating curve for the nearby Sespe Creek is applied and scaled to the flows of

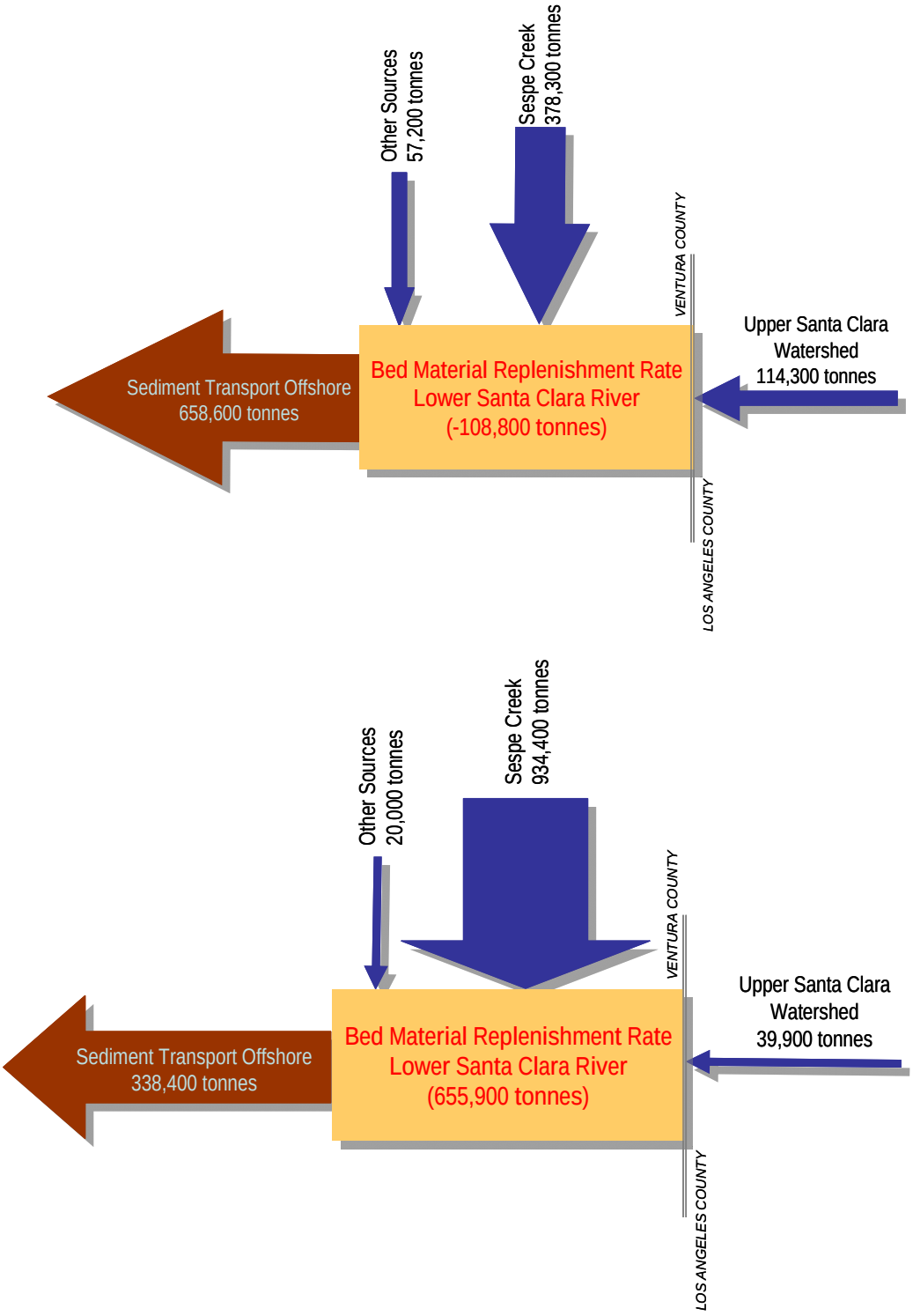

Figure 5-22. Illustration of the conceptual model of sediment transport dynamics within the lower Santa Clara River presented in Simons, Li & Associates (1983). Case A demonstrates a degradational (incision) event, based on the Simons, Li & Associates (1983) analysis of data from the January 25, 1969 flood. Case B shows an aggradational event based on their analysis of data from the February 10, 1978 flood.

the Santa Paula. A sediment rating curve does exist for Hopper Creek, but is based on fewer points than the other gauges. The ability to transport sediment offshore was estimated from gauging records on the Santa Clara River at Montalvo (USGS 11114000), representing the lower end of the LSCR. When the net input from the three supply sources exceeded the transport capacity at Montalvo, the morphological result should be net aggradation in the channel. As Sespe Creek provides the largest individual input of sediment of all the supply sources, net flood effects can be conceptualized as a competition between sediment supplied from Sespe Creek versus discharge to transport the sediment supplied by the upper river.

Table 5-16. Storm coarse sediment (>0.5 mm) yield.

Date	Sediment In (tonnes)				Sediment Out (tonnes)	Net supply to the Mainstem (tonnes)
	Santa Clara River near Los Angles/Ventura Co. Line	Hopper Creek	Sespe Creek	Santa Paula Creek*	Santa Clara River near Montalvo	
2-Mar-38	109,000	149,000	93,000	4,000	804,000	-449,000
25-Jan-69	582,000	108,000	338,000	22,000	1,346,000	-296,000
25-Feb-69	631,000	37,000	209,000	33,000	1,699,000	-789,000
10-Feb-78	39,000	26,000	752,000	11,000	557,000	271,000
4-Mar-78	55,000	61,000	175,000	5,000	873,000	-576,000
16-Feb-80	36,000	72,000	38,000	1,000	304,000	-157,000
1-Mar-83	49,000	44,000	263,000	4,000	696,000	-336,000
12-Feb-92	34,000	18,000	130,000	2,000	335,000	-151,000
10-Jan-95	51,000	59,000	350,000	5,000	689,000	-224,000
10-Jan-05	259,000	66,000	345,000	13,000	1,003,000	-320,000

* Sediment yield determined from Sepse Creek sediment rating curve.

Numerous data assumptions were necessary to construct the sediment budget. One simplification implicit in both the Simons, Li & Associates (1983) analysis and here is that the sediment rating curve is deemed to be time invariant; that is, floods of a particular magnitude will always produce the same amount of sediment and vary only according to their duration. In reality, hillslope sediment supply is probably highly variable in time (see Section 3). Second, the analysis does not account explicitly for sediment supply from other sources *within* the LSCR (*e.g.,* sediment supplied by small South Mountain tributaries), which may be considerable (Warrick, 2002)(see Table 4-2). A third major assumption is in data accuracy: the estimated net aggradation or incision is simply the residual from the surrounding estimates of sediment input and output (positive for aggradation, negative for incision). If, for instance, we assume that the sediment discharge at Montalvo has an error of ±50% (as Section 4.4.3), then, in Figure 5-22, the error value for Case A is approximately 330,000 tonnes, while in Case B it is approximately 170,000 tonnes. Under this scenario, only the aggradation in Case B may have been significant. Indeed, under this assumption, the event of February 10, 1978 could have been the only event with a significant effect on channel morphology of the five events analyzed by Simons, Li & Associates (1983). Fortunately, the repeat thalweg surveys demonstrating net incision (Section 5.3.3) provide corroboratory evidence that channel bed degradation was occurring in the LSCR in the period 1969–1980, adding confidence in the physical meaning of the results. It is, however, important to view the sediment budget as a device primarily for indicating relative change rather than absolute.

The results in Table 5-16 indicate a general trend towards channel bed incision in the LSCR for the largest floods of record. Similar to Simons, Li and Associates (1983), only the flood of February 10, 1978 is predicted to have resulted in channel bed aggradation (Figure 5-23a, b), whereas there has been a far greater overall loss of sediment from the LSCR, totaling approximately 3.0 million metric tons[6]. Converting this mass of sediment into a depth provides an estimate of net overall incision in the LSCR from the largest flood events of approximately 0.12 m since 1938[7]. This is a credible value in comparison with the overall incision measured along the thalweg in the LSCR, estimated at 0.7 m in the period 1949–2005 (see Section 5.3.4) from thalweg survey data, especially as there are two distinct reasons why this estimate will underestimate incision. First, the sediment budget from Table 5-16 does not represent sediment transport by smaller flood events (or even all the large events: events in 1998 and February 2005 could not be analyzed due to lack of sufficient data). Second, and more critically, the thalweg elevation survey data also includes the net effect of sediment removed mechanically through aggregate mining and so not all the 0.7 m average thalweg incision results from sediment transport processes.

To understand the potential impact of flood events of different relative magnitudes further, the recurrence interval of the each notable flood event for the major components of the LSCR was explored (Table 5-17). The maximum recurrence interval for each flood is a function of the period of record at each gauge and, as recurrence interval (RI) is derived from annual instantaneous flood peak data, there can be only one RI in any water year: judgment is necessary for the secondary floods of 1969, 1978, 1998 and 2005. Data in Table 5-17 show, for example, that the "degradational" flood of January 1969 was the largest on record in both the upper and lower Santa Clara River (RI = 53 years and RI = 54 years, respectively), whereas Sespe Creek experienced only a 14-year flood. Conversely, in the "aggradational" flood of February 1978, Sespe Creek experienced its largest flood on record at the time, (a 34-year RI event) in comparison to the 11-year RI flood on the USCR and the equivalent of a 7–8 RI event on the LSCR. At least in general, a pattern emerges: when flows are relatively higher in the USCR, incision occurs; whereas aggradation may occur when the highest flows are generated in Sespe Creek, which produces more sediment per unit area than does the USCR. As, on balance, incision is the more common flood outcome during the period of record (Table 5-16), the implication is that when the relative magnitude of flood events is roughly equal across the watershed tributaries, incision results. Such a watershed-level conceptualization is necessarily a simplification and will mask reach-level impacts: for instance, the flood of January 2005 represents the largest flood on record in Sespe Creek (and Santa Paula Creek) but also the second largest in the upper and lower Santa Clara River and net incision is predicted to result. However, as reference to Figure 5-20e shows (integrating the effects of the 1995 event, the poorly-documented 1998 event, and the 2005 flood), incision has been highly localized, suggesting that the balance of flood magnitudes, although instructive, is not the only variable determining the effect of individual flood events.

[6] It is probable that the sediment transport efficiency at the Montalvo gauge in 1938 is over-estimated: the rating curve for flow (and so sediment transport) at the gauge is based on USGS flow measurements at various dates from 1968 to 2004 (http://nwis.waterdata.usgs.gov/ca/nwis/ measurements/?site_no=11114000), whereas in 1938 the Montalvo reach had no levees and bed elevations were probably 2–3 m higher than in 1969 (Figure 5-19b), suggesting far less efficient sediment transport through the reach due to overbank flows.

[7] Assuming a bulk density of 1,900 kgm^{-3} (Lave and Burbank 2004), a channel length from Montalvo to the LA County Line of approximately 54.8 km, and assuming that processes of incision are focused not on the full active channel width (reach averages values of 146–570 m through the LSCR) but instead on some sub-set of the channel bed represented here by the flow width of the 1.5-year recurrence interval event (reach average values of 104–360 m through the LSCR) (*e.g.,* part of the overall active channel width documented in Table 5-12).

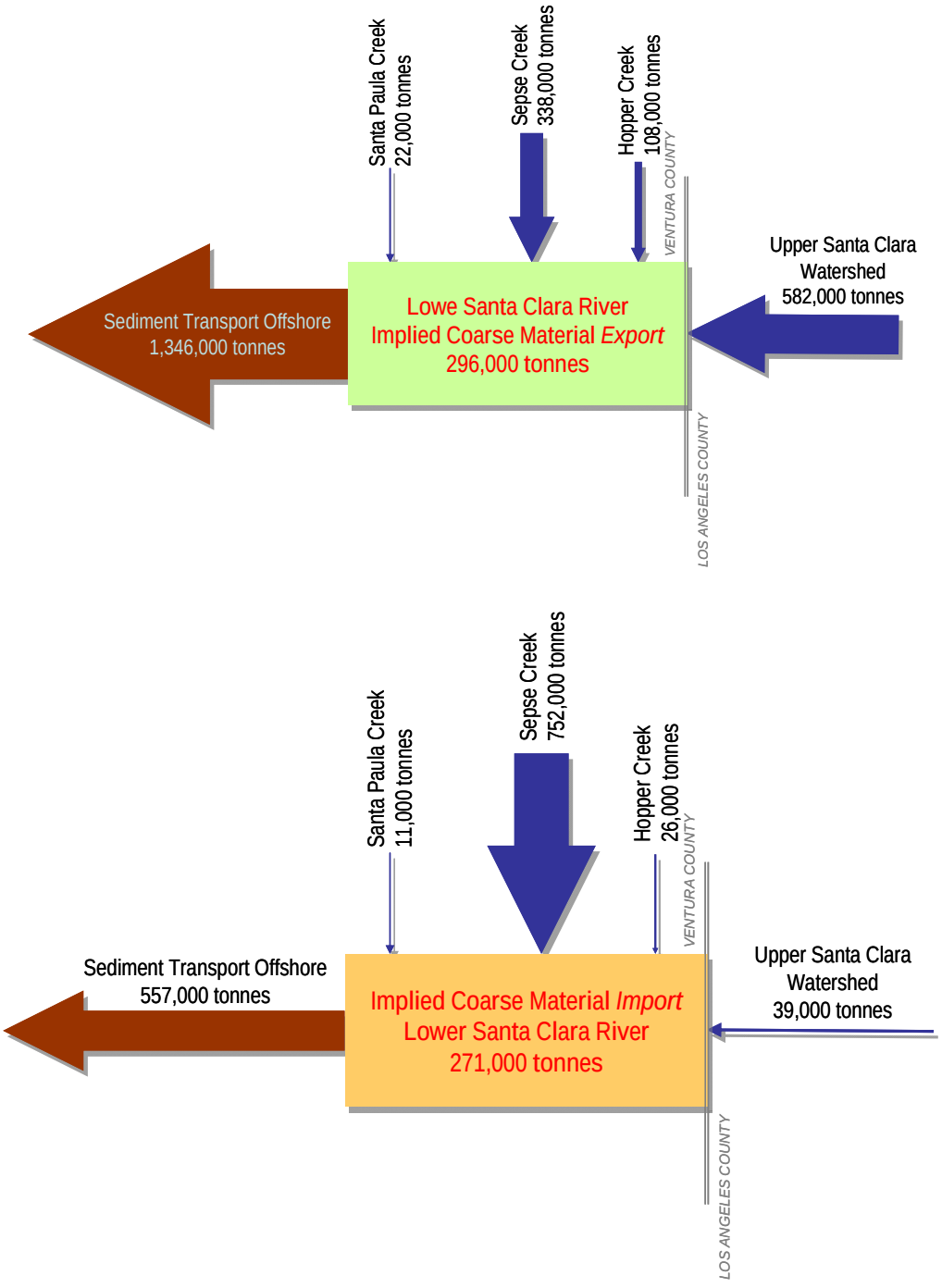

Figure 5-23. Re-calculation of coarse sediment budget for floods of January 25, 1969 (case A) and February 10, 1978 (case B). Note that the 1969 flood is still predicted to result in net incision, and the 1978 flood in net aggradation despite the different method and data used, compared to Simons, Li & Associates (1983).

Table 5-17. Flow discharge and recurrence intervals (RI) for the largest recorded floods on the Santa Clara River (Los Angeles/Ventura County Line and Montalvo stations), Sespe Creek, and Santa Paula Creek.

	SCR at Los Angeles/Ventura Co. Line[1]		Sespe Ck. near Fillmore[2]		SCR at Montalvo[3]	
Date	Flow (cfs)	RI (years)	Flow (cfs)	RI (years)	Flow (cfs)	RI (years)
Mar. 2, 1938	27,296*		56,000	9.7	120,000	18.0
Jan. 23, 1943	*no data*		44,000	7.6	80,000*	-
Apr. 3, 1958	7,070	3.5	28,400	5.2	52,200	4.9
Feb.10–11, 1962	9,100	4.1	25,600	4.5	47,700	4.2
Dec. 29, 1965	32,000	17.7	21,600	3.6	51,900	4.5
Dec. 6, 1966	*data gap*		21,600	3.8	35,000	3.2
Jan. 25, 1969	68,800	53.0	60,000	13.6	165,000	54.0
Feb. 25, 1969	62,500		45,000		152,000	
Feb. 11, 1973	12,800	6.6	38,300	6.2	58,200	5.4
Feb. 9-10, 1978	22,800	10.6	73,000	34.0	98,610	
Mar. 4, 1978	16,600		49,800	-	102,200	9.0
Feb. 16, 1980	13,900	7.6	40,700	6.8	81,400	6.0
Mar. 1, 1983	30,600	13.3	56,000	11.3	100,000	7.7
Feb. 14–15, 1986	12,300	5.6	*no data*		43,700	3.4
Feb. 12, 1992	12,300	5.6	44,000	8.5	104,000	10.8
Jan. 10, 1995	17,100	8.8	65,000	22.7	110,000	13.5
Feb. 3, 1998	*no data*		62,500	17.0	*data gap*	
Feb. 23, 1998	*no data*		*data gap*		84,000	6.8
Jan. 10, 2005	32,000[4]	26.5	85,300	68.0	136,000**	27.0
Feb. 24, 2005	*data gap*		*data gap*		82,200**	6.5

[1] Source: USGS 11108500
[2] Source: USGS 11113000
[3] Source: USGS 11114000
[4] Source: USGS 11109000
* estimated value (no gauging information available),
** estimated at Freeman Diversion [source: VCWPD]
no data = gage malfunction or outside of years of gage operation (SCR at Los Angeles/Ventura County Line)
data gap = currently unable to access the data.

Overall, the existence of the extensive LSCR valley alluvium and floodplain implies that, over the long-term, the majority of flood events resulted in net sediment transport into the LSCR and significant overbank deposition. Conversely, storm-based sediment budgets during the period of data record have indicated a trend of net sediment transport out of the LSCR, a fact corroborated by bed elevation records (Section 5.3.4) indicating net incision. One mechanism to explain this effect may involve flow confinement due to levees in combination with a narrower, deeper channel resulting from instream aggregate mining. Disconnecting the floodplain has, therefore, likely resulted in an accentuated net export of sediment from the SCR watershed either to, or beyond, the Santa Barbara Littoral Cell (see Section 6.2.1).

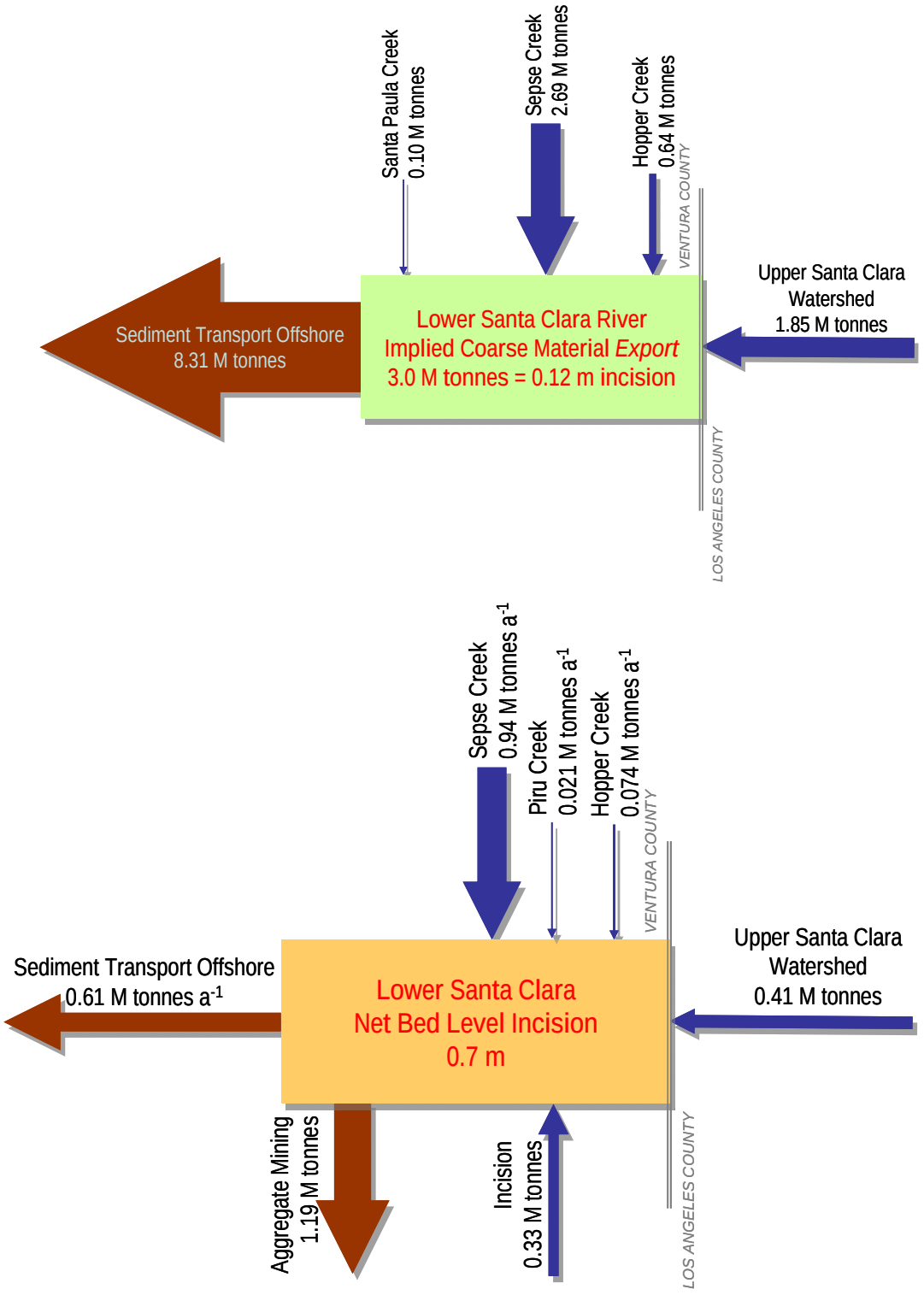

Figure 5-24. Case A: Integration of storm based sediment budgets based the largest recorded flood events only (data in Table 5-16). Net incision implied for the LSCRr is 0.12 m whereas from bed elevation records, net incision is 0.7 m. Case B: Sediment including an estimate of sediment removed directly by aggregate mining (scenario A in Table 5-18) resulting in very close agreement between sediment inputs and outputs.

5.4.2 Sediment Budget Accommodating Aggregate Mining

The residual term of 3.0 M tonnes of net sediment export over 67 years implied by the storm-event-based sediment budgets (*i.e.*, 0.045 M t a^{-1}), suggests net incision in the channel (as observed), but does not account for the direct impact of sediment removal caused by instream aggregate mining (Figure 5-24). By comparison, the average rate of instream sediment extraction in the period 1960–1977 is estimated to be approximately 1.7 M tonnes per year, and mining is known to have begun by at least 1950, and to have continued to 1989 (Noble Consultants, 1989; SCREMP, 1996). Therefore, like many other examples of aggregate mining in California (Kondolf and Swanson, 1993; Kondolf, 1997), the rate of extraction far exceeded the rate of natural sediment replenishment. Over the period 1949-1989, therefore, the net sediment export from the LSCR may be in the order of 60–70 M tonnes, depending on what assumptions are used for the periods without stated extraction rates (see Table 5-18).

Table 5-18. A 57-year sediment budget for the Lower Santa Clara River (1949-2005), inclusive of aggregate mining.

INPUTS		OUTPUTS	
Component	**Supply rate (M t a^{-1})**	**Component**	**Export rate (M t a^{-1})**
Scenario A – High			
USCR[1]	0.41	Aggregate mining[3]	1.19
Hopper[1]	0.074	Montalvo[4]	0.61
Piru[1]	0.021		
Sespe[1]	0.94		
Net channel incision[2]	0.33		
Total	1.775	**Total**	1.8
Scenario B – Low			
USCR[4]	0.37	Aggregate mining[6]	1.02
Hopper[4]	0.07	Montalvo[4]	0.61
Sespe[4]	0.85		
Net channel incision[5]	0.19		
Total	1.48	**Total**	1.63

[1] Rates from Warrick 2002
[2] Assuming net incision of the entire active width of the channel (see Section 5.3.2)
[3] Assuming a rate of 1.7 M t a^{-1}, sustained from the period 1949-1989
[4] Integrated from sediment transport rate calculations (see Section 5.1.1)
[5] Assuming net incision of the 1.5-year recurrence interval width of the channel (see Section 5.3.2)
[6] Assuming a rate of 1.7 M t a^{-1} 1960-1986, and a lower rate of 1.0 M t a^{-1} 1 in the early mining period 1949-1960, and in the period 1986-1989 as mining operations progressively finished.

Total sediment inputs and output for the period (inputs from County Line gauge, Sespe Creek, Hopper Creek, Santa Paula Creek, output from Montalvo gauge) can be inferred from suspended sediment data presented by Warrick (2002) (see Table 4-2) or by integrating the total coarse sediment transport implied by the sediment rating curves (e.g., Figure 5-2 to Figure 5-4; Appendix C). These values include all events (rather than just the large storms, as Section 5.4.1), but because they are based on mean daily flows they will underestimate transport potential of the largest peak flood discharges. The net supply of sediment to the LSCR from incision of channel bed (both through transport processes and mechanical removal by mining) is estimated from the 0.70 m average change in the thalweg elevation data over the LSCR length,

multiplied by the active channel width or the 1.5-year recuurence interval width estimate (for high and low estimates, respectively), to provide a sediment volume. The various sediment masses combine as:

Tributary sediment input – (mined sediment + sediment export at Montalvo) = channel incision.

Or, alternatively, as a mass balance:

Tributary sediment input + channel incision = mined sediment + sediment export at Montalvo

Recognizing the various errors and alternative sources of data, two scenarios are developed in Table 5-18, using different assumptions to represent potentially high and potentially low rates of supply and export. Despite the potential for large sources of error, the approximate balance between rates of sediment supply and sediment transport and mechanical export (especially for Scenario A) provide some corroboration both for the observed changes in bed elevation in the LSCR, and the overall effect of instream aggregate mining. In particular, it implies that, without instream aggregate mining, there would have been far less incision in the LSCR.

5.4.3 Reach-level Differentiation of Sediment Budget

A volumetric sediment budget was constructed for each of the 11 reaches of the LSCR. The apparent success in achieving an approximate mass balance between LSCR-averaged values for sediment input and output provides some confidence that the data representing bed-level changes (Section 5.3.3) can be used reliably to construct volumetric sediment budget at the reach level. Volumetric change is estimated using reach length, the average active channel bed width, and reach-averaged bed elevation change data (Table 5-19). Different volumes of sediment would result if a different metric for affected width was used (i.e., the "fully-scoured width", or the "1.5-year recurrence interval flow width", see Section 5.3.2), but the result would remain relatively similar between reaches. The implied mass of sediment is calculated using a bulk density of 1,900 kgm^{-3} (Lave and Burbank, 2004). Annualized rates of aggradation are provided for comparison with rates estimated in Table 5-16 and Table 5-18.

Results in Table 5-19 predict that sediment supplied from the upper watershed (including Castaic, Piru and Hopper creeks) is deposited progressively in the reaches upstream of Sespe Creek. Note that the estimated annual rate of sediment aggradation in Reaches 7–11 of 344,000 t is equivalent to or less than the sediment supplied by the USCR and Hopper Creek in the largest storm events (325,000 t in January 2005; 690,000 t in January 1969). This aggradation is presumably related, at least in part, to velocity reductions in flood waters from the USCR as they meet frequently larger flood discharges emanating from Sespe Creek, and they may have occurred more frequently in recent decades because of flood flow reductions above Sespe Creek resulting from regulation of flows by Santa Felicia Dam on Piru Creek. Downstream, Reaches 5 and 6, between Sespe and Santa Paula creeks, function to transport approximately the same amount of sediment as supplied to them.

Notable sediment losses occur in Reaches 1-4 and, in Reaches 2-4, apparently resulting from a combination of aggregate mining and fluvial processes. The combination of knickpoint creation, as a product of aggregate mining, and the containment of flood flows through levee construction, has resulted in a narrower, deeper, channel than existed previously. Narrower, deeper, channels are more effective at transporting sediment than shallower, wider channels of the same cross-section area, providing a mechanism whereby the present day LSCR is apparently capable of transporting out a greater volume of sediment than supplied to it in the majority of large storm events (Table 5-16).

Table 5-19. Reach level sediment budget for the Lower Santa Clara River, 1949-2005, inclusive of aggregate mining.

	Reach										
	1	**2**	**3**	**4**	**5**	**6**	**7**	**8**	**9**	**10**	**11**
Centerline reach length[1] (m)	6,412	9,967	4,715	3,503	2,545	6,803	5,267	5,710	4,745	4,445	6,076
Active width (m)	222	350	265	384	456	474	570	422	542	555	146
Reach average bed elevation change, 1949-2005[2] (m)	**-1.96**	**-3.90**	**-1.24**	**-1.13**	0.05	**-0.05**	0.86	0.58	0.42	0.42	0.83
Volume change (M m^3)	**-3.99**	**-29.18**	**-1.16**	**-0.83**	0.02	**-0.39**	4.23	2.53	1.47	1.65	0.46
Sediment balance[3] (M t)	**-7.57**	**-55.45**	**-2.21**	**-1.58**	0.04	**-0.73**	8.04	4.80	2.79	3.14	0.88
Rate of change (M ta^{-1})	**-0.133**	**-0.973**	**-0.039**	**-0.028**	0.001	**-0.013**	0.141	0.084	0.049	0.055	0.015

Notes:
[1] Derived from HEC-RAS output
[2] Derived from thalweg surveys 1949-1993, and data from 2005 LiDAR imagery.
[3] Derived using a bulk density of 1,900 kgm^{-3} (Lave and Burbank 2004).
Negative values (net incision and net loss of sediment) are highlighted in bold.

By far the greatest net loss of sediment has occurred in Reach 2, which saw both considerable aggregate mining, and the earliest containment of flood flows. One explanation for this phenomenon is that the levees prevented the channel from widening in response to incision, as is usually observed following knickpoint erosion (Schumm et al., 1984; Simon, 1989), and so recovery has not been possible. As extensive aggregate mining is not a factor in the history of Reach 1, it is possible that the significant reduction in channel width caused by levee construction has, in itself, been a sufficient mechanism by which to promote channel incision.

5.5 Summary: Fluvial Geomorphic Processes in the Lower Santa Clara River

5.5.1 Linkages: Interpretation of Morphological Changes in the LCSR 1929-2005

River channels change over time in response to natural environmental variations and to a suite of human influences. The present-day LSCR is functionally on the boundary between meandering and braided river forms, in terms of its relationship between gradient, discharge, and bed material grain size. The result (where natural processes prevail) is an unusual compound channel morphology, poorly described or analyzed in the published literature, that is essentially braided at lower flows but more akin to a low-sinuosity meandering channel during large flood discharges. The channel morphology of the semi-arid LSCR is affected primarily by large flood flows, rather than by the moderate discharges that are frequently used to characterize response in temperate river channels. The topography, situation, and latitude of the Santa Clara River watershed means that most of these important large discharges occur during years falling in the El Niño component of ENSO oceanic circulations. As ENSO occurrences have been more frequent since approximately 1969, there has been a corresponding increase in the number of large flood events in the LSCR over the last three decades.

The impact of individual large flood events depends primarily on the balance of discharge derived from the USCR versus Sespe Creek, the dominant tributary within the LSCR. If flows are relatively greater from Sespe Creek than from the USCR and sustained over a day or more, net aggradation is likely in the LSCR. We know also that the sediment yield from individual floods must depend on the amount of sediment delivered from hillslopes, and this may vary greatly according to recent earthquake activity in causing landslides, and the extent and frequency of wildfires in relation to high rainfall events. The fact that most large floods since 1930 have resulted in net incision, rather than aggradation, is likely due to the influence of human activities in the watershed because, over geological timescales, net aggradation in the LSCR must have been required to build the extensive deposits of the Oxnard Plain.

The active width of channel bed of the 60 km LSCR has become narrower by almost 50% from 1938-2005 (from 483 to 252 m). Further, over large stretches, the direct correspondence between active width and flood magnitude that might be expected in a semi-arid river has diminished over time. As such, few reaches of the LSCR now vary in active width commensurately with flood discharges. The LSCR has incised on average by 0.7 m from 1949–2005. Incision is focused in the lower parts of the river, where the maximum single-station incision is 7.65 m. Incision gives way to aggradation towards the upper end of the LSCR (maximum single-station aggradation of 3.1 m) such that over the period of record, the gradient of the LSCR has increased slightly from 0.0040 to 0.0041. In part due to human impacts, the downstream end of the LSCR now has a markedly greater stream power (a measure of the potential to transport sediment) than farther upstream, contrary to upstream-downstream trends in stream power found in most natural rivers. Such changes in the LSCR over the period of record help to explain why flood events now result in the net export of sediment from the watershed (*i.e.*, net incision).

Recent human activities in the watershed provide additional context for these patterns. Population in the SCR watershed increased ten-fold (from 31,000 to 314,000) from 1940-2004, and with it have come additional pressures for floodplain development, flood protection, and water resources. Three aspects are of particular note. First, intensive in-channel aggregate mining occurred in the lower LSCR from approximately 1950s until 1989 when in-channel mining was halted for fear of channel incision impacts on nearby infrastructure (*e.g.*, bridges). Second, progressive levee construction along the LSCR for flood control since the 1960s has seen approximately 40 km of levees built, covering about one-third of the total bank length of the LSCR, and resulting in a much narrower active channel bed. Plans exist for further levee projects in the LSCR (VCWPD, 2005). Third, several large dams have been constructed in the watershed, of which the completion of Santa Felicia Dam on Piru Creek in 1955 has probably had the largest impact on flows in the LSCR: overall, flow regulation facilities throughout the watershed have reduced water flows to the SCR by approximately 26%, and sediment yields by approximately 22%.

These impacts correlate with differences in channel response along the LSCR, and a sediment budget analysis of the LSCR, using flow and sediment gauging records combined with records of morphological change from the thalweg surveys and aerial photographs, suggests that these human impacts are responsible for much of this recent channel response. For example, the predicted net sediment export for large floods since 1938 is sufficient only to explain 0.12 m of the overall average incision in the LSCR of 0.70 m. However, if an estimate for sediment removal caused by aggregate mining is included into the budget, then an approximate mass balance is achieved (1949–2005) between estimates of sediment supplied from gauged tributary sources and sediment supplied through net channel incision (from thalweg surveys) versus sediment lost from the lower watershed through flow processes (i.e., sediment transport past the Montalvo gauge) and though mechanical removal by aggregate mining.

We are less certain of the cause-and-effect linkages for river channel changes in the LSCR from approximately 1820 to the early 1930s, a period beginning with extensive Euro-American settlement of the watershed and ending with the availability of channel thalweg surveys and aerial photographs used in the analyses above. Plat maps from around 1850 indicate that the river channel was in approximately the same position as it is currently, and other inferences can be drawn from ground photographs, narrative accounts, reconstruction of rainfall records back to 1770, and accounts of early groundwater extraction and irrigation practices. The watershed was subject to intensive cattle grazing from approximately 1820 until severe droughts in the 1860s and 1870s, after which irrigated agriculture quickly took over. Evidence elsewhere in western US would suggest that the period of ranching resulted in extensive soil erosion from hillslopes which could have exacerbated channel aggradation in the LSCR. Comparing maps to more recent images at the river mouth suggests that the mouth has built out into the ocean in this period, which would be consistent with an argument for high sediment yields during ranching.

Groundwater extraction in the Oxnard Plain from about 1890 caused rapid decreases in the surface elevation of alluvial aquifers. Upon formation of the forerunner to United Water Conservation District in 1925, irrigation methods switched to large-scale surface water diversions (from regulating Piru Creek) partly to recharge groundwater levels and to counter saltwater intrusion of alluvial aquifers. Decreasing groundwater levels may have caused the death of large riparian trees and in-channel vegetation, although the manual clearance of riparian vegetation for agriculture was also a common practice. Whichever mechanisms prevailed, this reduction in riparian vegetation could have reduced the resistance of the banks and bed of the LSCR to erosion during flood events. This may have allowed either the channel to become wider, or for flood flows to more effectively erode the channel bed. Finally, the flood discharge generated by the St. Francis Dam flood disaster in March 1928 event is estimated to be 3-5 times higher than any subsequent, natural flood event, and to consist of a wave of water that, from narrative and photographic evidence, caused both extensive erosion and deposition in floodplain lands.

Overall, the LSCR has undergone significant changes during the latter parts of the twentieth century, especially below the confluence with Santa Paula Creek where the channel is now very much deeper and narrower than in the historical past. The changes have occurred primarily in response to in-stream gravel mining activity, probably in conjunction with the construction of levees, but the changes themselves occur during very large flood events: the changes are, therefore, "climatically enacted but culturally prepared" (Downs and Gregory, 2004; see Section 3). Conversely, over the majority of recent geological time, large floods must have resulted in net aggradation to produce the extensive floodplain deposits that are now the (largely disconnected) Oxnard Plain.

Apportioning out changes explicitly to natural and human influences is confounded because not only have multiple human activities occurred on overlapping timeframes, but climate has changed also. So, not only do individual large floods appear capable transporting out more sediment to the lower reaches than supplied to them because of changes initiated by aggregate mining, and perpetuated by (progressive) levee construction, but there has also been an increased frequency of large flood events since 1969, corresponding with more frequent ENSO occurrences. Therefore, greater overall amounts of net sediment export have occurred than would have been the case, for example, in the 1944–1968 "quiet" ENSO period. Whether enhanced ENSO activity is occurring in response to climate change remains to be proven. However, there is clearly a significant morphodynamic legacy resulting from processes initiated by channel mining that, 18 years after the cessation of in-stream mining, is not abating. Rapid, partial recovery of the channel occurred upstream of Freeman Diversion Dam but additional local scour has occurred immediately downstream of the dam as might be expected.

Between Santa Paula and Sespe Creeks, the LSCR appears to be morphologically similar to its form in the 1930s although this is not to infer a "pre-European" reference condition, as the river will have responded to the integrated impacts of earlier human activities related to ranching and riparian forest clearance, groundwater abstraction, and the San Francis Dam break disaster. However, the reach still possesses nearly natural processes of flow and sediment transport because of the unregulated flows of Sespe Creek, and because the reach has not seen intensive instream aggregate mining or extensive levee construction. These factors seem likely to explain the semi-natural form of the reach.

Farther upstream, the increase of large flood events since 1969 is played out against a backdrop of somewhat reduced flows following the regulation of Piru Creek since 1955, and the potential impact of extensive upstream urbanization in Los Angeles County since about 1970. Channel narrowing and mild aggradation has occurred possibly because the reduced magnitude of large flow events causes channel sediments from the USCR to deposit out preferentially until such time that the reaches can become more efficient at sediment transport by establishing a narrower channel with steeper gradient to offset the reduction in flow magnitudes. An alternative or overlapping causal mechanism is provided by the rapid expansion of the city of Santa Clarita just upstream which may have resulted in a pulse of construction sediment working downstream. In the longer term, urban infrastructure usually causes a reduction in the relative concentration of sediments in flow and, eventually, to net channel incision, as observed in the Santa Ana watershed to the south of the SCR (Warrick and Rubin, *in press*). Investigating this effect in the upper reaches of the LSCR will require long-term channel morphology surveys and/or monitoring of sediment concentrations. A further alternative is that the aggradation results from episodically high sediment supply rates stemming from the increased frequency of large flood events since 1969.

5.5.2 Conceptual Model of Fluvial Processes in the LSCR

The various analyses performed in this section indicate that morphological changes in the LSCR are a complex response to numerous factors. From sediment transport calculations for individual large flood events, it appears that the *duration* as well as the *relative magnitude* of flood events from Sespe Creek is critical to the overall impact of individual events. Frequently, net incision occurs during large flood events, due in part to impacts related to aggregate mining and levee construction, but net aggradation is still possible if a large flood from Sespe Creek (the primary provider of sediment to the LSCR) is of sufficient duration. Further, the flood events in 1969 and 2005 are notable not only because of their magnitude, but also because in each year a secondary flood occurred within a month of the initial, largest flood. In both cases, the greatest net morphological change occurred in the second, smaller flood which was presumably more effective due to wet conditions that prevailed following the first event. As such, *antecedence* is a third factor in defining the net impact of individual events. Finally, while large flood events appear to cause the majority of flow-related morphological change in the LSCR from 1949–2005, a sediment budget analysis suggested that they are insufficient to explain overall morphological change in the LSCR; in addition, the volume of *sediment removed mechanically* had to be accommodated. Into the future, the cessation of mining means that mechanical sediment removal will not need to be accommodated explicitly in morphological changes, but that it will need to be incorporated along with other *contemporary and historical human activities* (*e.g.,* the existence of levees and Freeman Diversion Dam, flow regulation, urbanization, ranching, groundwater abstraction, St Francis dam disaster) in conditioning the channel response to individual floods events. The balance of impacts will alter in different reaches, so that *position* within the LSCR is an additional important variable, along with pre-existing *reach morphology* which will condition the detail of changes. Further, it is not possible with current sediment gauging data to account explicitly for *sediment supply variations* during individual flood

events caused by earthquake-induced landslides, or fire-flood sequences. Functionally and morphologically, large stretches of the LSCR are not the same as they were 70–80 years ago. However, relative to other rivers in the region, it has been remarkably little affected by human activity and thus has an intrinsic conservation value that can be fostered by judicious management practices.

6 ESTUARINE AND COASTAL PROCESSES

6.1 Physical Characteristics

6.1.1 Geologic Setting

The Santa Clara River delta and estuary lie within the Oxnard Plain, which occupies the seaward edge of the Ventura Basin, a large structural trough that plunges westward into the Santa Barbara Channel (Orme, 1982). Sedimentation within the Ventura Basin was primarily controlled by climate and tectonics during the Neogene period (24–2.7 Ma) and the current Quaternary period (2.7 Ma to recent time). While storm-induced flows in the Santa Clara River delivered sediment to the mouth and the Ventura Basin, tectonic deformation caused the central point of the Ventura Basin to subside intermittently, thereby affording space for further fluvial deposition (O'Hirok, 1985). Periodic transgression of tidal elevation across the Oxnard Plain has resulted in depositional sequences of both fluvial and marine sediments. The most recent depositional phase followed the late Pleistocene-Holocene transgression, in which sea level rose over 300 ft from 12,000 to 5,000 years ago, drowning the Santa Clara River mouth (Swanson *et al.*, 1990). Following this period of relatively rapid sea level rise, littoral accretion moved the shoreline seaward to its current location and a narrow barrier-lagoon system formed across the seaward edge of the Oxnard Plain (O'Hirok, 1985; Thompson, 1994).

The Santa Clara River Estuary (SCRE) lies along the axis of the active Oak Ridge fault (Figure 2-4). The Oak Ridge fault is a thrust fault that dips to the south at a shallow angle (< 30°) and forms a ridge south of the fault trace that parallels the Santa Clara River (Jennings, 1994). The slip rate of the fault is 3.5–6 mm yr^{-1} (Peterson and Wesnousky, 1994), which results in relative uplift of the SCRE in comparison with the region to the north.

6.1.2 Topography

Bed elevations taken in 2002 within the SCRE indicate an elevation range from approximately +0.3 m (+1.0 ft) Mean Seal Level (MSL) to approximately +2.4 m (+8.0 ft) MSL from the mouth to the extent of estuary flooding approximately 900 m (3,000 ft) upstream at the Harbor Blvd. Bridge (Figure 6-1) (ESA, 2003). The elevation of the sand barrier that closes the mouth is highly variable and can reach elevations in excess of +2.1 m (+7 ft) MSL (Swanson *et al.*, 1990). The current area of potential inundation within the estuary is approximately 0.42 m^2 (105 ac). The area of potential inundation for the estuary is defined primarily by the elevations of average yearly highest tide (+1.37 m MSL, +4.5 ft MSL) and observed extreme high tide (+1.58 m MSL, +5.2 ft MSL) for the region (see Table 6-1). Elevation data collected by ESA (2003) show that the median elevation within the current (2002) estuary is +1.13 m (+3.7 ft) MSL and the majority of the total estuary area is between +1.22 m (+4 ft) and +1.52 m (+5 ft) MSL (Figure 6-2). Levees adjacent to the estuary are 0.61 to 1.52 m (2 to 5 ft) higher than the maximum estuary bed elevation. The earthen levee that partially separates the Santa Clara River estuary and riparian forests from the adjacent campgrounds reaches approximately +3.05 to +3.56 m (+10 to +13 ft) MSL (ESA, 2003).

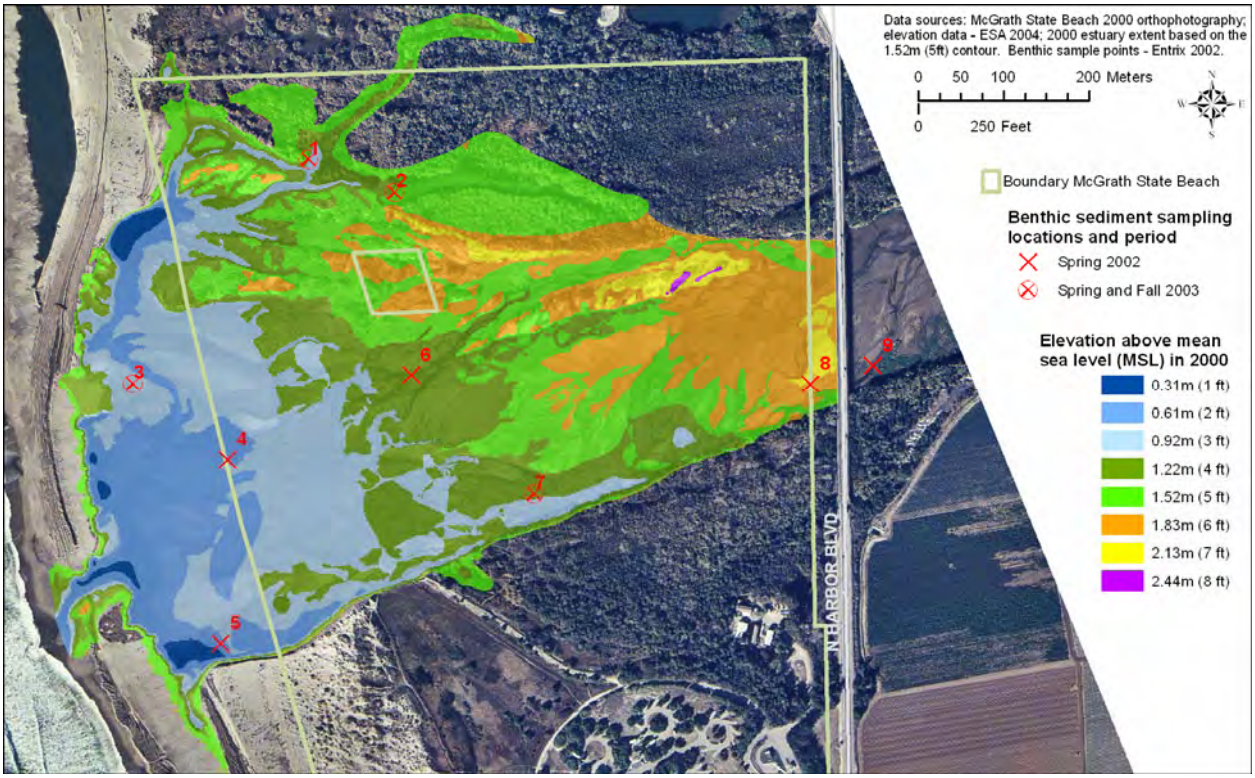

Figure 6-1. Topography (2000) and benthic sediment sampling locations within the Santa Clara River estuary (reproduced from ENTRIX, 2002; Aquatic Bioassay & Consulting Laboratories, 2004; ESA, 2003).

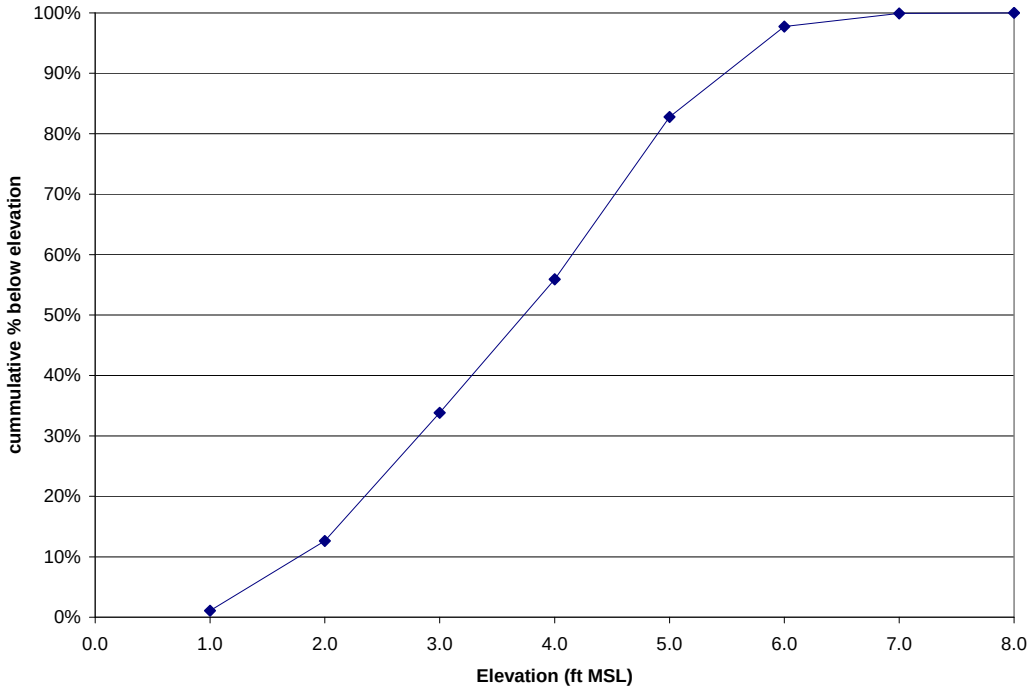

Figure 6-2. Topographic characteristics of the Santa Clara River estuary in 2000 (from ESA, 2003).

6.1.3 Tidal and Wave Dynamics

Tides

The tides at the mouth of the Santa Clara River are mixed semidiurnal (O'Hirok, 1985), meaning that in general there are two high tides (a lower high and a higher high) and two low tides (a higher low and a lower low) per day, although there are days in which there is only one high tide and one low tide. The mean tidal range at the Rincon Island gauge (approximately 20 km west northwest of the Santa Clara River mouth) is 1.13 m (3.71 ft), with the average yearly highest tide at +1.37 m (+4.5 ft) MSL and the average yearly lowest tide at -1.40 m (-4.6 ft) MSL (Table 6-1). The tidal prism within the SCRE calculated from 2002 topographic data (ESA, 2003) is approximately 56,634 m^3 (2.0 million ft^3). Tidal prism here is defined as the volume of water that can enter and exit the SCRE between the lowest bed elevation recorded in the estuary (0 m MSL, 0 ft MSL) and mean higher high water (+0.79 m MSL, +2.6 ft MSL). Mean sea level elevation has been projected to rise 1.5 to 2 mm yr^{-1} (approximately 6–8 inches per century) along the Southern California coast (Noble Consultants, 1989). In general, storm-induced increases in tidal elevation are relatively small (less than 0.3 m [1 ft]) in comparison with tidal fluctuations (Noble Consultants, 1989).

Table 6-1. Tidal elevations from Rincon Island (1962–1990).

Tidal Datum	Elevation (m MSL)	Elevation (ft MSL)
Extreme high (observed January 1983)	+1.58	+5.2
Average yearly highest	+1.37	+4.5
Mean higher high water (MHHW)	+0.79	+2.6
Mean high water (MHW)	+0.58	+1.9
Mean low water (MLW)	-0.55	-1.8
Mean lower low water (MLLW)	-0.85	-2.8
Average yearly lowest	-1.40	-4.6
Extreme low (predicted)	-1.65	-5.4

Source: NOAA, 1988

Waves

The effective wave energy modifying the coast is a function of wave direction, height, and period. Waves breaking onshore at the Santa Clara River mouth often approach from due west and are generated in the winter by low pressure systems over the Gulf of Alaska, and during the remainder of the year by the Hawaiian high pressure cell driving winds and swells to the east. Late summer tropical storms and Southern Hemisphere cyclones generate large swells from the south and south-southwest (O'Hirok, 1985). The average wave height along this shoreline is 1 m but ranges from 0.3 m to 7 m (Orme, 1982, as cited in O'Hirok, 1985).

Breaking wave type (plunging, spilling, or surging) influences the relative onshore movement of beach material. The most common wave type at the mouth of the Santa Clara River is a mixed plunge-spill breaker (O'Hirok, 1985). Owing to predominant deposition along this short segment of the coast, the foreshore is rarely steepened enough to generate surging waves. The width of the surf zone is a function of the slope of the near-shore bottom, wave height, tidal stage, and discharge. The submerged delta formed off the Santa Clara River can create surf zones greater than 250 m wide. Surf zones measured during high spring tides are narrower, as waves break closer to the steeper foreshore. When river discharge is low and sediment moved onshore by wave action forms a barrier that closes the Santa Clara

River mouth, the surf zone can decrease to less than 100 m with waves breaking only once (O'Hirok, 1985).

6.1.4 Estuary Hydrology and Hydraulics

Water in the SCRE is supplied predominantly by flow from the Santa Clara River and effluent from the waste water treatment plant, with local agricultural runoff and wave overwash also contributing to the overall supply (Swanson *et al.*, 1990). Observed water surface elevations within the SCRE range from +1.07 (+3.5 ft) MSL (Swanson *et al.*, 1990; USFWS, 1999) to +2.83 (+9.3 ft) MSL (USFWS, 1999) and the estuary can extend 914 m (3,000 ft) upstream during flooded conditions (Swanson *et al.*, 1990). The Santa Clara River discharge is very low most of the year (less than 0.03 m^3s^{-1} [1 cfs]), but storms that occur during winter and spring can increase discharge by several orders of magnitude within a few hours. At the mouth of the Santa Clara River, the City of San Buenaventura Water Reclamation Facility (waste water treatment plant) discharges an average of 31,797 m^3 day^{-1} (8.4 million gallons day^{-1}) of treated freshwater into the SCRE (City of San Buenaventura, 1999), which is equivalent to an average year-round stream flow of approximately 0.4 m^3s^{-1} (14 cfs). During the winter months when river flows dominate and generally maintain an open mouth, effluent discharge is a relatively small portion of total discharge volume. However, the average daily effluent discharge is far more than the average summer and fall streamflow that would be expected from an unregulated southern California river when the mouth is closed (ESA, 2003). Discharge of treated effluent from the waste water treatment plant while the mouth is closed can cause the water level of the SCRE to rise above the sand barrier and cause the barrier at the mouth to breach at a time of year when this would not occur under natural conditions (Swanson *et al.*, 1990, as cited in ESA, 2003).

In addition to the Santa Clara River mouth breaching as a result of impounded discharge causing erosion of the barrier beach, the mouth has been mechanically breached in the past to alleviate the risk of flooding adjacent to the estuary. Known recent authorized breaches include an emergency breach as part of the 1994 McGrath Lake oil spill and occasional breaches associated with the Ventura Port District annual winter dredging disposal operations (ESA, 2003). The McGrath Beach State Park 1979 General Plan indicated that park personnel would routinely breach the estuary barrier to prevent flooding of the campground caused by high groundwater. Due to natural resource considerations, this practice ended by 1985 (ESA, 2003).

6.1.5 Sediment Particle Size

The surface sediments within the SCRE are characterized by highly stratified layers of coarse sand with relatively small amounts of silt and clay (ESA, 2003), although cobble and boulder-sized sediment have also been observed being transported from the estuary during storm events (O'Hirok, 1985; J. Warrick, *pers. comm.*). Deposition of silt and clay-sized material has been observed due to fluvial delivery following storm events (USFWS, 1999) and flocculation (aggregation of fine sediment) induced by mixing of river and ocean water (O'Hirok, 1985). Grain size data collected during a closed phase of the estuary in spring of 2002 indicated that surface sediments were composed, on average, of 16% gravel, 64% sand, and 20% silt and clay (ENTRIX, 2002). Locations with greater that 12% gravel are restricted to the upper estuary, upstream of the waste water outfall channel. The surface samples collected at the 9 sample sites throughout the SCRE illustrated the degree of spatial variability of particle sizes (Figure 6-1). The D_{50} of the samples ranged from 0.04 mm (coarse silt) in the main channel to 2.41 mm (fine gravel) at the upstream extent of the estuary with a mean D_{50} value of 0.76 mm (coarse sand) (ENTRIX, 2002). Particle size data from four sites reoccupied during spring and fall 2003 (Sites 1, 2, 3, and 7) show the temporal variation in surface particle sizes within the SCRE (Aquatic Bioassay & Consulting Laboratories, 2004).

The Aquatic Bioassay & Consulting Laboratories (2004) study showed that sediments near the waste water outfall channel (Sites 1 and 2) were composed mostly of fine sands and were poorly sorted. The station located in the lagoon towards the barrier beach (Site 3) was fine silt in the spring and coarse silt in the fall. The bed at the station located in the main channel (Site 7) was composed of coarse sand in the spring and coarse silt in the fall. The shift in median particle size at the station in the main channel can be attributed to seasonal flow dynamics. During the spring after winter storms, sediments were coarser due to scour of fines and delivery of coarser sediments from upstream. In the fall, sediments are finer due to accumulation of fines during inundation in quiescent conditions (Aquatic Bioassay & Consulting Laboratories, 2004).

6.2 Sedimentation Dynamics

Sediment deposition dynamics at the mouth of the Santa Clara River and within the SCRE are driven by both fluvial and littoral sediment transport processes. Understanding how these processes interact to mediate deposition and subsequent Santa Clara River mouth closure dynamics is fundamental to understanding: (1) the fate of sediment within this fluvial-littoral interface, (2) the current and future geomorphic state of this mouth/estuary complex, and (3) the current and projected future ecological state of this system with respect to vegetation dynamics and fish passage. The following is a compilation of the current understanding of historical and present fluvial process and delta-building dynamics, longshore transport and shoreline dynamics, and barrier deposition and closure dynamics associated with the Santa Clara River mouth and estuary.

6.2.1 Fluvial Processes and Delta Dynamics

The Santa Clara River discharges a considerable amount of sediment primarily during high intensity, low recurrence storm events. Estimates of sediment discharge from the Santa Clara River by mass (tonnes yr^{-1}) and by volume (m^3 yr^{-1}) are shown in Table 6-2. In general, the coarser sediment (> 0.065 mm) that is delivered from the Santa Clara River during storm events contributes to the building of near-shore and offshore deltas, which in turn provides sediment for littoral transport (and down-coast beach deposition) and supplies sediment that builds the barrier beach and causes mouth closure during periods of low river discharge. Overall, the yield of sand and gravel from the Santa Clara River has been suggested to have decreased by approximately 25% from pre-development rates (Brownlie and Taylor, 1981).

Table 6-2. Summary of sediment discharge estimates for the Santa Clara River.

Sediment Discharge Class	Sediment Discharge (tonnes yr^{-1})	Sediment Discharge (m^3 yr^{-1})
Suspended Sediment	$3.5x10^6$ *[for 1950 to 1999]* (Warrick and Milliman, 2003)	
Sand		$1.35x10^5$ (Noble Consultants, 1989) $5.71x10^5$ (PRC Toups, 1980)
Sand & Gravel	$9.6x10^5$ *[for 1928–1975]* (Brownlie and Taylor, 1981)	$9.12x10^5$ *[for 1971–199]* (Willis and Griggs, 2003)
Total Sediment	$3.3x10^6$ *[for 1928–1975]* (Williams, 1979) $3.5x10^6$ *[for 1928–1999]* (Warrick, 2002)	

The high discharge events in the Santa Clara River that deposit sediment to the offshore delta are dominated by hyperpycnal flows (Warrick, 2002; Warrick and Milliman, 2003). Hyperpycnal flows are flows in which the river discharge is denser than ocean water due to high suspended sediment concentration. Buoyancy theory suggests a hyperpycnal threshold for suspended sediment concentration of approximately 40 g L^{-1} (approximate total flow density of 1,040 kg m^{-3}) for southern California rivers (ocean density = 1,025 kg m^{-3}) (Warrick, 2002). During the 1969 flood events, Santa Clara River suspended sediment concentrations exceeded the hyperpycnal threshold of 40 g L^{-1} for periods of hours to days. Warrick and Milliman (2003) suggest that the hyperpycnal threshold is surpassed during Santa Clara River flows less than 1 to 3 times the value of the mean annual flow (recurrence interval of approximately 1–4 yrs) and that approximately 75% of the estimated 170 million tonnes of sediment delivered from the Santa Clara River between 1950 and 1999 was delivered during hyperpycnal events. The density and velocity associated with hyperpycnal flows from the Santa Clara River cause the suspended sediment to pass through the estuary and near-shore zone, and be deposited on the offshore delta. This deposited sediment is then stored in the offshore delta and can be considered a potential loss of immediate beach sand supply (Warrick and Milliman, 2003). Hyperpycnal events with a low exceedence probability (> 100 year recurrence interval) have the potential to deposit sediment out of the littoral cell in offshore basins, essentially resulting a net loss of sediment within the system (Warrick and Milliman, 2003). This sediment routing can lead to local erosion by evacuating bed sediment that is deposited within the estuary.

The offshore delta of the Santa Clara River varies temporally with respect to volume due to variability in sediment input from the Santa Clara River and sediment erosion and subsequent down-coast deposition. The offshore delta had an estimated volume of 191 million m^3 (250 million yd^3) in 1989 (Noble Consultants, 1989). The largest recorded input of sediment from the Santa Clara River to the offshore delta occurred during the floods of 1969, in which approximately 9.94 million m^3 (13.0 million yd^3) of sediment was deposited (Noble Consultants, 1989). Drake (1972) determined that approximately 75% to 95% of the total load from the 1969 flood was deposited within 20 km from the Santa Clara River mouth, and that sand delivered from the Santa Clara River during the 1969 flood was initially deposited in a near-shore river mouth delta and was subsequently transported 1 to 1.5 km offshore onto the Santa Clara River delta. Following the 1969 flood events, bathymetric surveys conducted by the Ventura County Flood Control District and the U.S. Army Corp of Engineers (USACE) between December 1975 and May 1978 show a maximum seasonal gain in delta volume of approximately 3.10 million m^3 during fall/winter of 1977/1978 (~3x gain observed in two previous fall/winter surveys) as a result of deposition from a flooded Santa Clara River and a loss of approximately 1.20 million m^3 of sediment from the delta during winter 1975/1976 (USACE, 1980) due to lack of storms and subsequent sediment supply from the Santa Clara River. These data collectively suggest that the delta can be a significant source of sediment due to replenishment from the Santa Clara River during storm events, but prolonged periods between major storms can cause delta depletion which can lead to down-coast beach erosion. The mechanism of down-coast sediment delivery (longshore transport) and down-coast shoreline dynamics are discussed in Section 6.2.2.

Near-shore deltas form at the mouth of the Santa Clara River during more frequently occurring hypopycnal (river discharge is less dense than ocean water) storm events. O'Hirok (1985) suggested that near-shore delta formation and evolution at the mouth of the Santa Clara River can be described by application of jet theory (Bates, 1953), in which three zones exist: zone of flow establishment (constant velocity), zone of transportation (constant rate of velocity decrease), and zone of established flow (residual velocity decays rapidly through turbulence) (Figure 6-3). Deceleration in the transition zone

results in sediment deposition and delta building. Decelerations can be induced by density differences between incoming river water and ocean water. During hypopycnal flow events such as the flood event of March 1983, O'Hirok (1985) suggests that there is deposition of buoyant deltas (deposition as a function of flood water mixing with more dense sea water) and friction deltas (deposition as a function of decreased discharge resulting in accelerated sediment deposition and delta bifurcation) at the mouth of the Santa Clara River. Near-shore delta deposits from hypopycnal flows are ephemeral features subject to immediate wave impact and longshore transport, as well as local deposition at the mouth of the Santa Clara River which leads to barrier formation and subsequent mouth closure. The details of Santa Clara River mouth closure dynamics are discussed in Section 6.2.3.

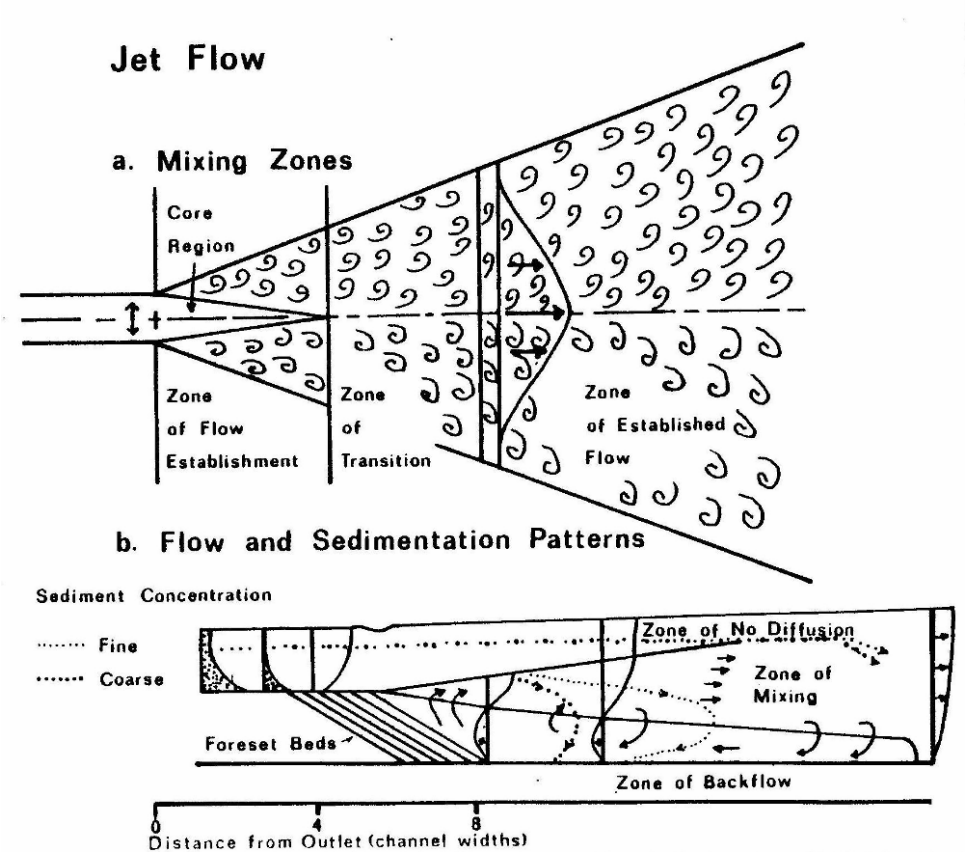

Figure 6-3. Conceptual description of sediment deposition from jet flow (O'Hirok, 1985, after Bates, 1953).

6.2.2 Longshore Transport Processes and Shoreline Dynamics

The sediment discharged from the Santa Clara River is transported down-coast via longshore transport as a part of the Santa Barbara Littoral Cell. Littoral cells are discrete coastal regions that can be considered closed systems within which sediment is transported. The Santa Barbara Littoral Cell, which is associated with the Santa Barbara Channel, is adjacent to the Santa Maria Littoral Cell and extends from Point Conception to Mugu submarine canyon (Figure 6-4). The portion of the littoral cell (subcell) for which the Santa Clara River specifically contributes sediment extends from Ventura Harbor at the northern extent to Channel Islands Harbor at the southern extent. Although Ventura River north of Ventura

Harbor does contribute sediment to this subcell, Ventura Harbor is considered the northern subcell extent. The strength and direction of the longshore current is a function of incoming wave height, direction of wave approach, and beach slope. In response to prevailing wind direction of 247° in the area of the Santa Clara River mouth and wave shelter from offshore islands, the longshore current generally flows down-coast in a southeasterly direction (O'Hirok, 1985; Noble Consultants, 1989). Longshore velocity can reach 2 m s^{-1} (Orme, 1982, as cited in O'Hirok, 1985). The direction of the current is subject to reversal during the summer months when occasional tropical storms generate large swells from the south (Orme, 1982; as cited in O'Hirok, 1985). Although longshore current reversals are frequent, sediment transported during these conditions represent a small portion of average total annual volume (Noble Consultants, 1989). Estimates by PRC Toups (1980) suggest that the Santa Clara River delivers approximately 65% of all sediment transport down-coast (O'Hirok, 1985).

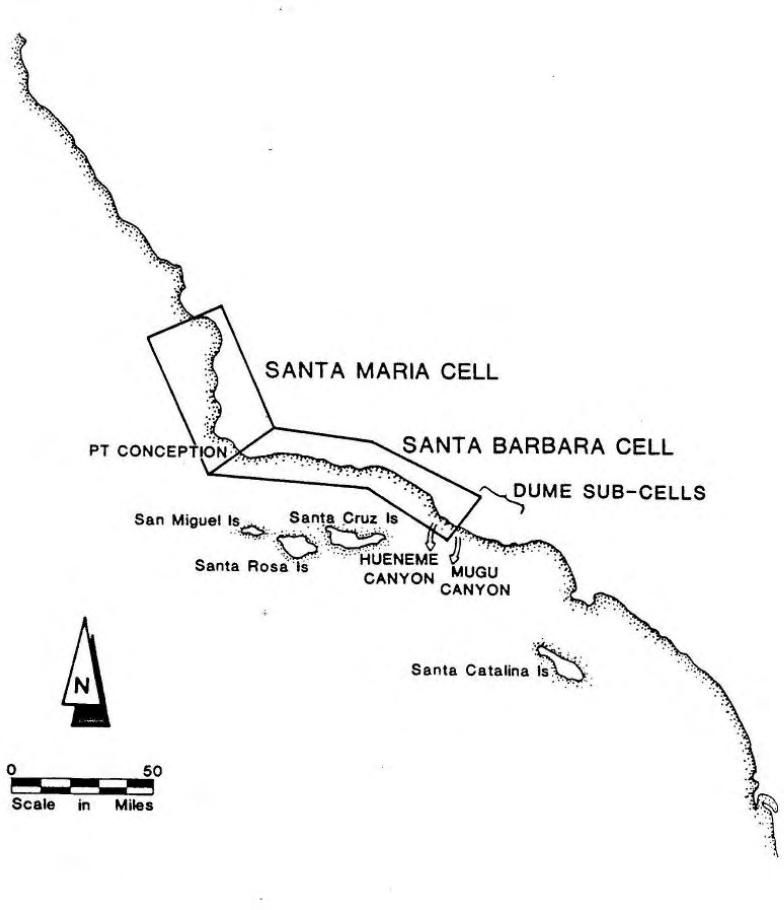

Figure 6-4. Location and extent of the Santa Barbara Littoral Cell (Noble Consultants, 1989).

Historical surveys show that the shoreline has changed considerably over the past 150 years immediately around the Santa Clara River mouth. From 1855 until artificially stabilized in the 1950s, the shoreline north of the Santa Clara River experienced a net seaward advance of several hundred feet while at the same time large retreats and advances down-coast occurred in response to fluctuations of the Santa Clara River offshore delta. Stabilization was affected by emplacement of a groin field (1962–1967), construction of Ventura Harbor (1963) in Pierpoint Beach, and establishment of a sand bypassing program for Ventura Harbor (Thompson, 1994). The shoreline directly adjacent to the Santa Clara River advanced seaward

approximately 101 m (330 ft) between surveys made in 1933 and 1948, retreated approximately 76 m (250 ft) from 1948 to 1961, and advanced approximately 98 m (320 ft) from 1961 to 1987 (during the 1969 flood a temporary delta extended seaward of the existing shoreline 607 m [2,000 ft]) (Thompson, 1994). Pronounced accretion between 1947 and 1955 was a result of the sediment made available in the offshore delta from the 1938 flood (Inman, 1950; Oceanographic Services, Inc., 1977; as cited in O'Hirok 1985). In the period directly after the 1969 flood events, there was considerable beach erosion at Oxnard Shores south of the Santa Clara River mouth, with subsequent shoreline advance in the early 1980s that yielded the approximate 150 m wide beach that currently exists (Orme, *pers. comm.*, 2005a). The overall net accretion that has occurred at the Santa Clara River mouth from 1855 to 1987 is approximately 274 m (900 ft) (Thompson, 1994).

In an effort to better quantify the relationship between observed beach erosion/deposition dynamics and sediment availability, Noble Consultants (1989) developed a sediment budget for the Santa Barbara Littoral Cell. The sediment budget analysis included numerical modeling of fluvial inputs from the Santa Clara River, analysis of net changes in sediment volume as computed by beach profile data, and estimates of annual longshore transport rates from dredging records from the Santa Barbara Harbor, Ventura Harbor, and Channel Islands Harbor. The sediment budget results indicate a yearly net loss of sand (as calculated from beach profile data) of approximately 298,176 m^3 (390,000 yd^3) between 1948 and 1966. The period between 1948 and 1963 represents pre-harbor conditions and was interpreted to be indicative of 'natural' conditions. An annual average net gain of sand of approximately 764,555 m^3 (1.00 million yd^3) was experienced between 1966 and 1970, which essentially records the effects of the 1969 flood. From 1970 to 1987, the average net gain was reduced to about 55,048 $m^3\ yr^{-1}$ (72,000 $yd^3\ yr^{-1}$). Dredging records between 1970 and 1987 indicate that approximately 489,315 $m^3\ yr^{-1}$ (640,000 $yd^3\ yr^{-1}$) on average is dredged from the Ventura Marina (up-coast of the Santa Clara River) and approximately 909,820 $m^3\ yr^{-1}$ (1.19 million $yd^3\ yr^{-1}$) on average is dredged from Channel Islands Harbor (down-coast of the Santa Clara River) (Noble Consultants, 1989). The dredged spoils are deposited down-coast of the harbor entrances on the beach and in the near-shore zone, and the sediment is subsequently entrained within the longshore current.

O'Hirok (1985) suggested that small symmetrical sand deposits lying between the dunes and the foreshore are remnants of spoil dredged from the Ventura Marina. Taking into account annual longshore transport reversals, the average annual net littoral transport rate near Ventura Harbor was determined to be 382,277 m^3 (500,000 yd^3) and the average annual net littoral transport rate near the Channel Islands Harbor was determined to be approximately 841,010 m^3 (1.10 million yd^3) (Noble Consultants, 1989). Combining this littoral transport rate in the vicinity of Ventura Harbor with a modeled average annual sand delivery rate from the Santa Clara River of approximately 133,797 m^3 (175,000 yd^3) (*i.e.*, sand from the Santa Clara River that is transported down-coast) yields an estimated average annual littoral transport rate of approximately 516,075 m^3 (675,000 yd^3) (Noble Consultants, 1989).

6.2.3 Barrier Deposition and Mouth Closure Dynamics

Typical of southern California rivers, barrier formation causes periodic closure of the mouth of the Santa Clara River. High-energy winter storms cause the mouth to remain open by both onshore wave action and increased offshore river discharge. Lower-intensity wave action and sediment deposition, and lower river discharges in the summer months facilitate onshore sediment transport and sediment deposition at the mouth, increasing mouth closure frequency and duration compared with the rest of the year (Swanson et al., 1990; Smith, 1990, as cited in ESA, 2003). When tidal range decreases during periods of low river discharge, the sediment transport capacity decreases due to a decrease in tidal prism, resulting

in mouth closure. Specific mechanisms shown to be important in mediating barrier closure and morphology in southern California lagoons include onshore migration of shore-parallel bars and longshore migration and eventual closure of the lagoon outlet (O'Hirok, 1985; Schwarz and Orme, in press). In general, the combination of river discharge dynamics, sediment availability from the near-shore river delta, sediment availability from longshore transport, and tidal dynamics contribute to barrier formation and mouth closure at the Santa Clara River. The closure dynamics of the Santa Clara River mouth can be a key component in determining the salinity regime of the system and subsequent vegetation establishment dynamics, as well a key component in controlling the migration of fish in and out of the watershed.

Data on the status of the mouth of the Santa Clara River suggest that the mouth is open more often than it is closed. Data collected daily by the City of San Buenaventura from 1984 to 1997 indicate that Santa Clara River mouth was open approximately 71% of the total time, with 1991 having the lowest daily frequency of an open mouth (51% of the year) and 1993 and 1995 having the highest daily frequency of an open mouth (96% of year) (City of San Buenaventura) (Figure 6-5). On a seasonal basis, the data collected by the City of San Buenaventura (1997) indicate that the mouth was open with the highest daily frequency in March (89% of time) and with the lowest daily frequency in August (57% of time) (Figure 6-6). The influence of extended storms on the status of Santa Clara River mouth has also been documented. El Niño-influenced river flows caused the mouth to stay open from December 1997 to August 1998 (Orme, pers. comm., 2005b). In general, these data reflect the storm-induced discharge patterns of the Santa Clara River from 1984 to 1999 (i.e., the mouth stayed open more during wetter years and wetter months), as well as the influence of mouth breaches due to the water treatment plant discharge and mechanical breaches.

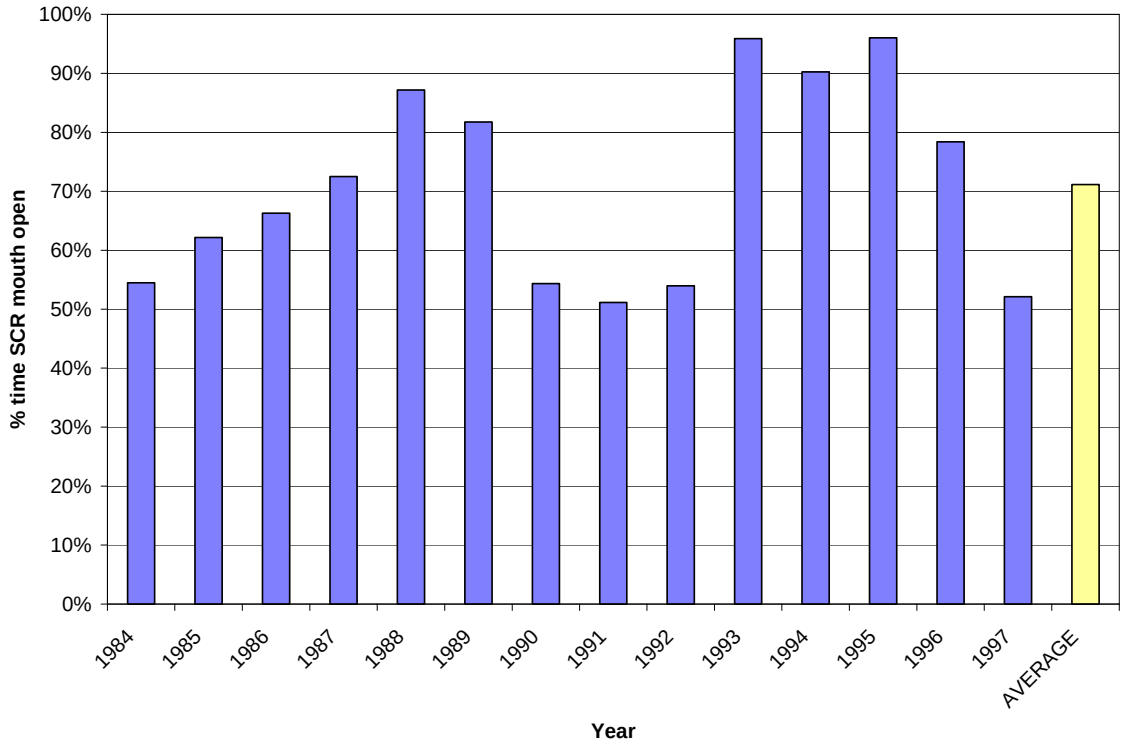

Figure 6-5. Percentage of time that the Santa Clara River mouth was open on an annual basis (1984–1997). (City of Ventura).

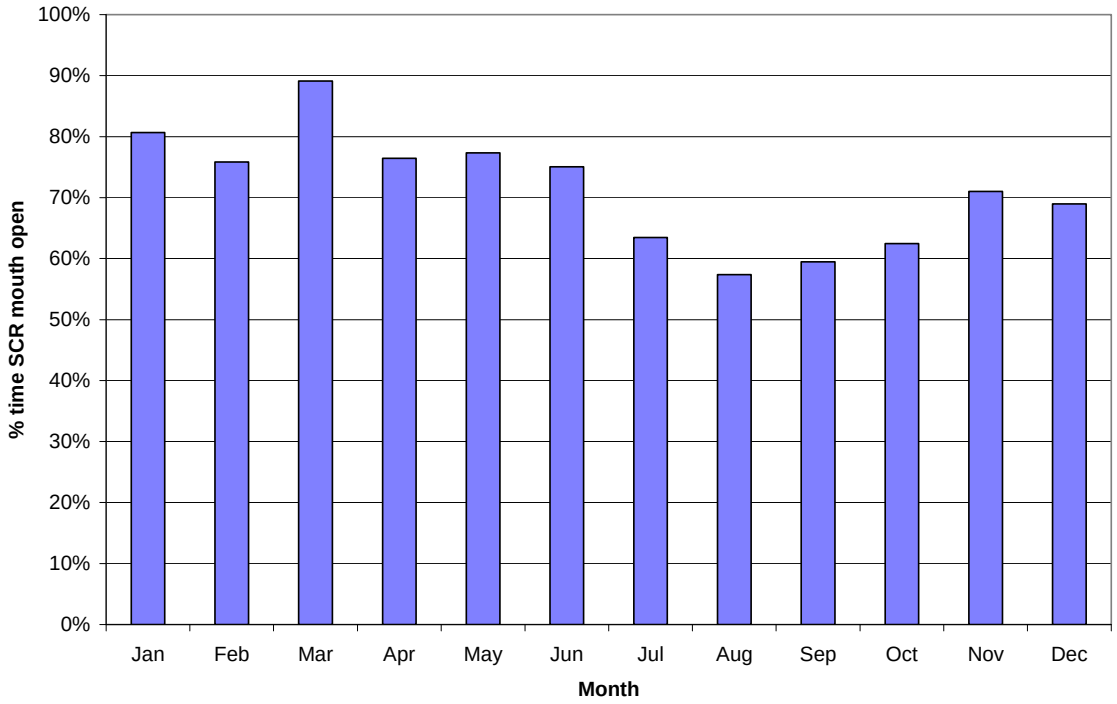

Figure 6-6. Percentage of time that the Santa Clara River mouth was open on a monthly basis (1984-1997). (City of Ventura).

The mechanics of a single barrier formation (mouth closure) and barrier erosion (breaching) at the mouth of the Santa Clara River following a single spring storm event have been documented, providing an insight into the processes and rates of barrier construction. O'Hirok (1985) examined a closure at the Santa Clara River mouth that occurred from April 16 to May 19, 1982 and breaching/resealing that occurred from May 20 to June 25, 1982 (Figure 6-7a-f and Figure 6-8a-f). Following a series of storms in April 1982, secondary barrier building began around the breached primary barrier and an offshore bar formed at the interface between river discharge and the ocean (Figure 6-7a). This accumulated bar caused breaking waves to then refract in many directions as they broke onshore. Continued onshore bar migration was facilitated by decreasing river discharge, increasing tidal range, decreasing wave height, and decreasing wave steepness. Decreased river discharge caused building of the secondary bar (Figure 6-7b). Secondary bar material was made up of silt over sand at the surface and gravel on the margins. As the bar continued to migrate onshore, river flow was divided into two channels (termed 'middle-formed bar') until the bar fused to the secondary barriers approximately 7 days after the closure began, creating a single outlet for river flow (Figure 6-7c).

Longshore transport (including a weak current reversal) and overwash by tidal action caused extension and increased the elevation of the secondary barriers, until a period of increased wave height and steepness caused increased onshore sediment movement and closure of the Santa Clara River mouth (approximately 34 days after closure began) (Figure 6-7d-f). As water elevation increased from a continuous low discharge (0.33 m^3s^{-1}) into the lagoon, the barrier was breached by overspill and the resulting high velocities in the channel (3 ms^{-1}) caused sediment approximately 300 mm in diameter to be

transported within the downcutting and widening (to 20 m) lagoon channel (Figure 6-8a,b). Longshore transport and overwash built up sediment around the breach (Figure 6-8c-e). Increasing tidal range and low intensity waves caused barrier sealing approximately 30 days after breaching (Figure 6-8f) (O'Hirok, 1985). O'Hirok (1985) concluded that mouth closure occurs at the Santa Clara River during 'tidal dominance' when wave energy is low, longshore current is slow, and river power is minimal. O'Hirok (1985) further concluded that tidal delta morphology (large flood-tidal delta and smaller ebb tide delta), which can contribute to mouth closure dynamics, was controlled by the magnitude of tidal prism, lagoon geometry, wave energy, longshore current, and quantity of longshore drift.

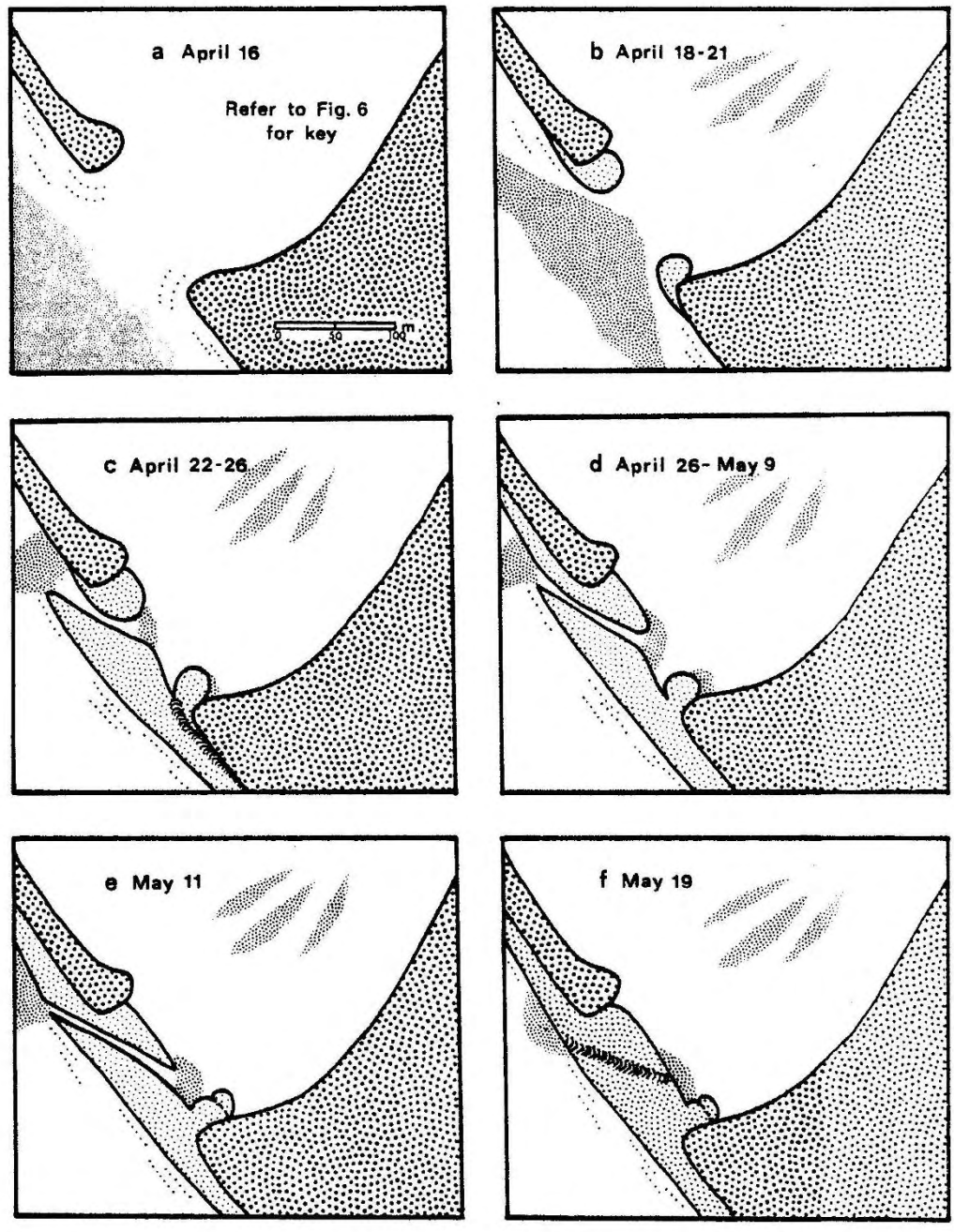

Figure 6-7. Time series of Santa Clara River mouth closure (April 16-May 19, 1982) (O'Hirok, 1985).

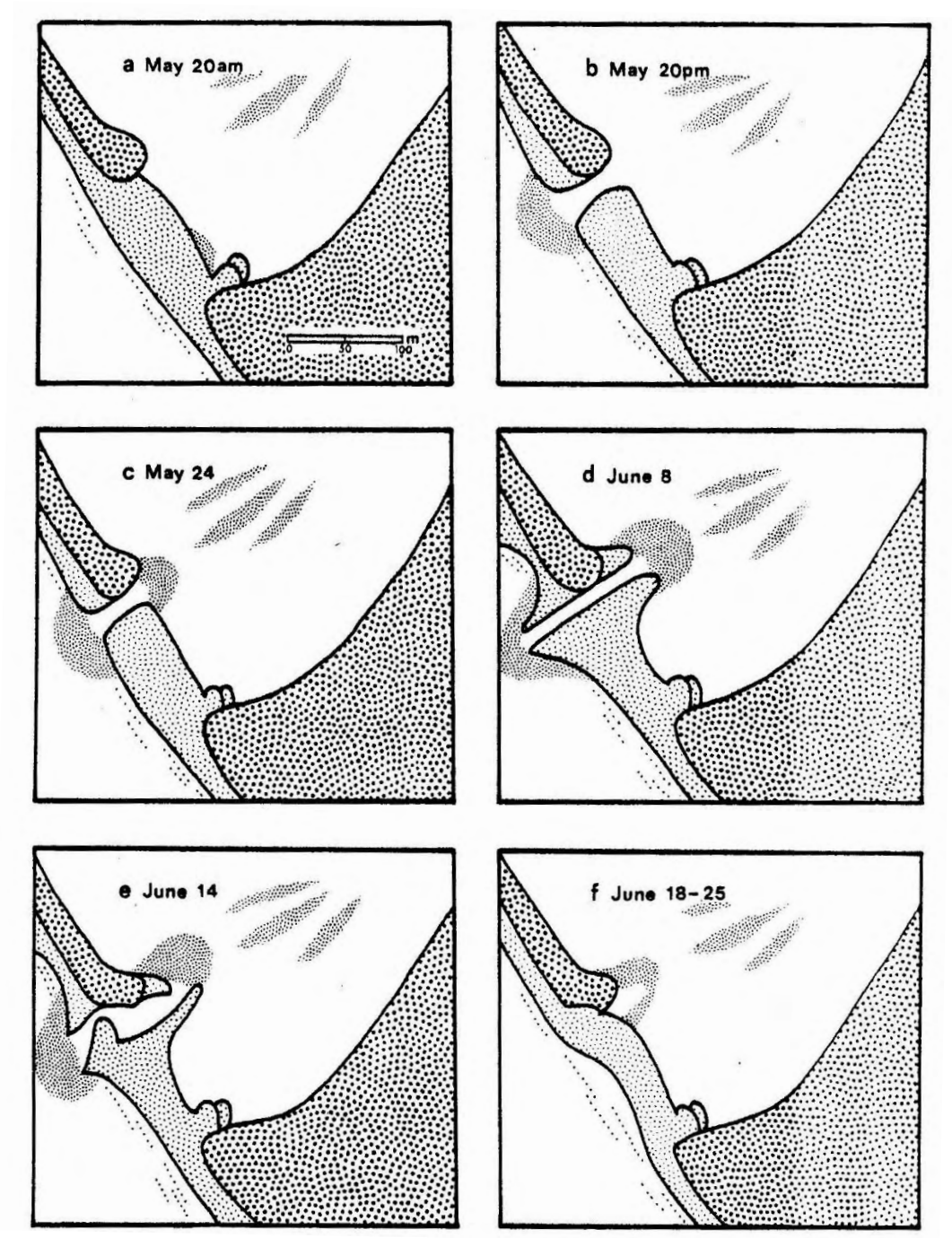

Figure 6-8. Time series of Santa Clara River mouth breach and closure (May 20-June 25, 1982) (O'Hirok, 1985).

6.3 Estuary Historical Change Analysis (1855-2002)

The SCRE has undergone considerable changes over the past 150 years. Agricultural encroachment and development within the historical estuary footprint have contributed to an approximate 75% decrease in estuary extent (Swanson *et al.*, 1990). A thorough narrative describing the overall changes of the SCRE with respect to anthropogenic impacts (levees, agriculture reclamation, and development) from 1855 to 1987 is given in the report by Swanson *et al.* (1990). The goal of the analysis presented in this study is to describe the historical geomorphic change of the entire Santa Clara River mouth and estuary in relation to the most recently documented (2002) extent of the active channel at the river mouth. Describing the change in the morphology of the entire mouth complex provides a context for understanding the evolution of the current estuary geomorphic dynamics. The active channel delineation used in the analysis is the approximate 1978/1980 flooding extent as described by Simons, Li & Associates (1983), with some modification due to erosion since the 1978/1980 floodway delineation. The active channel is essentially defined by the left and right bank levees upstream of Harbor Blvd. Bridge, the water treatment plant levee on the right bank downstream of Harbor Blvd Bridge, and the left bank terrace adjacent to the McGrath State Park campground on the left bank downstream of the Harbor Blvd Bridge (Figure 6-9). The active channel extent was superimposed on an 1855 U.S. Coast and Geodetic Survey (USC&GS) map of the Santa Clara River mouth and a series of aerial photographs of the Santa Clara River mouth from 1927 to 2002 (see Appendix G).[8]

Figure 6-9. Approximate active channel extent in July 2002. (Photo courtesy of California Coastal Conservancy)

[8] The 1855 USC&GS map and other historical aerial photography were georeferenced (no topographic correction) to the 2002 orthophotography (CA State Plane IV). Georeferencing of the 1855 map relied on an existing lat/long grid on the original scanned map and interpretation of surface features (bluff locations, abandoned channels, river mouth locations) against a 2002 NOAA IfSAR digital terrain model.

Summary – Historical Map and Photographic Interpretation

1855 The map of the Santa Clara River mouth from 1855 shows a meandering river channel with a broad floodplain and an extensive estuary/lagoon complex with a distributary channel network at the southern extent of the mouth complex. The shoreline and the river mouth (and associated estuary) are inland and the mouth/estuary complex is further north compared with the 2002 location. The extent of the SCRE is approximately 3.5 km^2 (870 ac) (Swanson *et al.*, 1990) (see Figure G-1).

1927 The shoreline and river mouth shown in the 1927 photograph advanced in comparison with the 1855 position. The river meandered through an active channel that extended an additional 762 m (2,500 ft) to the north and 305 m (1,000 ft) to the south in comparison with current conditions. A significant portion of the historical estuary to the north appears to be filled in and the mouth/estuary complex appears to have moved to the south (to approximate present location). Agriculture encroachment at the southern extent appears to have caused infilling of the distributary's channel network. Vegetation establishment within the active channel is not prevalent (see Figure G-2).

1945 The shoreline and river mouth shown in the October 1945 photograph advanced to the north and remained relatively stable to the south in comparison with the 1927 position. The sediment deposited from the St. Francis Dam failure (1928) and following 1938 floods (approximate 50-year event) is evident in the 1945 photograph. Vegetation within the main channel is still absent, presumably from scour associated with the 1938 flood event. The distributary channel network at the southern extent appears in-filled due to agricultural encroachment. Although the mouth/estuary complex appears to have expanded with shoreline advance, the area to the north appears to have been filled in more relative to the 1927 photograph.

1947 The shoreline and river mouth shown in the August 1947 photograph eroded slightly to the north and remained relatively stable to the south in comparison with the 1945 position. The estuary extent in comparison to the 1945 photograph appears relatively stable. Vegetation within the active channel is beginning to establish and stabilize the bed. The main channel at the mouth apparent in the 1945 photograph appears to have been filled, and the new main channel that empties into the estuary appears to be further north.

1958 The shoreline and river mouth shown in the April 1958 photograph have eroded landward at both the north and south ends in comparison with the 1947 photograph. A decade without a major discharge event from the Santa Clara River (*i.e.,* instantaneous discharge was less than 1,416 $m^3 s^{-1}$ [50,000 cfs] between 1947 and 1958) led to considerable vegetation development within the active channel. Riparian forest development at the southern portion of the active channel extent within the mouth/estuary complex led to a quasi-stable channel exiting to the north.

1969 The shoreline and river mouth shown in the February 1969 photograph appear relatively unchanged when compared with the 1958 photograph. Levees on both banks established upstream of the Harbor Blvd. Bridge have been established by 1969. The effects of the January and February 1969 floods within and around the Santa Clara River mouth are apparent in the photograph: a scoured channel network evident is evident on north side of the channel

(upstream of Harbor Blvd. Bridge) where the flow overtopped the levee; the impact of levee overtopping on the destruction of Ventura Marina is evident; and considerable deposition of sediment on the south side of channel upstream of Harbor Blvd is apparent. The location of the channel within the mouth/estuary complex is still to the north, but bank erosion induced by the 1969 flood is evident on riparian forest terrace to the south.

1993 The shoreline and river mouth shown in the April 1993 photograph have advanced seaward considerably at the north and south ends when compared with the 1969 photograph. A temporary storm-induced delta at the river mouth from the event in February 1993 (two months prior to when the photograph was taken) is also apparent. By 1993, the channel within the Santa Clara River mouth/estuary complex has migrated south to a location that is close to the current (2002) position.

2002 The shoreline and river mouth shown in the July 2002 photograph have eroded to the north and advanced to the south when compared with the 1969 photograph. Vegetation establishment is prevalent within the active channel due to a several years of relatively low flows (*i.e.*, instantaneous discharge less than 1,416 m^3s^{-1} [50,000 cfs] between 1998 and 2002). Further erosion of the riparian forest to the south and associated sediment deposition and riparian forest development to the north (when compared with the 1993 photograph) moved the main estuary channel at its present location (see Figure 6-9).

6.4 Conceptual Model and Projected Trajectory of the Santa Clara River Estuary

In order to understand the trajectory of the morphology of the SCRE, a conceptual model of geomorphic processes in the context of existing conditions was developed. Table 6-3 details the system variables that potentially affect the geomorphic dynamics of the SCRE. Understanding of the relative effects of these system variables on the estuary, in conjunction with the observations of estuarine evolution over the past 150 years described in the previous section, are key to developing a conceptual understanding of current and projected future geomorphic state of the SCRE.

The conceptual model for the current and projected geomorphic state of the Santa Clara River Estuary is illustrated in Figure 6-10. Overall, current storm flows within the lower Santa Clara River are constrained compared with historical conditions due to the network of flood-control levees. The discharge from the Santa Clara River watershed to the Santa Clara River mouth during lower-intensity (more frequent) storm events is less dense than the adjacent ocean water (hypopycnal) whereas discharge from higher-intensity (less frequent) storm events is dense with sediment in comparison with the adjacent ocean water (hyperpycnal). Hypopycnal events result in near-shore delta deposits that supply sediment for down-coast littoral transport and deposition, and supply sediment for barrier formation that occurs periods of low river discharge. Hyperpycnal events result in sediment deposition on the offshore delta and have the potential to deposit sediment in offshore basins during infrequent high-magnitude events. Sediment deposited in the offshore delta has the potential to be resuspended during storm events and transported down-coast. Overall, these conditions result in Santa Clara River storm flows that will maintain a river mouth and estuary that will remain in a fixed location on the Oxnard Plain in comparison with historical conditions, will migrate within the current active channel during high discharge events, and will supply sediment for mouth closure (near-shore deposition) and down-coast beach building (near-shore and offshore deposition). Although sediment loading to the Santa Clara River mouth is reduced compared with historical levels, hyperpycnal events still occur with often enough frequency to maintain the mouth/estuary. Furthermore, the decreased tidal prism within the mouth/estuary due to anthropogenic

encroachment does not offset the effects of hyperpycnal events to conclude that the mouth will not be self-maintaining.

Table 6-3. Elements of a conceptual understanding of the Santa Clara River Estuary.

Potential Impact on Estuary Development	Description
Sediment loading to the mouth has decreased due to dam and mining effects	• Less sediment is available to the off-shore delta compared with historical conditions • Potential for decrease in mouth closure frequency and decrease in down-coast beach replenishment
Magnitude of flows have decreased for given storm events due to dam effects	• Potential for more frequent mouth closure compared with historical conditions • Potential for increased sediment deposition in estuary
Tidal prism has decreased due to in-filling and levees	• Tide cannot maintain the mouth the way it was maintained historically • Potential to increase the frequency of mouth closure and sedimentation within the estuary
Levees have constrained flows	• Levees have caused position of estuary on the larger Oxnard Plain to remain stable relative to historical conditions • Constraining of flows causes local bed scour and channel migration relative to historical conditions.
Sea level rise	• Potential for drowning of mouth, causing landward migration • Potential for increased sediment deposition

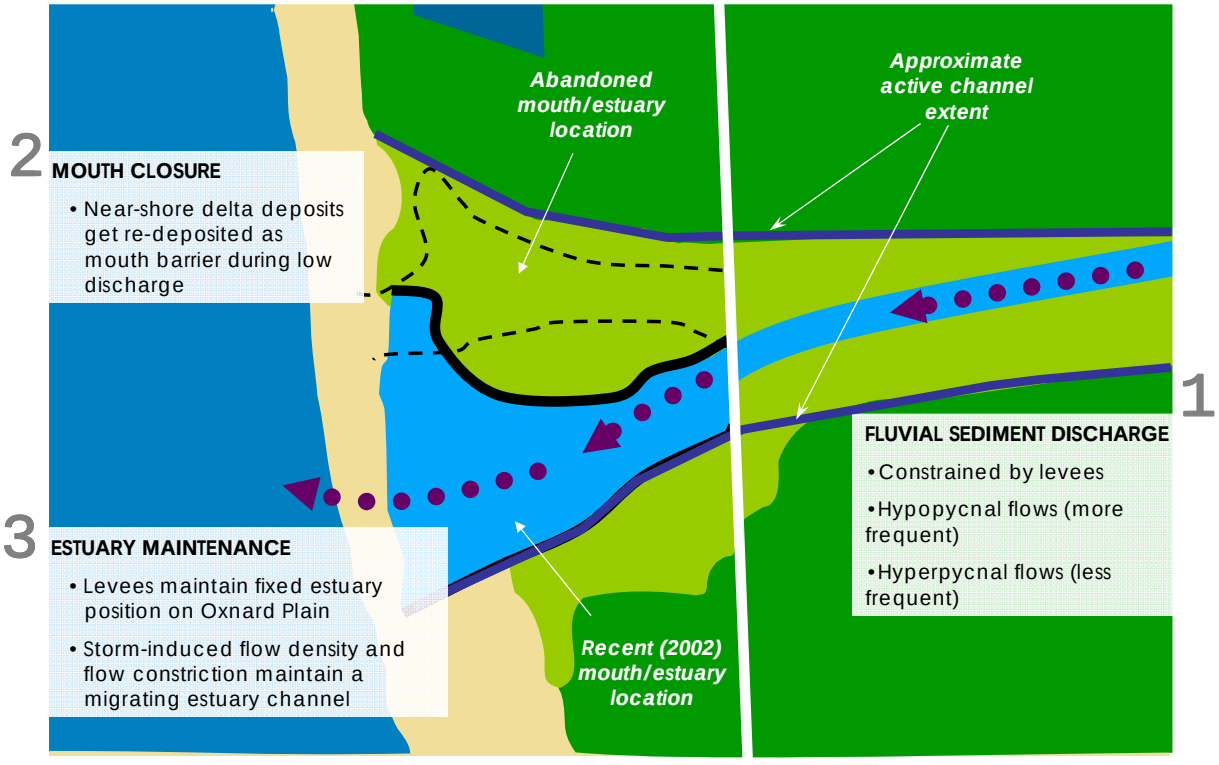

Figure 6-10. Conceptual model of the current and future maintenance of the Santa Clara River mouth/estuary complex.

7 SYNTHESIS

This report has identified and discussed the dominant geomorphic processes of the Santa Clara River watershed, with an emphasis on determining *what* has changed over time and *why*. Geomorphic processes and resulting conditions in the lower Santa Clara River (LSCR) are depicted by summary conceptual models of processes of hillslope sediment transport (Section 4.6) and estuarine dynamics (Section 6.4) based on available scientific literature. A conceptualization of processes in the lower mainstem river (section 5.5) is presented with an emphasis on the effects of human activities and large floods (Figure 3-1; Sections 5.1, 5.2), and is based on studies of scientific literature plus a detailed examination of channel morphological changes since approximately 1930 (Sections 5.3) supported by several sediment budgets derived from a sediment transport analysis (Section 5.4).

The geomorphic evolution of the lower river corridor depends strongly on rates of sediment supply and transport and how they vary over time. Rates and processes of hillslope sediment production and delivery to the mainstem have been summarized in Section 4. Particular attention was given to recent data documenting the prevalence of weak bedrock throughout the watershed (Section 4.2), the importance of dry raveling in maintaining a continuous supply of sediment (Section 4.2.1), the effect of shallow landslides (Section 4.2.3), the potential sediment legacy from the 1994 Northridge earthquake (Section 4.2.4) and from the widespread fires of 2003 (Section 4.2.5, and more recently in 2006), in combination with long-standing human impacts of rangeland conversion and fire management (Section 4.3). Available rates of hillslope processes are summarized in Section 4.4 and show that sediment supply from hillslopes is extremely dynamic: rapid uplift, periodic slope-destabilizing earthquakes, seasonally intense rainfall, and frequent fires all contribute to hillslope erosion rates in the Santa Clara River watershed that are among the fastest on record for the continental United States, with localized rates that rival the fastest in the world (Section 4.4.4). Sediment delivery to the mainstem Santa Clara River is episodic due to its semi-arid Mediterranean climate, and occurs predominantly during floods associated with fairly frequent moderate to big storms, interspersed by multi-year droughts (Section 4.5.1). Sediment delivery to the mainstem is likely to be highest during big storms that follow fires, due to enhanced runoff and sedimentation that result from post-fire hillslope processes (Section 4.5.2). Other influences on sediment supply and transport include flow regulation, notably of Piru Creek since 1955 by Santa Felicia and Pyramid dams, the flood that followed the collapse of the St. Francis Dam in 1928 (Section 5.2.1), the legacy of aggregate mining especially in the LSCR (Section 5.2.2), the progressive increase in the number of rock-revetted levees in the lower river (Section 5.2.3), the reduction in channel and riparian vegetation following flow diversion for irrigated agriculture and clearance (Section 5.2.4), and the prospect of future effects of urban growth in the upper watershed (Section 5.2.5). The integrated impact of these features on the morphology of the lower mainstem is described analytically in Sections 5.3 and 5.4, and summarized in Section 5.5.

The conceptual model of fluvial geomorphic processes for the LSCR was developed from a sediment budget model first advanced by Simons, Li & Associates (1983). The sediment budget estimates in Section 5.4, based of sediment gauging records throughout the watershed, illustrate whether the LSCR will incise or aggrade during individual floods based on a mass balance between sediment transport inputs from major tributaries versus sediment outputs from the mouth of the LSCR. In general, the output of the model indicates that, under channel conditions since about 1930, net incision is the most likely result in large storms events, but net aggradation in the LSCR can occur on occasions when flows in Sespe Creek, the major tributary, are high and of a sustained duration relative to those from the upper

SCR watershed. In this way, the model helps provide a means for assessing the patterns and types of flood risks and erosion hazards in the river corridor—factors that are ultimately related to whether the river is incising or aggrading. Comparing the model results to net morphological change inferred from adjustments in channel bed elevation and width over time indicated that natural fluvial processes, on their own, are insufficient to account for all the observed changes in channel morphology. However, adding an estimate for morphological change based on the volume of sediment mined directly from the channel improves the model appreciably. Ultimately the uncertainties inherent in applying a simple model to a complex river system will always be significant. It was suggested finally, that, in addition to factors of the duration and relative magnitude of flood events and sediment removed mechanically from the channel, morphological change during individual flood events will also depend on antecedent river conditions, the impact of contemporary and historical human activities, and sediment supply variations, factors that are all more difficult to quantify.

The conceptual model of the estuary describes the processes that are fundamental to estuary maintenance, integrating several studies of sedimentation dynamics, including recent research on the importance of hyperpycnal flows, the potential effect of sediment supply reductions due to historical aggregate mining and dam construction, and observations of bar deposition and mouth closure dynamics to conclude. There is the possibility that confinement of the lower mainstem channel by levees has resulted in increased suspended sediment concentrations in flood discharges at the estuary, such that of the frequency of floods with hyperpycnal flow conditions has increased. (Hyperpycnal flow occurs when the river discharge is much denser than ocean water due to high suspended sediment concentrations—see Section 6.2.1). Prior to channel confinement by levees, large flood flows would spread out and deposit fine sediments on the floodplain of the LSCR, reducing flow velocities and suspended sediment concentrations, such that flows entering the estuary and Pacific Ocean would be buoyant (and less prone to becoming hyperpycnal), in comparison with current conditions. Hence, levee construction since about 1960 may have not only affected fluvial processes of erosion and deposition in the lower mainstem river, but also caused changes to the dynamics of estuary formation and the replenishment of coastal sediment.

7.1 Key Information Gaps Affecting River Corridor Management Decision-making

The Santa Clara River is part of a large, complex, and highly dynamic watershed. This synthesis of information is intended to inform a cause-and-effect approach to understanding the geomorphic processes that shape the lower river. Developing this understanding further will provide a rational basis for prioritizing land acquisitions, and for developing corridor management strategies and restoration plans. Additional data and models that could assist in this endeavor are identified below.

- **Repeat channel survey data:** following the 2005 floods, an airborne Light Detecting And Ranging (LiDAR) survey was flown progressively under receding water conditions. It provides the first source of channel bed elevation data since a 1993 ground survey. This data, in comparison with the 1993 survey was used to discern recent trends in the bed of the LSCR, especially since the construction of the Freeman Diversion Dam in 1991. However, with the post-dam data temporally restricted to just two data points, additional surveys in low water conditions after future flood events are critical in determining more rigorously trends in morphological change in the LSCR and as the basis for planning future management strategies for the lower river.

- **Additional sediment transport measurements:** it was indicated in Section 5.1.3 that few bedload samples have been taken during high flows in the LSCR, making sediment transport modeling problematic because coarse material transport is estimated from sediment transport equations that may have limited validity in the Santa Clara River. The sediment loads in the Santa Clara River are so high, and such an important component of planning for river management, that resources should be committed for regular sampling of both bedload and suspended load in major tributaries during high flow events.
- **Event-based sediment transport investigations:** throughout this report, the importance of large floods for sediment transport has been emphasized, including the concentration of the large events in ENSO years (Section 5.1.2). It is therefore logical to plan studies to coincide with predicted ENSO events with, for instance, LiDAR channel survey data obtained before and after the event, and suspended and bedload sediment transport measurements obtained in a concentrated period throughout such events.
- **New sediment routing model:** recent developments in numerical modeling of sediment transport include the development of fractional sediment transport models that separate sand and gravel-cobble sediment fractions, models that can estimate the evolution of bedload sediment waves, and models that can accommodate a pulsed sediment supply. Each of these developments represents a fundamental advance in the ability to understand rivers like the Santa Clara that have a high fine and coarse sediment load components, and large, pulsed, sediment inputs at tributary junctions during extremely large flow events. The model should be run using short time-step integrating hydrological data pertaining to gauged flood events rather than using a design flood basis. In addition, the model could be run changing watershed inputs of water and sediment to simulate the impact of various human activities (*e.g.*, flow regulation of Piru Creek, upstream urban development).
- **Investigation of Northridge landslide effect on sediment supply:** the sediment legacy of the landslides triggered by the Northridge earthquake may be an important consideration for restoration along the lower river corridor (see Section 4.2.4). Subsequent storms have undoubtedly mobilized much of the earthquake-related landslide sediment downstream, but exactly how much of it remains in the watershed is unknown. Additional field reconnaissance might shed further light on this issue and individual landslides should be visited and surveyed.
- **Investigation of wildfire effects on sediment supply:** similarly, additional investigation of the effects wildfires on sediment delivery from hillslopes is warranted. Wildfires are a natural part of the sediment supply dynamic of the Santa Clara River watershed (see Section 4.2.5). For instance, post-dating the initial draft of this report, in September 2006, the Day Fire burned large areas of the Santa Paula, Sespe, Hopper and Piru Creeks, covering an area of approximately 664 km^2 (164,000 acres) or nearly 16% of the entire watershed of the Santa Clara River. Most studies of wildfire effects on sediment yields have occurred in small watersheds leading to valid concerns for how wildfire impacts can be aggregated over large spatial extents.
- **Estimation of long-term coarse sediment yield:** while reasonably reliable estimates of hillslope sediment production are available, there is only limited information about how much coarse sediment is transported downstream to the lower river corridor. Coarse sediment is arguably the most important part of the load in this case because it is most relevant to channel- and floodplain- forming processes and to littoral transport and beach replenishment. The high hillslope sediment production rates reported here suggest that the coarse load may be far higher than implied by previous sediment yield data. Quantifying the rate of coarse sediment delivery

to the lower river corridor is a major challenge, but might be achieved by comparing estimates of total load with estimates of suspended sediment yield to derive a residual coarse load, or by bathymetric surveys of reservoir sedimentation.

- **Develop a better understanding of the relationship between historical sediment supply changes and channel morphological change:** most of our data regarding channel change post-dates 1930. However, significant increases in sediment load caused by ranching on hillslopes in the mid-nineteenth century, together with reductions in riparian vegetation caused by irrigation, diversions and clearances in the early twentieth century may have had profound morphological impacts on the river that are currently undocumented. A dedicated historical study of early phase human impacts on the Santa Clara River would help elucidate the extent to which these pre-1930 impacts affected channel form, and the extent to which their legacy must be accommodated in future river management strategies.

Pursuing these types of information to fill data gaps will allow for a better understanding of the dynamics of the Santa Clara River and estuary, and provide managers with useful tools to predict how the river will change and the likely outcomes of restoration and management scenarios, including the development of the Santa Clara River Parkway.

8 REFERENCES

Ahnert, F. 1970. Functional relationships between denudation, relief, and uplift in large, mid-latitude drainage basins. American Journal of Science 268: 243-263.

AMEC (AMEC Earth and Environmental). 2004. Santa Clara River Enhancement and Management Plan (SCREMP) – Public Review Document. Prepared for the Ventura County Watershed Protection District, Los Angeles County Department of Public Works, and the SCREMP Project Steering Committee.

Anderson, H. W., G. B. Coleman, and P. J. Zinke. 1959. Summer slides and winter scour, dry-wet erosion in southern California mountains. Berkeley, California, U.S. Department of Agriculture, Forest Service, Pacific Southwest Forest and Range Experiment Station.

Andrews, E.D., R.C. Antweiler, P.J. Neiman, and F.M. Ralph. 2004. Influence of ENSO on flood frequency along the California Coast. Journal of Climate 17:337-348.

Aquatic Bioassay & Consulting Laboratories. 2004. Santa Clara River estuary macroinvertebrate bioassassment monitoring. Ventura California, Aquatic Bioassay & Consulting Laboratories, Inc.

Azor, A., E.A. Keller, R.S. Yeats. 2002. Geomorphic indicators of active fold growth: South Mountain-Oak Ridge anticline, Ventura Basin, southern California. Geological Society of America Bulletin 114: 745-753.

Bagnold, R.A. 1960. Some aspects of river meanders. U. S. Geological Survey Professional Paper 282-E:135-144.

Bagnold, R.A. 1966. An approach to the sediment transport problem from general physics. U. S. Geological Survey Professional Paper 422-I.

Bagnold, R.A. 1973. The nature of saltation and of bedload transport in water. Proceedings of the Royal Society of London, series A: 332:473-504.

Bagnold, R.A. 1977. Bed-load transport by natural rivers. Water Resources Research 13: 303-312.

Barnard, R.S. and W.N. Melhorn. 1982. Morphologic and Morphometric Response to Channelization: The case history of Big Pine Creek Ditch, Benton County, Indiana. *In* R.G. Craig and J.L. Craft eds., Applied Geomorphology. George Allen & Unwin, London, 224-239.

Bates, C.C. 1953. Rational theory of delta formation. American Association of Petroleum Geologists Bulletin 37: 2119-2161.

Benda, L., and T. Dunne. 1997. Stochastic forcing of sediment supply to channel networks from landsliding and debris flow. Water Resources Research 33: 2849-2863.

Bierman P.R. 2004. Rock to sediment - Slope to sea with Be-10 - Rates of landscape change. Annual Review of Earth and Planetary Sciences 32: 215-255.

Bledsoe, B.P., and C.C. Watson. 2000. Observed thresholds of stream ecosystem degradation in urbanizing areas: a process based geomorphic explanation. *In* Flug, M. and Frevert, D. eds., Watershed management 2000: science and engineering technology for the new millennium. Reston, VA: American Society of Civil Engineers.

Bledsoe, B.P., and C.C. Watson. 2001. Effects of urbanization on channel instability. Journal of the American Water Resources Association 37:255-270.

Blythe, A.E., D.W. Burbank, K.A. Farley, and E.J. Fielding. 2000. Structural and topographic evolution of the central Transverse Ranges, California, from apatite fissiontrack, (U/Th)/He and digital elevation model analyses. Basin Research 12: 97-114.

Booker, F.A. 1998. Landscape and Management Response to Wildfires in California. MS thesis, University of California, Berkeley.

Boughten, D.A., P.B. Adams, E. Anderson, C. Fusaro, E. Keller, E. Kelley, L. Lentsch, J. Nielsen, K. Perry, H. Regan, J. Smith, C. Swift, L. Thompson, and F. Watson. 2006. Steelhead of the south-central/southern California coast: population characterization for recovery planning. NOAA Technical Memorandum NMFS. October 2006.

Brownlie W.R., and B.D. Taylor, 1981. Coastal sediment delivery by major rivers in Southern California. Sediment Mangement of Southern California Mountains, Coastal Plains, and Shorelines, Part C, California Institute of Technology, Pasadena. Environmental Quality Laboratory Report 17-C, 314.

Brozovic, N., F. A. Booker, and W. E. Dietrich. 1997. A seventy year record of erosion and sedimentation from the San Gabriel Mountains, southern California American Geophysical Union, 1997 Fall Meeting 78.

Cayan, D.E., K.T. Redmond, and L.G. Riddle. 1999. ENSO and hydrologic extremes in the Western United States. Journal of Climate 12:2881-2893.

CDF (California Department of Forestry and Fire Protection). 2004. Fire and Resource Enhancement Program – Fire Perimeter GIS Data. http://frap.cdf.ca.gov.

CDMG (California Division of Mines and Geology). 1993. Update of mineral land classification of Portland cement concrete aggregate in Ventura, Los Angeles, and Orange Counties, California. DMG Open File Report 93-10. Sacramento, California, California Division of Mines and Geology.

CDSD (California Division of Safety of Dams). 2005. Website: http://damsafety.water.ca.gov/about.htm

Chang, H. 1985. Data received from Howard Chang, Professor at San Diego State University, 2 February 2005.

City of San Buenaventura. 1999. Annual report of analysis, City of San Buenaventura, Ventura Water Reclamation Facility, 1998. Prepared by City of San Buenaventura, California. 198 pp.

Cloud, W.K. and D.E. Hudson. 1975. Strong motion data for the San Fernando California, earthquake of February 9, 1971, *In* Oakshott, G.B. ed., San Fernando, California Earthquake of February 9, 1971. California Division of Mines and Geology Bulletin 196: 273-303.

Collins, B.D. and T. Dunne. 1990. Assessing the effects of gravel harvesting on sediment transport and channel morphology: a guide for planners. State of California Division of Mines and Geology, Sacramento, California. 26pp.

Corbett, E.S., and R.M. Rice. 1966. Soil slippage increased by brush conversion. Berkeley, California, U.S. Forest Service Pacific Southwest Forest and Range Experiment Station Research Note, PSW-128:1–8.

Culling, W.E.H. 1963. Soil creep and the development of hillside slopes. Journal of Geology 71:127-161.

Davis, W. M. 1892. The convex profile of badland divides. Science 20: 245.

DeBano, L.F. 1981. Water repellant soils, a state-of-the-art. Berkeley, California, United States Department of Agriculture, Forest Service, Pacific Southwest Forest and Range Experiment Station.

Densmore, A.L., and N. Hovius. 2000. Topographic fingerprints of bedrock landslides: Geology 28:371-374.

Deser, C., A. Capotondi, R. Saravanan, and A. Phillips. 2004. Tropical Pacific and Atlantic climate variability in CCSM3. Submitted to J. Climate CCSM# Special Issue.

Dietrich, W.E., and T. Dunne. 1978. Sediment budget for a small catchment in mountainous terrain. Zeitschrift für Geomorphologie, Supplement, 29: 191–206.

Dolan, J.F., and T. Rockwell. 2001. Paleoseismic evidence for a very large (M (sub w) >7), post-A.D. 1660 surface rupture on the eastern San Cayetano Fault, Ventura County, California; was this the elusive source of the damaging 21 December 1812 earthquake? Bulletin of the Seismological Society of America 91:1417-1432.

Downs, P.W. and K.J. Gregory. 2004. River Channel Management: towards sustainable catchment hydrosystems. Arnold, London.

Drake, D.E. 1972. Distribution and transport of suspended matter, Santa Barbara Channel, California, University of California, Santa Barbara, Santa Barbara, California.

Duvall, A., E.Kirby, and D. Burbank. 2004. Tectonic and lithologic controls on bedrock channel profiles and processes in coastal California. Journal Of Geophysical Research 109:F03002, doi:10.1029/2003JF000086.

Emmett, W.W. and G.M. Wolman. 2001. Effective discharge and gravel-bed rivers. Earth Surface Processes and Landforms 26:1269-1380.

ENTRIX. 2002. Resident species study Santa Clara River Estuary; Ventura water reclamation facility NPDES permit NO. CA0053651, CI-1822, Ventura water reclamation facility NPDES permit NO. CA0053651, CI-1822. Ventura, California, City of San Buenaventura.

Erskine, W. and R.F. Warner. 1988. Further assessment of flood- and drought-dominated regimes in south eastern Australia. Australian Geographer 29:257-261.

ESA (Environmental Science Associates). 2003. McGrath State Beach natural resources management plan (final). Los Angeles, California,

Prepared for the California Department of Parks and Recreation, Channel Coast District.

Faber, P. A., E. Keller, A. Sands, and B. M. Massey. 1989. The ecology of riparian habitat of the southern California coastal region: a community profile. Biological report 85(7.27). Mill Valley, California, U.S. Fish and Wildlife Service.

Ferguson, R.I. 1981. Channel Form and Channel Changes'. *In* Lewin, J. ed., British Rivers. George Allen & Unwin, London, 90-125.

Ferguson, R.I. 1987. Hydraulic and sedimentary controls of channel pattern. *In* Richards, K. S. ed., River channels: environment and process. Blackwell, Oxford, 129-158.

Ferrel, W.R., W.R. Barr, K.D. Mathews, R. Nagel, and J.S. Angus. 1959. Report on debris reduction studies for mountain watersheds: Los Angeles County Flood Control District, Dams and Conservation Branch.

Florsheim, J.L., E.A. Keller, and D.W. Best. 1991. Fluvial sediment transport in response to moderated storm flows following chaparral wildfire, Ventura County, southern California. Geological Society of America 103: 504-511.

Freeman, V. M. 1968. People-land-water: Santa Clara Valley and Oxnard Plain, Ventura County, California. Lorrin L. Morrison, Los Angeles.

Gabet, E.J. 2000. Gopher bioturbation: Field evidence for nonlinear hillslope diffusion. Earth Surface Processes and Landforms 25: 1419-1428.

Gabet, E.J. 2003a. Sediment transport by dry ravel. Journal of Geophysical Research 108:doi:10.1029/2001JB001686.

Gabet, E.J. 2003b. Post-fire thin debris flows: sediment transport and numerical modelling. Earth Surface Processes and Landforms 28: 1341-1348.

Gabet, E.J., and T. Dunne. 2002. Landslides on coastal sage-scrub and grassland hillslopes in a severe El Niño winter: The effects of vegetation conversion on sediment delivery. Geological Society of America Bulletin 114: 983-990.

Gabet, E.J., and T. Dunne. 2003a. Sediment detachment by rain power. Water Resources Research 39: 1002, doi:1010.1029/2001WR000656.

Gabet, E.J., and T. Dunne. 2003b. A stochastic sediment delivery model for a steep Mediterranean landscape. Water Resources Research 39: 1237, doi:1210.1029/2003WR002341.

Gabet, E.J., O.J. Reichman, and E.W. Seabloom. 2003. The effects of bioturbation on soil processes and sediment transport. Annual Review Earth Planet Science 31: 249-273.

Gilbert, G.K. 1877. Report on the geology of the Henry Mountains. U.S. Geological Survey. Washington D.C.

Gilbert, G.K. 1909. The convexity of hilltops. Journal of Geology 17:344-350.

Gomez, B. 2006. The potential rate of bed-load transport. Proceedings of the National Academy of Sciences of the United States of America 103: 17170-17173.

,Gomez, B. and M. Church. 1989. An assessment of bed load sediment transport formulae for gravel bed rivers. Water Resources Research 25: 1161-1186.

Graf, W.L. 1983. Flood-related change in an arid region river. Earth Surface Processes and Landforms 8: 125-139.

Graf, W.L. 1988a. Fluvial processes in dryland rivers. Springer-Verlag, Berlin.

Graf, W.L. 1988b. Applications of catastrophe theory in fluvial geomorphology. *In* Anderson, M. G. ed., Modeling geomorphological systems. J. Wiley and Sons, Chichester, 33-47.

Harp, E.L., and R.W. Jibson. 1996. Landslides triggered by the 1994 Northridge, California earthquake. Bulletin of the Seismological Society of America 86: 319-332.

Harvey, M.D., and C.C. Watson. 1986. Fluvial processes and morphological thresholds in incised channel restoration. Water Resources Bulletin 22: 359-368.

Hauksson, E. 1994. The 1991 Sierra Madre earthquake sequence in southern California: Seismological and tectonic analysis. Bulletin of Seismology Society of America 84: 1058-1074.

Heimsath, A.M. 1998. The soil production function. Ph.D. dissertation, University of California, Berkeley.

Heimsath, A.M., W.E. Dietrich, K. Nishiizumi, and R.C. Finkel. 1997. The soil production function and landscape equilibrium. Nature 388: 358-361.

Horton, R.E. 1945. Erosional development of streams and their drainage basins; hydrophysical approach to quantitative morphology. Bulletin of the Geological Society of America 56: 275-370.

Inman, D.L. 1950. Report on beach study in the vicinity of Mugu Lagoon, California. Beach Erosion Board, Technical Memo 14: 1-47.

Inman, D.L., and S.A. Jenkins. 1999. Climate change and the episodicity of sediment flux of small California rivers. Journal of Geology 107:251-270.

Iverson, R.M., M.E. Reid, and R.G. LaHusen. 1997. Debris-flow mobilization from landslides. Annual Reviews of Earth and Planetary Science 25: 85–138.

Jennings, C.W. 1994. Fault activity map of California and adjacent areas (with location and ages of recent volcanic eruptions), California Division of Mines and Geology, San Francisco.

Johannesson, J., and G. Parker. 1989. Linear theory of river meanders. *In* Ikeda S. and G. Parker eds., River Meandering. Water Resources Monograph 12, American Geophysical Union, Washington D.C., 181-214.

Keefer, D.K. 1984. Landslides caused by earthquakes. Geological Society of America Bulletin 95: 406-421.

Kirchner, J.W., R.C. Finkel, C.S. Riebe, D.E. Granger, J.L. Clayton, and J.G. King. 2001. Mountain erosion over 10 yr, 10 k.y., and 10 m.y. time scales. Geology 29: 591-594.

Knighton, A.D. 1998. Fluvial forms and processes. Arnold, London.

Knighton, A.D. and G.C. Nanson. 1993. Anastomosis and the continuum of channel pattern. Earth Surface Processes and Landforms 18: 613-625.

Kondolf, G.M. 1994a. Geomorphic and environmental effects of instream gravel mining. Landscape and Urban Planning 28: 225-243.

Kondolf, G.M. 1994b. Environmental planning in regulation and management of instream gravel mining in California. Landscape and Urban planning 29: 185-199.

Kondolf, G.M., and R.R Curry. 1986. Channel erosion along the Carmel River, Monterey County, California. Earth Surface Processes and Landforms 11: 307-319.

Kondolf, G.M., and W.V.G. Matthews. 1991. Unmeasured residuals in sediment budgets - a cautionary note. Water Resources Research 27: 2483-2486.

Krammes, J.S. 1960. Erosion from mountain side slopes after fire in Southern California. Research Note No. 171, PSW Forest and Range Experiment Station, U.S.D.A. Forest Servive, Berkeley, California.

Krammes, J.S. 1965. Seasonal debris movement from steep mountain slopes in southern California, in Proceedings, Federal Inter-Agency Sedimentation Conference, Jackson Miss.: US Department of Agriculture Miscellaneous Publications 970: 85-88.

Krammes, J.S., and R.M. Rice. 1963. Effect of fire on the San Dimas Experimental Forest. Arizona Watershed Symposium, Proceedings of the 7th Annual Meeting, Phoenix, AZ, 31-34.

Laak, D. 2005. Personal Communication with Phil Mineart, URS Corp. Ventura County Watershed Protection District, Ventura, California. 8 June.

Larsen, E.W. 1995. The mechanics and modeling of river meander migration. Unpublished dissertation, University of California at Berkeley.

Larsen, E.W., and S.E. Greco. 2002. Modeling channel management impacts on river migration: a case study of Woodson Bridge State Recreational Area, Sacramento River, California, USA. Environmental Management 30: 209-224.

Lave, J., and D. Burbank. 2004. Denudation processes and rates in the Transverse Ranges, southern California: erosional response of a transitional landscape to external and anthropogenic forcing. Journal of Geophysical Research 109: F01006, doi:01010.01029/02003JF000023.

Lawler, D.M. 1992. Process dominance in bank erosion systems. *In* Carling, P. A. and G. E. Petts, eds., Lowland floodplain rivers. J. Wiley and Sons, Chichester, 117-143.

Leopold, L.B. 1968. Hydrology for urban planning – a guidebook on the hydrologic effects of urban land use. U.S. Geological Survey Circular 554, Washington, DC.

Lynch, H.B. 1931. Rainfall and stream run-off in Southern California since 1769, Metropolitan Water District of Southern California, Los Angeles, CA.

Macklin, M.G., and J. Lewin. 1993. Holocene river alluviation in Britain. Zeitschrift für Geomorphologie Supplement-Band, 88: 109-122.

Mather, A.E., J.S. Griffiths, and M. Stokes. 2003. Anatomy of a 'fossil' landslide from the Pleistocene of SE Spain. Geomorphology 50: 135-149.

Meigs, A., D. Yuleb, A. Blythec, and D. Burbank. 2003. Implications of distributed crustal

deformation for exhumation in a portion of a transpressional plate boundary, Western Transverse Ranges, Southern California. Quaternary International 101-102: 169-177.

Mensing, S.A., J. Michaelsen, and R. Byrne. 1999. A 560-year Record of Santa Ana Fires Reconstructed from Charcoal Deposited in the Santa Barbara Basin, California. Quaternary Research 51: 295-305.

Metcalf, J.G. 1994. Morphology, chronology, and deformation of Pleistocene marine terraces, southwestern Santa Barbara County, California. M.S. thesis, University of California, Santa Barbara.

Miller, D. J., and J. Sias. 1998. Deciphering large landslides: linking hydrological, groundwater and slope stability models through GIS. Hydrological Processes 12: 923-941.

Minnich R.A. 1983. Fire mosaics in Southern-California and Northern Baja California. Science 219, 4590: 1287-1294.

Nanson, G.C. and J.C. Crooke. 1992. A genetic classification of floodplains. Geomorphology 4: 459-486.

NOAA (National Oceanic and Atmospheric Administration). 1988. Tide Tables. National Ocean Survey.

Noble Consultants. 1989. Coastal Sand Management Plan, Santa Barbara, Ventura County Coastline. Irvine, California, Prepared for BEACON (Beach Erosion Authority for Control Operations and Nourishment).

Oceanographic Services, Inc. 1977. Stability on the beaches in the Hollywood beach area, prepared for Howorth, Anderson and Lafer.

O'Hirok, L.S. 1985. Barrier beach formation and breaching, Santa Clara River mouth, California. Masters thesis, University of California, Los Angeles.

Orme, A.R. 1982. Temporal variability of a summer shorezone. *In* Thorne, C.E. ed., Space and time in geomorphology, Allen and Unwin, London, 285-313.

Orme, A.R. 1998. Late Quaternary tectonism along the Pacific coast of the Californias: a contrast in style. *In* R.L. Stwewart and Vita-Finzi, C. eds. Coastal Tectonics. Geological Society, London. Special Publication 146: 179-197.

Orme, A.R. 2005a. Personal Communication. University of California, Los Angeles. Santa Clara River, California, 6 March.

Orme, A.R. 2005b. Personal Communication. University of California, Los Angeles. 29 July.

Orme, A.R., and R. G. Bailey. 1971. Vegetation conversion and channel geometry in Monroe Canyon, Southern California. Yearbook - Association of Pacific Coast Geographers 33: 65-82.

Parker, G. 1976. On the cause and characteristic scale of meandering and braiding in rivers. Journal of Fluid Mechanics 76: 459-480.

Parker, G., and D. Andres. 1976. Detrimental effects of river channelization Proceedings of Conference Rivers 76: 1248-1266.

Peterson, M.D., and S.G. Wesnousky. 1994. Fault slip rates and earthquake histories for active faults in southern California. Bulletin of Seismological Society of America 84: 1608-1649.

Petts, G.E. 1984. Impounded rivers: perspectives for ecological management. J.Wiley and Sons, Chichester.

PRC Toups Corp. 1980. Vern Freeman diversion project, final environmental impact report. Prepared for United Water Conservation District.

Pulling, H.A. 1944. A History of California's Range-Cattle Industry, 1770–1912. Ph.D. dissertation, University of Southern California.

PWA (Philip Williams & Associates). 1997. Santa Clara River Enhancement Plan for Reach Five (contains PWA study – "A Geomorphic Evaluation of Meander Migration and Identification of Effective Bank Stabilization Locations").

PWA (Philip Williams & Associates). 2003. RFP Scoping Document – Santa Clara River Parkway Floodplain Restoration Feasibility Study, Ventura County, California. Prepared for the California Coastal Conservancy.

Rice, R.M., and G.T. Foggin. 1971. Effect of high intensity storms on soil slippage on mountainous watersheds in southern California. Water Resources Research 7: 1485-1496.

Rice, R.M., E.S. Corbett, and R.G. Bailey. 1969. Soil slips related to vegetation, topography, and soil in southern California. Water Resources Research 5: 647–659.

Richards, K.S. 1982. Rivers: form and process in alluvial channels. Methuen, London.

Roberts, C.R. 1989. Flood frequency and urban induced channel change: some british examples. *In* Beven K. and P. A. Carling eds., Floods: Hydrological, Sedimentological and Geomorphological Implications. J.Wiley and Sons, Chichester, 57-82.

Rockwell, T. 1988. Neotectonics of the San Cayetano fault, Transverse Ranges, California. Geological Society of America Bulletin 100: 500-513.

Rockwell, T.K., E.A. Keller, M.N. Clark, and D.L. Johnson. 1984. Chronology and rates of faulting of the Ventura terraces, California, Geological Society of America Bulletin 95: 1466-1474-513.

Roering, J.J., K.M. Schmidt, J.D. Stock, W.E. Dietrich, and D.R. Montgomery. 2003. Shallow landsliding, root reinforcement, and the spatial distribution of trees in the Oregon Coast Range. Canada Geotechnical Journal 40: 237-253.

Roering, J.J., P. Almond, P. Tonkin, and J. McKean. 2002. Soil transport driven by biological processes over millennial time scales. Geological Society of America 30: 1115-1118.

Schumm, S.A. 1981. Evolution and response of the fluvial system, sedimentologic implications. Society of Economic Paleontologists and Mineralogists Special Publication 31: 19-29.

Schumm, S.A. 1985. Patterns of alluvial rivers. Annual Review of Earth and Planetary Sciences 13: 5-27.

Schumm, S.A., M.D. Harvey, and C.C. Watson. 1984. Incised channels: morphology, dynamics and control. Water Resources Publications, Littleton, CO.

Schwartzberg, B. and P. Moore. 1995. A history of the Santa Clara River, Santa Clara River enhancement and management plan.

Schwarz, K.M. and A.R. Orme. *In press*. Opening and closure of a seasonal river mouth: The Malibu estuary-barrier-lagoon system, California. Zeitschrift für Geomorphologie.

Scott, K., and R.P. Williams. 1978. Erosion and sediment yields in the Transverse Ranges, Southern California. Geological Survey Professional Paper 1030.

SCREMP (Santa Clara River Enhancement Management Plan). 1996. Flood Protection Report (Final Draft). Aggregate Subcommittee.

Seabloom, E.W., O.J. Reichman, and E.J. Gabet. 2000. The effect of hillslope angle on pocket gopher (*Thomomys bottae*) burrow geometry. Oecologia 125: 26-34.

Shen, H.W., S.A. Schumm, J.D. Nelson, D.O. Doehring, M.M. Skinner, and G.L. Smith. 1981. Methods for assessment of stream-related hazards to highways and bridges. Technical Report for US Department of Transportation FHWA/RD-80/160, Colorado State University, Fort Collins, Colorado.

Sherman, D.J., K.M. Barron, and J.T. Ellis. 2002. Retention of beach sands by dams and debris basins in Southern California. Journal of Coastal Research 36: 662-674.

Simon, A. 1989. A model of channel response in disturbed alluvial channels. Earth Surface Processes and Landforms 14: 11-26.

Simons, Li & Associates. 1983. Hydraulic, erosion and sedimentation study of the Santa Clara River Ventura County, California. Prepared for Ventura County Flood Control District, Ventura, California.

Smith, J.J. 1990. The effects of sandbar formation and inflows on aquatic habitat and fish utilization in Pescadero, San Gregorio, Waddell, and Pomponio Creek estuary/lagoon systems, 1985-1989. Prepared by San Jose State University, Department of Biological Sciences, San Jose, California for California Department of Parks and Recreation.

Sommerfield, C.K., and H.J. Lee. 2003. Magnitude and variability of Holocene sediment accumulation in Santa Monica Bay, California. Marine Environmental Research 56: 151-176.

Swanson, M.L., M. Josselyn, and J. McIver. 1990. McGrath State Beach Santa Clara River Estuary Natural Preserve: restoration and management plan, Page 75. Ventura County, California, California Department of Parks and Recreation.

Thompson, W.C. 1994. Shoreline geomorphology of the Oxnard Plain from early U.S. Coast Survey Maps. Shore and Beach, July 1994: 39-50.

Titus, R.G., D.C. Erman, and W.M. Snider. *In press*. History and status of steelhead in California coastal drainages south of San Francisco Bay.

Trecker, M.A., L.D. Gurrola, and E.A. Keller. 1998. Oxygen-isotope correlation of marine terraces and uplift of the Mesa Hills, Santa Barbara, California, USA. Geological Society Special Publication 146: 57– 69.

Trimble, S.W. 1977. The fallacy of stream equilibrium in contemporary denudation studies. American Journal of Science 277: 876-887.

University of Southern California. 2004. William Mulholland & the Collapse of the St.Francis Dam. Available online at: http://www.usc.edu/isd/archives/la/scandals/st_francis_dam.html

URS (URS Corporation). 2005. Santa Clara River Parkway Floodplain Restoration Feasibility Study—Water Resources Investigations. Prepared for the California Coastal Conservancy. April 2005.

URS (URS Corporation). 2006. Re: Revised set-up and verification of hydraulic model of Santa Clara River, memorandum. Letter to Bill Sears, Stillwater Sciences. 13 September 2006.

USACE (United States Army Corp of Engineers). 1980. Survey report for beach erosion control, main report. Prepared for Ventura County.

USDA Forest Service (United States Department of Agriculture, Forest Service). 1954. Fire-flood sequences on the San Dimas Experimental Forest: United States Department of Agriculture, Forest Service, California Forest and Range Experiment Station 6.

USFWS (U.S. Fish and Wildlife Service). 1999. Santa Clara River Estuary, Ecological Monitoring Program. I*n* G. M. Prepared by Greewald, L.S. Snell, G.S. Sanders, and S.D. Pratt, eds., Ventura, California, USFWS.

Van den Berg, J.H. 1995. Prediction of alluvial channel pattern of perennial rivers. Geomorphology, 12: 250-279.

VCFCD (Ventura County Flood Control District). 1999. Detention Dams and Debris Basins Manual, Public Works Agency: Hydrology Section.

VCWPD (Ventura County Watershed Protection District). 2005. Integrated Watershed Protection Plan, Fiscal Year 2005, Zone 2. Prepared by Ventura County Watershed Protection District, Ventura, California. 16 May 2005.

Voight, B. 1978. Rockslides and Avalanches, Developments in geotechnical engineering. Elsevier, Amsterdam.

Wald, D.J., and T.H. Heaton. 1994. A dislocation model of the 1994 Northridge, California earthquake determined from strong ground motions. U.S. Geological Survey. Denver Colorado, U.S. Geological Survey, 94-278.

Warner, R.F. 1987. Spatial adjustments to temporal variations in flood regime in some Australian rivers. *In* Richards, K. S. ed., River channels: environment and process. Blackwell, Oxford, 14-40.

Warner, R.F. 1994. A theory of channel and floodplain responses to alternating regimes and its application to actual adjustments in the Hawkesbury River, Australia. *In* Kirkby, M. J. ed., Process models and theoretical geomorphology. J. Wiley and Sons, Chichester, 173-200.

Warrick J.A. and D. Rubin. 2007. Suspended-sediment rating-curve response to urbanization and wildfire, Santa Ana River, California. Journal of Geophysical Research – Earth Surface 112, F02018, doi:10.1029/2006JF000662

Warrick, J.A. 2002. Short-term (1997–2000) and long-term (1928–2000) observations of river water and sediment discharge to the Santa Barbara channel, California. Ph.D. dissertation, University of California, Santa Barbara.

Warrick, J.A. 2003. Land sources and ocean dispersal of river sediment in southern California. Seminar given at INSTAAR, University of Colorado. http://instaar.colorado.edu/other/seminar_mon_presentations/warrick_2003.pdf

Warrick, J.A. 2004. Historical Erosion Rates of Coastal California, What is "Natural?", Headwaters To Oceans (H2O) Conference. http://www.coastalconference.org/pdf/thursday_2004/4A/Warrick-Historical_Erosion_Rates_of_Coastal_California.pdf.

Warrick, J.A. 2005. Personal Communication. United States Geological Survey (USGS) Santa Clara, California. 6 March.

Warrick, J.A., and J.D. Milliman. 2003. Hyperpycnal sediment discharge from semiarid southern California rivers: implications for coastal sediment budgets. Geological Society of America Bulletin 31: 781-784.

Wells, W.G., II. 1981. Some effects of brushfires on erosion processes in coastal Southern California. *In* T. Davies, and A. Pearce, eds., Erosion and sediment transport in Pacific Rim Steeplands, 305-342.

Wells, W.G., II. 1985. The influence of fire on erosion rates in California chaparral. *In* J. J. DeVries, ed. Proceedings of the chaparral ecosystems research conference Water Resources Center, 62: 57-62.

Wells, W.G., II. 1987. The effects of fire on the generation of debris flows in southern California. *In* Costa J.E. and G.F. Wiezorek, eds., Debris flows/avalanches: Processes, recognition and mitigation: Reviews in Engineering Geology 7: 105-114.

Wells, W.G., II., and P.M. Wohlgemuth. 1987. Sediment traps for measuring on slope sediment movement. USDA Forest Service, Pacific Southwest Forest and Range Experiment Station Research Note, PSW-393.

Wells, W.G., II., P.M. Wohlgemuth, and A.G. Campbell. 1987. Postfire sediment movement by debris flows in the Santa Ynez Mountains, California. *In* Beschta, R. L. ed., Erosion and sedimentation in the Pacific Rim, 275-276.

Williams, G.P. and M.G. Wolman. 1984. Downstream Effects of Dams on Alluvial Rivers. Professional Paper 1286, US Geological Survey, Washington D.C.

Williams, R.P. 1979. Sediment discharge in the Santa Clara River basin, Ventura and Los Angeles Counties, California. U.S. Geological Survey, Menlo Park, California.

Wolman, M.G. 1967. A Cycle of Sedimentation and Erosion in Urban River Channels. Geografiska Annaler 49A:385-395.

Wolman, M.G., and L.B. Leopold. 1957. River flood plains: some observations on their formation. Professional Paper 271, U.S. Geological Survey, Washington D.C.

Wolman, M.G., and Miller, J.P. 1960. Magnitude and frequency of forces in geomorphic processes. Journal of Geology 68: 54-74.

Wolter, K., and M.S. Timlin. 1993. Monitoring ENSO in LOADS with seasonally adjusted principal component index. Proc. 17th Climate Diagnostics Workshop, Norman, OK, NOAA, 52-57.

Yeats, R.S. 1981. Quaternary flake tectonics of the California Transverse Ranges. Geology 9: 16-20.

APPENDIX A: GEOLOGIC SETTING

The Santa Clara River watershed lies within the Transverse Ranges and is bounded on the north by the Big Pine Fault, on the northeast and east by the San Andreas Fault, and on the south by South Mountain, Oak Ridge, and the Santa Susana Mountains (Figure 2-4). The Transverse Ranges are part of a structurally complex region that bisects the Pacific-North America tectonic plate boundary.

The last 28 million years of evolution of the Transverse Ranges can be divided into three periods. From roughly 28 to 18 million years ago (Ma), northward migration of the San Andreas transform fault gradually converted the plate boundary from a subduction margin to a transform margin.

Between approximately 18 and 5 Ma, the Transverse Ranges experienced a trans-tensional phase that resulted in clockwise rotation of the regional stress field, and produced an array of west-trending left-lateral structures and extensional basins. These basins were eventually filled with sheared rocks and extremely thick successions of marine sediments. Low-grade metamorphism of crystalline bedrock and local volcanism were common during this time.

Over the last 5 Ma, the region was characterized by a compressional regime, associated with restraining bend tectonics that developed due to the intersection of the San Andreas (a right-lateral strike slip fault) and Garlock (a left-lateral strike slip fault), north of the Santa Clara River. Left-lateral motion along the Big Pine Fault has contributed to regional compression during this time (Bohannon and Howell, 1982). The axes of regional fold and thrust structures were oriented east to west, across the predominantly north-northwest to south-southeast trending orientation of the plate boundary. Many faults that were generated by earlier crustal extension and rotation are believed to have been reactivated during this period, as reverse or thrust faults. Seismic activity along many of these faults has continued throughout the Quaternary (Yeats, 1981; Rockwell, 1988; Azor *et al.,* 2002; and Orme and Orme, 2002), and is at least partly responsible for of present day seismic hazards in southern California.

Earthquake-generating ruptures along faults are discreet in space and time, with long (order 10^2 year) recurrence intervals for large ruptures. These observations highlight the fact that historic records of seismic activity are unlikely to reflect the full range of potential seismic hazards in an area. Potentially destructive earthquakes can occur along faults that are unknown, either because they are buried or have been dormant over observed records (Greensfelder, 1971; Rockwell, 1988; Figure 2 of Knopoff, 1996).

Persistent tectonic instability has exposed a wide variety of highly deformed, folded, fractured, and faulted rock types in the Transverse Ranges (Yeats, 1981; Rockwell *et al.*, 1984; Rockwell, 1988). The eastern margins of the upper watershed (located in the central Transverse Ranges) predominantly consist of igneous and metamorphic rocks, including Precambrian gneiss and schist and late Cretaceous granite. West of the San Gabriel Fault, in the lower watershed, are younger (late Cretaceous to Pleistocene) clastic sedimentary rocks of both marine and continental origin.

The mainstem of the Santa Clara River follows the axis of a broad sedimentary syncline, occupying a broad braided alluvial channel that contrasts starkly with the steep, bedrock-confined tributaries that feed it. On the flanks of the synclinal valley are thick (~12,000 m) intensely folded and faulted sequences of sedimentary rocks of the Topatopa and Santa Susana Mountains. Tertiary volcanic rocks and interbedded marine mudstones, siltstones, sandstones, and conglomerates are steeply tilted and thrusted

over younger unconsolidated Quaternary sediments along the San Cayetano Fault to the north and the Oak Ridge Fault to the south (Rockwell, 1988). Folds in the sedimentary rock display strongly asymmetric geomorphology, with forelimbs containing nearly vertical and locally overturned beds, and backlimb beds dipping gently away from the fold axis (Azor *et al.*, 2002). Landslides are common near ridges, where weak and deformed Pliocene mudstones are located.

REFERENCES CITED:

Azor, A., E.A. Keller, R.S. Yeats. 2002. Geomorphic indicators of active fold growth: South Mountain-Oak Ridge anticline, Ventura Basin, southern California. Geological Society of America Bulletin 114: 745-753.

Bohannon, R.G., and D.G. Howell. 1982. Kinematic evolution of the junction of the San Andreas, Garlock, and Big Pine faults, California. Geology 10: 358-363.

Greensfelder, R. 1971. Seismologic and crustal movement investigations of the San Fernando earthquake. California Geology, Special San Fernando Earthquake Edition, 24: 4-5.

Knopoff, L. 1996. A selective phenomenology of the seismicity of Southern California. Proc. Natl. Acad. Sci. 93: 3756-3763.

Orme, A.J, and A.R. Orme. 2002. Tectonic geomorphology and San Andreas Fault System: A Field Trip Guide for the Association of American Geographers. Unpublished field notes.

Rockwell, T.K., E.A. Keller, M.N. Clark, D.L. Johnson. 1984. Chronology and rates of faulting of the Ventura terraces, California, Geological Society of America Bulletin 95: 1466-1474-513.

Rockwell, T. 1988. Neotectonics of the San Cayetano fault, Transverse Ranges, California. Geological Society of America Bulletin 100: 500-513.

Yeats, R.S. 1981. Quaternary flake tectonics of the California Transverse Ranges. Geology 9: 16-20.

APPENDIX B: WATERSHED IMPACTS CHRONOLOGY

Factor	Pre-1850	1851–1870	1871–1890	1891–1900	1901–1910	1910–1920	1921–1930	1931–1940	1941–1950	1951–1960	1961–1970	1971–1980	1981–1990	1991–2000	2000–present
Climate															
Floods	**1811** **1815** **1820–21** **1824–25** **1840**	**1861–62:** worst in 19th century, made an inland sea; eroded land; numerous landslides	**Dec 26, 1883–Jan/Feb, 1844:** 34 hours of rain; 15 in. **Feb 15 1884:** rained for 4 days; banks swept bare of cottonwoods, oak, sycamore. **Feb 17**: house and barns floating down river. No water shortage for 10 yrs (Hardison acct., p. 21)	**1892 – 93**	**1909:** river flowed through Sta. Paula, damaged Saticoy Bridge abutment and nearby farmlands	**1911:** damaged railroad bridges and irrigation systems **1914:** washed away homes and farm buildings in Bardsdale, and State 23 bridge	**March 12–13, 1928:** St. Francis Dam failure (est. 500,000–800,000 cfs); 23,700 ac of orchards lost; $5.5M dollars damage; 385 killed; 1,250 home lost; peak of wall of water at 78 ft; water 25 ft deep at Sta. Paula 42 mi downstream; parts of Ventura Co. under 70 ft of mud & debris	**1932:** Montalvo gage initiated **March 1938** [2] (120,000 cfs): Ventura Co. losses $2.5M; hundreds of acres of land damaged; Saticoy Bridge lost two spans; Newhall Ranch Bridge destroyed; Sta. Paula STW destroyed; comparable to 1914, but < 1862 & 1884			**Jan 1969** [1]: largest recorded flood (165,000 cfs). Hwy 126 closed at Piru for two weeks, Willard Bridge nearly destroyed, planes removed from airport. Montalvo STW damaged. **Feb 1969:** caused more damage than Jan; 500 ft of Hwy 118 bridge washed out; 2,000 ft of levee damaged; Ventura Marina 'destroyed'	**March 1978** [5] (102,200 cfs) several hundred ac ag land lost to erosion, second most damaging flood	**Jan 27– 31, 1983**: [6] (100,000 cfs) most flood damage near the coast Hwy 101; Hwy 118 on north bank, Sepse Ck; Hwy 23 bridge on the south	**Feb 10–12 1992** [4]: (104,000 cfs) storms following heavy rain through Jan; Fillmore STW threatened; rock slope protection lost; ag. lands damaged **Jan 10 & March 10, 1995** [3] **:** (110,000 cfs) rock groins damaged south bank Hwy 101 loss of ag land and damage upstream Hwy 118 **1995:** new gage Hwy 118 **Feb 23, 1998:** (84,000 cfs) at Saticoy groin damage south bank beyond Hwy 101; some orchard losses; Sespe Ck. close to its 1978 max flood flow	**Jan 11 2005 flood**
Fire							**Ridge fire:** (28,000 ac) upper Piru	**1932 Matilija fire:** (139,000 ac) on Sespe Ck./ Sta. Paula & severe silting					**1985 Ferndale fire:** (46,000 ac) near Sta. Paula **1988 Piru fire:** (25,000 ac) lower Puru	**1996 Grand July:** (11,000 ac) NW Fillmore **1997 Hopper Fire** **1998 Piru:** (12,500 ac) in lower Piru **1998 El Niño:** severe debris flows	
Known Channel Changes (from aerial photographs)															
Channel Management															
Channelization, levees, bank protection							St. Francis Dam disaster prompts start of levees and groins			**1959:** 1,950 linear ft river bed pilot channeling (42,300 cu. yds material removed); pilot channeling continues to mid-1960s, cinl. by agg. firms	**1961:** completion of South Mt to Hwy 101 levee by USACE (25,000 ft); earthern berm completed to Victoria Ave. Bridge site; Saticoy Auxilliary Dike 25,000 on north bank **1969 onward:** various groins built by VCWPD	**1973–79:** bank protection from southbank across from Sespe Ck. **1976:** Victoria Ave Bridge completed, berm turned to levee blocking historical flow path (maintained by VCWPD)	**1983–93:** groins on south bank near Ventura Road **1986–96:** 2,760 ft bank protection south bank along Bailard landfill rip-rap; increased **1996** **1984:** bank protection at Sudden Barranca Other, undated bank protection in Los Angeles County	
Regulation						**1912:** Dry Canyon. Resr (4.5 sq mi) taken out of operation in 1966 due to seepage problems	**1928:** St. Francis Dam disaster								
								1934: completion of Bouquet Resr. (13.6 sq.mi.)		**1955:** UCWD completed 200 ft high Sta. Felicia Dam (Lake Piru) on Piru Ck (421 sq.mi)		**1971–72:** completion of Castaic Lake (154 sq.mi) and Pyramid Lake (293 sq.mi upstream of Lake Piru)			
Abstraction							**1930:** SCVWD began Piru Ck diversions								
								1931: SCVWD began Sta. Paula diversions		**1954–56:** Lower River Project improved diversion at Saticoy etc.					
													1989–91: Freeman Dam completed		

Aggregate Extraction					Start of small-scale agg. mining in river						Earliest SCR river permits issued	Acceleration of agg. permits	**1986–1992:** VC created red line for mining depth in river; above Freeman no real bed change **1989:** most agg. mining finished	**1967–1986:** agg. mining and extreme flood flows lowered the river profile tens of feet across Sta. Paula g/w subbasin (UWCD/CLWA 1996). **1996:** one active in channel mine left in LAC; 3 out-of-river in LAC & VC	
Management Policy							Govt. control over river increases from here. **1925:** SCR Protective Assoc formed; supported by ag, oil and agg. industries; not urban. **1927:** SCWCD formed 11,000 ac ag. area VC and OP		**1944:** formation of VCFCD (now VCWPD). **1950:** formation of UWCD from SCVWD					**1992:** 31.5 mi of Sespe Ck designated wild and scenic	
Irrigation Infrastructure & groundwater			First wells on OP	**By 1890s:** water demands high enough to need pumped water supplies	**Early 1900s:** 16,000 ac irrigated in VC.	**1912:** 17,000 ac irrigated by surface flows of SCR **1919:** 31,700ac irrigated in VC.	**1925:** 35,000 ac irrigated in VC.		**1949:** 107,689 ac irrigated in VC; only 4,900 of 74,800 dry-farmed areas remained		**1965:** 2,500 ac irrigated by surface flows of SCR due to reduction in surface flow **1969:** 101,140 ac irrigated in VC.	**1980:** 106,480 ac irrigated in VC.			
Land Use Changes															
Land cover (change)	**1769:** consistent source of water, tall & thick oaks and cottonwoods, willows, grass; earth "spongy, insecure & whitish"	**mid-1850s:** growth of timber and willows along the Ck., freshwater marsh	invasive mustard plant introduced; still tules in the swampy part of the river												
Agriculture	**1920s–1860s:** livestock raising; intro. of new grasses; mostly cattle	**1860s:** following drought switched to sheep; caused more erosion and remove root of grasses. **1860–70s:** flood & droughts shift focus from livestock to ag. (*e.g.*, barley, corn, flax, alfalfa, oats)	**1878:** 85% of crop = wheat, barley, corn (8,400 ac in VC). **1875:** intro. lima beans	**1898–1919:** sugar beet on OP, lowering OP water table. **1890s:** citrus intro.; Limoneira Co. in Sta. Paula required irrigation		**Post-WWI:** citrus becomes the main crop. **1917:** 29,000 ac orchards			**1950:** 66,000 ac orchard						
Urbanization	**1782:** first mission established. **1848-onward:** American land ownership patterns										**1969:** USCV urban uses = 39% (compare right) urban area 72,600 ac	**1980:** USCV urban water demand surpasses ag. 51:49; urban area 121,870 ac; industrial +136%, residential +68%; commercial +64%			
Road and rail construction			**1876:** branch line of SP ran east from Newhall to Soledad Cyn practically on the riverbed. **1887:** branch line from Newhall to Ventura paralleling river; growth of Piru, Fillmore, Bardsdale		most roads in river bed	extensive development of paved roads. **1918:** Sierra Hwy bridge completed. **1921:** Mint Cyn bridge completed									

Ag = Agriculture
Agg = Aggregate
Ck = Creek
Co = County
Cyn = Canyon
Hwy = Highway
LAC = Los Angeles County
OP = Oxnard Plain
Resr = Reservoir
SCR = Santa Clara River
SCVWD = Santa Clara Valley Water District
SP = Southern Pacific
Sta = Santa
STW = Sewage Treatment Works
USCV = Upper Santa Clara Valley
VC = Ventura County
VCFCD = Ventura County Flood Control District
VCWPD = Ventura County Watershed Protection District

APPENDIX C: DETERMINATION OF COARSE SEDIMENT YIELD WITHIN THE SANTA CLARA RIVER WATERSHED

In order to understand the effects of coarse sediment discharge on in-channel geomorphic processes, it is necessary to examine coarse sediment yield within a watershed on two distinct time scales. Determining coarse sediment yield throughout a watershed for discrete storm events (i.e., short-term sediment yield) is important in understanding the key sources of coarse sediment within a watershed and how storm magnitude relates to net short-term channel aggradation or incision. Over the longer term, analysis of the magnitude and frequency of coarse sediment yield (termed coarse sediment magnitude-frequency) determines the channel 'dominant discharge,' or the discharge that transports the most sediment and contributes the most to channel morphology over a long period of record. Storm coarse sediment yield is a function of the relationship between flow and coarse sediment discharge (i.e., coarse sediment rating curve) and the discrete storm hydrograph. Coarse sediment magnitude-frequency is a function of the coarse sediment rating curve and the distribution of daily mean discharge over a period of record (i.e., flow frequency). Storm coarse sediment yield was determined for the Santa Clara River at the LA Co Line/Piru (USGS 11108500/11109000), Hopper Creek near Piru (USGS 11110500), Sespe Creek at Fillmore (USGS 1113000), Santa Paula Creek at Santa Paula (USGS 11113500), and the Santa Clara River at Montalvo (11114000). Coarse sediment magnitude-frequency was determined for the Santa Clara River at the LA Co Line/Piru, Sespe Creek at Fillmore, and the Santa Clara River at Montalvo. This appendix describes the methodology used within these analyses.

The coarse sediment discharge at each gage was calculated as a combination of coarse suspended sediment load and bedload. The suspended sediment data for the gages (provided by the USGS) was compiled and the coarse fraction (>0.5 mm for the storm coarse sediment yield analysis and >0.063 mm for the coarse sediment magnitude-frequency) of the suspended sediment sample for each flow measured was determined. A regression was then fit through each set of data (Figure C-1). The suspended load is coarser for the storm sediment yield analysis because it is assumed that suspended sediment below 0.5 mm will travel as washload and not deposit within channel (Simons and Li, 1983). Bedload discharge for each gage was determined for the range of flows represented in the suspended sediment dataset in several ways. At the LA Co Line/Piru gage, bedload discharge was determined as measured bedload (provided by the USGS) below 325 cfs and as 6% of total suspended load (value suggested for the mainstem Santa Clara by Williams [1979]) above 325 cfs, with a regression fit through the data (Figure C-2). Bedload discharge at the Hopper Creek gage and Sespe Creek gage was calculated as 10% of the total suspended load (as suggested by Williams [1979] for Southern California Rivers) and a regression was fit through the data (with a break in slope at 325 cfs at the Sespe Creek gage). Bedload for the Montalvo gage was calculated as 6% of the total suspended load and a regression was fit through the data (with a break in slope at 325 cfs). The fitted coarse suspended sediment discharge estimate (for >0.5 mm and >0.0625 mm) was then added to the fitted bedload estimate for each gage to result in two coarse sediment rating curves per gage (Figure C-3). Due to the lack of Santa Paula Creek sediment data and the similarity in watershed characteristics between Santa Paula Creek and Sespe Creek (Warrick 2002, Appendix A), the coarse sediment rating curves for Sespe Creek were applied to Santa Paula Creek.

The storm hydrograph data for each gage were compiled for days in which the daily peak discharge was the annual maximum or the daily peak discharge equaled or exceeded the mean annual

discharge (i.e, a discharge with a recurrence interval of at least 2.33 years). For storms after water year (WY) 1987, 15-min flow data was available from the USGS. For several storms before WY 1987, 1-hour flow data was extracted from hydrograph plots in Simons and Li (1983). There are several significant storm events in which 15-min or 1-hour incremental flow data was not available for certain gages. For these storms, daily mean flow was used to determine the storm coarse sediment yield (see below).

The distribution of daily mean flows (i.e., flow frequency) for the Santa Clara at the LA Co Line/Piru gage, Sespe Creek at Fillmore gage, and the Santa Clara River at Montalvo gage were determined by dividing flows into log-based bins. The bins started at $10^{-1.3}$ (0.05 cfs) and the exponent increased by 0.1 past 10^{0} (1 cfs) to $10^{5.1}$ (112,946 cfs). A regression was then fit to the relationship between the number of days in each bin (flow frequency) and the midpoint of each bin. The daily mean flow bin with the highest frequency of occurrence was 38.6 cfs for the LA Co Line/Piru gage, 0.5 cfs for the Sespe Creek gage, and 0.5 cfs for the Montalvo gage (Figure C-4).

The total coarse sediment yield for each individual storm considered was determined from the coarse sediment rating curve for sediment >0.5 mm (tons day^{-1}) and the storm hydrograph data (cfs). The sediment yield for each incremental discharge value in the daily hydrograph was determined by entering the incremental discharge data into the coarse sediment rating curve (tons/day), determining the fraction of the day that the incremental discharge represented (day), and multiplying the coarse sediment discharge by the fraction of the day represented for each incremental discharge (tons). These values were then summed to get the coarse sediment yield for the entire day (tons). For storms in which flow hydrograph data were not available, storm coarse sediment yield was determined from the gage-specific relationship between storm coarse sediment yield using storm hydrograph data and coarse sediment yield using daily mean discharge (Figure C-5). As there was no storm hydrograph data for Hopper Creek (USGS 11110500) available, storm sediment yield for this gage was determined from daily mean discharge.

The total long-term coarse sediment yield for the gages for the range of flows represented by the daily mean flow record was determined as a product of the flow frequency for each daily mean flow bin (days) and the coarse sediment rating curve for sediment >0.0625 mm (tons day^{-1}) (Figures C-6 to C-8). The computed 'dominant discharge' for the gages is, in all cases, the largest flow on record.

REFERENCES CITED:

Inman, D.L. and P.M. Masters, 1991. Coastal sediment transport concepts and mechanisms. State of the Coast Report, San Diego Region, Coast of California Storm and Tidal Waves Study. U.S. Army Corps of Engineers, Los Angeles District, Chap. 5.

Willis, C. M., and G. B. Griggs. 2003. Reductions in fluvial sediment discharge by coastal dams in California and implications for beach sustainability. Journal of Geology 111: 167-182.

Wolman, M.G. and L.B. Leopold. 1957. River flood plains: some observations on their formation. Professional Paper 271, U.S. Geological Survey, Washington D.C.

Wolman, M.G. and J.P. Miller. 1960. Magnitude and frequency of forces in geomorphic processes. Journal of Geology 68: 54-74.

Williams, R.P. 1979. Sediment discharge in the Santa Clara River basin, Ventura and Los Angeles Counties, California. Menlo Park, California, U.S. Geological Survey.

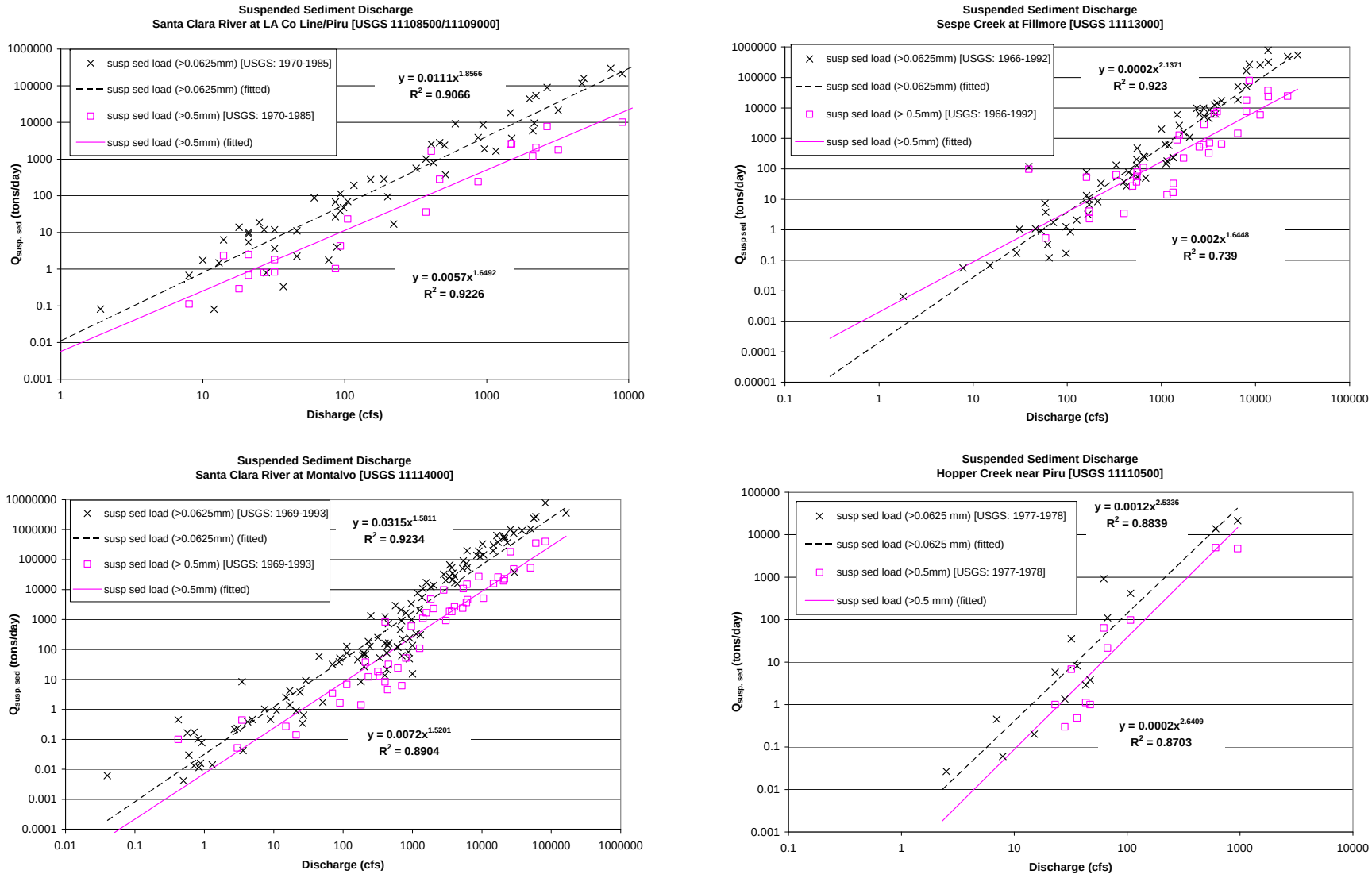

Figure C-1. Coarse suspended sediment discharge for Santa Clara River watershed gauges.

NOTE: Data from 1/26/72 - 2/10/73 were not included for the Montalvo gage due to the effects of gravel mining (per Brownlie and Taylor [1981])

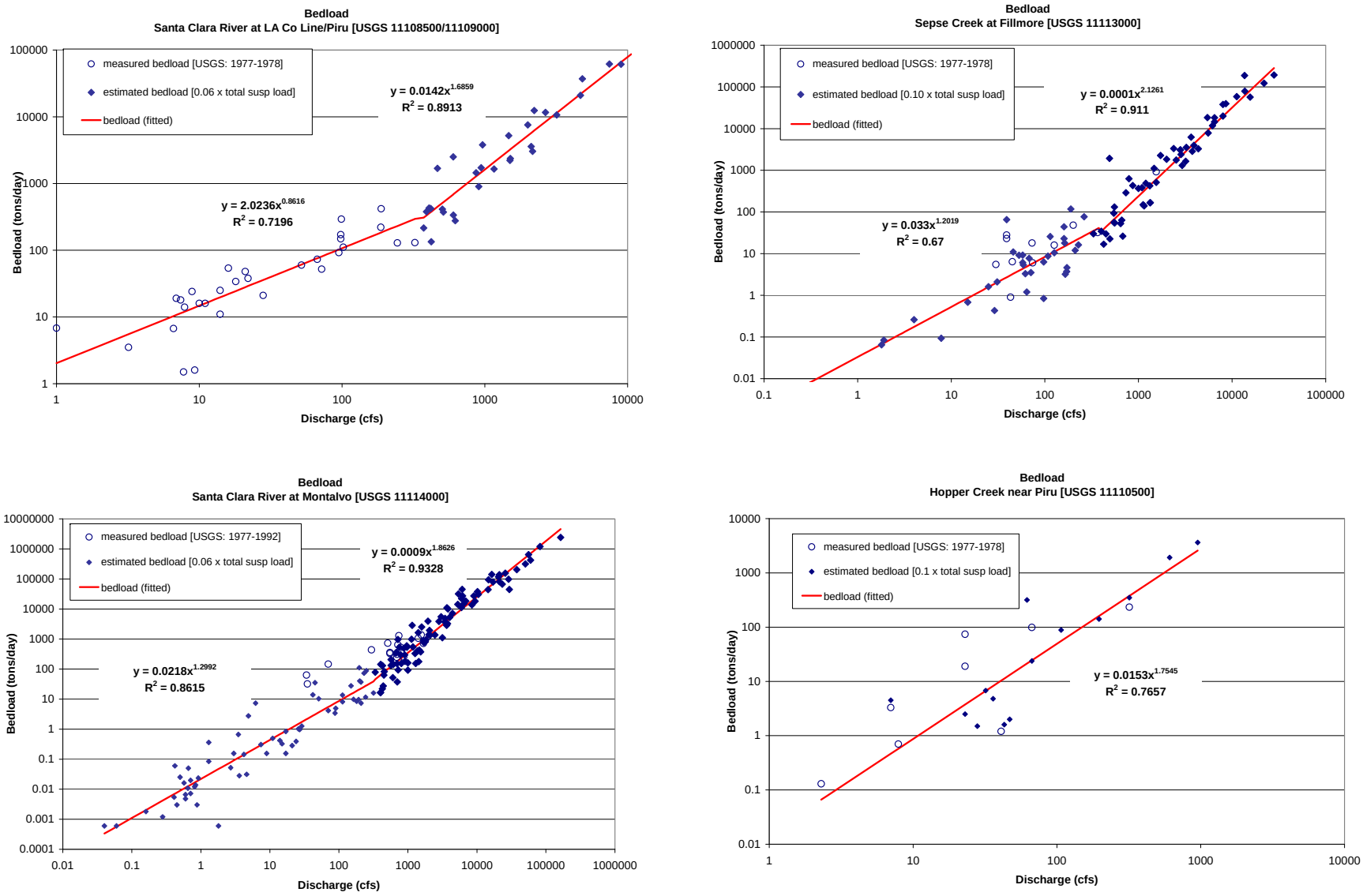

Figure C-2. Bedload estimates for Santa Clara River watershed gauges.

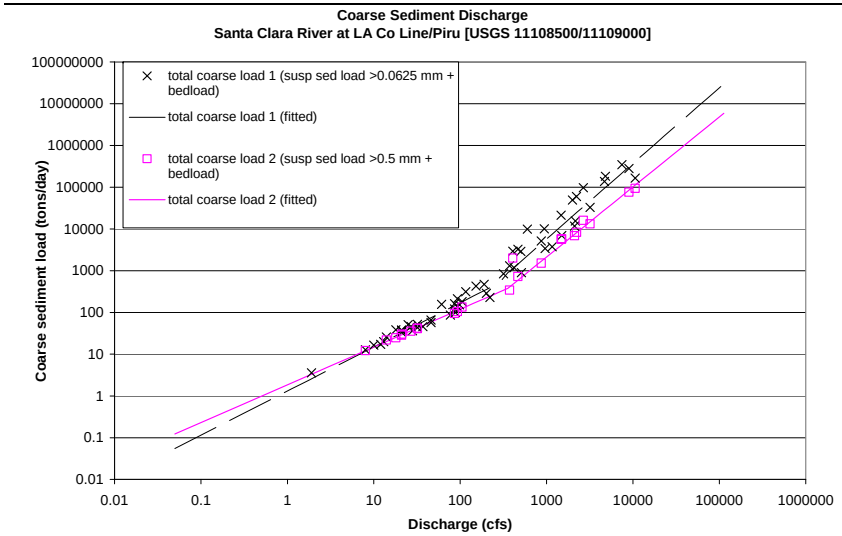

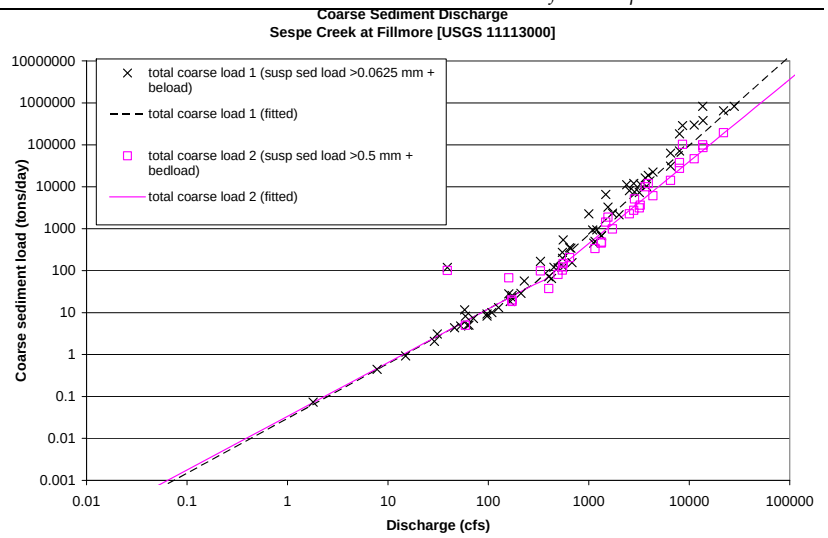

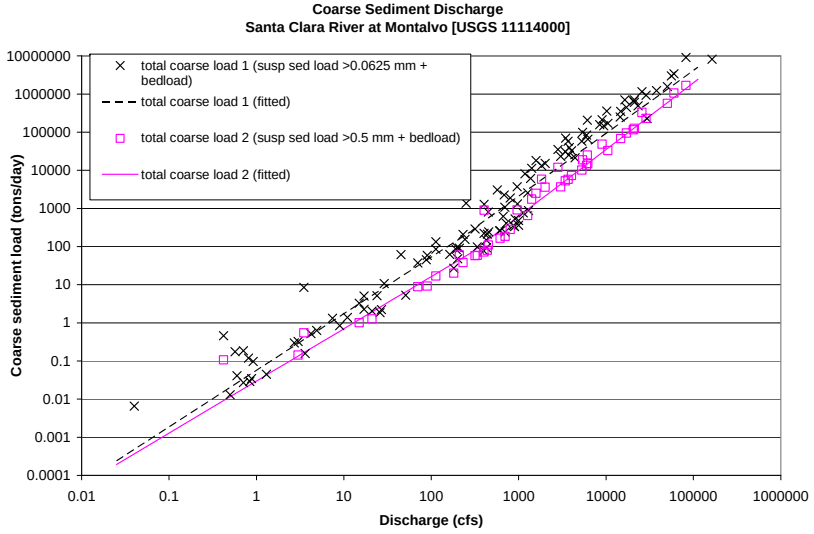

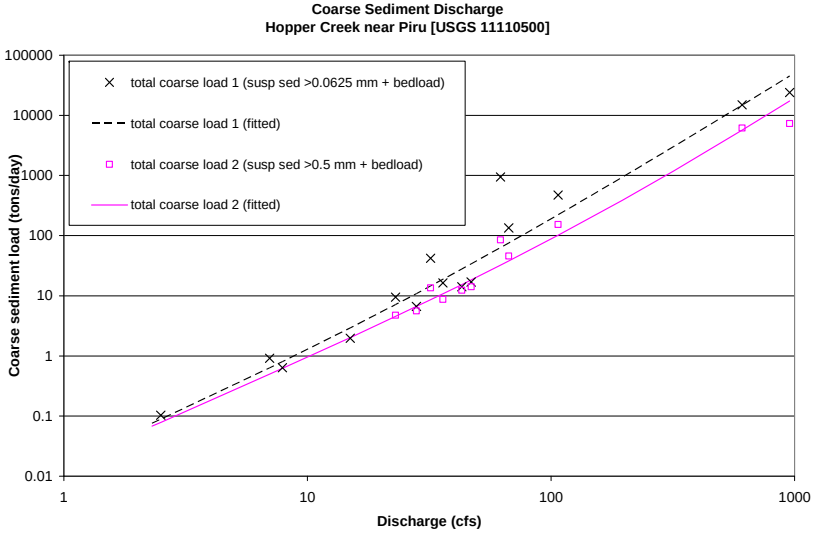

Figure C-3. Total coarse sediment discharge for Santa Clara River watershed gauges.

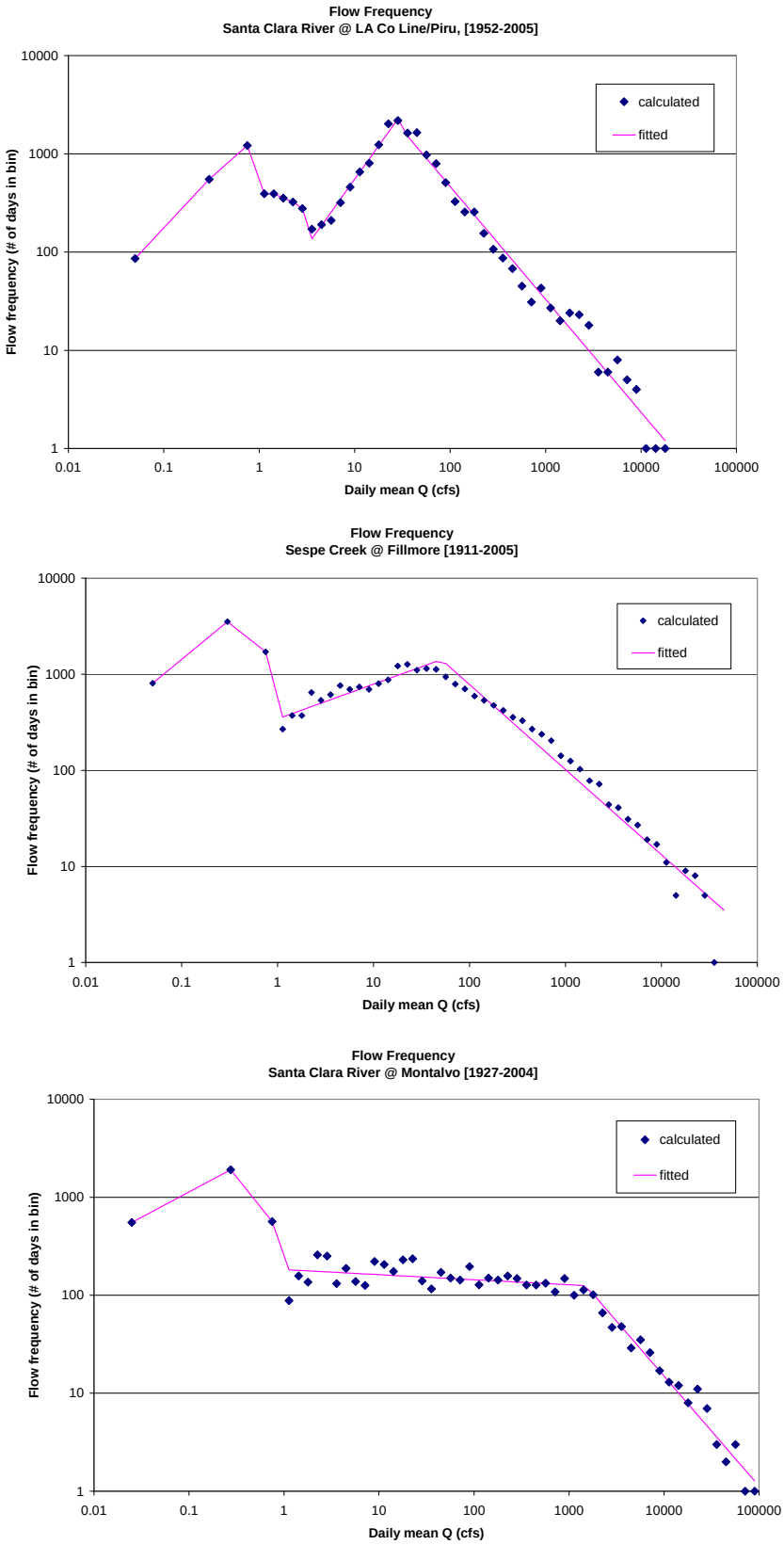

Figure C-4. Daily mean flow frequency distributions for Santa Clara River watershed gauges.

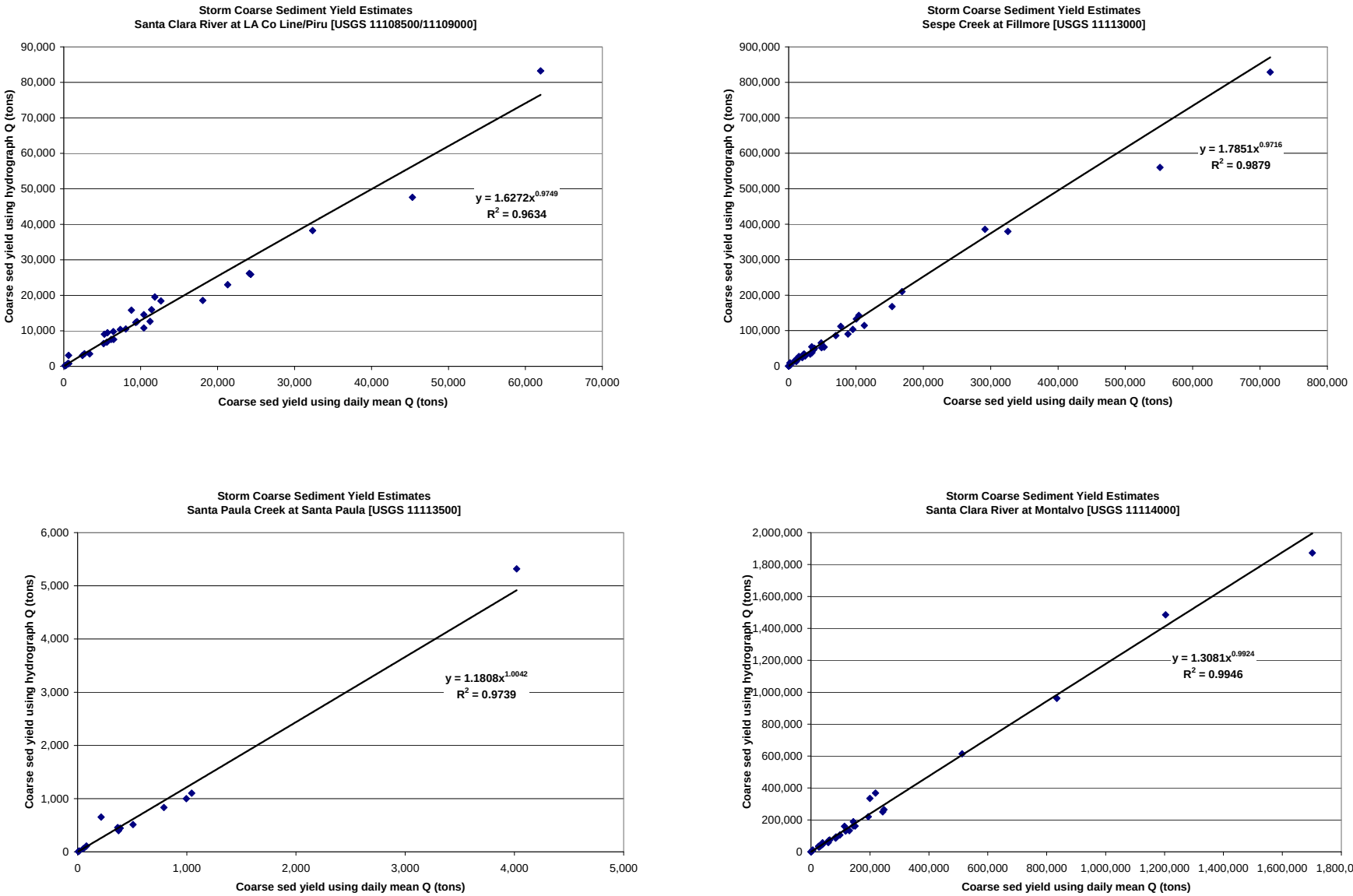

Figure C-5. Relationship between storm coarse sediment yield using storm hydrograph data and data and daily mean discharge data for Santa Clara River watershed gauges.

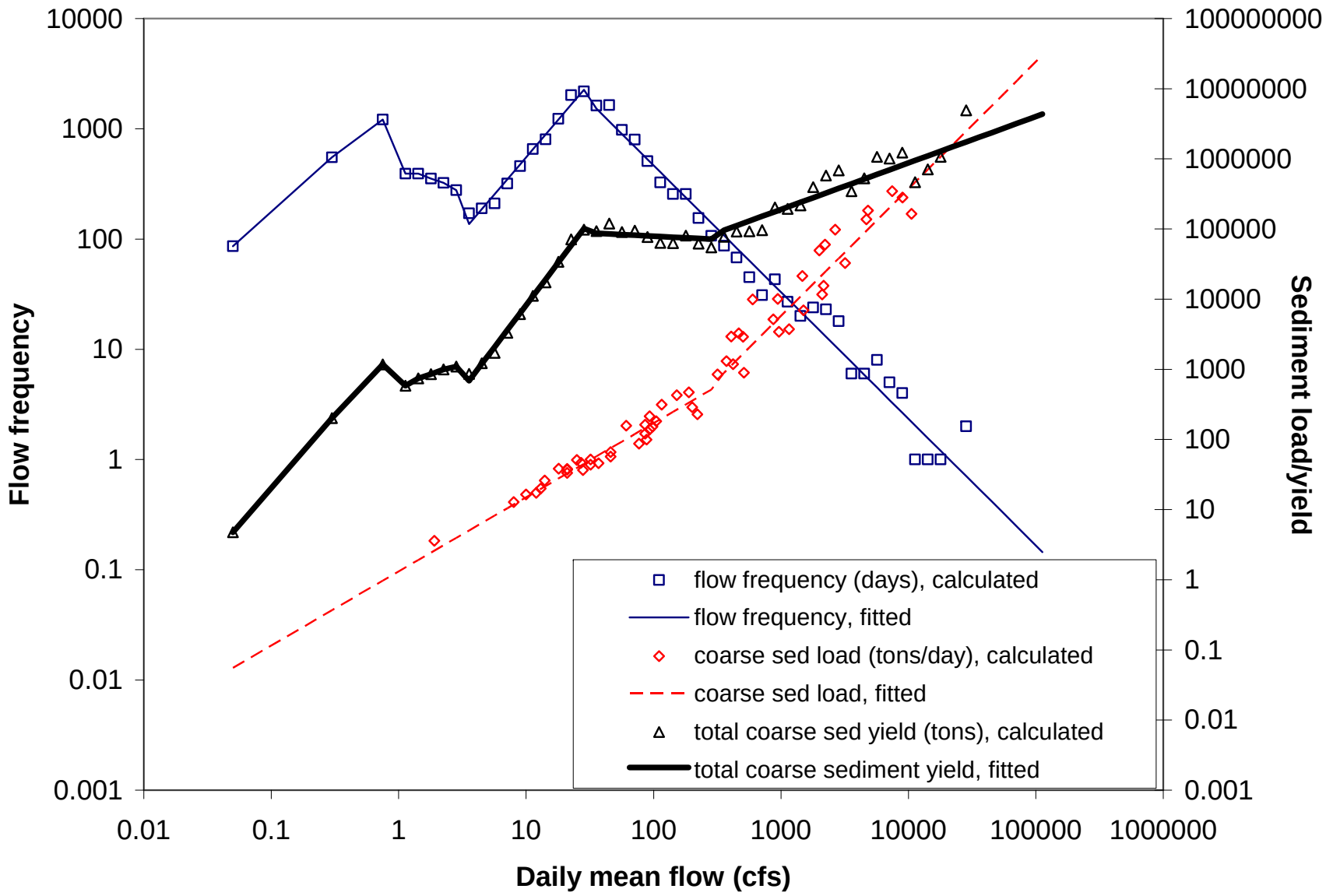

Figure C-6. **Flow frequency and coarse sediment load for long-term daily mean flow record for Santa Clara River at Los Angeles County Line (USGS 11108500/1110900).**

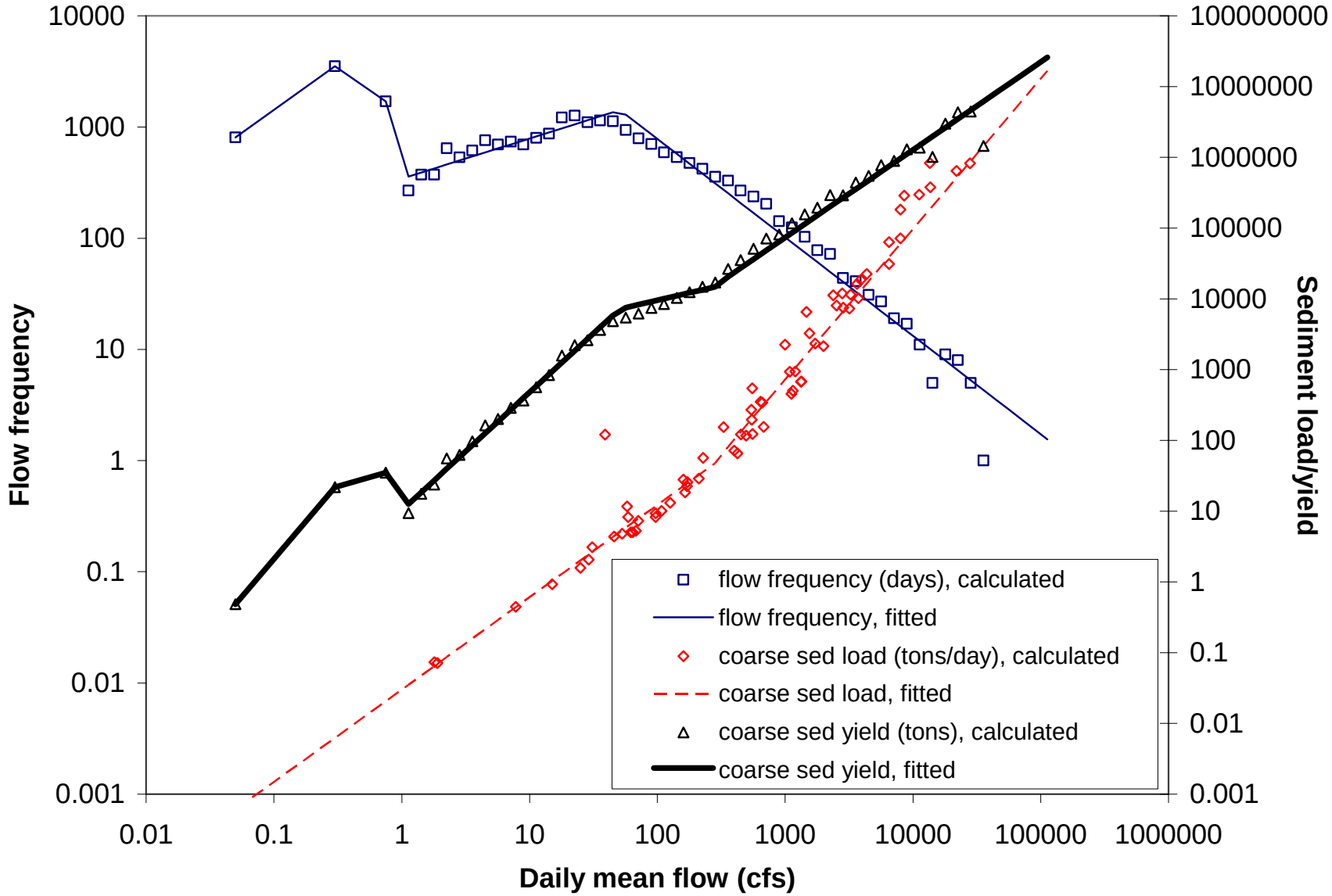

Figure C-7. Flow frequency and coarse sediment load for long-term daily mean flow record for Sespe Creek at Fillmore (USGS 11113000).

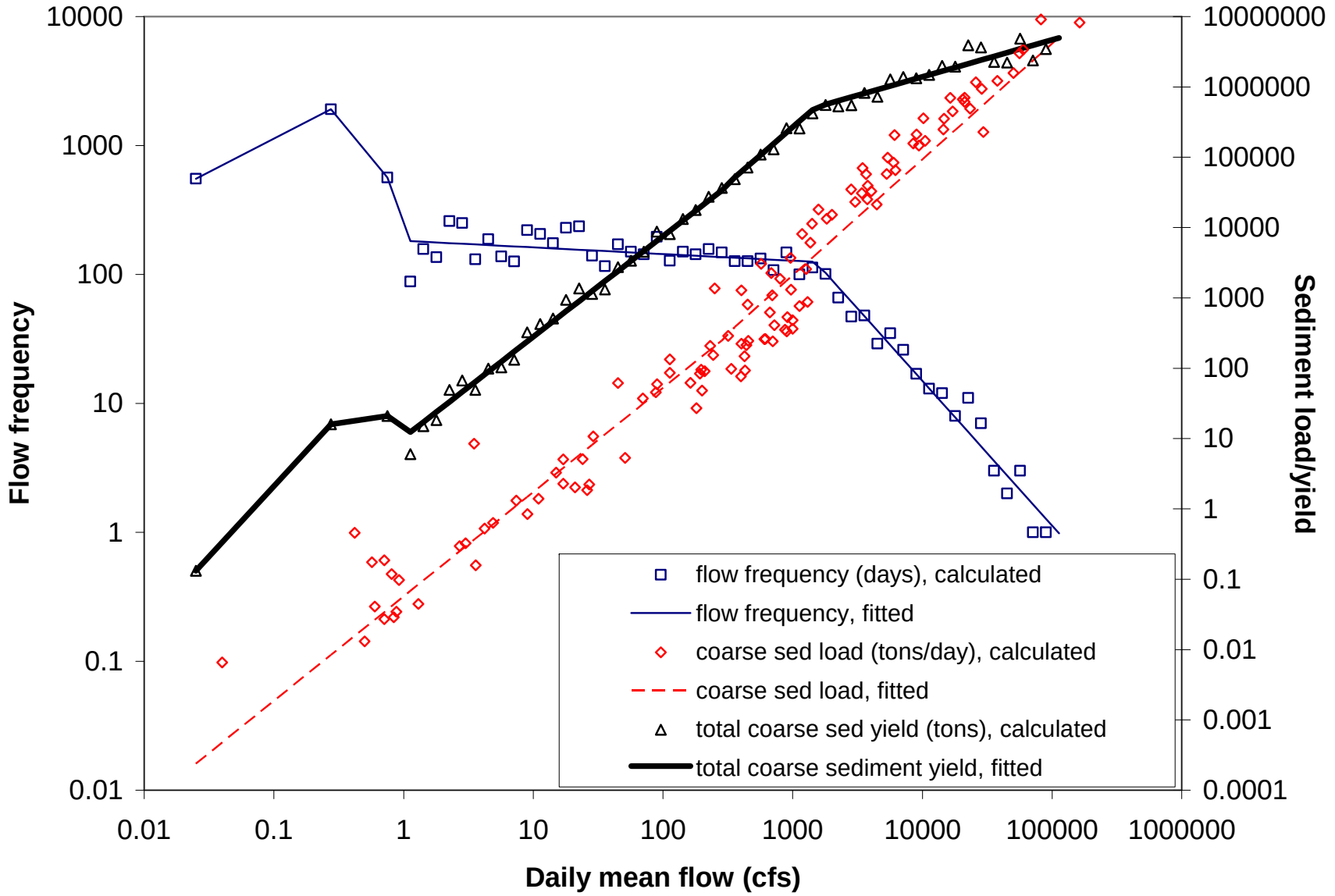

Figure C-8. Flow frequency and coarse sediment load for long-term daily mean flow record for the Santa Clara River at Montalvo (USGS 11114000).

APPENDIX D: RECONNAISSANCE OBSERVATIONS FOLLOWING FLOODS IN JANUARY AND FEBRUARY 2005

Two large flood events occurred in the watershed during the period of this study, in January and February 2005. The January flood peak on the lower Santa Clara River at Freeman Diversion has been provisionally estimated at 3,851 m^3s^{-1} (136,000 cfs) (source: VCWPD), which would make the flood the second largest in recorded history (URS, 2005). The flood contribution from Sespe Creek was estimated at 2,415 m^3s^{-1} (85,300 cfs) (source: VCWPD), the highest on record (URS, 2005). In April 2005, field reconnaissance was undertaken in order to interpret geomorphic changes following the floods in conditions of low flow and prior to the re-emergence of extensive stands of in-channel vegetation. Orthophotography taken in early 2005 was not yet available to this study, although a series of oblique photographs were available and were especially useful in areas of restricted access.

Bank erosion was extensive in some locations and, especially in the vicinity of Saticoy, exhibited a pattern of alternate bank erosion not unlike a confined meandering river. Other erosion of note included activity around the Highway 23 bridge in Fillmore, which apparently constricted flow, causing extensive flooding to the south (left) bank (and erosion where the flow re-joined the river), and led to erosion of the face of the levee protecting a new development downstream of Highway 23. The river also developed a highly sinuous course downstream of the Sespe Creek confluence causing extensive scallop-shaped erosion scars in formerly occupied river bottomlands (see Figure 5-13). Upstream of Santa Paula, the river migrated left into South Mountain Road necessitating reconstruction of the road.

In Santa Paula, the river eroded both left and right banks downstream of Willard Bridge and removed part of the runway at Santa Paula Airport, exposing groins constructed in the 1950s to protect the right bank and since buried by the river. Extensive outer bend erosion occurred at the Hansen-Villanueva property. Upstream of Highway 118 at Saticoy, the river meandered to the right, opposite the United Water Spreading grounds, then left into a former gravel pit area. Downstream of the bridge, the river eroded banks alternately right and left. The river thalweg also eroded the left bank upstream of the Highway 101 bridge before turning abruptly across the channel and realigning itself to erode part of a levee downstream of the railroad bridge. The flows damaged incomplete sections of the Highway 101 bridge improvement. Little bank erosion was evident around the Victoria Avenue bridge but, upstream of Harbor Boulevard bridge, the river migrated to the right-most edge of the floodway course, realigning the estuary and removing large areas of river bottom vegetation.

REFERENCES CITED:

URS (URS Corporation). 2005. Santa Clara River Parkway Floodplain Restoration Feasibility Study—Water Resources Investigations. Prepared for the California Coastal Conservancy. April 2005.

APPENDIX E: METHODS FOR ASSESSING PLANFORM CHANNEL DYNAMICS OF THE LOWER SANTA CLARA RIVER: 1938-2005

INTRODUCTION

Historical aerial photography was utilized in a geographic information system (GIS) to delineate areas of flood disturbance for 7 selected historical floods (1938, 1945, 1969, 1978, 1992, 1995, and 2005) along a 60.4 km (37.5 mile) long reach of the lower mainstem Santa Clara River within Ventura County, California. This planform data was subsequently combined with channel profile and other data to perform a number of analyses designed to understand the fluvial geomorphic dynamics of the lower river. Many aspects of this analysis were modeled on similar work done by Graf (2000), Tiegs et al. (2005), and Tiegs and Pohl (2005).

PHOTO ACQUISITION

Imagery was acquired from a number of sources, including the Ventura County Watershed Protection District, Pacific Western Aerial Surveys, Ventura County Surveyors Office, AirPhoto USA, and IK Curtis. Historically, much of the aerial photography flown over the lower Santa Clara River Valley was commissioned by Ventura County to document flood damage (including damage caused by the 1928 Saint Francis Dam disaster), and so was particularly well suited to analyzing the effects of major floods along the Santa Clara River. For this analysis, photo sets were chosen to represent the effects of 7 major floods of interest (see Table E-1 and Figure E-1). Although suitable aerial photography exists to document major floods in 1980, 1983, and 1998, funding was not available to process these photo sets. The extent of coverage each aerial photo set provided was not uniform, as some photography, particularly early sets, were flown only to assess effects on the major towns in the valley.

Aerial photography was acquired in one of three different formats, depending upon availability and age: hardcopy contact prints, non-georeferenced digital images, or orthorectified imagery[9]. For hardcopy contact prints, each image was scanned at a resolution of 600 dpi in either 24 bit color or grayscale, depending on the color spectrum of the original image. Non-georeferenced photography was typically scanned by the supplier at resolutions ranging from 600 dpi to 1200 dpi.

[9] Georeferencing refers to the process of "rubber-sheeting" or matching features in an image to a "real-world" coordinate system. Georeferencing typically only considers horizontal referencing, whereas an orthorectified image will be referenced using both horizontal and vertical components, resulting in a more accurate representation of earth's surface.

Table E-1. Aerial photography sets used in planform dynamics assessment

Photography date(s)	Flood date	Estimated peak discharge (cfs) at Montalvo (USGS 11114000)	Original scale	Pixel resolution	Photo source[a]
September 1, 2005	February 21, 2005	82,200		1.0 feet	APUSA
Feb 1-4, 2005	January 10, 2005	136,000		0.5 feet	APUSA/VCWPD
	January 9, 2005	129,000			
January 31, 1995	January 10, 1995	110,000		1 meter	APUSA
November 1, 1992	February 12, 1992	104,000	1:24000	1 meter	PWAS
May 16, 1978	March 4, 1978	102,200	1:24000	1 meter	PWAS
March 2, 1969	February 25, 1969	152,000	1:12000	1 meter	VCWPD
February 26, 1969	January 25, 1969	165,000			
November 2, 1945 October 25, 1945 July 1, 1938	January 23, 1943	80,000[b]		1 meter	VCWPD
May 25, 1938 May 10, 1938	March 2, 1938	120,000		1 meter	VCSO

[a] APUSA = AirPhoto USA, VCWPD = Ventura County Watershed Protection District, PWAS = Pacific Western Aerial Surveys, IKC = IK Curtis, VCSO = Ventura County Surveyors Office

[b] Discharge from USACE 1968 (cited in Simons, Li & Associates, 1983)

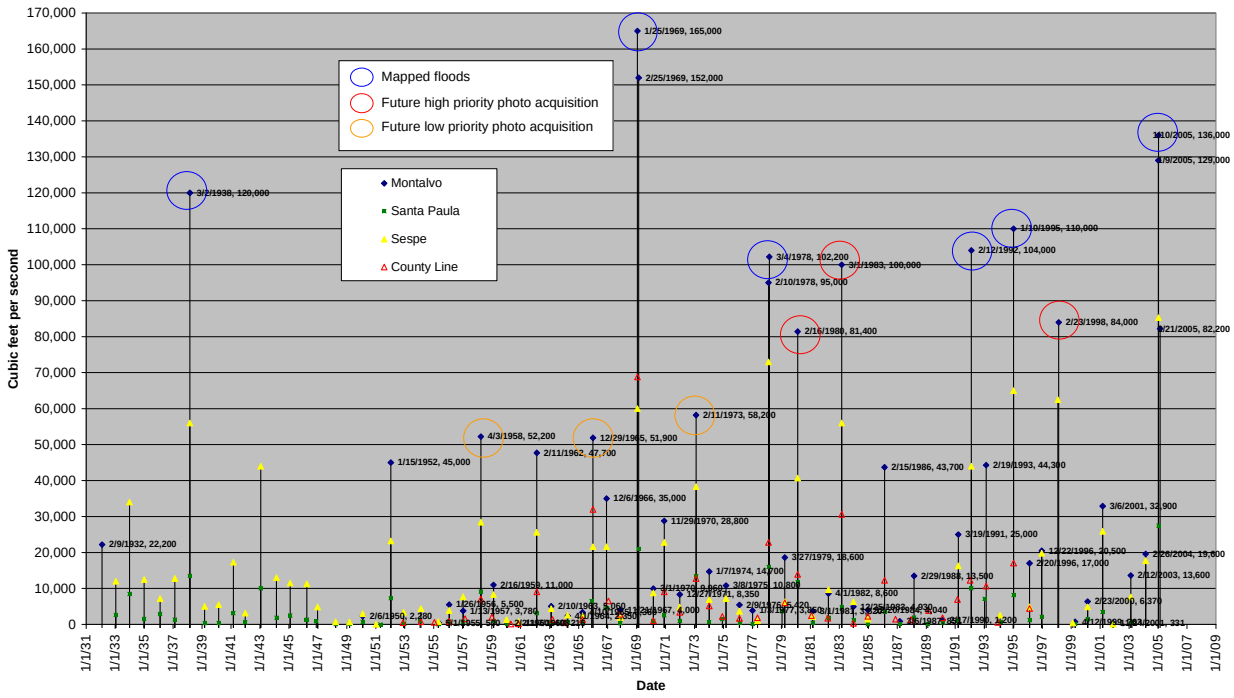

Figure E-1. Mapped historical flood extents and future imagery acquisition priorities for Santa Clara River planform mapping.

GEOREFERENCING

In order to extract and accurately compare river planform data from the acquired aerial photography, a common spatial context was necessary. Using a GIS, all imagery was georeferenced to a single spatial projection (California State Plane Zone 5, NAD 83). Orthophotography was obtained for 1995 and both photos sets flown in 2005; the remaining flood years were acquired either as hardcopy contact prints or non-georeferenced digital images. The ESRI ArcGIS georeferencing toolset was utilized to georeference the scanned hardcopy contact prints and digital imagery to the 2005 orthophotography, thus providing a highly accurate standard control point source for the entire photographic record. Control points were typically located using old barns, bridges, intersections, and other features that appeared unchanged between photos sets. Georeferencing methods utilized at least 10 control points per photograph; bilinear interpolation was used to produce pixel resolutions of 1 m. Orthorectified imagery was acquired at pixel resolutions ranging from 1 m to 0.5 ft (see Table E-1).

Spatial error in certain portions of photo sets due to imagery registration errors was occasionally significant – as high as 35 m. These errors were typically associated with image distortion at the outer edges of older photos, due to sub-standard aerial photography techniques, standard lens distortion, or oblique camera angles. However, spatial errors between most photo sets generally ranged between 3 and 15 m.

FLOOD SCOUR DIGITIZING

Each set of spatially referenced photography (each representing a particular flood) was used in a GIS to interpret two levels of flood-caused disturbance in the channel and floodplain areas. In addition, areas of apparently natural riparian vegetation[10] that remained after the flood were also mapped. For purposes of photo interpretation, these areas were defined as follows:

High disturbance: These areas are characterized by distinct channel and floodplain areas severely disturbed by flow (i.e. scoured to bare substrate), typically with 10% or less apparent remaining riparian vegetative cover. This category may include agricultural or developed lands with a high level of apparent disturbance by flood flows, thus identification of this type is not always based upon vegetative cover, sometimes relying on patterns of obvious scour.

Medium disturbance: This class is characterized by distinct areas of low to moderate apparent disturbance by flow, typically defined as areas with more than 10% but less than 80% apparent riparian vegetative cover. This type includes agricultural or developed lands with low to moderate apparent disturbance by flood flows, thus identification of this type is not always based upon vegetative cover, as with the high disturbance class.

Riparian vegetation: These areas were characterized by distinct zones of apparently natural riparian vegetation with little to no apparent disturbance by flood, typically containing more than 80% riparian vegetation. Areas in this class may have been inundated by floodwaters, but did not show significant signs of scouring or other disturbance that removed vegetation.

[10] In the context of the floodplain vegetation communities of the Santa Clara River, "riparian vegetation" may include types more typical of upland communities, such as coastal sage scrub, or non-native plant species which in some cases includes non-native species, but not agricultural lands

To record these areas, polygons were delineated around features within each flood year photo set using heads-up digitizing at a scale of 1:4500 in the GIS. While methods for digitizing generally followed those described by Tiegs and Pohl (2005), the data generated in this study were not converted to a raster format for analysis, but rather kept as polygons in an ESRI Geodatabase, as originally digitized. All subsequent analyses (see below) were conducted using the polygon representation, which allowed for a finer scale of resolution in analysis output.

In addition to spatial error related to georeferencing, polygon delineation likely resulted in unknown spatial errors due to difficulties in interpreting features of interest. These types of error are most likely to occur with older contact prints (i.e. 1938 and 1945) used in this study. Older photographic film typically had a coarser grain than more modern films resulting in lower feature resolution once the image was scanned and georeferenced, making interpretation of floodplain features more difficult. The grayscale color spectrum of older imagery (1938, 1945, and 1969) made interpretation of residual riparian vegetation more difficult in certain cases as well.

Capturing Incremental Changes in the 2005 Flood Season

Multiple large floods within a single flood season are not uncommon on the Santa Clara River (i.e., 1969 and 2005; see Table E-1); however, the incremental changes resulting from the individual floods are rarely documented due to relatively infrequent aerial photography flights. In 2005, however, AirPhoto USA performed two flights along the Santa Clara River, each capturing the effects of two separate, significant flood events. In January and February 2005, three significant peak flood flows occurred (see Table E-1). The two January floods were documented by aerial photography flown in February 2005. The additional effects of a third flood on February 21 were recorded by photography flown in September 2005.

The February photography was utilized first to develop the planform map documenting the effects of the January floods. The results from that analysis were then updated with analysis from the September imagery, documenting the incremental changes wrought by the February flood. It is important to note that these analyses were additive, because certain planform changes between the January floods and the February flood were not readily distinguished, such as whether an area which was highly disturbed in the January floods had only a moderate disturbance in the February flood.

QUALITY CONTROL

Each flood year polygon data set was checked for spatial and interpretive accuracy by a GIS analyst that was not associated with the digitization process for that particular year. This process ensured that the data sets were consistent and accurate between and across years. Assessments of spatial error were conducted by a GIS analyst not directly involved in georeferencing or digitization processes.

ANALYSES

The planform data digitized from the aerial photography sets were used to conduct a number of spatial analyses to support understanding of fluvial dynamics in the lower Santa Clara River. These analyses included calculation of historical flood disturbance probability, "last flood" spatial analyses, and average reach width calculations for each historical flood.

Locational Probability Model

The methods and nomenclature discussed below have been modeled on those of Graf (2000) and Tiegs (2005). For this analysis, we define a locational probability model as a graphical representation of the historical probability that any particular area within the floodplain and channel of the Santa Clara was

scoured (i.e. the "highly disturbed" category described above) by a major flood. As discussed above, aerial photographs chosen for use in this study were taken after major floods (see Table 1 and Figure 1) and thus represent the post-flood channel configuration for a particular flood.

Because the Santa Clara River is a flood event dominated system (see Section 5 of the main report) and each set of photography was taken shortly after a major flood event, it can be assumed that each photo set represents the dominant planform configuration of the channel until the next large flood documented by aerial photography. This approach differs from that of Graf (2000), Tiegs et al. (2005), and Tiegs and Pohl (2005), who assume that each photo set is representative of general channel conditions for a period of time from one photo set to the previous photo set. Thus, their approach does not appear to explicitly consider whether the photo is representative of the effects of particular floods, but rather describes general channel conditions over time.

There are numerous caveats to our assumption discussed above, the most important being that smaller floods occur between the photograph sets and likely result in reworking of the channel; however, it remains that major changes to the channel and floodplain of the Santa Clara River are accomplished by large floods. For this analysis, another significant caveat is the lack of aerial photographic coverage for three recent, major floods in 1980, 1983, and 1998; although suitable aerial photography exists to document these floods, funding limited the number of aerial photograph sets that could be processed.

To derive a disturbance probability model, the study area was divided into 11 reaches which were distinguished primarily by differences in stream power (see Section 5 of the main report for further discussion). A separate disturbance probability model was calculated for each of 10 reaches; Reach 11 was excluded from the analysis due to a lack of significant aerial photographic coverage. In order to build the disturbance probability model, the photo sets needed to be weighted based on the amount of time each represented in the overall study period[11] (1938-2007), on a reach basis. The weighting values were calculated for each flood year and reach using the following equation:

$$\text{Weighting value } (W_n) = \frac{\text{years represented by given photograph } (t_n)}{\text{total number of years in photographic record } (m)}$$

The value of t_n is the number of years between the documented flood of interest and the next photo documented flood. The value of m is the total number of years documented by aerial photography for a particular reach, from earliest photography set to most recent. Working through the equation for each flood year and reach gave the results displayed in Tables E-2 and E-3 below.

[11] Photography was acquired for selected floods between 1938 and 2005, thus this period represents the photographic record. For the purposes of calculating probability of disturbance, the "study period" was 1938-2007, since no major floods had occurred between 2005 and the year this study was completed, 2007.

Table E-2. Years represented by individual flood photography and total number of years in the photographic record, by reach.

Reach	Number of years represented by given flood photography (t_n)							Number of years in photographic record (m)
	1938	1945	1969	1978	1992	1995	2005	
1	7	24	9	14	3	10	2	69
2	-	24	9	14	3	10	2	62
3	31	-	9	14	3	10	2	69
4	31	-	9	14	3	10	2	69
5	7	24	9	14	3	10	2	69
6	7	24	9	14	3	10	2	69
7	-	-	9	14	3	10	2	38
8	-	-	9	14	3	10	2	38
9	31	-	9	14	3	10	2	69
10	31	-	9	14	3	10	2	69

Table E-3. Weighting values for individual floods photography and reaches.

Reach	Weighting value (W_n)						
	1938	1945	1969	1978	1992	1995	2005
1	0.10	0.35	0.13	0.20	0.04	0.14	0.03
2	-	0.39	0.15	0.23	0.05	0.16	0.03
3	0.45	-	0.13	0.20	0.04	0.14	0.03
4	0.45	-	0.13	0.20	0.04	0.14	0.03
5	0.10	0.35	0.13	0.20	0.04	0.14	0.03
6	0.10	0.35	0.13	0.20	0.04	0.14	0.03
7	-	-	0.24	0.37	0.08	0.26	0.05
8	-	-	0.24	0.37	0.08	0.26	0.05
9	0.45	-	0.13	0.20	0.04	0.14	0.03
10	0.45	-	0.13	0.20	0.04	0.14	0.03

Weighting values were assigned to flood year and reach polygon layers in the GIS. All of the flood year layers were then combined in the GIS (using the "union" function), resulting in numerous smaller polygons, all of which retained their original assigned probability for each year and reach. For each individual polygon, all the years weighting values were summed, resulting in a probability of scour for each (Table E-4). The probability field was then used to illustrate locational probability in a map (see Figure 5-16) for each reach.

Table E-4. Example of GIS data table with summed weighting values or probability of scour ("SumProb") for each polygon.

Polygon	1938	1969	1978	1992	1995	2005	SumProb	Shape_Area
1	0.45	0	0	0	0	0	0.45	1459947.254
2	0	0.13	0	0	0	0	0.13	1710181.258
3	0	0.13	0	0	0	0	0.13	825.8837909
4	0	0.13	0	0	0	0	0.13	321.74415
5	0.45	0.13	0	0	0	0	0.58	1037.485881
6	0	0.13	0	0	0	0	0.13	1777.786451
7	0	0.13	0.2	0	0	0	0.53	181.1416506
8	0	0.13	0.2	0	0	0	0.53	113.8613641
9	0	0.13	0.2	0	0	0	0.53	5636.241047
10	0	0	0	0.04	0	0	0.04	46170.7421
11	0	0	0	0.04	0	0	0.04	435.8034547
12	0	0	0	0.04	0	0	0.04	2020.878413
13	0	0	0	0	0.14	0	0.14	327800.4409
14	0	0	0	0	0.14	0	0.14	40539.56361
15	0	0	0	0	0	0.03	0.03	222838.8706
16	0	0	0	0	0	0.03	0.03	66320.23549

Width of Active Channel Bed in Successive Floods

Knowledge of the last known flood disturbance for any particular area of the floodplain is critical to understanding the age of geomorphic surfaces and thus the approximate age of riparian vegetation growing there. The flood scour layers were manipulated in the GIS to derive a map of "last flood" scour areas for the entire study reach. All flood year layers were combined in a GIS using the "union" command, resulting in numerous smaller polygons each retaining information on the years in which the particular polygon was inundated. Using a "max number" algorithm, the most recent year was chosen from the GIS data and copied to a new field; the value in the new field (the "last flood" field) now contained the date of the most recent scour event for any particular polygon. The value of the "last flood" field was then used to produce a map of last flood scour for the entire study reach (see Figure 5-17).

Reach Width Analysis

In order to help inform an understanding of the behavior of the lower Santa Clara River, a geomorphological analysis was undertaken using the "active channel width" (i.e. the scoured area or "high" classification) of each documented flood (see Section 5). In order to facilitate the analysis, reach average widths were calculated for each documented flood based upon the area of scour documented for each flood (as calculated in the GIS). A channel centerline was established as the basis for reach length, then width was derived from the simple relationship between length, width and area:

Width = Area/Length

Reach-based areas for each documented flood were exported from the GIS and imported to Microsoft Excel, where the calculations were completed using the Pivot Tables function.

REFERENCES CITED:

Graf, W.L. 2000. Locational probability for a dammed, urbanizing stream: Salt River, Arizona, USA. Environmental Management 25: 321-335.

Simons, Li & Associates. 1983. Hydraulic, erosion and sedimentation study of the Santa Clara River Ventura County, California. Prepared for Ventura County Flood Control District, Ventura, California.

Tiegs, S.D., J.F. O'Leary, M.M. Pohl, and C.L. Munill. 2005. Flood disturbance and riparian diversity on the Colorado River Delta. Biodiversity and Conservation 14: 1175-1194.

Tiegs, S.D., and M. Pohl. 2005. Planform channel dynamics of the lower Colorado River: 1976-2000. Geomorphology 69: 14-27.

APPENDIX F: BED ELEVATION CHANGE ALONG THE SANTA CLARA RIVER (1929-2005)

Table F-1. Bed elevation along the Santa Clara River (1929-2005).

Sub-reach (start)	Land-mark	Station (ft)	Elevation (ft NAVD88)																
			1929	1949	1967	1967 (1968 COE)	1967 & 1968 (1970 COE)	1968 & 1971 (1972 COE)	1968 & 1971 (1973 COE)	1975	1978	1979	1980	1983	1986	1989	1992	1993	2005
	SCR mouth																		
		00+00		4.5		2.5													6.6
		10+00		5.5		4.5												6.0	6.5
		20+00		7.5		6												8.0	6.4
REACH 1																			
	Harbor Blvd (28+00)																		
		30+00		10.5		8					8							10.0	6.1
		40+00		12.5		9.5					10				7.5			12.0	7.8
		50+00		14.5		11.5					12.5				9.5			13.5	9.0
		60+00		16.5		13.5					14.5				11.5			15.0	11.7
		70+00		17.5		16					16.5				12			16.5	12.9
		80+00		18.5		20					18.5				14.5			18.5	15.2
		90+11		20.5		23.5					20.5				16			21.0	17.4
		100+00		22.5		25.5					22.5				20			22.5	20.1
		110+00		26.5		27					24.5				23		20	24.5	22.0
		120+00		29.5		29					27				26		24	28.0	24.2
		130+00		31.5		31					29.5				28		26	30.5	25.9
		140+00		34.5		32					32				29.5		28	32.0	29.0
		150+00		37.5		34					34.5				31.5		32	33.5	
		160+00		40.5		37					37				35		35.5	35	32.3
		170+00		43.5		40					39				37		38	37.0	33.6
		180+00		45.5		43					41				39.5		42	39.0	36.3
		190+00		48.5		45					44				41.5		44	42.0	38.4
		200+00		50.5		46.5					45.5				43.5			45.5	40.9
		210+00		52.5		50					49				46			48.0	43.3
		220+00		54.5		53					51.5				48.5			50.5	45.3
		230+00		56.5		55					54				51			53.0	47.1
REACH 2																			
	Hwy 101 bridge																		
		240+00		58.5	58	56.5				59	50	56.5	60	57	53		51	55	52.0
		250+00		59.5	63	58.5				61	57	59.5	63	58.5	55		55	57.5	57.7
		260+00		60.5	67	61.5				62	62.5	62	65	61	58.5		58.5	60.5	60.9

Sub-reach (start)	Land-mark	Station (ft)	Elevation (ft NAVD88)																
			1929	1949	1967	1967 (1968 COE)	1967 & 1968 (1970 COE)	1968 & 1971 (1972 COE)	1968 & 1971 (1973 COE)	1975	1978	1979	1980	1983	1986	1989	1992	1993	2005
		270+00		62.5	71	64.5				63.5	64.5	65	67	64	61.5		60.5	62.5	65.6
		280+00		65.5	73	67.5				65.5	67.5	67	69.5	67	65.5		62	64.5	67.3
				72	74	70				68	69.5	68.5	72	69.5	67		63	67	68.8
		300+00		78	77	72.5				71	72	71	74	72	69		65	69	71.7
		310+00		82.5	79	75				73.5	74.5	73.5	76	74	72.5		69	72	73.3
		320+00		84.5	81.5	78				75.5	76	74.5	78	76.5	75.5		71.5	74	76.6
		330+00		87	84	81				77.5	78	78	80.5	79	77		72	77	79.4
		340+00		90.5	86	84.5				80	80	79	83.5	81.5	79.5		74.5	79.5	81.5
		350+00		92.5	89	86				82.5	82.5	82	85	84	82		78	82	83.7
		360+00		97	92	88				83	85	85	87	86.5	86		81.5	85	86.0
		370+00		98.5	94	89.5				83	88	87.5	88	88.5	88		84	87	87.9
		380+00		100.5	96	92.5				83.5	90.5	89	89	91	92		85	90	89.7
		390+00		101.5	98.5	94				95	93.5	92	92	94	94.5		87.5	93	92.0
		400+00		103.5	102	95.5				98.5	97	94.5	95	95	96		91	95.5	95.1
		410+00		108.5	105	98				100	97.5	97	97.5	97.5	98		93	97.5	96.8
		420+00		114.5	107.5	102				102	99	99	99	99	98		95.5	100	99.0
		430+00		116.5	109.5	105				104.5	102	101.5	101	101.5	101.5		97	102.5	101.6
		440+00		120.5	110.5	107.5				106.5	105	105	103	104	104		101	106	103.7
	Hwy 118 bridge																		
		450+00		122.5	112	112				110	107	108.5	106.5	105.5	105.5		104.5	108.5	106.9
		460+00		126.5	118	117				115	110	111	112	109	109		107	111.5	110.5
		470+00		132.5	123	122.5				116.5	112.5	113.5	116	113	112.5		111.5		112.8
		480+00		136.5	127	126.5				118	118.5	118.5	119	115.5	115.5		112.5	118	116.7
		490+00		138.5	130	129				125	124	123	122	121	121		115.5	121	118.5
		500+00		144.5	132	132				129	124.5	128.5	126	123.5	124.5		118	124	121.6
		510+00		147	134	135.5				131	126	131	131	128.5	128		123	127.5	123.7
		520+00		150.5	138.5	139.5				138.5	131	136	134.5	132	133		129	130.5	126.3
		530+00		152.5	144.5	145				145.5	139	141	137.5	139	139		132	133.5	129.5
		540+00		156.5	151.5	149				153	143.5	144	140.5	141	141		135	136	131.9
		550+00		159.5	156		155			156	148	147	142.5	143	143		139	139	134.4
		560+00		161.5	159.5		158			160	150	149.5	144.5	145	144.5		140.5	142.5	137.5
REACH 3																			
	Freeman Diversion (568+00)																		
		570+00		164.5	162		160.5			164.5	154.5	154.5	149	150	148		163.5	163	164.6
		580+00		169.5	164		163			168.5	161	158.5	152.5	153.5	152.5		165	165	165.4
		590+00		172.5	165		165			173	166.5	162.5	158	158	157		166	167	167.5
		600+00		174.5	166.5		167.5			173.5	165	165	162.5	162.5	161		167	169	169.8
		610+00		177.5	171.5		171.5			175	168.5	169	166.5	166.5	167.5		169	172	174.1

Sub-reach (start)	Land-mark	Station (ft)	Elevation (ft NAVD88)																
			1929	1949	1967	1967 (1968 COE)	1967 & 1968 (1970 COE)	1968 & 1971 (1972 COE)	1968 & 1971 (1973 COE)	1975	1978	1979	1980	1983	1986	1989	1992	1993	2005
		620+00		180.5	176.5		175.5			178	173.5	174.5	170	170	169		171	174	176.4
		630+00		183.5	182		179			179	176.5	175.5	173	173	170		172	177	177.9
		640+00		185.5	185		180.5			181.5	180	176.5	175.5	175.5	172.5		175.5	180	181.9
		650+00		188.5	193		183			183	183.5	178	178.5	178.5	175		178	183	184.2
		660+00		190.5	195		191.5			186	187	183.5	180.5	182	176.5		180.5	186	185.5
		670+00		194.5	197		193.5			189	190	188	182	186	182		183	189	189.4
		680+00		196.5	200		195.5			192	193.5	191.5	186.5	191	186.5		185.5	192.5	192.9
		690+00		198.5	204		199			195	197	194.5	190	194.5	191		191	196	195.1
		700+00		202.5	206.5		202			198	200	198	196	197	194		194	200	197.3
REACH 4																			
	Shell Rd [from LiDAR] (714+40)																		
		710+00		208	209		206			204	203	202.5	202.5	200	196		197.5	204	199.9
		720+00		210.5	212.5		208			209	207	207	207.5	203	198.5		200.5	206.5	201.7
		730+00		214.5	214.5		210			214	211.5	212	211.5	209	204		204.5	208.5	211.0
		740+00		219.5	217		213.5			218.5	216.5	216.5	214	215.5	208		209	212	213.2
		750+00		223	220		218			221.5	221	221	218	222	212.5		216	216	216.3
		760+00		224.5	222.5		220			223.5	225.5	225.5	220	227	221.8		219	221	217.8
		770+00		226.5	225		223			226	228.5	228.5	222	228	222.5		223	225	222.5
		780+00		230.5	229		226.5			228	231	231.5	227	230	225		224.5	227.5	226.6
		790+00		232.5	234		229.5			231	233	233.5	231	232	227		227.5	230	230.7
		800+00		234.5	237		234.5			234	235.5	235.5	233	234.5	229		231	233	233.7
		810+00		236.5	240.5		236			236	236	239	237.5	238.5	230.5		235	237	239.6
		820+00		239.5	245		236			238	236.5	242.5	241.5	243	233.5		239	240	242.6
REACH 5																			
	Santa Paula Cr confl. (830+00 - 835+00)																		
		830+00		245	246.5		241			241	246	246	243.5	247	241		242.5	240	245.5
		840+00		248.5	248		243.5			243.5	249	250	247	248	243.5		245	244.5	247.4
		850+00		252.5	252		247			246	249	254	251	251.5	245		247	249	251.4
		860+00		254.5	253		250	253		252.5	252	258	255	253	250		249.5	254	254.8
		870+00		258.5	257.5		254	255		257	258	259.5	258.5		254		252.5	258.5	257.4
		880+00		260.5	262		257	258.5		261	261	261.5	261.5		257		255.5	261.5	261.7
		890+00		265.5			260.5	261.5			264		264		260.5			264.5	266.1
		900+00	269	268.5			265				267		268		263			267	269.0
		910+00	270	273			267				273							271	272.2
		920+00	273	276			270				278							275	278.9
REACH 6																			
	East side of South Mountain [from LiDAR] (925+60)																		
		930+00	278.5	279.5			273				281		272.5					278	281.8

Sub-reach (start)	Land-mark	Station (ft)	Elevation (ft NAVD88)																
			1929	1949	1967	1967 (1968 COE)	1967 & 1968 (1970 COE)	1968 & 1971 (1972 COE)	1968 & 1971 (1973 COE)	1975	1978	1979	1980	1983	1986	1989	1992	1993	2005
		940+00	278.5	281.5			277.5				284		276.5					281	284.4
		950+00	288.5	284.5			282				287.5		280					284.5	284.8
		960+00	291.5	288.5			283.5				291		283					287	287.3
		970+00	292.5	293			286				295		285.5					290	291.3
		980+00	294.5	294.5			291				297.5		290					293.5	294.4
		990+00	296.5	296.5			294				299.5		294					297	298.5
		1000+00	298.5	298.5			298				301		298.5			300		300	301.6
		1010+00	303	302.5			301				303.5		302			302.5		303	304.7
		1020+00	304.5	306.5			305				306		304.5			306.5		306	307.3
		1030+00	310	310.5			309.5				307.5		306.5			310.5		308.5	310.4
		1040+00	311	314.5			313.5				308.5		311			313		311	314.0
		1050+00	316	318.5			316				311		316			315.5		315	317.7
		1060+00	318.5	320.5				320.5			317		321.5			320		318.5	319.2
		1070+00	323.5	322.5				322			325		327			326		322.5	326.0
		1080+00	326	326.5				325.5			328		330			332		326	328.6
		1090+00	334	330.5				331			331		333			334.5		330	332.5
		1100+00	336.5	339.5				334			335.5		335.5			337.5		334	336.3
		1110+00	338	344.5				337			338		339			339.5		337	339.1
		1120+00	340	344.5				340			341		344			342.5		340.5	342.6
		1130+00	343	346.5				343.5			344.5		348			346.5		343.5	344.7
		1140+00	346	351				348			348.5		351			351		347	348.9
		1150+00	352	355.5				350			353		355			358		349.5	350.9
REACH 7																			
	Sespe Cr conf. (1165+00 - 1210+00)																		
		1160+00	356.5	359.5				354.5			357.5		359					353	356.5
		1170+00	364	361.5				360			359		363					358	361.4
		1180+00	370	363				366			364		368					364.5	365.8
		1190+00	372.5	366.5				371			371		373					370	373.6
		1200+00	375.5	371				376.5			376.5		378.5					375.5	376.6
		1210+00	377.5	376.5				380.5			380		383.5					379.5	380.4
		1220+00	385	381				386			386		388.5					384	385.0
		1230+00	390	384.5				390			390							388.5	388.4
		1240+00	392	390.5				395			394.5							393.5	395.2
		1250+00	397.5	394.5				398.5			399							398	400.0
	Hwy 23 bridge [from HECRAS] (1254+50)																		
		1260+00	400.5	400.5				403			404.5							403	403.6
		1270+00	404.5	404.5				407			408							409	407.9
		1280+00	409.5	409.5				412			413							413.5	411.8

Sub-reach (start)	Land-mark	Station (ft)	Elevation (ft NAVD88)																
			1929	1949	1967	1967 (1968 COE)	1967 & 1968 (1970 COE)	1968 & 1971 (1972 COE)	1968 & 1971 (1973 COE)	1975	1978	1979	1980	1983	1986	1989	1992	1993	2005
		1290+00	414	417				419			417							418	415.3
		1300+00	423	422.5				423			420.5							422.5	425.2
		1310+00	427	428.5				427										426.5	429.7
REACH 8																			
	1 mile East of Chambers-berg Rd [from LiDAR] (1321+60)																		
		1320+00	433.5	432.5				432			433							432	433.7
		1330+00	438	438.5				439			439							437	437.4
		1340+00	444	441.5				444.5			443							441.5	443.6
		1350+00	447	444.5				449			448							447	448.9
		1360+00	450.5	448.5				452.5			453							452	453.7
		1370+00	454.5	454.5				460			459							457	456.8
		1380+00	460	460.5				462			466							463	463.8
		1390+00	466.5	468.5				467			471.5							468.5	469.2
		1400+00	472	472.5				473			475.5							474.5	473.4
		1410+00	481	478.5				478			481							479.5	479.7
		1420+00	486.5	485				481			487							485	485.7
		1430+00	493.5	488.5				485			493							489.5	490.7
		1440+00	497.5	496				492.5			498.5							495	495.6
		1450+00	502.5	500.5				499			505							499.5	500.9
		1460+00	505	505				505			510.5							506	507.9
		1470+00	512	512.5				510			516							512	514.1
		1480+00	519.5	518				514.5			521.5							518.5	520.7
		1490+00	525.5	522.5				519			527								525.3
		1500+00	528.5	527.5				523			532.5								530.5
REACH 9																			
	Hopper Cr confl. [from LiDAR] (1506+00)																		
		1510+00	534	532.5					527		534								535.8
		1520+00	539	537.5					535.5		542								541.8
		1530+00	546.5	543.5					540.5		547.5								547.6
		1540+00	548.5	548.5					547		553								552.0
		1550+00	556.5	556.5					552		559								557.2
		1560+00	564.5	563					559		564.5								563.9
		1570+00	571	568.5					565		570								567.2
		1580+00	575.5	576.5					570		576								572.8
		1590+00	578.5	578.5					576										581.6
		1600+00	583.5	585					582.5										586.3
		1610+00	587	590.5					586.5										591.3
		1620+00	591.5	595.5					594										597.2

Sub-reach (start)	Land-mark	Station (ft)	Elevation (ft NAVD88)																
			1929	1949	1967	1967 (1968 COE)	1967 & 1968 (1970 COE)	1968 & 1971 (1972 COE)	1968 & 1971 (1973 COE)	1975	1978	1979	1980	1983	1986	1989	1992	1993	2005
		1630+00	596	600.5					598										602.3
		1640+00	606	607.5					602.5										607.2
		1650+00	612	612.5					608.5										612.5
		1660+00	617.5	616.5					614										618.8
REACH 10																			
	Piru Cr confl. (from LiDAR) (1670+00)																		
		1670+00	622	622.5					618										622.2
		1680+00	628	626.5					623.5										627.2
		1690+00	632.5	631					628										632.0
		1700+00	639	639					633.5										638.4
		1710+00	642.5	645					642.5										645.5
		1720+00	652.5	653					651										651.1
		1730+00	655.5	658.5					657.5										660.0
		1740+00	662.5	664.5					663										664.9
		1750+00	670	670					667.5										672.4
		1760+00		675.5					674										680.4
		1770+00		681					679										685.1
		1780+00		686.5					685										689.7
		1790+00		693					690										695.0
REACH 11																			
	2.5 miles East of Piru Cr [from LiDAR] (1796+80)																		
		1800+00		698.5					693.5										700.6
		1810+00		703					701.5										705.8
		1820+00		708					708										711.1
		1830+00		713					710.5										716.2
		1840+00		715.5					715.5										720.1
		1850+00		721					719.5										725.6
		1860+00		725.5					724		727							730	730.9
		1870+00		732.5					728.5		733							735.5	735.8
		1880+00		738.5					737.5		740							739.5	739.5
		1890+00		745					743.5		747.5							743.5	744.1
		1900+00		753					750		754							749	749.3
		1910+00		755					757		759							755.5	753.7
		1920+00		760.5					760.5		764							762	758.7
		1930+00		766.5					763.5		768							767.5	764.8
		1940+00		772.5					769		772							772.5	769.8
		1950+00		778.5					777.5		779							777	775.8
		1960+00		783					786.5		785.5							781.5	781.8

Sub-reach (start)	Land-mark	Station (ft)	Elevation (ft NAVD88)																
			1929	1949	1967	1967 (1968 COE)	1967 & 1968 (1970 COE)	1968 & 1971 (1972 COE)	1968 & 1971 (1973 COE)	1975	1978	1979	1980	1983	1986	1989	1992	1993	2005
		1970+00		788.5					796		790.5							786	790.0
		1980+00		791					801.5		796							791.5	796.8
		1990+00		793					804.5		800.5							803	803.2
		2000+00		798.5					809		806.5							807.5	808.4
		2010+00		805					815		811.5							813	814.2
		2020+00		813					821		816.5							818	820.4
	LA Ventura Co Line																		
		2030+00		818.5					826.5		821							823	825.8

Table F-2. Net bed elevation change for discrete time periods along the Santa Clara River.

Sub-reach (start)	Land-mark	Station (ft)	Difference in elevation (ft)															
			1929-1949	1949-1967	1949-1967 (1968 COE)	1949-1967 & 1968 (1970 COE)	1949-1968 & 1971 (1972 COE)	1949-1968 & 1971 (1973 COE)	1949-1975	1949-1978	1949-1979	1949-1980	1949-1983	1949-1986	1949-1989	1949-1992	1949-1993	1949-2005
	SCR mouth																	
		00+00			-2													2.11
		10+00			-1												0.5	0.96
		20+00			-1.5												0.5	-1.07
REACH 1																		
	Harbor Blvd (28+00)																	
		30+00			-2.5					-2.5							-0.5	-4.39
		40+00			-3					-2.5				-5			-0.5	-4.75
		50+00			-3					-2				-5			-1.0	-5.55
		60+00			-3					-2				-5			-1.5	-4.77
		70+00			-1.5					-1				-5.5			-1.0	-4.63
		80+00			1.5					0				-4			0.0	-3.35
		90+11			3					0				-4.5			0.5	-3.1
		100+00			3					0				-2.5			0.0	-2.39
		110+00			0.5					-2				-3.5		-6.5	-2.0	-4.49
		120+00			-0.5					-2.5				-3.5		-5.5	-1.5	-5.32
		130+00			-0.5					-2				-3.5		-5.5	-1.0	-5.63
		140+00			-2.5					-2.5				-5		-6.5	-2.5	-5.47
		150+00			-3.5					-3				-6		-5.5	-4.0	-37.5
		160+00			-3.5					-3.5				-5.5		-5	-5.5	-8.16
		170+00			-3.5					-4.5				-6.5		-5.5	-6.5	-9.95
		180+00			-2.5					-4.5				-6		-3.5	-6.5	-9.22
		190+00			-3.5					-4.5				-7		-4.5	-6.5	-10.11
		200+00			-4					-5				-7			-5.0	-9.63
		210+00			-2.5					-3.5				-6.5			-4.5	-9.17
		220+00			-1.5					-3				-6			-4.0	-9.22
		230+00			-1.5					-2.5				-5.5			-3.5	-9.42
REACH 2																		
	Hwy 101 bridge																	
		240+00		-0.5	-2				0.5	-8.5	-2	1.5	-1.5	-5.5		-7.5	-3.5	-6.49
		250+00		3.5	-1				1.5	-2.5	0	3.5	-1	-4.5		-4.5	-2.0	-1.78
		260+00		6.5	1				1.5	2	1.5	4.5	0.5	-2		-2	0.0	0.35
		270+00		8.5	2				1	2	2.5	4.5	1.5	-1		-2	0.0	3.07
		280+00		7.5	2				0	2	1.5	4	1.5	0		-3.5	-1.0	1.84
				2	-2				-4	-2.5	-3.5	0	-2.5	-5		-9	-5.0	-3.2
		300+00		-1	-5.5				-7	-6	-7	-4	-6	-9		-13	-9.0	-6.32
		310+00		-3.5	-7.5				-9	-8	-9	-6.5	-8.5	-10		-13.5	-10.5	-9.2
		320+00		-3	-6.5				-9	-8.5	-10	-6.5	-8	-9		-13	-10.5	-7.9
		330+00		-3	-6				-9.5	-9	-9	-6.5	-8	-10		-15	-10.0	-7.63

Sub-reach (start)	Land-mark	Station (ft)	Difference in elevation (ft)															
			1929-1949	1949-1967	1949-1967 (1968 COE)	1949-1967 & 1968 (1970 COE)	1949-1968 & 1971 (1972 COE)	1949-1968 & 1971 (1973 COE)	1949-1975	1949-1978	1949-1979	1949-1980	1949-1983	1949-1986	1949-1989	1949-1992	1949-1993	1949-2005
		340+00		-4.5	-6				-10.5	-10.5	-11.5	-7	-9	-11		-16	-11.0	-9.04
		350+00		-3.5	-6.5				-10	-10	-10.5	-7.5	-8.5	-10.5		-14.5	-10.5	-8.8
		360+00		-5	-9				-14	-12	-12	-10	-10.5	-11		-15.5	-12.0	-11.04
		370+00		-4.5	-9				-15.5	-10.5	-11	-10.5	-10	-10.5		-14.5	-11.5	-10.65
		380+00		-4.5	-8				-17	-10	-11.5	-11.5	-9.5	-8.5		-15.5	-10.5	-10.83
		390+00		-3	-7.5				-6.5	-8	-9.5	-9.5	-7.5	-7		-14	-8.5	-9.49
		400+00		-1.5	-8				-5	-6.5	-9	-8.5	-8.5	-7.5		-12.5	-8.0	-8.43
		410+00		-3.5	-10.5				-8.5	-11	-11.5	-11	-11	-10.5		-15.5	-11.0	-11.72
		420+00		-7	-12.5				-12.5	-15.5	-15.5	-15.5	-15.5	-16.5		-19	-14.5	-15.46
		430+00		-7	-11.5				-12	-14.5	-15	-15.5	-15	-15		-19.5	-14.0	-14.88
		440+00		-10	-13				-14	-15.5	-15.5	-17.5	-16.5	-16.5		-19.5	-14.5	-16.76
	Hwy 118 bridge																	
		450+00		-10.5	-10.5				-12.5	-15.5	-14	-16	-17	-17		-18	-14.0	-15.64
		460+00		-8.5	-9.5				-11.5	-16.5	-15.5	-14.5	-17.5	-17.5		-19.5	-15.0	-16.04
		470+00		-9.5	-10				-16	-20	-19	-16.5	-19.5	-20		-21	-132.5	-19.68
		480+00		-9.5	-10				-18.5	-18	-18	-17.5	-21	-21		-24	-18.5	-19.83
		490+00		-8.5	-9.5				-13.5	-14.5	-15.5	-16.5	-17.5	-17.5		-23	-17.5	-20
		500+00		-12.5	-12.5				-15.5	-20	-16	-18.5	-21	-20		-26.5	-20.5	-22.86
		510+00		-13	-11.5				-16	-21	-16	-16	-18.5	-19		-24	-19.5	-23.3
		520+00		-12	-11				-12	-19.5	-14.5	-16	-18.5	-17.5		-21.5	-20.0	-24.18
		530+00		-8	-7.5				-7	-13.5	-11.5	-15	-13.5	-13.5		-20.5	-19.0	-23.02
		540+00		-5	-7.5				-3.5	-13	-12.5	-16	-15.5	-15.5		-21.5	-20.5	-24.63
		550+00		-3.5		-4.5			-3.5	-11.5	-12.5	-17	-16.5	-16.5		-20.5	-20.5	-25.11
		560+00		-2		-3.5			-1.5	-11.5	-12	-17	-16.5	-17		-21	-19.0	-24.05
REACH 3																		
	Freeman Diversion (568+00)																	
		570+00		-2.5		-4			0	-10	-10	-15.5	-14.5	-16.5		-1	-1.5	0.07
		580+00		-5.5		-6.5			-1	-8.5	-11	-17	-16	-17		-4.5	-4.5	-4.11
		590+00		-7.5		-7.5			0.5	-6	-10	-14.5	-14.5	-15.5		-6.5	-5.5	-5.04
		600+00		-8		-7			-1	-9.5	-9.5	-12	-12	-13.5		-7.5	-5.5	-4.68
		610+00		-6		-6			-2.5	-9	-8.5	-11	-11	-10		-8.5	-5.5	-3.45
		620+00		-4		-5			-2.5	-7	-6	-10.5	-10.5	-11.5		-9.5	-6.5	-4.07
		630+00		-1.5		-4.5			-4.5	-7	-8	-10.5	-10.5	-13.5		-11.5	-6.5	-5.62
		640+00		-0.5		-5			-4	-5.5	-9	-10	-10	-13		-10	-5.5	-3.63
		650+00		4.5		-5.5			-5.5	-5	-10.5	-10	-10	-13.5		-10.5	-5.5	-4.35
		660+00		4.5		1			-4.5	-3.5	-7	-10	-8.5	-14		-10	-4.5	-4.96
		670+00		2.5		-1			-5.5	-4.5	-6.5	-12.5	-8.5	-12.5		-11.5	-5.5	-5.1
		680+00		3.5		-1			-4.5	-3	-5	-10	-5.5	-10		-11	-4.0	-3.57
		690+00		5.5		0.5			-3.5	-1.5	-4	-8.5	-4	-7.5		-7.5	-2.5	-3.41
		700+00		4		-0.5			-4.5	-2.5	-4.5	-6.5	-5.5	-8.5		-8.5	-2.5	-5.2
REACH 4																		

Sub-reach (start)	Land-mark	Station (ft)	Difference in elevation (ft)															
			1929-1949	1949-1967	1949-1967 (1968 COE)	1949-1967 & 1968 (1970 COE)	1949-1968 & 1971 (1972 COE)	1949-1968 & 1971 (1973 COE)	1949-1975	1949-1978	1949-1979	1949-1980	1949-1983	1949-1986	1949-1989	1949-1992	1949-1993	1949-2005
	Shell Rd [from LiDAR] (714+40)																	
		710+00		1		-2			-4	-5	-5.5	-5.5	-8	-12		-10.5	-4.0	-8.11
		720+00		2		-2.5			-1.5	-3.5	-3.5	-3	-7.5	-12		-10	-4.0	-8.83
		730+00		0		-4.5			-0.5	-3	-2.5	-3	-5.5	-10.5		-10	-6.0	-3.55
		740+00		-2.5		-6			-1	-3	-3	-5.5	-4	-11.5		-10.5	-7.5	-6.26
		750+00		-3		-5			-1.5	-2	-2	-5	-1	-10.5		-7	-7.0	-6.69
		760+00		-2		-4.5			-1	1	1	-4.5	2.5	-2.7		-5.5	-3.5	-6.68
		770+00		-1.5		-3.5			-0.5	2	2	-4.5	1.5	-4		-3.5	-1.5	-3.98
		780+00		-1.5		-4			-2.5	0.5	1	-3.5	-0.5	-5.5		-6	-3.0	-3.95
		790+00		1.5		-3			-1.5	0.5	1	-1.5	-0.5	-5.5		-5	-2.5	-1.84
		800+00		2.5		0			-0.5	1	1	-1.5	0	-5.5		-3.5	-1.5	-0.79
		810+00		4		-0.5			-0.5	-0.5	2.5	1	2	-6		-1.5	0.5	3.08
		820+00		5.5		-3.5			-1.5	-3	3	2	3.5	-6		-0.5	0.5	3.13
REACH 5																		
	Santa Paula Cr confl. (830+00 - 835+00)																	
		830+00		1.5		-4			-4	1	1	-1.5	2	-4		-2.5	-5.0	0.48
		840+00		-0.5		-5			-5	0.5	1.5	-1.5	-0.5	-5		-3.5	-4.0	-1.14
		850+00		-0.5		-5.5			-6.5	-3.5	1.5	-1.5	-1	-7.5		-5.5	-3.5	-1.15
		860+00		-1.5		-4.5	-1.5		-2	-2.5	3.5	0.5	-1.5	-4.5		-5	-0.5	0.25
		870+00		-1		-4.5	-3.5		-1.5	-0.5	1	0		-4.5		-6	0.0	-1.15
		880+00		1.5		-3.5	-2		0.5	0.5	1	1		-3.5		-5	1.0	1.22
		890+00				-5	-4			-1.5		-1.5		-5			-1.0	0.55
		900+00	-0.5			-3.5				-1.5		-0.5		-5.5			-1.5	0.51
		910+00	3			-6				0		-273					-2.0	-0.78
		920+00	3			-6				2		-276					-1.0	2.89
REACH 6																		
	East side of South Mountain [from LiDAR] (925+60)																	
		930+00	1			-6.5				1.5		-7					-1.5	2.32
		940+00	3			-4				2.5		-5					-0.5	2.89
		950+00	-4			-2.5				3		-4.5					0.0	0.27
		960+00	-3			-5				2.5		-5.5					-1.5	-1.25
		970+00	0.5			-7				2		-7.5					-3.0	-1.7
		980+00	0			-3.5				3		-4.5					-1.0	-0.14
		990+00	0			-2.5				3		-2.5					0.5	1.97
		1000+00	0			-0.5				2.5		0			1.5		1.5	3.11
		1010+00	-0.5			-1.5				1		-0.5			0		0.5	2.23
		1020+00	2			-1.5				-0.5		-2			0		-0.5	0.79
		1030+00	0.5			-1				-3		-4			0		-2.0	-0.08
		1040+00	3.5			-1				-6		-3.5			-1.5		-3.5	-0.49
		1050+00	2.5			-2.5				-7.5		-2.5			-3		-3.5	-0.82
		1060+00	2				0			-3.5		1			-0.5		-2.0	-1.29

Sub-reach (start)	Land-mark	Station (ft)	Difference in elevation (ft)															
			1929-1949	1949-1967	1949-1967 (1968 COE)	1949-1967 & 1968 (1970 COE)	1949-1968 & 1971 (1972 COE)	1949-1968 & 1971 (1973 COE)	1949-1975	1949-1978	1949-1979	1949-1980	1949-1983	1949-1986	1949-1989	1949-1992	1949-1993	1949-2005
		1070+00	-1				-0.5			2.5		4.5			3.5		0.0	3.47
		1080+00	0.5				-1			1.5		3.5			5.5		-0.5	2.1
		1090+00	-3.5				0.5			0.5		2.5			4		-0.5	2.03
		1100+00	3				-5.5			-4		-4			-2		-5.5	-3.19
		1110+00	6.5				-7.5			-6.5		-5.5			-5		-7.5	-5.44
		1120+00	4.5				-4.5			-3.5		-0.5			-2		-4.0	-1.86
		1130+00	3.5				-3			-2		1.5			0		-3.0	-1.76
		1140+00	5				-3			-2.5		0			0		-4.0	-2.06
		1150+00	3.5				-5.5			-2.5		-0.5			2.5		-6.0	-4.58
REACH 7																		
	Sespe Cr conf. (1165+00 - 1210+00)																	
		1160+00	3				-5			-2		-0.5					-6.5	-3.04
		1170+00	-2.5				-1.5			-2.5		1.5					-3.5	-0.12
		1180+00	-7				3			1		5					1.5	2.78
		1190+00	-6				4.5			4.5		6.5					3.5	7.14
		1200+00	-4.5				5.5			5.5		7.5					4.5	5.56
		1210+00	-1				4			3.5		7					3.0	3.86
		1220+00	-4				5			5		7.5					3.0	4
		1230+00	-5.5				5.5			5.5							4.0	3.88
		1240+00	-1.5				4.5			4							3.0	4.72
		1250+00	-3				4			4.5							3.5	5.5
	Hwy 23 bridge [from HECRAS] (1254+50)																	
		1260+00	0				2.5			4							2.5	3.05
		1270+00	0				2.5			3.5							4.5	3.44
		1280+00	0				2.5			3.5							4.0	2.3
		1290+00	3				2			0							1.0	-1.73
		1300+00	-0.5				0.5			-2							0.0	2.71
		1310+00	1.5				-1.5			-428.5							-2.0	1.17
REACH 8																		
	1 mile East of Chambers-berg Rd [from LiDAR] (1321+60)																	
		1320+00	-1				-0.5			0.5							-0.5	1.19
		1330+00	0.5				0.5			0.5							-1.5	-1.06
		1340+00	-2.5				3			1.5							0.0	2.12
		1350+00	-2.5				4.5			3.5							2.5	4.42
		1360+00	-2				4			4.5							3.5	5.19
		1370+00	0				5.5			4.5							2.5	2.28
		1380+00	0.5				1.5			5.5							2.5	3.28
		1390+00	2				-1.5			3							0.0	0.65
		1400+00	0.5				0.5			3							2.0	0.85
		1410+00	-2.5				-0.5			2.5							1.0	1.15
		1420+00	-1.5				-4			2							0.0	0.66

Sub-reach (start)	Land-mark	Station (ft)	Difference in elevation (ft)															
			1929-1949	1949-1967	1949-1967 (1968 COE)	1949-1967 & 1968 (1970 COE)	1949-1968 & 1971 (1972 COE)	1949-1968 & 1971 (1973 COE)	1949-1975	1949-1978	1949-1979	1949-1980	1949-1983	1949-1986	1949-1989	1949-1992	1949-1993	1949-2005
		1430+00	-5				-3.5			4.5							1.0	2.17
		1440+00	-1.5				-3.5			2.5							-1.0	-0.4
		1450+00	-2				-1.5			4.5							-1.0	0.37
		1460+00	0				0			5.5							1.0	2.94
		1470+00	0.5				-2.5			3.5							-0.5	1.62
		1480+00	-1.5				-3.5			3.5							0.5	2.69
		1490+00	-3				-3.5			4.5								2.81
		1500+00	-1				-4.5			5								2.96
REACH 9																		
	Hopper Cr confl. [from LiDAR] (1506+00)																	
		1510+00	-1.5					-5.5		1.5								3.26
		1520+00	-1.5					-2		4.5								4.29
		1530+00	-3					-3		4								4.14
		1540+00	0					-1.5		4.5								3.5
		1550+00	0					-4.5		2.5								0.67
		1560+00	-1.5					-4		1.5								0.87
		1570+00	-2.5					-3.5		1.5								-1.3
		1580+00	1					-6.5		-0.5								-3.73
		1590+00	0					-2.5										3.14
		1600+00	1.5					-2.5										1.27
		1610+00	3.5					-4										0.76
		1620+00	4					-1.5										1.72
		1630+00	4.5					-2.5										1.8
		1640+00	1.5					-5										-0.33
		1650+00	0.5					-4										-0.04
		1660+00	-1					-2.5										2.28
REACH 10																		
	Piru Cr confl. (from LiDAR) (1670+00)																	
		1670+00	0.5					-4.5										-0.32
		1680+00	-1.5					-3										0.74
		1690+00	-1.5					-3										0.97
		1700+00	0					-5.5										-0.56
		1710+00	2.5					-2.5										0.46
		1720+00	0.5					-2										-1.88
		1730+00	3					-1										1.54
		1740+00	2					-1.5										0.38
		1750+00	0					-2.5										2.36
		1760+00						-1.5										4.87
		1770+00						-2										4.05
		1780+00						-1.5										3.21
		1790+00						-3										1.97

Sub-reach (start)	Land-mark	Station (ft)	Difference in elevation (ft)															
			1929-1949	1949-1967	1949-1967 (1968 COE)	1949-1967 & 1968 (1970 COE)	1949-1968 & 1971 (1972 COE)	1949-1968 & 1971 (1973 COE)	1949-1975	1949-1978	1949-1979	1949-1980	1949-1983	1949-1986	1949-1989	1949-1992	1949-1993	1949-2005
REACH 11																		
	2.5 miles East of Piru Cr [from LiDAR] (1796+80)																	
		1800+00						-5										2.07
		1810+00						-1.5										2.75
		1820+00						0										3.13
		1830+00						-2.5										3.21
		1840+00						0										4.56
		1850+00						-1.5										4.56
		1860+00						-1.5		1.5							4.5	5.37
		1870+00						-4		0.5							3.0	3.34
		1880+00						-1		1.5							1.0	1.04
		1890+00						-1.5		2.5							-1.5	-0.93
		1900+00						-3		1							-4.0	-3.72
		1910+00						2		4							0.5	-1.29
		1920+00						0		3.5							1.5	-1.8
		1930+00						-3		1.5							1.0	-1.75
		1940+00						-3.5		-0.5							0.0	-2.68
		1950+00						-1		0.5							-1.5	-2.69
		1960+00						3.5		2.5							-1.5	-1.16
		1970+00						7.5		2							-2.5	1.47
		1980+00						10.5		5							0.5	5.77
		1990+00						11.5		7.5							10.0	10.17
		2000+00						10.5		8							9.0	9.93
		2010+00						10		6.5							8.0	9.17
		2020+00						8		3.5							5.0	7.35
	LA Ventura Co Line																	
		2030+00						8		2.5							4.5	7.29

APPENDIX G: ESTUARY HISTORICAL PHOTOS

Note: The aerial photographs from 1945, 1947, 1958, 1969, and 1993 that were used in the historical analysis are proprietary and could not be reproduced within this report. These photographs can be found in the University of California at Santa Barbara (UCSB) archive collection.

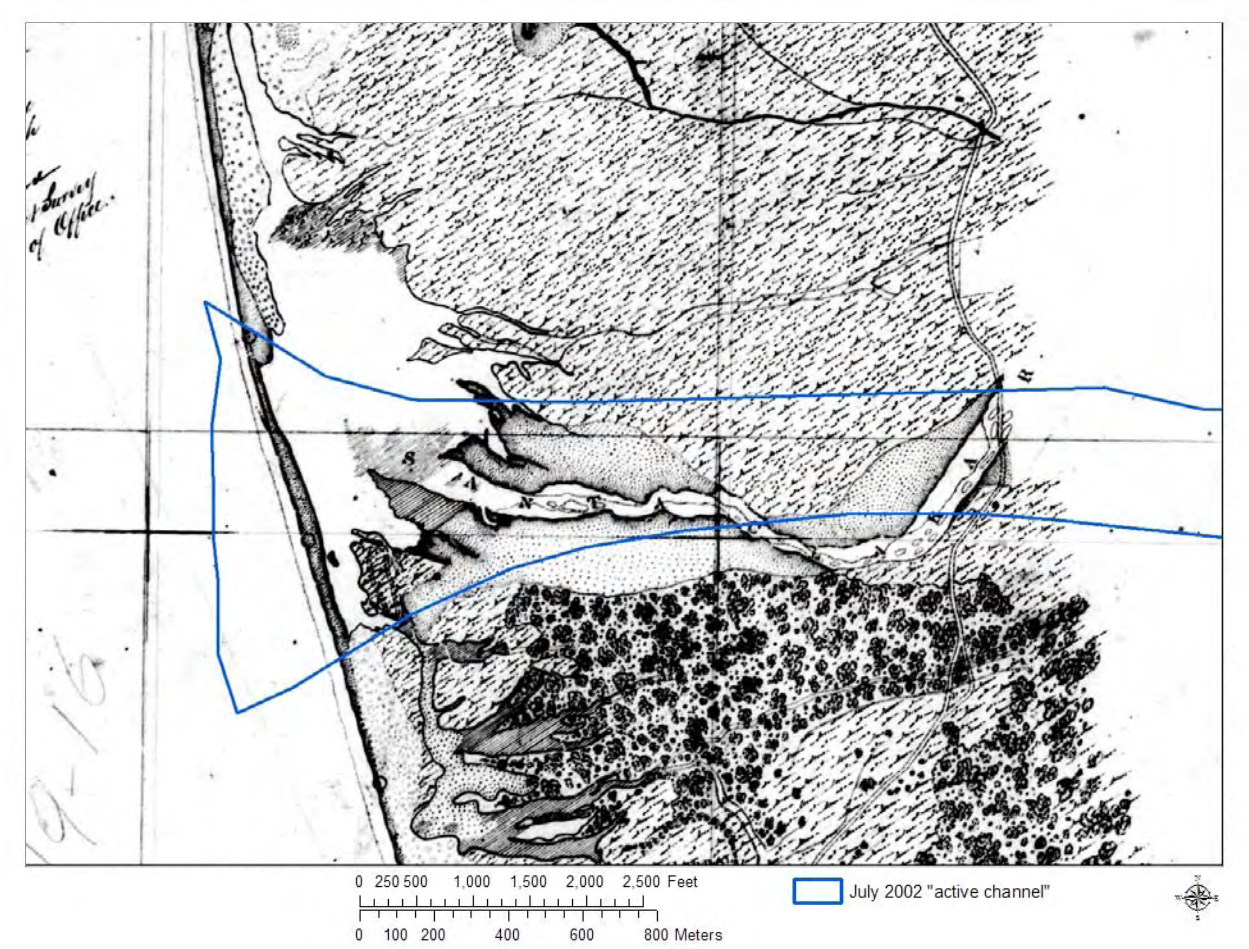

Figure G-1. Approximate 2002 active channel and estuary extent compared to 1855 conditions (Source: United States Coastal and Geodetic Survey).

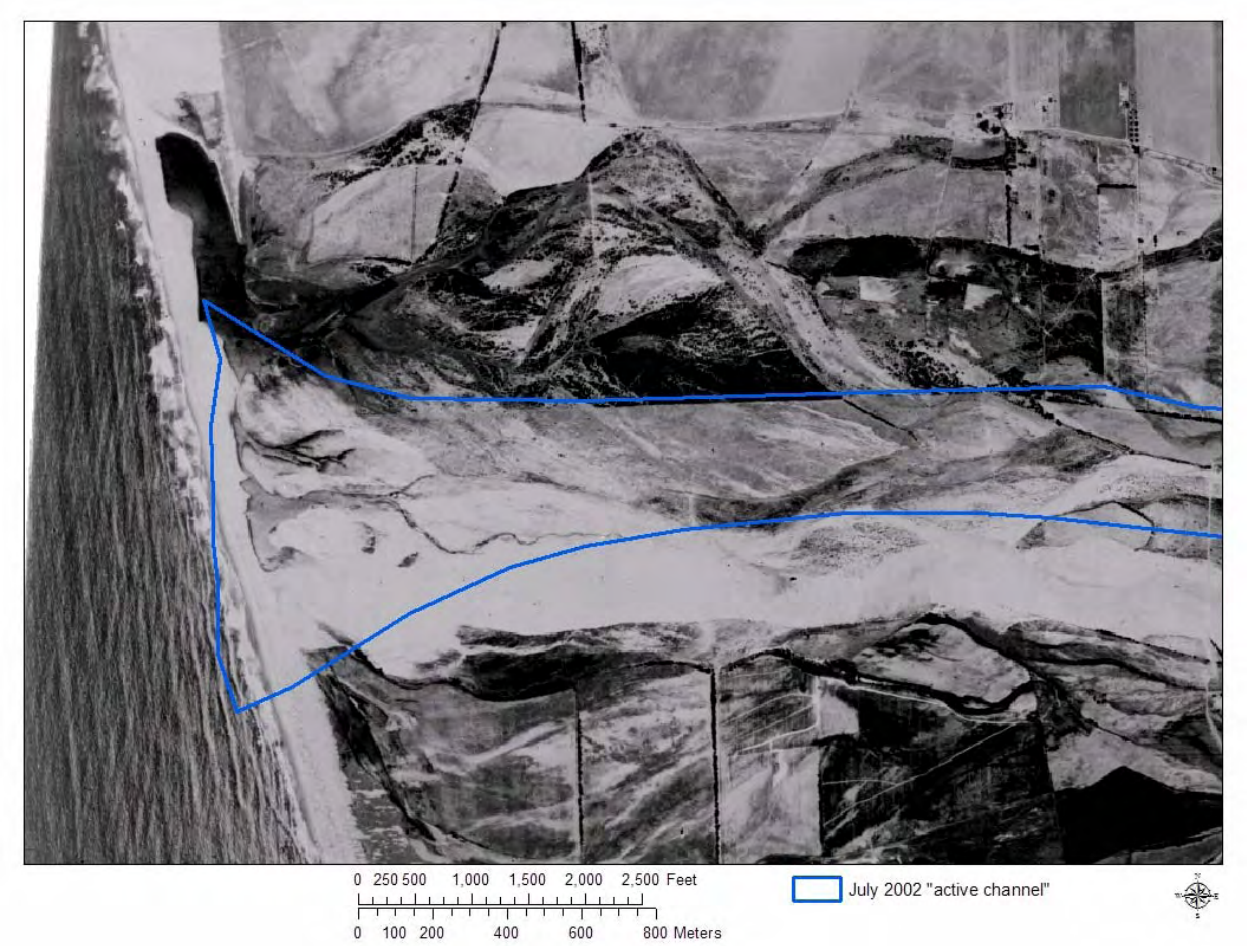

Figure G-2. Approximate 2002 active channel and estuary extent compared to 1927 conditions (Source: California Coastal Conservancy).